THE DEVELOPMENT OF A COMPUTER ASSISTED BIOPSY PROCEDURE FOR EARLY DIAGNOSIS OF LUNG CANCER.

Linda M Sutherland

PhD
University of Edinburgh
1991

The work described in this Thesis has been carried out by me.

Linda M Sutherland

ABSTRACT

The diagnosis of peripheral lung lesions is done by pathological testing of tissue samples collected from the lung by needle biopsy. Lesion positional information is obtained by direct measurement of film negatives taken from two perpendicular X-ray views. Accurate positioning of the biopsy needle, based on this information and under manual control, is difficult to achieve. Sampling accuracy of lesions less than 2cm in diameter (those offering the best chance of a cure if accurate diagnosis is obtained) is poor.

The aim of this project was to devise a means of accurately sampling small peripheral lesions (less than 2cm diameter) with a computer guided biopsy needle using a 'C-arm' rotatable X-ray machine to supply the positional information.

The existing needle biopsy technique is evaluated and a practical error analysis done using a developed mechanical analogue of the X-ray and patient arrangement to determine how the technique might best be developed to reveal all the necessary geometrical information. A marker arrangement is developed which will reveal such geometrical information.

The possible methods of image analysis which might be applied to obtain the relevant X-ray information from the C-arm T.V. monitor are examined. In view of the complicated X-ray image obtained these techniques are dismissed and a manual technique is developed instead in which the information is input to the computer by the surgeon using a mouse. The technique is evaluated using an optical analogue of the X-ray machine.

A biopsy machine, its computer control system and the mechanism by which the biopsy needle is positioned pointing towards the lesion is developed. Accuracy and reproducibility studies of

needle positioning are also detailed and indicate that with selected X-ray views needle positioning should lie within 2-5mm of the centre of the lesion, the exact error being dependent upon the lesion position and depth relative to the biopsy machine.

Details of the biopsy machine link-up to the C-arm X-ray machine, its accuracy testing and the first clinical trials are given. Problems, inherent to the X-ray machine, are detailed and recommendations for further work are made.

ACKNOWLEDGEMENTS

I wish to acknowledge the help of the following:

Dr Norman MacLeod and Prof. Jack Ponton for their supervision, guidance, support and encouragement throughout this work.

Prof. D C Flenley, Dr A Wightman and Dr W MacNee, of the Department of Respiratory Medicine at the Edinburgh City Hospital, for their help during clinical evaluation.

The Scottish Home and Health Department and the SERC for funding this work.

The Chemical Engineering technicians for all the assistance and advice given, especially Kenny Fee for his patience and workmanship during construction of the apparatus.

Chris Hewlett for much help in obtaining the correct format by alterations and additions to 'MEMO'

My office mates- Caroline, Jennifer, Catriona and John for their sympathy and understanding when needed.

My parents for their encouragement and support throughout my student days and beyond.

CHAPTER 1

LITERATURE SURVEY

1.1. Introduction - Functions of the Lung

The lungs have many functions including water evaporation (important for heat and fluid regulation), filtration of toxic materials from the circulation and blood storage. Their main purpose, however, is to provide a medium across which gaseous exchange can occur between atmospheric air and blood.

Atmospheric air is drawn into the body through either the nose or mouth and passes down through the trachea, which divides into two bronchi, one leading to the left lung, the other to the right, as illustrated in Figure 1.1. These bronchi branch out further into all the lobes of the lung, gradually becoming much shorter and narrower, and terminate in alveoli, air sacs of about 0.3mm in diameter.

The pulmonary artery carries blood from the right ventricle of the heart and splits into two, one branch going to each lung. There they subdivide into numerous blood vessels and capillaries of approximately 5 - 20 microns in diameter. These capillaries surround the alveoli and result in a gaseous exchange surface area of between 50 - 100 m^2 and a very thin blood - gas barrier of about 0.5 microns.

Gas exchange is carried out by simple diffusion: Oxygen in the inspired air and at a relatively high partial pressure diffuses into the blood, which has a low partial pressure of oxygen. Carbon dioxide, at a high partial pressure in the blood diffuses out into the airways and is expired.

The capillaries, containing oxygenated blood, join to form the pulmonary vein which returns blood to the left atrium of the heart. The blood passes through to the left ventricle from where

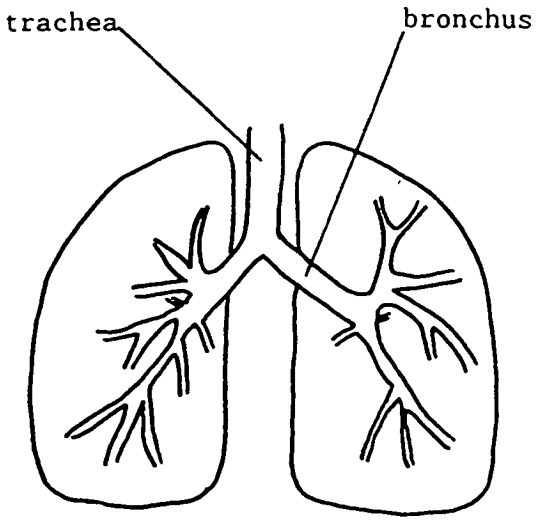

Figure 1.1 - The Anatomy of the Tracheobronchial Tree

it passes out to the rest of the body via the aorta.

If the lungs are diseased the lung function becomes impaired. Common conditions include tuberculosis, pneumoconiosis, emphysema and lung cancer. Lung cancer is the major cause of premature death in industrialised countries. Most lung cancer, if caught in an early stage, is potentially curable. However, by the time lung cancer is diagnosed it is often well advanced with a poor prognosis.

1.2. Rates of Incidence and Death for Cancer

Over the period 1940 - 1983 the U.S. incidence rate of various cancers altered (1). The incidences of stomach and uterine cancers decreased by 70% over the period but now appear to be levelling off. However laryngeal and kidney cancer rates greatly increased as did pancreatic cancer. Breast cancer incidence increased by 30%, prostate, colon and bladder cancer by over 65%, thyroid by over 75% and lung cancer incidences soared by 225% among men and 400% among women.

The U.S. mortality rates do not always display similar trends to the incidence rates. Laryngeal cancer mortality among males and kidney cancer mortality among females decreased. Mortality rates for prostate, colon and bladder cancers showed no major change and for thyroid cancer have decreased. Breast cancer mortality has remained constant but lung cancer mortality has increased, remaining comparable with the incidence rate.

Lung cancer incidence and mortality rates exceed those for other cancer sites (1). The male incidence rate underwent a massive increase but levelled off in the mid 1970's and is expected to decrease. The female incidence rate is considerably lower than for men but is rapidly increasing , as illustrated in Figure 1.2

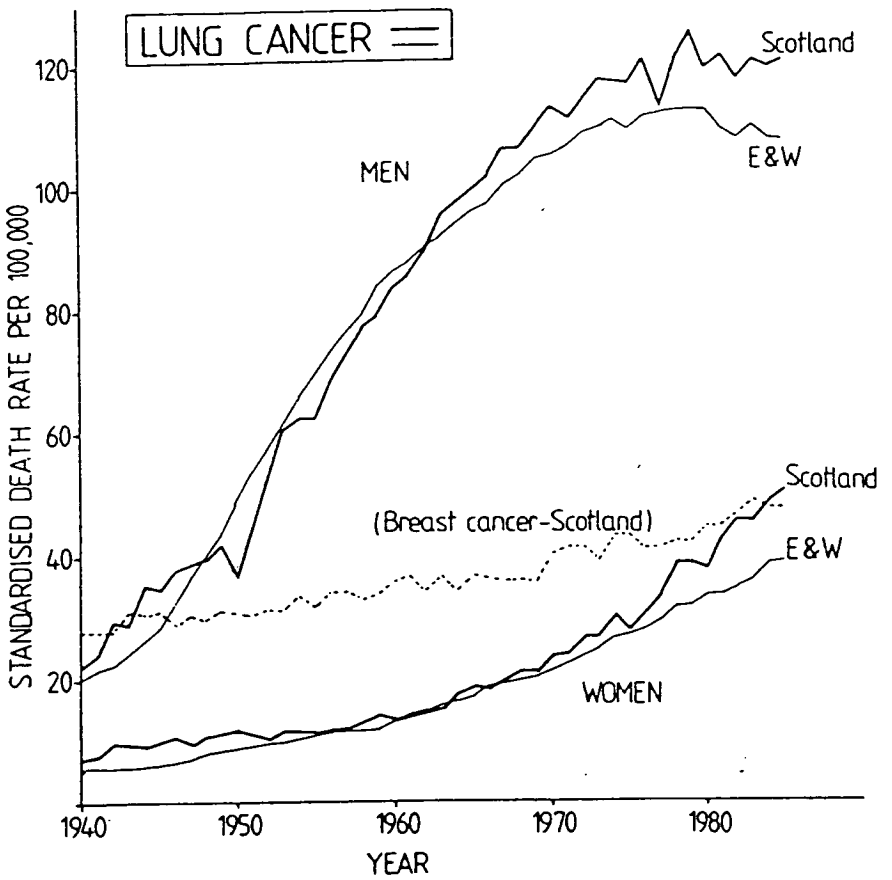

Figure 1.2 - U.K. Lung Cancer Incidence Rates for Men and Women over the period 1940 to 1985.

(2), following a similar trend to the male rate but lagging almost 20 years behind. It has recently overtaken breast cancer as the major cause of death among women.

34,772 people died from lung cancer in 1982 in the U.K. alone (3). The incidence rate for Scotland, at 120 per 100,000, is the highest in the world.

1.3. Cancer Manifestation Versus the Immune System

It may initially seem strange that cancers at one site within the body can be controlled, even cured, while at others can progress almost unhindered. The word 'cancer', however, is an umbrella term covering a wide range of different diseases, each requiring an individual treatment approach. Different cancers attack different sites within the body and one site may be attacked by several different cancers. Thus the system is complicated by different patterns of spread and responses to therapy (4). It is impossible to describe in detail the numerous biological and biochemical changes which occur in cancer, indeed many are not yet understood; but a brief summary of the known and postulated general cellular changes and immune response to these changes is given below.

The actual process by which cancer occurs is unknown. All cells have the ability to multiply and replace those cells lost by death or exfoliation in the normal cell cycle but usually, once a critical mass is reached, they cease multiplying, thus preventing overgrowth. In cancerous cells, however, multiplication does not stop at the critical mass and uncontrolled growth continues until eventually the patient dies.

It is generally assumed that the plasma membrane (the cell surface) will be affected in a cancerous cell. Certain cell surface molecules may occur in large amounts, e.g. proteins,

glycoproteins or glycolipids (5). Interferons (a complex set of proteins and glycoproteins) are also produced. They have a potent anti-tumour effect.

Several cell types within the body exhibit anti-tumour effects. These include natural killer (NK) cells, macrophages, T-lymphocytes, B-lymphocytes and cells which secrete cytotoxic factors.

In a normal healthy body a large quantity of these NK cells exist in lymph, a plasma-like fluid which bathes the body tissues. They are a form of lymphocyte and can rupture (or 'lyse') the plasma membrane of tumour cells and virally infected cells allowing the cell contents to escape. It is thought that these NK cells play an important part in the mechanism of host defence against neoplasia (6,7,8).

T-lymphocytes have a delayed hypersensitivity and respond to antigens on the cancerous cell, reacting to produce lymphokines. These lymphokines can modulate NK cell activity (9) and activate and influence the behaviour of macrophages (10).

B-lymphocytes bind to antigens and result in the production of immunoglobulin, a form of antibody. The antibody is large and is generally confined to the bloodstream. Antibodies do not play a large part in carcinoma rejection: Cell mediated immune responses do (11).

Mononuclear phagocytes are scavenger cells which engulf and digest bacteria, cells, cell debris, etc. It is generally believed that phagocytes play a fundamental role in immune stimulation, antigen recognition and in lymphocyte (white blood cell) proliferation and differentiation.

Unlike NK cells phagocytes do not normally display cytotoxicity

towards cancerous cells. They require to be 'activated' (becoming 'activated macrophages') in a process which may take several days to perform. Mononuclear phagocytes can be activated by many naturally occurring and synthetic materials such as lymphokines, bacterial lipopolysaccharide, double stranded RNA, chronic exposure to noxious gases such as cigarette smoke and various microorganisms. Once activated these macrophages can display cytotoxicity towards cancerous cells while leaving normal cells unharmed. They carry out 'phagocytosis', consisting of two separate steps. The first step is recognition and attachment of the particle. The second step is the fusion of the plasma membrane with the lysosomal membranes and release of lysosomal enzymes into the cell (10). Tumours with a high concentration of infiltrating macrophages sometimes have a lower growth rate than those with low macrophage concentration (12, 13). However others (14) have observed the opposite effect of tumour growth enhancement. It has therefore been suggested that activated macrophages can induce both suppressor cells and cytotoxic cells but the conditions favouring one rather than the other have not yet been determined.

These activated macrophages only retain their tumoricidal properties for a short time, decay rapidly and are unable to undergo reactivation. Unfortunately the process of macrophage activation may also be accompanied by side reactions, one of which is the suppression of NK cell activation but the link between NK cells and macrophages is unknown (15).

Generally it appears that NK cells, present before immunisation, act as the first line of defence prior to macrophage and T-lymphocyte responses. Thereafter, however, their actions are interlinked, often unpredictable , and not always beneficial.

Several possibilities exist for tumour cells to evade the defence system (4):

- When tumours result from chemical carcinogens tumour cells may have different levels of immunogenicity. Those cells releasing large quantities of antigens will be destroyed but those releasing small quantities may remain. Eventually, after continuous stimulation to low quantities of antigens, the immune system will become tolerant and will not reject the tumour cells.

- Many aetiologic agents, whether viral or chemical, are immunosuppressants and thus prevent a host immunologic reaction. Once established the tumour itself may produce immunosuppressants.

- Very early cancers, consisting of only a small number of cancerous cells, may not be recognised as such and continue to multiply and become established. By the time they are recognised the cancer is too far advanced for the immune system to deal with.

1.4. Lung Cancer Metastasis

Tumour cells are able to spread from the site of origin (primary tumour) to surrounding structures and other organs (secondary tumour). This is done by a process known as metastasis in which cancerous cells separate from the tumour, float away in body fluids (lymph, blood), lodge in another site and continue to divide.

There are several common sites of lung cancer metastasis:

- A peripheral tumour can invade the pleura or chest wall. Fluid accumulates in the pleural space and assists in the spread of tumour cells.

- Mediastinal tumours can invade the trachea, bronchi, oesophagus, laryngeal and phrenic nerves or blood vessels.

-Once into the blood stream secondary tumours may occur in the brain, liver, bone marrow, bone and suprarenal glands.

1.5. Types of Lung Cancer

There are many different histological types of lung cancer. Matthews et al (15) and Rosenow and Carr (16) describe the four main types which between them make up over 90% of all lung cancer occurrences.

- Squamous (epidermoid) cell is a slow growing cancer which constitutes around 40-70% of all lung cancers (17). Most squamous carcinoma are observed in males. They often ulcerate, bleed and obstruct a major bronchus. Squamous carcinoma manifests itself mainly within the central area of the lung (67%) (often obstructing a major bronchus) but sometimes peripherally (33%). As a result abnormalities are initially identified by radiography or cytology. Peripheral lesions may be cavitated or necrotic.

- Small (oat) cell carcinoma is a rapidly spreading form of cancer which is manifest mainly in the proximal area (root) of the lung. It accounts for 20-30% of all bronchial carcinoma.

- Adenocarcinoma makes up 10% of lung cancers. It does not spread as quickly as small cell carcinoma and is associated with pulmonary diseases, eg tuberculosis. Such lesions are mainly peripheral (75%) and identified radiographically.

- Large cell carcinoma occurs in 10-15% of lung cancers and is mainly peripherally located.

1.6. Symptoms of Lung Cancer

Lung cancer is not often detected until it has become symptomatic, around 10 years after it first began (17). It may present many different symptoms:

- Haemoptysis- coughing up of blood. A common symptom although it is also attributable to other causes such as tuberculosis and pneumonia. It is associated with ulceration in the bronchus.

- Thrombophlebitis - inflammation of the wall of a vein, commonly in the leg.

- Chest pains from local spread of the tumour.

- Clubbing of fingers and toes - thickening of the tissues at the base of the finger and toe nails so that the normal angle between the nail and digit is filled in. The nail becomes convex in all directions. It occurs in about 30% of lung cancer cases although it can also occur naturally as a harmless congenital abnormality.

- Hypoglycaemia - glucose deficiency in the blood stream causing muscular weakness and incoordination, mental confusion and sweating.

- Breathlessness, although this is more often attributed to a resulting complication of lung cancer.

- Cough or change in smokers cough due to a tumour in the bronchus causing irritation.

-Pneumonia

- Weight loss, tiredness and anorexia

-Recent onset of epilepsy, behaviour disorders or vomiting are common indications of a cancer spread to the brain. Enlargement of the liver may indicate a liver metastasis.

These symptoms are not associated solely with lung cancer and further investigation is necessary before a diagnosis can be made.

1.7. Causes of Lung Cancer

Squamous and small cell carcinoma are associated with asbestos fibres, polycyclic hydrocarbons, coal tar, radioactive chemicals, and probably the best known carcinogen, tobacco smoke.

Large cell and adenocarcinomas are linked with chemical gases and fine dusts of less than 0.5 microns diameter (which includes asbestos, silica and coal dusts)

Other known carcinogens include nickel (18), arsenic, chloromethyl ether and printing ink (2) as well as chromates.

Current epidemiological evidence suggests that some cancer forms are caused by other chemicals and viral infections.

Over 30% of all cancers and 90% of lung cancers are caused by smoking (19). The lung cancer incidence rate for non-smokers (including ex-smokers) is 10 -13 per 100,000 compared with the overall incidence rate of 120 per 100,000 in Scotland. Tobacco smoke contains over 4,700 different chemical substances (2) which include carcinogens and mutagens such as benzyprene, polonium 210 and nitrosamines.

Different tobacco types have different associated lung cancer risks - pipe and cigar tobacco have almost one quarter of the lung cancer risk associated with cigarette tobacco (20). Filter tips have ventilated filters which dilute the inhaled smoke with air, reducing the quantity of tar and nicotine inhaled. However these low tar cigarettes still have high risk factors which increase with the quantity of cigarettes smoked daily, the duration of smoking and the tendency to inhale.

DeVita, Hellman and Rozenburg (21) describe how cancer arises from a sequential two stage process of initiation followed by promotion, where each step change is produced by different agents, these agents determining the site and type of lung cancer.

Tobacco smoke is generally regarded as being a promoting agent since the risk of lung cancer decreases soon after smoking has ceased, although it is only after 10 non-smoking years that the lung cancer risk approaches that of a lifelong non-smoker. If, therefore a smoker comes into contact with an initiator he is very susceptible to lung cancer.

Smokers, however, do not merely increase their own lung cancer risk but also increase the risk for those around them. It is now believed that passive smoking may put many people into the high risk category. This increased risk for non-smokers is most easily examined for smokers' non-smoking spouses (22, 23, 24, 25). Estimates of increased lung cancer risk vary between 30% and 50% but most agree that the risk increases with the amount smoked by the spouse and the longterm exposure to tobacco smoke. Outwith the home 'environmental' passive smoking is difficult to analyse but will play a significant role in risk increase.

Such passive smoking is generally associated with squamous cell and small cell carcinoma, i.e. the histological types commonly

associated with active smoking (22, 24, 26).

Although smoking accounts for a large proportion of lung cancers only a fraction of smokers develop the disease. Studies of patients diet were compared with that of a control group and reveal that a high dietary intake of certain vitamins and minerals may have a preventative effect for lung cancer. Vitamin A, from animal products and green and yellow vegetables is required for normal growth and differentiation of respiratory membranes and inhibits neoplastic transformation (27). This is most evident for male non-smokers over the age of 60 (28). It provides protection against squamous and small cell carcinoma but not adenocarcinoma (29). Other vitamins and minerals examined include Vitamin C, Vitamin E and selenium. It appears unlikely that Vitamins C and E give protection against cancer but it is possible that selenium may provide protective action (27).

Silica, encountered in the pottery industry, quarrying and mining can also cause lung disorders. When silica fibres are inhaled into the lung they become deposited in the alveoli. Alveolar macrophages engulf the fibres and die. The length, diameter and shape of the particles influences how toxic such inhaled particles can be. Particles of > 3-4 microns diameter are trapped by cilia lining the airways and are expelled by cough or sneeze. Finer particles, in the range 0.1-1.0 microns diameter are deposited in the alveoli.

Asbestos, generally regarded as being a promoting agent of lung cancer, is the most important occupational health hazard. For asbestos workers the lung cancer risk increases with duration of employment in the industry but there appears to be excessive risk for those employed less than six months in total (30). For surveyed UK workers diagnosed as having asbestosis, lung cancer was present at death in 44% of cases (31). Of these,

adenocarcinoma was the most common histological type, present in 41% of the lung cancer cases. Squamous carcinoma is also common (17).

Radiation exposure affects lung cancer risk. Japanese atomic bomb survivors had a lung cancer risk of at least twice the normal rate (32). 222Radon and radon daughter products, decay products of uranium, are suspected as increasing the lung cancer rate. Uranium miners may be exposed to such sources by inhaling dusts (33, 34).

People with a personal history of respiratory problems such as chronic bronchitis, emphysema, and asthma are at higher risk of developing lung cancer (35). Those with parents who died of lung cancer are at risk 5 times higher than normal and a parental malignancy of any type also increases the risk.

Susceptibility may be enhanced if a person is in contact with more than one carcinogen. An asbestos worker who smokes is 4-7 times more likely to develop lung cancer than an asbestos worker who does not smoke (2) and is 92 times more likely to develop lung cancer than a person who neither smokes nor works with asbestos (21) i.e. the agents have synergistic effects.

1.8. Rate of Growth of Lung Cancer

Collins, Loeffler and Tivey (36) suggest that if lung cancer begins as a single mutated cell, 10 microns in diameter, and this divides into 2 cells, and these two divide into four, etc then in twenty such doublings the tumour will be 1mm in diameter and in 30 doublings will be 1cm in diameter, as illustrated by Figure 1.3. By 40 doublings they estimate the tumour to weigh about 1Kg and the cancer will be approaching termination.

All cells undergo a cell cycle of resting, DNA synthesis and

duplication of chromatin, followed by mitosis (cell division) (4). The growth rate of tumours depends upon the number of cells in a cycle, the length of the cycle and the fate of the daughter cells. Only a fraction of cells, the growth fraction (GF), are involved in the active cycle. The growth fraction is given by:

$$GF = P / (P + Q)$$

where P is the number of cells actively proliferating and Q is the Quiescent cells not involved in the active cycle. The value of the GF varies over the range 30-80% (4).

Spratt and Harlan (37), estimating the rate of growth and duration of primary pulmonary carcinomas approximated the tumour shape with a sphere and measured tumour diameters on roentgenograms at different stages in the tumour growth. They used the information to decide upon the site of cell division within the tumour. They recognised three possible different growth processes:

- All fully grown cells within the tumour divide. In this case an exponential plot of tumour volume versus time will be obtained.

- Only fully grown cells on the tumour periphery divide, those inside the tumour being inert. In this case the plot of radius versus time will be linear.

- Either of the above may apply but the growth rate may vary because of limited space for growth, lack of food, etc. The resulting radius vs time plot should reveal periods of varying growth along with periods of stagnancy.

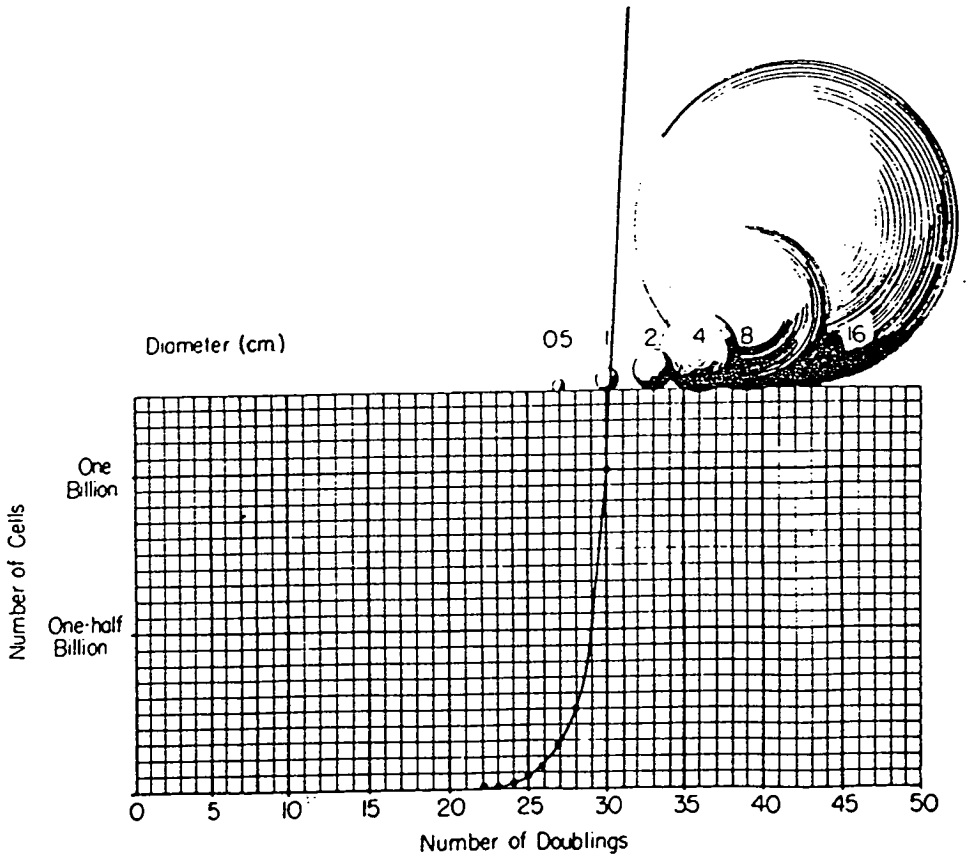

Figure 1.3 - Growth Curve of a Hypothetical Tumour

Results tentatively suggested that all parent cells within the tumour divide but this was by no means conclusive: A few plots showed linearity suggesting that only the peripheral cells divide. However, several problems are inherent in this growth rate estimation:

- Tumours are rarely spherical (or even approximately spherical), are not visible with clearly defined boundaries and do not grow at a constant rate but are limited by lack of blood supply, attack from immune cells etc (3).

- Lesions are unlikely to be detected radiographically until they are at least 1 - 1.5 cm in diameter, often larger, by which time they will have already been established for around 10 years. Early growth patterns cannot therefore be observed.

- It is necessary to treat the lung cancer patient and therefore longterm uninterrupted tumour growth cannot be observed.

- Not all tumours are solid - some are cavitated or necrotic, in which case the rate of external growth does not indicate the rate of cell proliferation.

Several authors have tried to assign a tumour growth factor to observed tumours. These vary widely between patients and histological cancer types (37, 38, 39) and it is not possible to assign growth constants to cell types. Tumour volume doubling times, in which the exponential radius versus time plot is an inherent assumption, also vary widely: 30 - 160 days (40) and 7 - 500 days (41). Tumour doubling time is the overall result of a number of factors, including growth fraction, extent of cell loss, grade of differentiation and mean tumour cell cycle time. Generally the volume doubling time for small cell carcinoma is

short (<1 month) whereas squamous, large cell and adenocarcinoma are slower. The doubling time remains approximately constant for an individual tumour but on occasions when they change they do so towards the end of the tumour life, becoming larger (43). Benign nodules usually either have a much slower or a much faster doubling time than malignant tumours (41). Nodules which do not alter size for over 2 years or are calcified are generally regarded as benign although occasionally calcification can occur in malignant tumours.

1.9. Detection of Lung Cancer

It is desirable to detect and diagnose lung cancer at an early stage when it is treatable and chances of longterm survival are higher. Unfortunately the average tumour size at detection varies between 3 - 4cm (43).

It is generally assumed for most cancers that regular mass screening (annual or 6 monthly) of entire populations over a certain age range or alternatively of high risk groups (smokers, asbestos workers, etc) will indicate many cancers while they are still asymptomatic, i.e. at an early stage when treatment will be more effective, decreasing the mortality rate. This is particularly true for breast and cervical cancers (32) but there is doubt whether mass lung cancer screening will be beneficial (40, 45, 32, 46). Such lung cancer screening commonly involves lateral and posteroanterior (back-front) chest X-rays (abnormalities appear as shadows) and sputum cytology (testing cells taken from bronchopulmonary secretions).

Sputum samples found to contain cancerous cells are often indicative of lung cancer. Sputum testing was found to have a sensitivity of approximately 71% and is around 99% specific (47). Results are better with central than peripheral lesions. In

tests, squamous cells appeared in sputum in 80% of patients with squamous cell carcinoma, and in 36% of patients with no carcinoma. These false positive results tended to occur in the sputum of heavy smokers.

Shadows may arise for many different reasons. Tuberculosis (TB) sufferers and former TB victims have calcified (bony) lesions which show up clearly on radiographs whereas a pulmonary haemorrhage often gives a diffuse shadow. Tumours may appear differently, depending upon the histological type of cancer. They may be necrotic or occasionally calcified and will hence appear similar to TB or Lung abscesses.

According to Boucot and Weiss (46) a general screening programme should be "inexpensive, simple, convenient, reliable, sensitive and specific; and it should provide a good yield of curative cases".

A 5 year screening trial has been reported, involving 10,040 male smokers (45). They were split into two screening schedules:

- Annual chest radiographs

- Annual chest radiographs along with 4-monthly sputum cytology examinations.

In the dual screening programme sputum cytology examination and chest radiographs generally detected different lung cancer cases, as shown in Table 1.1. Lung cancer mortality for the dual programme was expected to be less than for radiographic screening alone since more cases were treated earlier. This assumption was proved wrong.

Table 1.1 - Method of Detection versus Lung Cancer Cell Type in Dual Screen of 4968 Men.

Histology	Determined by cytology	Determined by radiograph	Determined by both	Interval cases	Total
Epidermoid	20	8	8	10	46
Adenocarcinoma	5	44	3	21	73
Large Cell	1	3	0	2	6
Oat Cell	1	5	3	12	21
Carcinoid	0	0	0	1	1
Total	27	60	14	46	147

* Interval cases were determined during the screening period but by means other than the two screening methods studied.

Sputum cytology detects only squamous and adenocarcinoma, both slow growing types. Although these tumours did not, in general, appear on the radiographs they are still potentially curable when they are eventually detected radiographically.

There is hence controversy about the effect of dual screening on lung cancer survival. Generally radiographic screening will not detect the tumour until it is at least 1cm in diameter. Sputum cytology may detect central cancers at an earlier stage but not much earlier than radiography and so the dual programme does not appear to have much effect on survival when compared with radiographic screening alone.

All patients in the programme underwent regular chest radiography and the effect of radiographic screening on lung cancer mortality was not investigated. However, the overall 5 year survival rate for both screening schedules was 35% compared with an estimated 13% in the US generally.

A massive 3 year study involving 55,000 men aged 40 or over has been carried out (49). Two groups were formed: The test group contained 29,723 men who underwent regular 6-monthly chest radiographs. 25,311 men in the control group had a chest

radiograph taken at the beginning and end of the study period.

101 patients in the test group developed lung cancer. 65 of these were detected radiographically but the remaining 36 were symptomatic at detection. The 5 year survival rates for patients who developed lung cancer was 23% in the test group compared with 6% in the control group. Of the patients who underwent surgical resection 32% in the test group and 23% in the control group survived 5 years. The author suggests that early radiographic detection resulted in improved resectability of lung cancer although the 5 year survival of resectable patients was similar in both groups.

Another 10 year study (46) involved 6,136 male volunteers, aged 45 years or over, drawn from the general population who initially showed no signs of any respiratory abnormalities. 121 new cases of lung cancer were found over the period. Of these lung cancer cases 67 had regular 6 monthly X-rays but 25% of these were detected only after symptoms developed. Of the 54 cases who had greater than 6 months between their last screening and detection 50% were symptomatic.

Survival rates between the radiographic and symptomatically detected lung cancers for those undergoing regular 6 monthly checks were similar in the longterm, i.e. 13% and 11% at 5 years respectively, but in the short term (1 year) those detected radiographically had much higher survival rates, 63% compared with 11%. For those who had greater than 6 months between their last checkup and detection of cancer the 1 year survival was again better for radiographically detected than symptomatic, 69% compared with 7%, and 8% and nil for the 5 year survival respectively.

Although high risk groups have a higher expected lung cancer incidence and screening may yield a higher proportion of lung

cancers the associated 'cure' rate is low because the prognosis for these patients is bad.

Mass screening is hindered by false positive tests. Chest X-ray screening is 97% specific (46). On the surface this would appear satisfactory but the 3% of patients with false positive results represents a considereble number in mass screening programmes. All require further clinical study, which is expensive on resource time and funding.

Mass screening is expensive, but when TB was rife and a major killer such screening processes were worthwhile. If TB patients are found in early stages (and chest X-rays normally revealed early stages) they can be cured by chemotherapy. Lung cancer 'finds' were regarded as an added bonus of the system. The cost benefits at that time, in terms of patients cured, were thus high. Nowadays TB incidence is low and chest screening among either mass population or high risk groups, yielding only a very small cure rate, has a very low cost benefit (46). Current asymptomatic lung cancer patients have usually been detected by regular industrial screening of high risk groups, such as asbestos workers.

Abnormalities of < 1cm in diameter, and often larger, are not usually visible on chest radiographs. They tend to be obscured by the ribs or do not have a large difference in X-ray attenuation from that of the surrounding tissue and so are missed by the radiologist.

Other detection methods may pick up such obscured lesions. Tomography is an X-ray technique which involves focussing X-rays at a certain depth and deliberately blurring out structures at other depths. This may pick out lesions obscured behind ribs.

A great improvement on this technique has been computed

tomography (CT). Its use in lung disease is detailed elsewhere (50). Collimated X-rays are focussed on a thin 'slice' of patient, 2-13mm thick, without interference from blurring of surrounding structures. Several views are taken from different angles and the images are projected onto sensitive scintillation detectors, allowing accurate measurement of transmitted radiation. the images are matched by a computer using the X-ray attenuation information. The resulting image can be displayed either on a T.V. monitor as a grey level picture, on radiographic film or stored as intermediate information on a disc for future analysis.

In order to locate a lesion several such slices must be built up. To locate lesions of less than 1cm in diameter a maximum slice separation of 1 cm is required. 10 consecutive slices however delivers a radiation exposure of 3.5 r to the skin (51). Conventional Tomography can reliably detect nodules down to 6mm diameter whereas CT can detect those of 3mm reliably. Although it can often detect tumours at an earlier stage and reveal more information about the extent of spread of disease. CT has not been widely used in routine chest examinations. The equipment is vastly expensive compared with that for conventional radiography.

Ultrasound, used to scan many sites within the body, is inappropriate for the lungs due to their air content. Peripheral lesions may, however, be observed through the rib spaces at full expiration.

The tumour visibility may be improved using radio-nuclides (66) (a high activity and low radiation dose is required). These radioactive tracers are administered either orally or intravenously and, after a time delay accumulate at the site of inflammation. A gamma camera will detect the gamma radiation emitted as the radionuclide decays. This technique is commonly

used to detect blood clots which have travelled to the lung and cannot be observed easily on radiographs. Labelled microspheres are administered and become trapped in the lung capillaries, illustrating abnormalities.

197Hg (with a half life of 65 hours) is commonly used in locating small lung tumours with X-rays.

Gallium scanning may also be used to detect some types of lung cancer. Ga67, with a half life of only 78 hours is able to be used within the body. It binds to lymphocytes and is therefore drawn into and concentrated in inflamed areas of the body (52). It is also absorbed into bone, liver and spleen and some leaves in the urine. Ga67 can detect small cell carcinoma of the lung but is expensive and not readily available (51). As a detection or location technique this may be satisfactory, but it is not a suitable technique for mass screening.

Research is currently underway on 'biomarkers' and tumour markers for use as detection agents for cancers. These are antigens, hormones or enzymes which are secreted by cancerous cells and are hence present in abnormally large quantities in body fluids when cancer is present (15, 53, 54). Lung Tumour Associated Antigen (LTAA) has been discovered in serum from lung cancer patients. 35 - 75% of lung cancer patients show elevated levels of calcitonin (55). Springer et al, using T-antigen, (57) claim to detect 90% of $T^{1}M^{0}N^{0}$ NSCC in the lung with a high (unquantified) specificity. The population size was, however, small. Serum levels were raised in 69% of newly diagnosed SCC of the lung. Serum NSE was raised in 39% of patients with limited stage SCC, 87% with extensive stage disease, 84% with 1 or 2 metastasis sites and all patients with metastasis at 3 or more sites (58). However, none of these markers are specific either to cancer sites or to histological types of cancer. In addition many

people, e.g. heavy smokers, have high levels of such antigens etc in the absence of cancer. Ideally such chemical markers could be used in mass screening for early detection, staging and siting of cancers. Thereafter they may also be useful in monitoring response to therapy (58, 59, 60, 61).

Hence, although their uses are presently limited, tumour markers have a major potential for improving cancer detection.

1.10. Diagnosis of Lung Cancer

Once an abnormality in the lung has been indicated, further tests are required for diagnosis. To accurately diagnose cancer and also to find its cell type at present requires direct histological examination of the suspected cancer itself and hence that a tissue sample be taken from the indicated abnormality (or 'lesion').

Several investigative methods exist for inspecting and sampling the lesion for cell typing and the pleura and nodes for testing for metastases.

Mediastinoscopy may be carried out under general anaesthetic to examine the mediastinum and associated nodes (41) and they may be biopsied directly. The patient is positioned supine and a small incision is made in the neck, above the suprasternal notch and a 'tunnel' cleared between the fascia and the trachia. The fascia is cut to allow access to the lymph nodes. The mediastinoscope, a hollow, rigid instrument, 8cm long by 2 cm wide, is inserted through the tunnel and directed towards the lymph nodes for examination and sampling, if required.

Thoracotomy, again carried out under general anaesthetic, involves surgically opening the chest cavity to inspect and/or sample the lungs, pleura, chest wall, etc and thus enable more

accurate staging. The operation can, however, be extremely distressing and painful for the patient. Many patients are old, ill and may not be fit enough to undergo such a traumatic experience as surgery or even general anaesthetic.

Several other techniques much less invasive, simpler to perform and generally much less costly, have been developed in recent years.

The normal investigative procedure for the lung involves the insertion of a fibre-optic bronchoscope through the respiratory tract into the bronchi and the removal of cell samples from suspect areas for test. The patient is placed in the supine position with head held back and the end of the fibrescope, which is coated in lubricant, is inserted through the nasal passages. The surgeon, viewing the position of the fibrescope end through the eyepiece, directs it down trachea, into the correct lung and bronchus until the suspect tumour is observed. A long brush or forceps is then inserted down through the tubes of the fibrescope and by either brushing or snipping, cell samples are taken from the suspicious areas, transferred to slides, soaked in formalin and sent to the pathology laboratory. The bronchoscope, however, cannot obtain samples either from the superior segments of the lower lobes or from the medial sections of the upper lobes as it cannot bend sufficiently to reach these areas. The fibreoptic bronchoscope can sample 28-38% of peripheral lesions and 19% of small nodules (41).

A bronchio-alveolar lavage may help when the fibrescope (7mm in diameter) cannot approach a lesion. This involves injecting 100-300ml of saline solution down through the fibrescope into the bronchus and out into the alveoli. By applying a backpressure most of the saline may be sucked back up the fibrescope, stored and examined for cancerous cells.

Alternatively, when the lesion cannot be viewed through the bronchoscope but is visible radiographically, a bronchial biopsy may be carried out under fibreoptic guidance. This involves directing the forceps out from the end of the bronchoscope through the bronchi towards the lesion and removing a small tissue sample from the tumour area.

General reported yields of these fibreoptic bronchoscope techniques are shown in Table 1.2.

It appears that for large, visible, centrally occurring tumours bronchial brushing is most accurate whereas for peripheral tumours bronchial biopsy under fluoroscopic guidance is preferred. Kvale et al (62) noted that in many cases, especially peripheral lesions, positive results were obtained by either brushing or biopsy and thus combining the two techniques increased the overall yield to 79%.

Tumour size is also important: Large tumours are more easily detected than smaller ones. Radke (63) suggested that fibreoptic bronchial biopsy may be satisfactory for lesions greater than 2cm diameter but unsatisfactory for those less than 2cm diameter.

These bronchoscope methods are satisfactory for sampling lesions which occur in central areas of the lung, but peripheral lesions, especially those less than 2 cm in diameter, cannot be approached by the fibrescope and transthoracic needle biopsy is carried out instead.

In this method a needle is passed through the chest wall and lung into the lesion and a cell sample drawn off for pathology or cytology. There are two main types of biopsy needle: Cutting needles and aspiration needles.

Cutting needles have a large bore and are thick walled. They are

Table 1.2- General reported diagnostic yields of positive specimens when using the flexible fibreoptic bronchoscope.

Authors	Tumour Information		percentage of positive specimens on using					Comments
	Diameter	Location	Bronch. Brushing	Bronch. Biopsy	Bronch. Brushing +saline	Bronch. washing (lavage)	Post bronch sputum	
P A Kval et al (62)	all	central visible	77	71	70	63	48	71 total
	all	peripheral	20	50	40	33	33	biplane fluoroscopy used in positioning (6 total)
Radke (63)	<2cm	peripheral		28				
	>=2cm	peripheral		64				biplane fluoroscopically guided
	all	peripheral		56				
Stringfield (97)	<2cm	<2 or >6 from hilum	48% 27%					not visible through bronchoscope
	>2cm	2-6cm from hilum	71%					
Ellis (98)	>4cm		57	81				
	<4cm		29	58				
Rudd (65)	all	all		96				29 biopsy forceps guided by fluoroscope

designed to remove a core of tissue for pathological examination. Aspiration needles are much finer, usually 18-22 gauge. They remove a much smaller tissue sample for cytology.

The patient is positioned on the table generally either in the prone or supine position to allow easy, usually vertical, needle access to the lesion. The skin is cleaned and a local anaesthetic is given along the proposed approach of the needle towards the lesion which, of course, must avoid puncture of arteries or any other organs. A small incision is made with a scalpel through the skin and subcutaneous tissue and the needle inserted and advanced, in a vertical direction, towards the lesion. The patient is asked to hold his breath as the needle breaks through the lung or 'pleura' to avoid the occurrence of tears to the lung surface. The patient resumes gentle breathing and the needle advance is continued until the appropriate depth is reached, sometimes indicated by a change in the lung consistency. The needle position is then viewed on the monitor, using the fluoroscope, and the depth is checked by taking an X-ray or fluoroscopic view from the side, perpendicular to the original vertical fluoroscope view, the needle remaining in position while this check X-ray is processed and studied. Any adjustments to the needle position are made at this stage. For cutting needle biopsy the inner stylet is fully inserted and the outer cutting edge then advanced, gathering tissue as it progresses through the tumour. The needle is then removed.

For aspiration needle biopsy the stylet in the needle annulus is removed and the surgeon blocks off the end with his thumb to avoid the ingress of air into the chest cavity which could cause pneumothorax, a partial collapse of the lung. A syringe is attached to the end of the needle and suction applied. The needle is sawed back and fore over a roughly 1cm distance to obtain tissue samples and, maintaining the suction, the needle is

withdrawn and the suction is released.

The tissue, held in the needle annulus, is transferred to glass slides, soaked in formalin solution and sent for pathological examination.

Immediately after the biopsy a frontal X-ray is taken, with the patient in an upright position, to ensure that pneumothorax has not occurred. Reported accuracies of percutaneous needle biopsies are shown in Table 1.3. There appear to be large discrepancies in the reported needle biopsy diagnostic accuracies, which are dependant on the lesion size, its position within the lung and the size of needle used.

Lesions greater than 2cm diameter have accuracies of 86% while lesions less than 2cm diameter are not so easily sampled and diagnostic accuracies are lower, around 69% (64).

Needle biopsies are most accurate for use on peripheral lesions greater than 2cm in diameter. They have also been used to sample lesions inaccessible to the bronchoscope (such as the mediastinal and hilar areas) with good accuracy, although Rudd et al (65) reported accuracies of only 61% for those lesions not accessible by bronchoscope. They used 'ultrathin' needles of 24-25 gauge which not only bend easily (although their final position was checked fluoroscopically) but also remove a very small piece of tissue for cytology. If the sample is badly crushed it becomes very difficult to diagnose disease and this may result in a low diagnostic accuracy.

Ultrathin needles are best used for the initial puncture of a mediastinal lesion when the cause is uncertain. Should accidental puncture of the heart or artery occur then the fine needle will not cause as much damage as one of smaller gauge, ie larger

Table 1.3 - Reported Accuracies of Percutaneous Needle Biopsies

Author	Tumour Information		Needle	Diagnostic	Common	Comments
	Diameter	Location	Type	Accuracy	Complications	
Harris et al (99)	all	all	cutting	92%	26% pneumothorax 19% haemorrhage	
Gibney (64)			aspirated	73.6%	30% pnuemothorax	
Berquist (100)	all	all	aspirated	82%	49% pneumothorax	
	>8cm	all		88%	11% haemoptysis	25 cases
	4-8cm	all		91%	26% haemorrhage	94 cases
	2-4cm	all		84%		193 cases
	1-2cm	all		69%		84 cases
	<=1cm	all		65%		34 cases
	<=1cm	peripheral		85%		
	1-2cm	peripheral		75%		
	>4cm	mediastinal		92%		
		central		78%		100 cases
		peripheral		82%		297 cases
		mediastinal		92%		24 cases
		pleural		88%		9 cases
Lalli (101)	all	all	aspirated	86%	24.2% pneumothorax (most work done by inexperienced residents)	
Dr Wightman (102)			aspirated	95%	15% pneumothorax	
Westcott (103)		all	aspirated	97%	7% haemoptysis 21% pneumothorax	
Zavala (104)	all	all	aspirated	87%		25 patients (used ultrathin needles of 24 or 25 gauge).
Rudd et al (65)	all those not accessible by bronchoscope			61%		

diameter. Once the lesion has been located and the surgeon is sure that the cause is not an artery, etc then a smaller gauge needle can be inserted to obtain a more sufficient sample.

Complications are more frequent for deeper lesions. This is especially so for cutting needles which can result in haemorrhages. It has been proposed that cutting needles be restricted to peripheral lesions where complication rates are low and aspiration needles be used elsewhere.

Generally percutaneous needle biopsy is only performed on cooperative patients who are able to maintain a fixed position and to suspend respiration on demand. Since a pneumothorax can easily occur such patients should be able to withstand such a complication.

Originally it was believed that the needle biopsy technique may encourage seeding to occur along the needle track but such occurrences are infrequent (41).

In order to correctly site the needle into the lesion with the minimum amount of repositioning requires that the lesion position within the lung is known, preferably relative to a radio-opaque external marker which can be seen by the surgeon. A marker, in the form of a file, paper clip or coin, is taped to the chest wall and used as a guide.

Several means exist for the determination of lesion position:

Two perpendicular radiographs may be used, one taken PA the other lateral. Both radiographs are approximately actual size. In such arrangements the source-detector distance is about 6m. The patient, with marker attached, is positioned up against the detector so magnification effects are negligible.

Provided that the patient holds his breath at the same point in the breathing cycle for each X-ray take it is possible to measure the distance and direction of the lesion from the external marker directly from the radiograph using a ruler.

One lateral radiograph in conjunction with a fluoroscope. The X-ray source is positioned either above or below the patient. the external marker may be positioned directly over the lesion by viewing the relative positions using a fluoroscope and, when correctly positioned, an indentation is made on the skin by pressing down firmly on the marker. An X-ray is taken from the side and to indicate the lesion depth and the marker is removed, its position indicated by the skin indentation.

1.11. Staging of Lung Cancer

The extent to which lung cancer has progressed at the time of detection is a major factor during consideration of the best treatment and in determination of the expected lifespan of the patient.

A cancerous tumour will begin initially as one cell and will grow to engulf many cells within the organ. The cancer may then spread to the lymph nodes and finally metastasise to other organs.

The extent of spread within the chest may be determined by X-ray, CT, bronchoscopy, mediastinoscopy, thoracotomy, etc. More distant metastases may be more difficult to detect. If the patient is symptomatic then the symptoms may suggest spread, for example brain metastases is related to behavioural problems. Otherwise routine testing of common sites of metastases should be done. Such sites include brain, liver, bone, and bone marrow.

Lung cancer staging is based on the 'Tumour - Nodal - Involvement - Metastasis' (TNM) system, described in detail by Little et al

Table 1.4 - Staging of Lung Cancer.

TNM Classification		Definition
Primary Tumour(T)		
	TX	Tumour proven by the presence of malignant cells in bronchopulmonary secretions but not visualised roentgenographically or bronchoscopically; or any tumour that cannot be assessed
	TO	No evidence of primary tumour
	T1S	Carcinoma in situ
	T1	Tumour 3cm or less in greatest diameter, surrounded by lung or visceral pleura, and without evidence of invasion proximal to a lobar bronchus at bronchoscopy
	T2	Tumour more than 3cm in greatest diameter, or a tumour of any size that either invades the visceral pleura or has associated atelectasis or obstructive pneumonitis extending to the hilar region. At bronchoscopy, the proximal extent of demonstrable tumour must be within a lobar bronchus or at least 2cm distal to the carina. Any associated atelectasis or obstructive pneumonitis must involve less than an entire lung and there must be no pleural effusion.
	T3	Tumour of any size with direct extension into an adjacent structure such as the parietal pleura or the chest wall, the diaphragm, or the mediastinum and its contents; or a tumour demonstrated bronchoscopically to involve a main bronchus less than 2cm distal to the carina ; or any tumour associated with atelectasis or obstructive pneumonitis of an entire lung or pleural effusion.
Nodal Involvement (N)		
	NO	No demonstrable metastasis to regional lymph nodes
	N1	Metastasis to lymph nodes in the peribronchial or the ipsilateral hilar region, or both, including direct extension
	N2	Metastasis to lymph nodes in the mediastinum
Distant Metastasis (M)		
	MX	Not assessed
	MO	No (known) distant metastasis
	M1	Distant metastasis present

Stage Grouping

Occult Carcinoma	Stage 1	Stage 2	Stage 3
TX NO MO	T1S NO MO T1 NO MO T1 N1 MO T2 NO MO	T2 N1 MO	T3; any N or M N2; any T or M M1; any t or N

Several of these TNM groupings combined form the stage grouping: An early cancer, confined to the initial organ of manifestation, is classed as stage 1 and a far spread cancer as stage 3.

Confusingly the staging system has recently been rearranged in an attempt to associate staging with survival rates (68). The TNM basis has been retained but the number of classifications has increased, as shown in Table 1.5. The individual stage classification has also changed with the addition of a stage 4 category. T1N1, previously classified as stage 1 is now in stage 2. The overall effect will be to improve the appearance of the mortality rates associated with each stage.

(67). It categorises the cancer into groups, depending upon the size and site of the primary tumour (T); the extent of the cancer spread to lymph nodes (N); and the extent of spread (metastasis) to other organs, such as the brain, liver, opposite lung and bones (M). These groups are described in an extract (16), shown in Table 1.4.

Several of these TNM groupings combined form the stage grouping: An early cancer, confined to the initial organ of manifestation, is classed as stage 1 and a far spread cancer as stage 3.

Confusingly the staging system has recently been rearranged in an attempt to associate staging with survival rates (68). The TNM basis has been retained but the number of classifications has increased, as shown in Table 1.5. The individual stage classification has also changed with the addition of a stage 4 category. T1N1, previously classified as stage 1 is now in stage 2. The overall effect will be to improve the appearance of the mortality rates associated with each stage.

According to (67), patients are often understaged when either cancerous lymph nodes or small distant metastases are not detected. They state that a quarter of patients may be understaged and hence receive insufficient treatment. Staging should be a repetitive process:Rather than relying merely on uninvasive testing using X-rays, bronchoscopy, etc the staging should be constantly updated as the surgeon gains more information both during surgery and from the pathological examination of resected tissues. Three main stage classifications are mentioned (69):

> Clinical classification based on results from physical examination, radiology, bronchoscopy, mediastinoscopy, mediastinotomy or thorascopy.

Table 1.5 - The New International Staging System for Lung Cancer: TNM Definitions

Primary Tumour (T)	
TX	Tumour proven by the presence of malignant cells in bronchopulmonary secretions but not visualised by roentgenography or bronchoscopy, or any tumour that cannot be assessed as in a retreatment staging.
T0	No evidence of primary tumour.
T1S	Carcinoma in Situ.
T1	A tumour that is 3cm or less in greatest dimension surrounded by lung or visceral pleura and without evidence of invasion proximal to a lobar bronchus at bronchoscopy.
T2	A tumour more than 3cm in greatest dimension, or a tumour of any size that either invades the visceral pleura or has associated atelectasis or obstructive pneumonitis extending to the hilar region. At bronchoscopy the proximal extent of demonstrable tumour must be within a lobar bronchus or at least 2.0 cm distal to the carina. Any associated atelectasis or obstructive pneumonitis must involve less than an entire lung.
T3	A tumour of any size with direct extension into the chest wall (including superior sulcus tumours), diaphragm, or the mediastinal pleura or pericardium without involving the heart, great vessels, trachea, oesophagus, or vertebral body, or a tumour in the main bronchus within 2.0cm of the carina without involving the carina.
T4	A tumour of any size with invasion of the mediastinum or involving heart, great vessels, trachea, oesophagus, vertebral body, or carina or with presence of malignant pleural effusion.
Nodal Involvement (N)	
N0	No demonstrable metastasis to regional lymph nodes.
N1	Metastasis to lymph nodes in the peribronchial or he ipsilateral hilar region, or both, including direct extension.
N2	Metastasis to ipsilateral mediastinal lymph nodes and subcarinal lymph nodes.
N3	Metastasis to contralateral mediastinal lymph nodes, contralateral hilar lymph nodes, or ipsilateral or contralateral scalene or supraclavicular lymph nodes.
Distant Metastasis (M)	
M0	No (known) distant metastasis
M1	Distant metastasis present - specify site(s)

Surgical evaluative classification using results from thoracotomy and biopsy.

Post surgical treatment classification based on the results of the pathological examination of resected tissue.

At each classification the stage is upgraded and initial stage 1 patients may end up classified as stage III (or now even stage IV). Over two thirds of patients have stage 3 (old classification) lung cancer when diagnosed as having lung cancer (70).

1.12. Treatment of Lung Cancer

Once cancer has been diagnosed and histologically typed the most suitable treatment must be sought. Lung cancer treatment is very much dependent on the cancer type and the extent of its spread. There are currently 3 major forms of treatment: Surgery, radiotherapy and chemotherapy. For treatment purposes the 4 main different histological types of lung cancer are split into 2 groups: Small cell carcinoma (SCC) and Non small cell carcinoma (NSCC).

1.12.1. Surgical Resection

NSCC's are best treated by surgical removal of the tumour (69). If the entire tumour can be removed the treatment can be curative. However, this requires that the cancer is in an early stage of development and has not metastasised (stage 1 or perhaps stage 2). Overall operable lung cancer has a 5 year survival rate of less than 10% compared with 69% for early operable lung cancers (57). Unfortunately, only 20% of patients are potentially surgically resectable. This treatment is especially promising in slow growing squamous carcinoma, in which metastases do not occur

until very late. It may prove satisfactory for SCC only in a very early stage but unfortunately for small cell carcinoma and large cell carcinoma metastases usually occur early in the tumour life. The amount of tissue removed in resection is dependant not only on the size of the tumour but also on the surgeons preferred resection method. Usually the treatment involves the removal of either a lobe of the lung or an entire lung but recently miniresections have been done on small peripheral lesions (71) without any increase in the mortality rate. This is particularly useful for older patients who may not cope well with a much larger resection. The remaining lung tissue must therefore cope with the entire output from the right ventricle of the heart. If the remaining lung tissue is normal then the patient should not display any symptoms such as breathlessness.

Only rarely are SCC's found at an early stage. Less than 2% of patients with SCC are staged as either T1 or T2 with NO (72). By the time that they are detected the tumours are usually spread,at least as far as the lymph nodes. These SCC cases are commonly treated with chemotherapy and occasionally radiotherapy, which act by killing the fast growing cells within the body to produce tumour regression. Unfortunately all cells are not destroyed and so these treatments usually only prolong life.

1.12.2. Radiotherapy

The principles of radiotherapy are described elsewhere (73). Radiotherapy is provided locally and requires precise location of the tumour to enable regular treatments to be given to the same area of tissue and also to allow shielding blocks to be positioned so that normal tissues are protected. Generally radiation attacks cells on the boundary between the advancing tumour and normal cells where a plentiful blood supply is available (73). The cells, (both normal and cancerous) absorb

ionising radiation and the DNA, contained within the cell may be either destroyed or deformed. Deformed DNA may, however, be repaired by enzyme processes and the cell will continue to divide. Further irradiation is therefore required. For this reason radiation doses must be spread out over a period of time. A moderate radiation dose is generally regarded as between 4000-5000 rads spread over several weeks and applied daily. Such radiotherapy often reduces tumour size but does not , in general, provide a cure. The tumour will divide at the same rate as before irradiation was commenced. Thus the treatment merely slows the tumour progress by the equivalent amount of time that is required for the tumour to regrow to its original preirradiated size (74) and this merely improves the short term survival and reduces pain. Before radiotherapy can be expected to cure lung cancer, tumour cells will need to be made more sensitive to its effects. This may be effected using a drug which is taken up by the tumour, but as yet none have proved successful (40). Although radiation is applied only to the site of affected tissues the resulting side effects apply more generally. These include a general feeling of lethargy, headache, anorexia or vomiting. For radiation applied to the lung other side effects include pneumonitis, an inflammation of the lung.

1.12.3. Chemotherapy

The principles of chemotherapy are described in detail elsewhere (75, 76, 77).Chemotherapeutic agents have a selectivity for cancer cells over normal host cells (4). Chemotherapy is used either for the majority of SCC or when NSCC has metastasised. Common therapeutic agents include Cyclophosphamide, CCNU, methotrexate, 5-flourouracil (CMF), vincristine, adriamycin and hexamethylmelanine. Cytotoxic drugs do not actually kill tumour cells but affect cell division. They inhibit one or more of the steps in the cell cycle. Alkylating agents, such as chlorambucil,

cyclophosphamide, etc damage the DNA template and prevent replication. Vincristine and vinblastine inhibit mitosis (4).The applied dosage of such agents is vitally important since small changes in dose can result in large changes in response rate. The dose chosen is very dependant upon the drug used, the age and physical condition of the patient and also on the tumour itself. Any previous therapy must also be considered. As in radiotherapy both tumour and normal cells can recover after chemotherapy and so the required dose is given in stages. Regular blood count readings will indicate if the cytotoxic effect on the immune system becomes excessive. The white cell count should not fall below 3,000 per mm3 or the platelet count below 80,000 per mm3 (77). When a single drug is administered a response is achieved in 30% of cases (69). A given dose of cytotoxic drug disables a constant fraction of cells. To eradicate the entire population of cancerous cells it is necessary to increase the drug dose to the maximum tolerated by the body or to start treatment when the number of cells is low enough to allow the tumour destruction at smaller, more tolerable doses (4). Often combination chemotherapy (using several anti-cancer agents) proves more successful since between them they provide a wider attack front and also inhibit the formation of resistance to individual agents. The different chemotherapeutic agents can be administered at different stages, so preventing the tumour cells from becoming resistant to each drug.

1.12.4. Combined Treatments

Several treatment modalities may be combined to improve the prognosis.

If an NSCC has progressed to the extent that surgical resection will not remove the whole tumour then aggressive radiotherapy may be used pre-operatively to reduce the tumour size. Radiotherapy or chemotherapy may be used post-operatively should a cancer

recur or a metastasis be discovered (78, 79).

Combining radiotherapy with combination chemotherapy can also increase the length of patient survival (69).

1.12.5. Side Effects

These therapeutic treatments are successful because they are toxic to fast growing cells such as cancers. There are many naturally occurring fast growing cells within the body, including hair, skin, nails,etc as well as the mutant cancer cells. As a result several unpleasant side effects occur which include nausea, vomiting, hair loss, low blood count, toxicity to bone marrow,high risk of infection, etc. It is possible to minimise such side effects and provide an acceptable quality of life for such patients.

1.12.6. Current Research

Several new treatment modalities are currently being researched. Most include some form of immunotherapy.

BCG is normally administered as part of the TB prevention process. It induces cell-mediated immunity to produce increased resistance. Post surgical BCG administration for early NSCC's may help prevent recurrence of cancer but for advanced NSCC and for all SCC BCG shows no effect (44, 78).

Monoclonal antibodies to specific antigens may be radiolabelled and/or toxin-labelled and could possibly be used to direct therapeutic agents to the site of antigen production, ie the tumour cells (80, 81).

Interferons are known to have a potent anti-tumour effect. They initiate cells to activate an anti-viral state and also enhance

the immunoregulatory system by activating NK cells. The exact method by which interferons act on tumour cells is unknown but it has been proposed that the interferons bind to the tumour cell-surface molecules and trigger off a 'messenger' which depresses the host genome. However, interferons provide disappointing results in NSCC of the lung in human trials (82).

It is suggested that immunotherapy may be best used post operatively in NSCC since it does not appear to have as severe side effects as the cytotoxic drugs used in chemotherapy (69, 81).

1.13. Lung Cancer Patient Survival Rate.

The definition of 'cure' as regards lung cancer patients is variable. Many believe that lung cancer is an incurable disease and that all such patients die of some cancer related disease - either another primary cancerous growth (a recurrent disease) or alternatively of a metastasis. Others believe that if a patient survives a certain length of time without cancer recurrence of any form then he has been cured. The commonly used endpoint for this theory is the 5 year disease free survival rate.

Rate of survival is very dependent on several factors: Patient age, nutrition, psychologic state, histologic type of lung cancer, stage of lung cancer progression and the state of the patients immune system (83) as well as the tumour location. Peripheral lesions have a much higher associated survival rate than centrally located lesions.

Treatment success is generally measured in terms of years of disease free survival. The overall 5 year survival rate for lung cancers is approximately 10-15% (16).

Table 1.6 - Table 1.11 - Available survival rates in terms of Cancer Group and Stage of Progression.

Table 1.6 Cancer Type - SCC
Stage - 1

Author	Stage	% Survival at Indicated Year 15	10	5	4	3	2	1	Treatment	Comments
Shields (105)	$T^1N^oM^o$			59					resection	11 survivors (both peripheral and central lesions in 5 year survival)
	$T^2N^oM^o$			28					80 resection and chemoth. 68 resection	peripheral survivors in 5 years
Meyer	1			83					resection and combination chemotherapy	only 6 patients
(32)	1					(<--33-->)			chemotherapy and radiotherapy	
	1				(<--10-->)				chemotherapy	
Rosenow and Carr (16)	1*						6		unspecified	

Table 1.7 Cancer Type - SCC
Stage - 2

Authors	Stage	% Survival at Indicated Year 15	10	5	4	3	2	1	Treatment	Comments
Meyer (106)	$T^2N^1M^0$			50					resection and combination chemotherapy	4 patients
Shields (105)	$T^1N^1M^0$			31					resection	
	$T^2N^1M^0$			9					resection	
Rosenow and Carr (16)	2*						5		unspecified	
Maurer et al (107)	limited*						24		unspecified	
Inde et al (108)	limited*			8	8	8	13	52	combination chemotherapy	32 patients

Table 1.8 Cancer Type - SCC
Stage - 3

Author	Stage	% Survival at Indicated Year 15	10	5	4	3	2	1	Treatment	Comments
Meyer (58)	T^3N^0, T^3N^1			25					resection and chemotherapy plus cranial radiation	4 patients
	N^2			0					radiation	4 patients
Shields (105)				3.6					resection	
Rosenow and Carr (16)	3*						3.8		unspecified	
Inde (108)	extensive*				3	5	12	42	combination chemotherapy	73 patients

Table 1.9 Cancer Type - NSCC
Stage 1

Authors	Stage	% Survival at Indicated Year 15	10	5	4	3	2	1	Treatment	Comments
Martini et al (109)	1					85	87	93	resection	
	$T^1N^oM^o$					89	91	94	resection	
	$T^2N^oM^o$					80	83	91	resection	
Jensik (110)	$T^1N^oM^o, T^2$	25	33	53					resection	
Cooper (111)	1			6					radiotherapy	operable lung cancer but refused (72% squamous cell)
Faber (79)	1		28	38					sleeve resection	
Paireselo (112)	1*			69			84		resection	
	1*			56					resection	all types
	1*			70					resection	squamous
	1*			65					resection	adenocarcinoma
	1*			66					resection	large cell
	T^1N^o			80					resection	all types (<20 patients)
	T^2N^o			63					resection	all types (<20 patients)
	T^1N^o			70					wedge resection	
	T^1N^o			68					lobectomy	
Little (67)	1*			55					resection	
Rosenow and Carr (16)	1*					47			unspecified	squamous
	1*					46				adenocarcinoma
	1*					43				large cell
Mountain et al (113)	1*		31	38		53			unspecified	
Paulson (114)	N°*				43		73		resection and pre-op. irradiation	
Shields (115)	T^1N^o		54	68					resection	
	T^2N^o		40	54					resection	

Table 1.10 Cancer Type - NSCC
Stage - 2

Author	Stage	% Survival at Indicated Year 15	10	5	4	3	2	1	Treatment	Comments
Holmes (78)	T^1N^1			75					resection	squamous
	T^1N^1			52					resection	adenocarcinoma
	T^2N^1			53					resection	squamous
	T^2N^1			25					resection	adenocarcinoma
Little (67)	2*			30					resection	
Pairelero (116)	N^1,N^2					7.4			resection	
Faber (79)	2			20					sleeve resection	
Martini (117)	N^2			30					resection	
Selawry (42)	2			30					resection	all types
Jensik (71)	1,2*		11	31	52				mini resection	
Rosenow and Carr (16)	2*						40		unspecified	squamous
	2*						14			adenocarcinoma
	2*						13			large cell
Mountain (113)	2*			9	12		31		unspecified	
Williams (112)	T^1N^1			53					resection	all types
	T^2N°			50					wedge resection	
	T^2N°			49					lobectomy	
Paulson (114)	N^1,N^2							15	resection with pre-op irradiation	
Shields (115)	T^1N^1					37			resection	
	T^2N^1					40			resection	

Table 1.11 Cancer Type - NSCC
Stage - 3

Author	Stage	% Survival at Indicated Year 15	10	5	4	3	2	1	Treatment	Comments
Jensik (71)	3			9					miniresection	
Little (67)	3*			15					resection	
Pairolero (116)	$T^3N^oM^o$			54					resection	all patients
	$T^3N^oM^o$			59					resection	NSCC patient
	$T^3N^oM^o$			85					resection	under 60 yrs
	$T^3N^oM^o$			28					resection	over 60 year
	$T^3N^oM^o$			54					resection and radiotherapy	
Burt (70)	T^3			7		13	22		resection	
	T^3M^o			2		21	29		resection	
	T^3M^o			22		22	30		resection and radiation	
	T^3M^o					0	9		incomplete resection	
	T^3M^o						10		unoperated	
Faber (79)	3			15						all types
Selawry (42)	3			15						all types
Rosenow and Carr (16)	3*						12		unspecified	squamous
	3*						8			adenocarcinoma
	3*						13			large

Early cancers have a much better prognosis than well progressed cancers. Tables 1.6 to 1.11 summarise the available survival rates in terms of cancer group and stage of cancer progression at the time of treatment commencement. Unfortunately discrepancies arise because of the recent alterations in the TNM staging criteria. Some references state merely the stage, not the TNM classification, and it is hence not possible to 'restage' such results to the new system. Where this has occurred the results remain within the authors stated stage but have been indicated with an asterisk. For all NSCC's surgery has been the chosen treatment, resulting in 5 year survival rates ranging from 38% to 70%. In one trial patients who refused surgical resection as a treatment were given radiotherapy: A 6% 5 year survival resulted.

Patients with surgically resectable NSCC have the best chance of complete recovery although in a limited number of cases patients are curable with aggressive chemotherapy (84).

Stage 2 NSCC's again undergo resection as the preferred treatment, 5 year survivals ranging from <5% to 75%. Squamous carcinoma have a much better prognosis than adenocarcinoma. In a few cases adjuvant treatment, in the form of post-operative radiotherapy, was administered and appeared to greatly improve results from 5% to 31% survival at 3 years.

Stage 3 NSCC's have a wide band of survival rates, 0 to 58%, depending upon the treatment administered. 5 year survival rates for resection alone range from 2 to 58%. Post operative radiotherapy appears to increase the 2% survival to 22% (70). Patients over 60 years of age undergoing resection have a 5 year survival of only 28% while those under age 60 have 85% survival.

Thus surgical resection is the best treatment for NSCC, either alone or with radiotherapy, but in unresectable NSCC radiotherapy

can, in some cases, provide disease free survival for 3 or more years (85).

SCC's are usually found in an advanced state and have hence been treated only with palliative therapies to improve the length and quality of remaining life . However, in a few cases, SCC's have been found in stage 1 and various treatments have been tried. It should be noted that the number of patients per trial is small, often fewer than ten. Early resection in SCC, especially peripheral lesions, can have promising results when compared with the traditional treatments.However adjuvant therapy may prove necessary to ensure that small, undetected metastases, if present, are destroyed.

Stage 2 and stage 3 SCC's, commonly treated with combination chemotherapy (i.e using several anti-cancer agents) have very low survival rates: 3 years for stage 2 and 5% at 3 years for stage 3 patients. It is generally accepted that radiotherapy is not an effective treatment for SCC. Attempts at resection appear encouraging with 5 year survival rates between 9 and 50% for stage 2. However there are very few patients in each set and these are, presumably, preselected.

Generally SCC is not at present ably treated, due mainly to its advanced stage at diagnosis. NSCC, if found early can have promising 'curative' results.

It is therefore apparent that to improve longterm survival and cure rate of cancer patients requires that new and more effective treatments are found as well as improving the methods of detection to allow cancers to be diagnosed at an early stage while they are potentially curable. The present screening techniques detect lung cancer only after the lesion has reached 1 cm in diameter. Lesions less than 2cm, however, are not

accurately diagnosed since they are difficult to locate within the chest. It is proposed to devise a computerised biopsy machine to attach to a rotatable fluoroscope with which more accurate biopsies may be carried out, thus improving the diagnostic accuracy of the biopsy technique, especially for small and deeply located lesions within the chest.

To do this it is essential to understand the mechanics of respiration and to appreciate difficulties involved in the biopsy procedure currently practised so that such problems may be eliminated, minimised or at least allowed for in the proposed biopsy machine.

CHAPTER 2

ANATOMY OF THE CHEST

2.1. Introduction

The chest wall is constructed from twelve pairs of ribs attached to the sternum at the front and the vertebral column at the back. The lowest point along any rib is at the side of the body with the anterior end being lower than the posterior, as shown in Figure 2.1

A network of muscles exists, illustrated in Figure 2.2 These:

a) are attached between adjacent ribs (intercostals)

b) span several ribs between attachments (subcostals)

c) connect the ribs to the sternum or vertebrae (transverse thoracis and levatores costorum)

A further thin dome-shaped muscle, the diaphragm, separates the thorax from the abdomen. It is attached around its outer edge to the vertebrae, the ribs and the sternum. When relaxed, pressure from the abdomen pushes it upwards into its dome shape.

Gray's Anatomy (86) details the relative positions of the lungs, heart, diaphragm, etc within the thorax.

Keith (87) states that the lung is composed of air sacs which are the distensible element of the lungs. The quantity and size of sacs in any part of the lung control the degree of extensibility. These sacs are not evenly spread with the result that there are varying degrees of extensibility throughout the lungs and hence they do not expand equally but move in certain definite directions during inspiration.

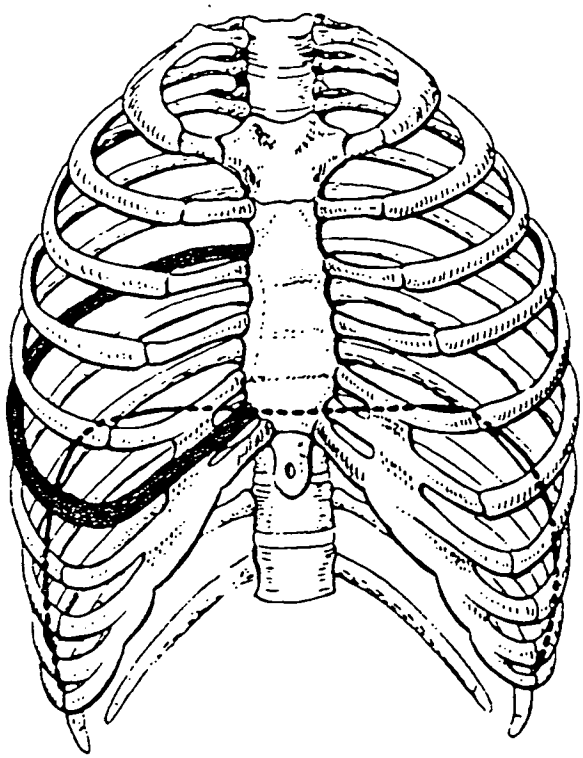

The dotted line represents the dome of the Diaphragm at the resting position.

Figure 2.1 - The Skeleton of the Rib Cage.

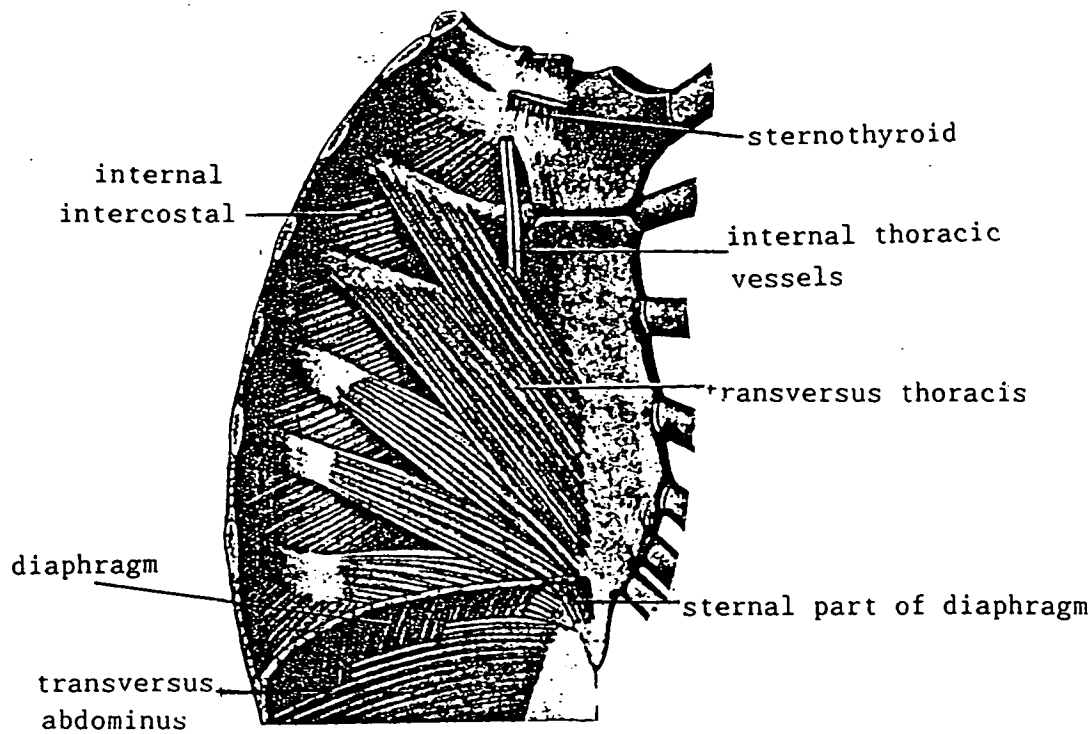

Figure 2.2 - The Network of Muscles which Surround the Ribs.

A membrane, the visceral pleura, covers the lung surface and another, the parietal pleura, covers the inner surface of the chest wall and the diaphragm and rises to cover the structures which lie in the middle of the thorax, as shown in Figure 2.3. The lung surface lies against the chest wall and a thin mucus film between the two pleura allow them to slide gently over each other. The lungs, however, do not completely fill the pleural cavity. A small section between the lungs and the diaphragm, called the costo-diaphragmatic recess, is empty.

2.2. Mechanics of Respiration.

There is a small negative pressure between the pleura, about -2.5mm at the resting position, which keeps the lungs expanded against the chest wall. During inspiration, caused by the combined action of the above muscles, the chest and diaphragm move away from the lungs, causing a larger negative pressure which pulls on the lungs and draws in air to fill them.

During gentle or quiet respiration fewer muscles act and according to respiration is possible without diaphragmatic movement or without the intercostals, but not without both.

The major contribution to quiet respiration comes from the diaphragm. On contraction it descends, pulling the bottom of the pleural cavity downwards, as shown in Figure 2.4 increasing the longitudinal dimensions of the thorax and resulting in inspiration while at the same time compressing the abdominal contents. The abdominal muscles relax, allowing the abdominal organs to descend and move forwards. This process accounts for most of the 500ml of air inspired. There is no movement of the upper two pairs of ribs. Rib pairs 3-7 follow two different types of movement at the same time. Firstly the 'bucket-handle' movement as illustrated in Figure 2.5, in which the rib pivots

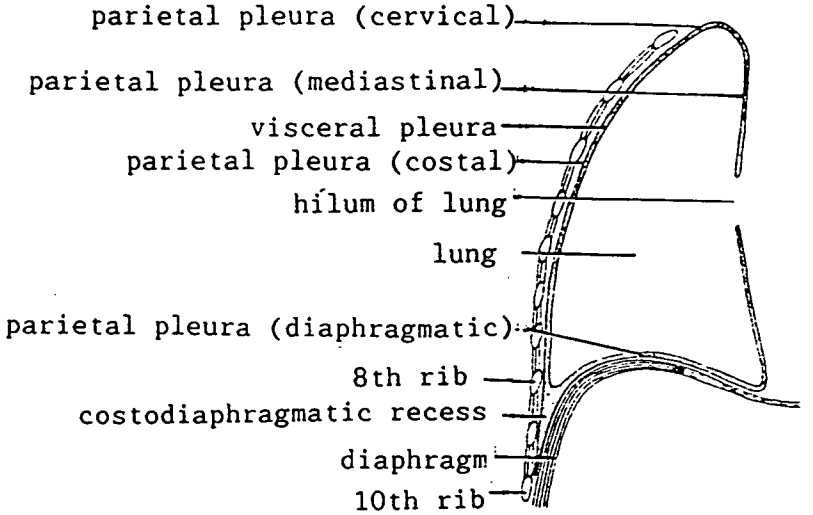

Figure 2.3 - A Section Through the Right Side of the Chest.

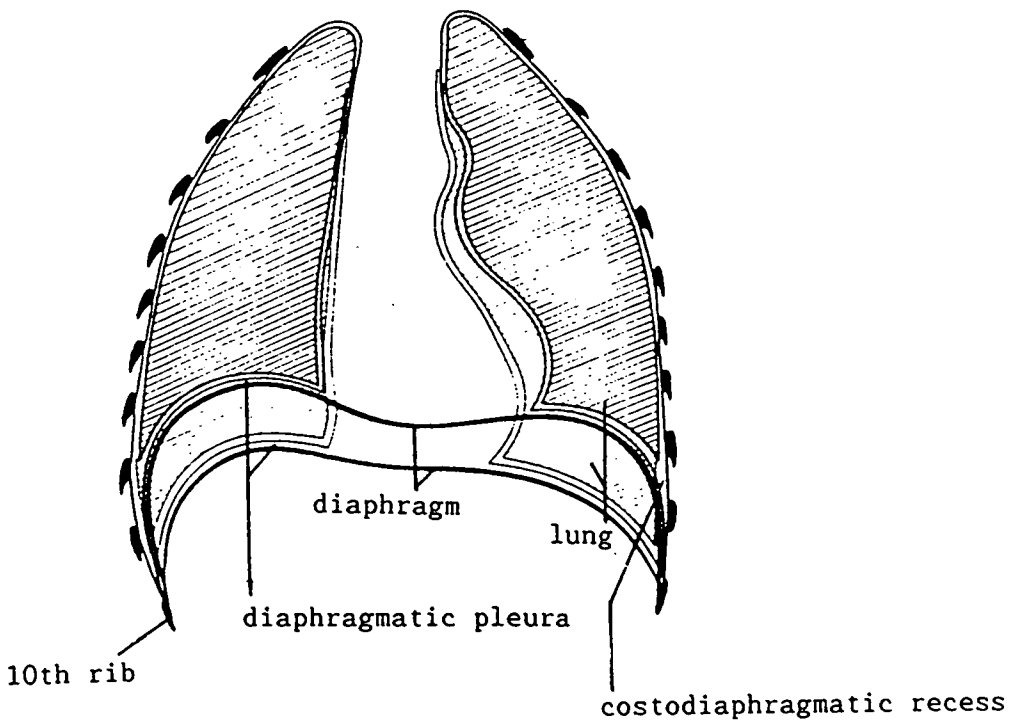

Figure 2.4 - An outline drawing illustrating the change in shape of the thoracic contents resulting from contraction of the diaphragm alone.

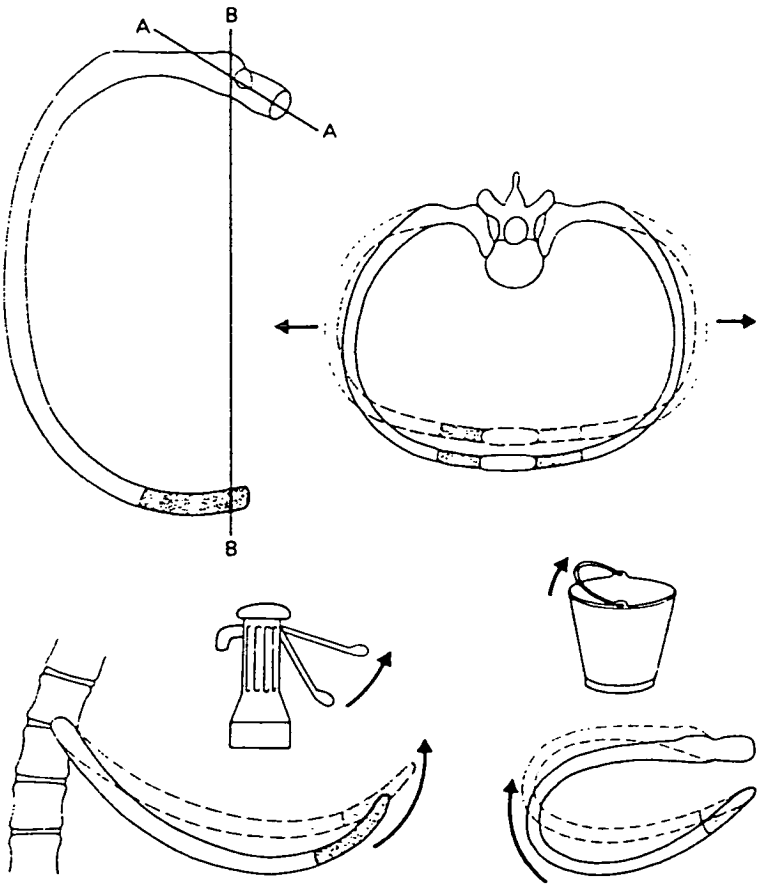

Figure 2.5 Movements of the ribs. The upper ribs move about two axes. Movement about axis A will elevate the anterior end of the rib, producing the 'pump handle' type of movement. Movement about axis B will elevate the middle of the rib, producing a 'bucket handle' type of movement. The lower ribs open out like calipers, as shown in the diagram at the top right.

around its anterior and posterior ends, moving upwards and outwards, increasing the lateral dimensions of the rib cage. Secondly the 'pump-handle' movement, which involves raising the anterior end of the rib and hence the sternum. This increases the anteroposterior (AP) dimension of the rib cage. The lower ribs, 7-10, undergo a caliper-like movement, increasing the lateral dimension but decreasing the AP dimension. These slight rib movements account for only a very small fraction of the air inspired during gentle respiration.

On slow relaxation of the intercostal muscles and the diaphragm gentle expiration occurs as the lungs undergo gradual elastic recoil and return to their resting position.

In deep inspiration the movements described above are greatly enhanced as the external intercostal muscles contract with greater force. The neck muscles also come into play raising the first and second rib pairs. Thus a much larger proportion of the lungs are used for respiration. In this enhanced breathing the rib cage movement is great, each 1cm increase in circumference of the chest increasing the chest capacity by around 200ml up to a maximum tidal volume of around 3 litres.

Forced expiration is caused by contraction of the abdominal muscles forcing the abdominal contents upwards against the diaphragm which returns to its dome shape, while at the same time pulling downward on the rib cage thus decreasing the volume of the chest cavity. To a lesser extent the internal intercostals also act by pulling the ribs downwards.

2.3. Lung Movement

It is desirable to know to what extent the lungs move during respiration. These movements are difficult to characterise because different breathing mechanisms act over different areas

of the lung. They are also modified by effects of posture.

2.3.1. Effects of Posture

Several Texts describe the effects of posture on respiration. In the standing position gravity acts on the diaphragm and abdomen in the inspiratory direction and on the rib cage in the expiratory direction. In the sitting position the abdominal wall pulls the ribs downwards and inwards due to the abdominal weight. The resulting change in shape of the chest wall causes a corresponding change in shape of the lung although Campbell (88) suggests that the elastic recoil of the lung away from the chest wall and diaphragm does not change appreciably. In the supine position gravity acts on both the rib cage and the abdomen in the expiratory direction and the resting volume is reduced. Campbell describes the probable distribution of pressure on the pleural surfaces at the resting volume and in the upright and lateral positions. In the upright position the lung recoils inwards, away from the diaphragm, as shown in Figure 2.6, with a pressure nearly equal to the pull of the abdominal weight whereas in the lateral position the diaphragm is distended by the lung and the abdomen which exert a cranial force on the lower section. Lung recoil in this lowermost region is probably nil whereas the upper region of the diaphragm is pulled cranially by the lung and caudally by the abdomen.

In the upright position the rib cage exerts a force equal and opposite to the lung recoil, but in the lateral position the weight of the chest fixes the lower part of the chest wall and only the upper chest wall moves.

2.3.2. Post Mortem Experimentation

Unfortunately experiments carried out on lungs either removed from the body or within a dead body are not characteristic of

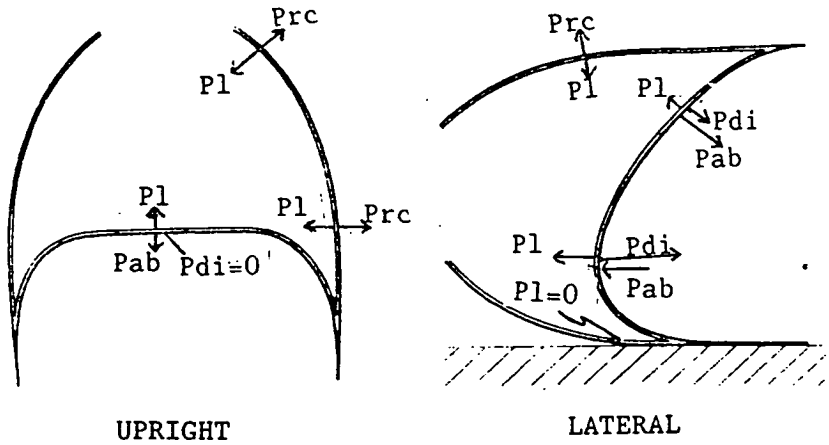

Figure 2.6 Diagram illustrating the probable distribution of pressures in the respiratory system at the end of a spontaneous expiration in the upright and lateral postures. The effect of gravity on the chest wall and lung is accounted for.

Pl = pressure exerted by the lung
Pab = pressure exerted by the abdomen
Pdi = pressure exerted by the diaphragm
Prc = pressure exerted by the rib cage

lung expansion during normal respiration. Rigor mortis and post mortem muscle changes invalidate any observations and inflation of the lung causes expansion in the direction of least resistance which is not the case during normal respiration where the action of the thoracic walls and/or the diaphragm determine the area and degree of lung expansion.

2.3.3. Positioning Within the Lung

Keith divided the lung into three different anatomical zones:

1) The root zone close to the main tract containing the bronchus, artery, vein, lymph glands and fibrous tissue. This zone is essentially less distensible than others.

2) The intermediate zone containing bronchial branches, veins and pulmonary tissue. Varying degrees of extensibility occur, the veins being the least distensible and the pulmonary tissue the most.

3) The outer or peripheral zone, up to 30mm deep with a more even and greater degree of extension.

Generally the air sacs are smaller in the root zone and larger in the outer zone and also smaller in the apical part and larger in the base of the lung. Correspondingly during inspiration the peripheral section of the lung extends more than the root and the base more than the apex.

In healthy bodies, therefore, by considering different areas of the lung it is possible to predict the directions and extents of these respiratory movements.

In the apex of the lung, during shallow breathing, very little or no movement might be expected as the upper ribs are stationary

and hence direct lung expansion is unlikely. However, Keith (87) describes anterior apical descent and attributes the effect to large diaphragm contractions. During deep respiration the dorsal part of the apex remains stationary and the anterior part again descends. This is an unexpected result since it was assumed that the anterior part would follow the general upward movement of the first and second rib pairs. However the diaphragm contraction must obviously generate a greater force.

In the lowest section of the lung, where most 'breathing' is conducted, relatively large movement due to lung expansion would be expected at all times, even during shallow breathing. During inspiration the lung expands and moves downwards following the diaphragm. As rib action is still present during shallow breathing a small amount of forward movement is expected, both movements being greatly enhanced during deep respiration. However Keith states that sometimes (infrequently) during deep respiration, the diaphragm descends and then rises to a higher position than when at rest as the abdominal viscera, instead of air, are drawn into the thoracic cavity. In this case the resulting longitudinal movement would be upwards.

In the mid-section, however, movement is uncertain. The rib cage, during inspiration, would tend to pull the lung upwards and outwards. The diaphragm, however, pulls down on the lung stretching it longitudinally. Although it has been stated above that the root of the lung displays little extensibility, Keith (87) mentions movement of the mediastinal surface, i.e. adjacent to the heart, trachea, etc. This occurs because the heart follows the movement of the sternum as well as the diaphragm, on which it rests. Since the heart is firmly attached to the root of the lung, the lung will undergo a translation following the direction of the heart movement. During shallow inspiration the diaphragm will probably exert the greater force, resulting in an overall

downwards movement of the mid-section, but in deep respiration the combined effect of the three movements is unknown, although almost certainly both the outward anterior and lateral movements will still take place. Keith summarised qualitative lung movement in a diagram, shown in Figure 2.7.

To obtain quantitative or qualitative information from experiment will require a large number of patients with readily identifiable lesions in different lung positions. Since it is unlikely that each individual will conform to the same size or shape and may in fact exhibit different rib cage movement, depending upon the shape of the skeleton or on habit, individual quantitative results may prove misleading or not generally representative. however upper limits on possible movement in different lung regions will prove useful information when considering the likelihood of a 'direct hit' with the biopsy needle.

2.3.4. Experimentation and Estimation Methods to detect the Extent of Lung Movement

In the case of the lowest lung section adjacent to the diaphragm, it may be possible to estimate probable lung (lesion) movement by examination of movements of the diaphragm, the abdominal wall or its contents during respiration. This has the advantage that any patient can provide the necessary information as a suitable identifiable lesion is not required. For many detailed abdominal examinations described in the literature ultrasound has been used in place of X-rays as the patient is not submitted to potentially harmful radiation and more detailed images may be obtained. Little is available in the literature as regards the relationship between diaphragm and lower lung movements.

As stated previously not all the lung and diaphragm are in contact: The costo-diaphragmatic cavity exists. Gray's Anatomy (86) states that in quiet respiration the lower limit of the lung

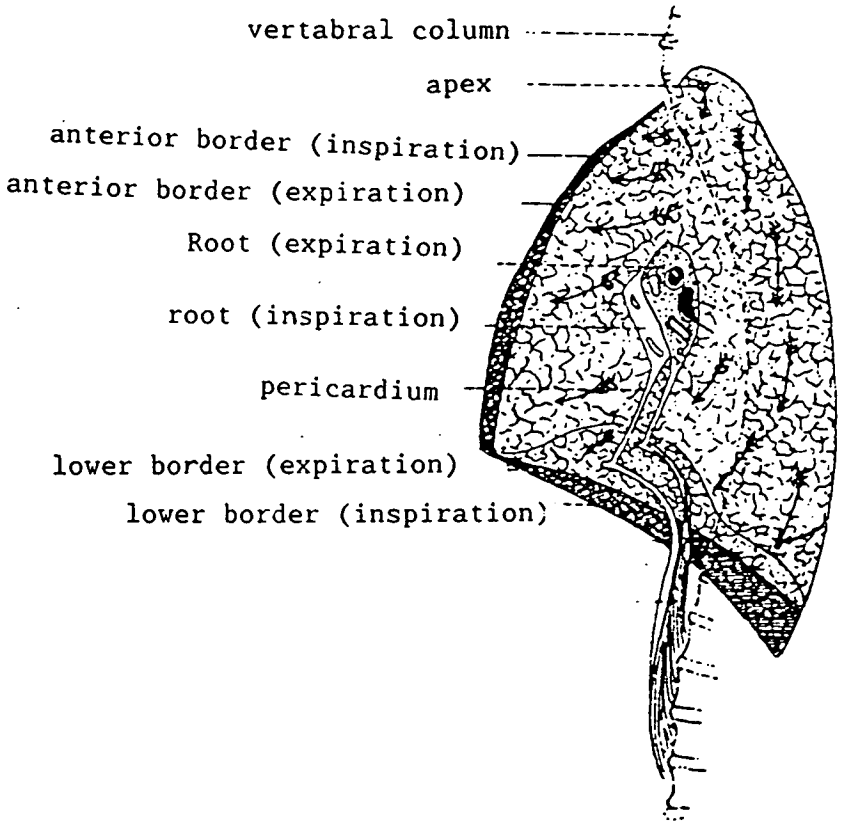

Figure 2.7 - Mediastinal aspect of the right lung to show the respiratory movement of the root. The arrows indicate the direction of the inspiratory movement of the various parts of the lung.

lies about 5cm above the lower limit of the pleura. Keith (87) estimated that 250 cm^2 of the diaphragm is in contact with the lungs. According to Hoover (90) excursion of the lower border of the lungs cannot be used to estimate diaphragm movement and cites a 6cm lung descent caused by a 1cm drop in diaphragm position. He does, however, refer to the Litten Diaphragm phenomenon (in which under certain lighting conditions a shadow can be seen passing down the chest between the lower ribs, caused by the diaphragm movement) as being appropriate in estimating movement of the lower border of the lungs. Assuming that diaphragm excursion will reveal some information on lower lung movement a general examination of the literature was carried out.

For diaphragm movement to be useful it is essential that it is not consciously controllable by the patient. Wade (94) investigated the extent of conscious control and concluded that, contrary to popular belief, the diaphragm is not under any direct control, the extent of its movement being determined solely by the depth of breath taken. During his studies he noted that the skeleton extends during deep respiration and he measured the extent of this vertical movement at the front of the thoracic cage using a Bowden cable attached to a small perspex plate strapped firmly to the patient's chest over the sternoxiphisternal joint. He concluded that the extent of vertical movement of the thoracic cage varies with different individuals, the effect being more enhanced in erect than supine subjects. With this finding, Wade realised that previous diaphragmatic measurements could be unreliable, since they were affected by vertical movements of the thoracic cage with deep respiration. He therefore measured and adjusted diaphragmatic movement accordingly, after allowing for geometric distortion to the image. His adjusted results revealed around 1.6cm average diaphragm movement when the patient is sitting or standing and 1.7cm when supine during quiet respiration. During deep respiration, however, this increased

dramatically with movement varying between 7cm and 13cm, averaging out at 10.3 cm when upright and 9.9cm supine. Table 2.1 illustrates results of other workers from which it is apparent that there is little difference in the extent of diaphragm movement during quiet respiration in different postures. Campbell (88) states that during quiet respiration the diaphragm contribution to tidal volume is estimated to be around 2/3 in sitting and standing positions and around 3/4 in the supine position. This agrees in general with the results in Table 2.1, with supine movement being greater if only fractionally.

As mentioned previously the anterior abdominal wall will often protrude during inspiration and indent during expiration, due respectively to the descent and ascent of the diaphragm with respiration. However the abdominal muscles may be consciously contracted by the patient and the degree of protrusion hence lessened. This often occurs when patients know that they are being examined and so breathe in an abnormal manner.

The abdominal wall is also affected by rib movement which serves to counteract the effects of diaphragm movement by pulling longitudinally on the abdominal wall as the vertebral column is lengthened. Observation of the abdominal wall is hence unsatisfactory for determining the degree of diaphragm movement and hence movements of the lower lung.

The abdominal contents will be affected by any movements of either the diaphragm or the abdominal wall. It may be possible to determine diaphragm movement in any patient by examination of the movements of certain of these abdominal contents with respiration.

The abdomen contains many organs The stomach, liver, intestines, etc for digestion and for excretion the kidneys, bladder, etc. The liver, kidneys and fundus of the stomach are in direct

Table 2.1 - Summary of reported diaphragm movements with different postures and extents of respiration.

AUTHOR	QUIET RESPIRATION		DEEP RESPIRATION	
	erect	supine	erect	supine
Wade (94)	1.6cm	1.7cm	10.3cm (range 7-13cm)	9.9cm
Fick (95)	1.5cm		3cm	
Hulkrantz (96)	---		10cm	
Weiss et al (91)	0.8±0.4cm	1.3±0.5cm	(range 1.2-7.5cm)	
Gray's Anatomy(86)	1.5cm		(range 6-10cm)	

contact with the diaphragm as shown in Figure 2.8, and are therefore more likely to reflect its excursions. Hoover (90) states that the descent of the liver during inspiration is an exaggeration of diaphragm movement because the liver rotates on a transverse axis during inspiration. However Weiss et al (91) assumed that hepatic excursion was a vertical translation without plastic deformation and compared diaphragm excursion with hepatic excursion in both erect and supine positions. They found results to be similar during quiet respiration, as shown in Table 2.2. Suramo et al (92) investigated cranio-caudal movements of the liver, pancreas and kidneys with the patient supine. Their results, along with others, are shown in Table 2.3. The liver appears to be the most mobile reaching a maximum excursion of around 8cm during maximum respiration but averaging out to around 5.5cm during maximum, 2.5cm during quiet and 0.9cm on suspended respiration. There is a discrepancy between the two results for liver movement during quiet respiration. Weiss' results were obtained using a gamma camera and adjustments made for motion correction. Suramo, however, used ultrasound.

It therefore seems obvious that diaphragm and hence cranio-caudal lower lung excursion is considerable, even in quiet respiration. As previously stated, the lower lung is the most extensible and hence its excursion should be the maximum expected of any part of the lung.

2.4. Reproducibility of Breath Holding

It is desirable to minimise this lung movement and hence stabilise the position of any lung lesion prior to X-raying and sampling.

The normal procedure in X-raying is to 'take' while the patient holds his breath at the end of deep inspiration, the point in the breathing cycle at which breath holding is generally most

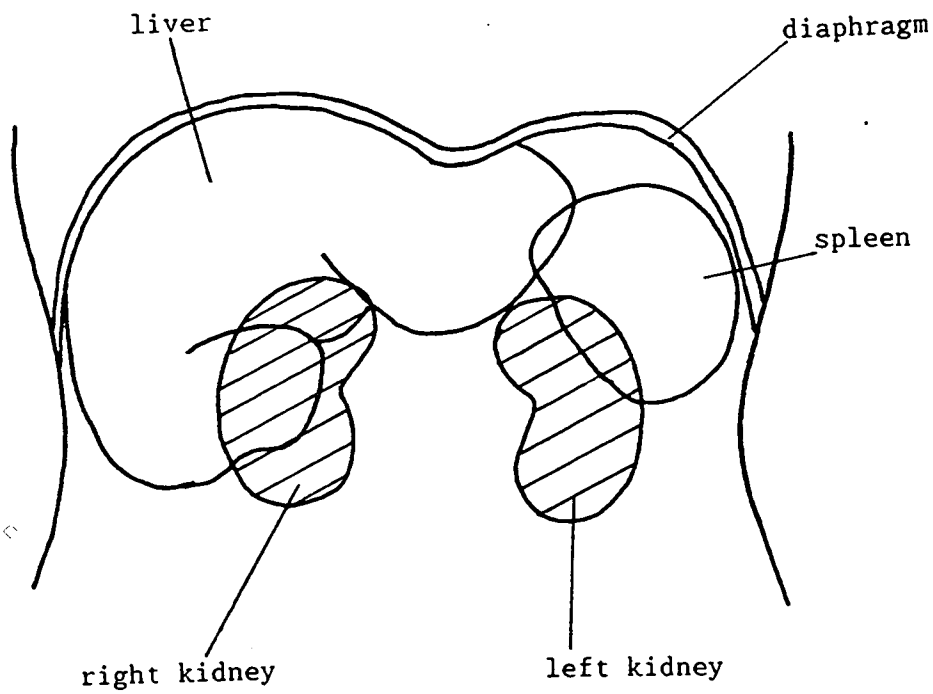

Figure 2.8 - The anatomy of the abdomen illustrating how several of the abdominal organs lie in contact with the diaphragm.

Table 2.2 - Hepatic and right hemidiaphragm excursion during quiet respiration (91).

	Computer determined hepatic excursion (cm)	Radiographically determined hemidiaphragm excursion (cm)
Erect	0.8 0.2* (n=18)	0.8 0.4 (n=26)
Supine	1.1 0.3 (n=12)	1.3 0.5 (n=25)

* = standard deviation

Table 2.3 - Movement of organs in respiration examined by ultrasound. Mean and Range (92).

Organ	Excursion	
	Maximum respiration (cm)	Normal respiration (cm)
Liver	5.5 (3-8)	2.5 (1-4)
Pancreas	4.3 (2-8)	2.0 (1-3)
Right Kidney	4.0 (2-7)	1.9 (1-4)
Left Kidney	4.1 (2-7)	1.9 (1-4)

reproducible. One thus obtains X-ray images detailing the expanded lung.

In a lung biopsy procedure two X-ray views are taken, one PA the other lateral, with a marker positioned on the patient's chest. Direct distance measurements of the lesion from the marker are taken from the radiographs and the lesion position found. the needle biopsy is then carried out while the patient breathes quietly. A fluoroscope ensures that the needle insertion point is directly above the lesion, the needle inserted to the required depth (taken from the lateral radiograph) and a further X-ray image is used to check the needle position prior to sampling. If the initial lesion positioning is erroneous then the needle will require repositioning. This is an unsatisfactory situation, especially if the lesion lies in the mediastinal region, since the risk of complications is increased.

If these X-rays are taken at full inspiration they will give a false impression of lesion position and depth. It is appropriate to X-ray at the mid-breathing-cycle. Reproducibility of breath holding mid-range is unreliable but even so, lesion position determination at this point must be more accurate than at full inspiration. However should breath holding reproducibility prove to be a problem several means exist by which it may be improved.

The most obvious is probably spirometry, in which the patient breathes into a mouthpiece and the volume of air inhaled and exhaled is measured. The patient is asked to hold his breath when an indicator reaches a preset, marked position.

Alternatively a suspended horizontal bar may be used as an indicator (92). The supine patient breathes in until the bar, suspended above the chest, just touches the skin. Reported results (Table 2.3) showed considerable improvement, as shown in

Table 2.4, with the 0.9cm liver excursion during suspended respiration decreasing to 0.2cm excursion, when using the bar.

Jones (93) describes a respiration monitor for use with body scanning as shown in Figure 2.9. It measures body circumference and displays the results by means of a pressure module linked to an LED bar. The patient inhales and holds his breath when the LED bar lights to a preset level This method, designed for use with CT scanning, does improve reproducibility of breath holding, as shown in Figure 2.10.

2.5. Conclusions

The process by which lung cancer becomes established and evades and confuses the immune system is not understood. Many substances have been proven carcinogenic (of which tobacco smoke is the main one) and much resources have been expended on public health education in an effort to reduce the lung cancer incidence rate. However the desired decrease has not yet materialised. There are probably three main reasons for this:

Lung cancer risk does not dramatically decrease immediately smoking is ceased but takes 10 years to approach the non-smoker level.

By the time that lung cancer is detected it will have been manifested for several years.

The general public reacts slowly to such health warnings. The general attitude may be that smoking did not adversely affect their parents' health and so will not affect their own health. It is therefore important that general practitioners continually emphasise the health risks associated with smoking.

Table 2.4 - Difference in the position of the organs (Mean and Range)

Organ	Difference	
	Suspended Respiration (cm)	Suspended Respiration + bar (cm)
Liver	0.9 (0-2.5)	0.2 (0-0.5)
Pancreas	0.6 (0-2)	0.1 (0-1)
Right Kidney	0.4 (0-2)	0.1 (0-1)
Left Kidney	0.4 (0-1.5)	0.1 (0-1)

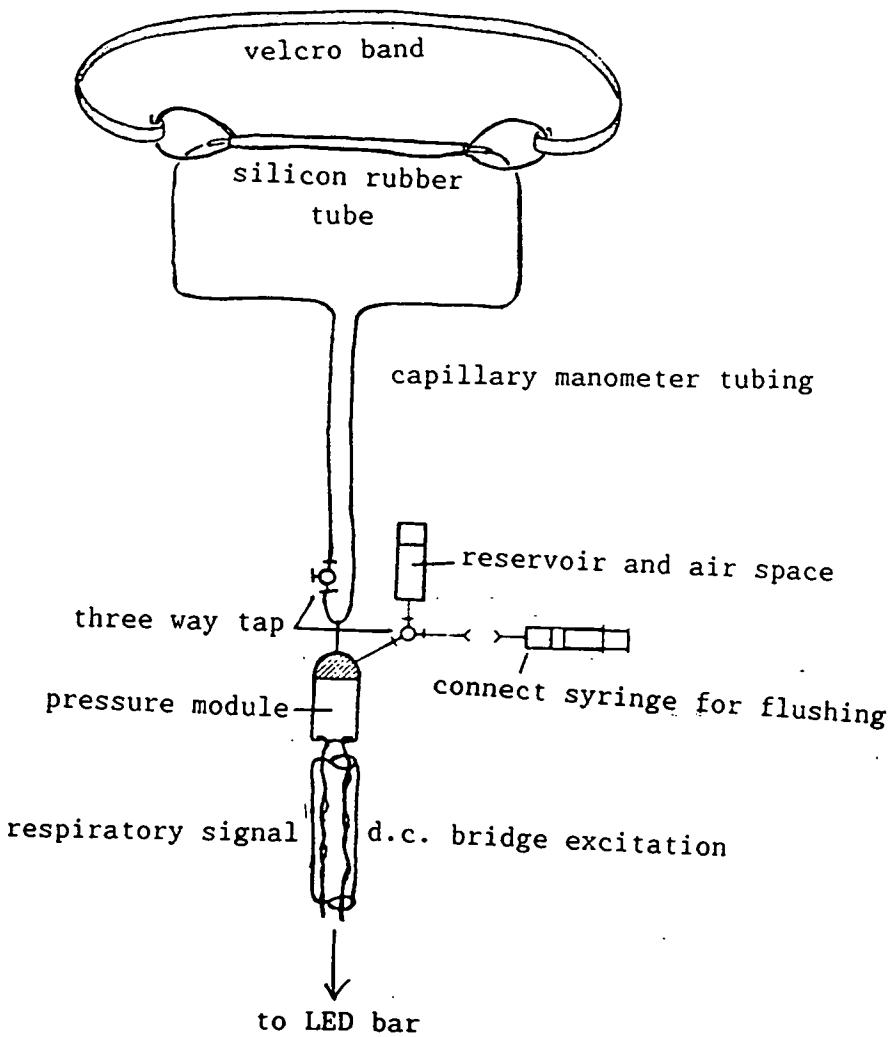

Figure 2.9 - A respiration monitor developed to limit organ movement between X-ray takes.

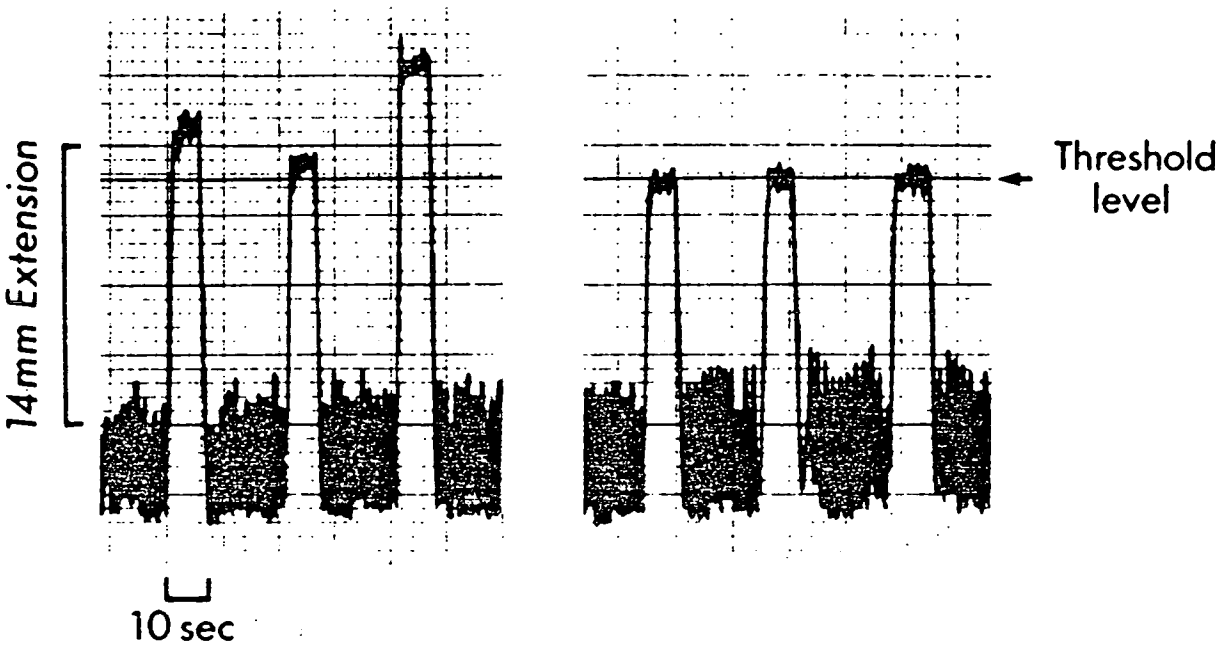

Figure 2.10 - Typical chart recorder traces for three cycles of held inspiration. The left hand diagram illustrates the results without using the respiration monitor and the right hand diagram illustrates the results when the respiration monitor is used.

Thus in the case of smoking, the reduction in the lung cancer incidence rate may not appear until many years after the initial non-smoking campaign began.

Screening can detect lung cancer at an early stage when lesions are around 1cm in diameter. However, present sampling techniques do not supply reliable diagnostic information until the lesions are greater than 2cm in diameter.

If the lung cancer is diagnosed at an early stage then available treatments can, in some circumstances, be curative. However, if diagnosed in a late stage then treatment can only prolong and improve the quality of remaining life.

New treatment modalities are constantly under investigation but as yet no 'wonder-drug' has emerged and it hence appears that, at the present time, the best means of improving longterm survival of such patients is to improve the available diagnostic techniques.

One of the main problems in diagnostic lesion sampling is respiratory movement during which the lesion can move by as much as 13cm during deep respiration and 1.7cm during shallow breathing. Techniques exist to aid reproducibility of breath holding to limit the extent of such movement while X-raying and needling.

Another problem is the accurate needling of suspect lesions in biopsy. The present research is directed towards this problem.

CHAPTER 3

DEVELOPMENT OF A PATIENT MARKER FOR THE BIOPSY MACHINE.

3.1. Introduction

The diagnostic accuracy of the needle biopsy technique for sampling small peripheral lung lesions is poor. Small, early, cancerous lesions, less than 2cm in diameter, are the most favourable for complete cure provided that they are correctly diagnosed and the cancer type is known.

The aim of this project is to develop a cheap and simple - and hence widely available - mechanical means of guiding a biopsy needle through the patient's chest wall to a point within the lung identified by the radiologist as a site of suspected cancer.

At present there are two stages in the biopsy procedure.

1. The detection of the lesion position within the lung. This is presently done using two perpendicular X-rays with an external marker positioned on the patients chest. The lesion position is estimated relative to the external marker.

2. Insertion of the needle through the chest wall and lung into the estimated lesion position.

Errors arise in both these stages. Lesion location is done with two perpendicular X-rays using the normal radiographic technique in which the full size X-ray appears on radiographic film. However, between these X-ray takes and the actual needling procedure the patient will probably have moved from the X-ray table and may also have changed posture, in which case the lesion position will have changed relative to the marker taped to the patient's chest. The actual needling itself is also error prone, especially since no quantitative guidance is used in angling the

needle to point towards the expected lesion position. It would be more satisfactory if the X-raying and needling were carried out without the patient moving between the two stages and also if the needle angling and depth of insertion were quantified and related by calculation to accurate measurements of the lesion position.

It was suggested to us by the late Professor D C Flenley that the relatively cheap, commercially available, C-arm X-ray machine might be used to answer many of these difficulties. The C-shaped arm, carrying the X-ray source and detector, may be rotated to lie at different angles relative to the patient and its X-ray pictures are displayed on a T.V. monitor. The different views needed to locate the lesion could hence be obtained without moving the patient.

It remained to devise some means of obtaining all the relevant dimensional information from each X-ray view to enable the lesion position to be calculated so that the sampling needle can be directed to it.

3.2. Methods of Angle Determination

In the existing lung biopsy process two perpendicular X-rays are taken - one PA (post-anterior), the other lateral. A radio-opaque marker, positioned on the skin acts as an external reference point to which cranio-caudal and lateral distances, as well as lesion depth, can be measured directly from the chest radiographs with a ruler.

This technique is in principle sound because:

1) In normal radiography the magnification on the detector is negligible since the source-detector distance is commonly around 6 metres and the patient is positioned close to the detector.Both recorded images are to the

same scale and are approximately actual size.

2) Since the X-ray views are essentially horizontal and vertical, the x and y coordinates of the lesion are recorded directly from them.

The rotatable C-arm X-ray machine consists of a point source of X-rays and an image intensifier, mounted on either end of a C-shaped arm, only 93cm apart, giving large magnification, dependent on the source-patient distance. The C-arm can be rotated through 120°, tilted and moved laterally, as shown in Figure 3.1 , (and locked at any position within this range) permitting a large angle range from which to choose appropriate angles of view. The patient is positioned lying on the trolley, between the source and the detector. The C-arm is rotated to a suitable angle of view and an X-ray taken. The procedure is repeated at a different angle and the images are displayed immediately on a T.V. monitor.

The geometry of the system is shown in Figure 3.2. To enable calculations of the lesion position to be made from image measurements, it is necessary to know the angles of orientation of both views and a conversion factor to relate the distances between points on the displayed T.V. image to the real corresponding distances, thus taking care of both view-dependent foreshortening and magnification effects. Angles of view may be obtained by several methods. The C-arm carries an angle scale, but it is not sufficiently finely graduated, nor is the structure carrying it sufficiently rigid, to furnish the required information with the necessary precision. Thus some alternative means of angle input or angle calculation is required. This might be obtained either directly from the C-arm itself using transducers or by comparison of the marker dimensions with the measured lengths of the marker images.

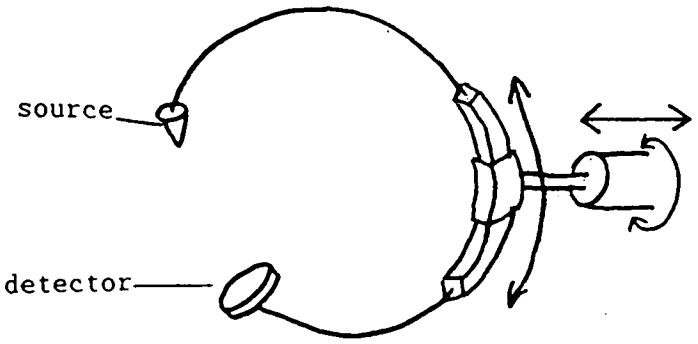

Figure 3.1 - Diagrammatic representation of the C-arm indicating the directions of rotation and lateral movement.

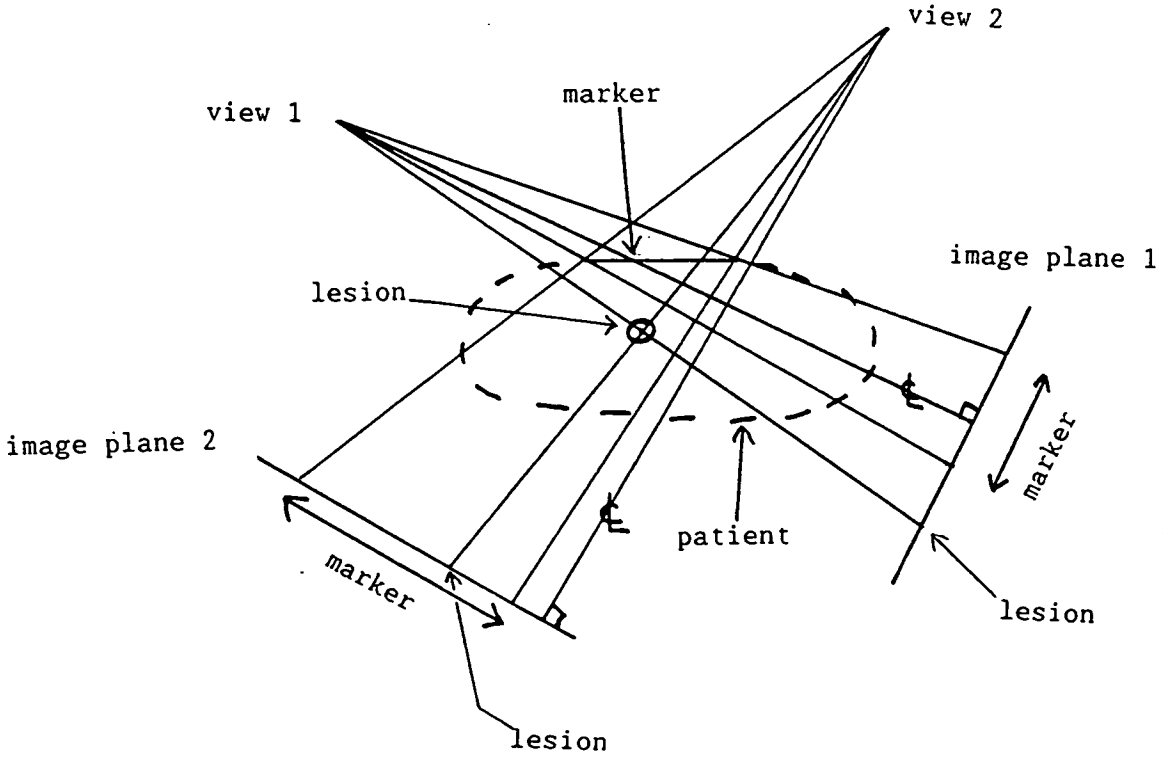

Figure 3.2 - Geometry of the Situation.

It is unsatisfactory to use transducers fixed to the C-arm mechanism for several reasons:

1. The C-arm angle scale reading is not necessarily the true viewing angle of the X-ray relative to the marker. That angle is also determined by marker orientation within the view.

2. It is undesirable to have trailing connections to transducers on the x-ray equipment.

3. The transducers would require regular calibration.

4. The C-arm equipment is not rigid so that angles would not be measured from a stable base.

5. The system would be specific to each particular X-ray machine

The angle required is that of the C-arm source above the plane of the marker and patient, rather than that of the C-arm orientation alone. This angle may be more easily and accurately determined from length measurements, taken from the image of a suitable marker system located on, or in a known relation to, the patient's chest. If the radio-opaque marker (to which the lesion position is referred) is correctly designed, comparisons of its known dimensions with the measured dimensions of its image may be used to evaluate both the angle of view and the magnification for each scene. Image measurements of apparent lesion distance from the marker for two or more scenes taken at different viewing angles can yield values of the true coordinates of the lesion relative to the marker.

3.3. The Patient Marker

The prime requirement of such a marker is that it should allow

evaluation of a magnification factor, to convert magnified T.V, image dimensions into the corresponding true dimensions projected onto the image plane. This is achieved using a sphere as a component of the marker, as its viewed diameter will not be affected by the angle of view. Thus the magnification factor F, is given by:

F=T.V. image diameter / sphere diameter

and takes account of the magnification due to the formation of the X-ray image by divergent rays from a point source.

It is also necessary to know the angle of orientation of the source to the marker for each view. This can be obtained from the image of the marker, if it incorporates X-ray opaque rods of known length. By comparing real and apparent rod lengths at known magnification, F, and using basic trigonometry, the centre-line viewing angle is derived, as illustrated in Figure 3.3, as:

$$\theta cl = \sin^{-1}((\text{image length} / F) / \text{rod length})$$

In the 3-dimensional case the image has to be located in two planes and at least two rods are required as components of the marker, preferably perpendicular to each other, lying in a horizontal plane on, or in a known relation to, the patient's chest.

3.3.1. Errors of Lesion Position Estimation

If image lengths are taken from the T.V. screen inaccuracies will arise from these measurements through imaging and measurement errors. It is estimated that these combined errors will be no larger than $\pm$1mm for each length. It is not immediately obvious how these individual errors will affect the uncertainty in the

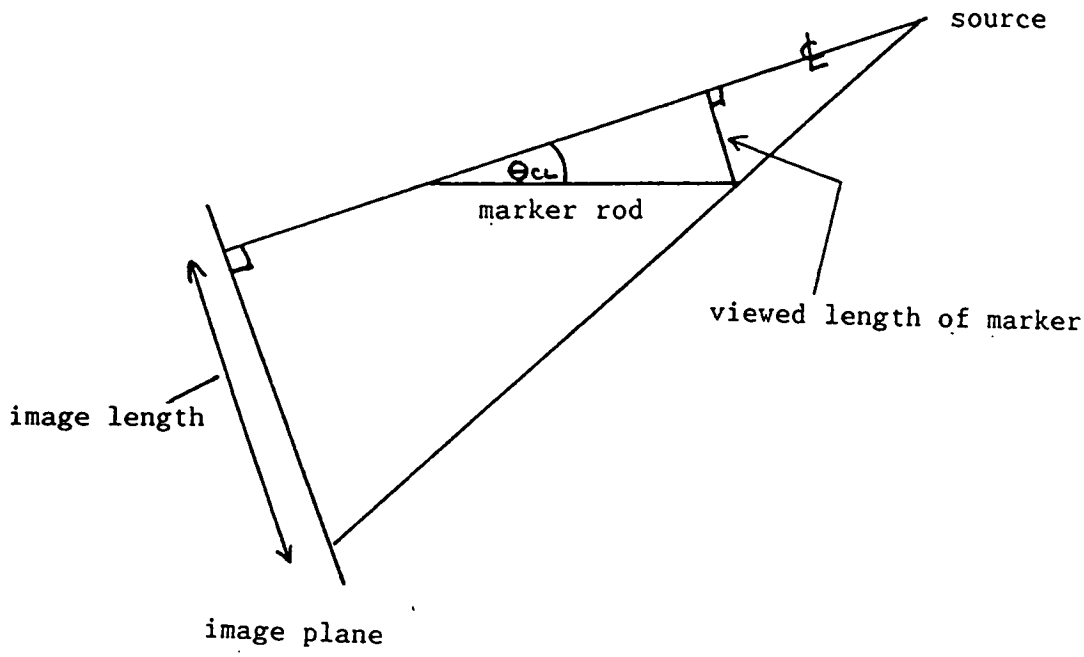

Figure 3.3 - Illustration showing how the centre-line viewing angle θ_{cl} is determined.

calculated lesion position and preliminary testing is necessary to assess whether, or in what circumstances, the method is of sufficient precision for practical use.

To determine the accuracy with which the lesion position (x,y,z) may be calculated in terms of marker dimensions, angles of C-arm orientation, errors in image measurement, distance of the source from the marker and different methods of angle determination is both complicated and difficult. It was therefore decided to reduce the problem initially to a 2-dimensional one and to carry out the investigation using a mechanical analogue.

3.4. Mechanical Analogue

A half scale, 2-dimensional lesion plotter apparatus was devised to investigate these error effects. For convenience this is based on the assumption that the centre of the marker 'sphere', point P, lies on the normal to the detector plane through the X-ray source, as shown in Figure 3.4.

3.4.1. Background Geometry

The basic geometry of the system, as proposed for use with the C-arm X-ray machine is shown in Figure 3.5. The X-rays from the point source cast shadows from both the rod and sphere marker and the patient on to the detector. The size of the images is dependent on the source-marker distance and the angle from which the system is viewed. It is necessary to work from the image lengths to the real system using available information. Initially only the marker dimensions, the image lengths and the source-detector distance are known. The extreme rays grazing the sphere in an actual observation correspond to lines drawn from the source to the extremities of a diameter of the image sphere as it appears in the image plane. If the marker is placed on such

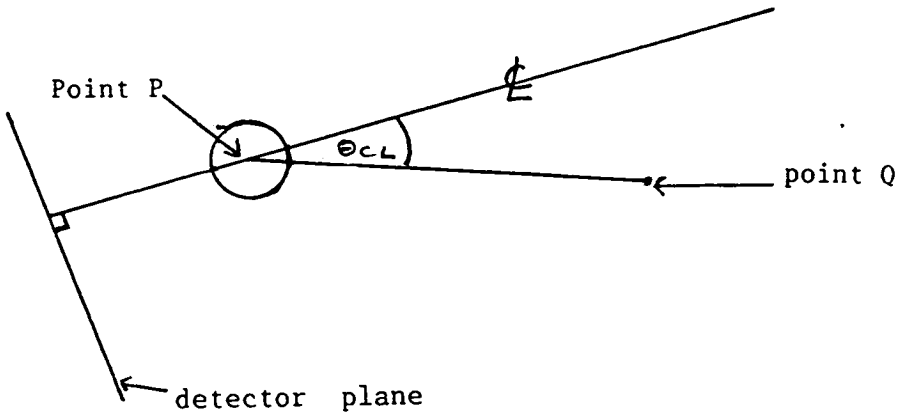

Figure 3.4 - The marker PQ and an illustration of the assumptions used in the mechanical analogue.

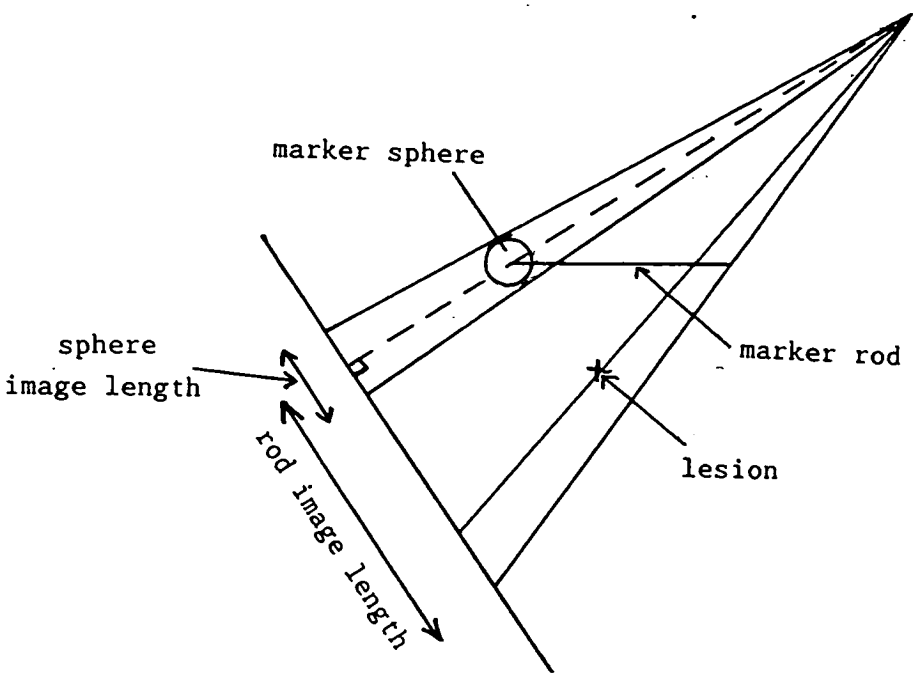

Figure 3.5 - Basic geometry of the proposed system of lesion location by X-ray imaging.

a full-scale drawing and moved towards or away from the point representing the source until both rays extending from the source are just tangent to the actual sphere, the correct source-sphere distance is obtained, as illustrated in Figure 3.6. Maintaining the centre of the sphere at this distance and rotating the marker about the sphere centre until the end of the rod coincides with the ray which intersects with the corresponding image point gives the correct orientation of the marker rod relative to the (X-ray) optic axis. This is the basis on which the apparatus has been designed.

3.4.2. The Mechanical Equipment

The mechanical analogue or plotter used to evaluate the effect of measurement errors on this scheme of lesion location is shown in Figure 3.7. It consists of two coplanar steel straight edges, S1 and S2, one of which (normally S1) represents a ray grazing the sphere, the other,S2, a ray passing through the end point of the rod. S1 and S2 rest on the horizontal draughting surface and are hinged together at one end, the lines of the opposed edges intersecting at the hinge axis, H. This axis is fixed perpendicularly in a third arm, A, which is in a plane parallel to that of S1 and S2, a little above the draughting surface. A has a vee-groove machined along the length of its underside, the centre line of which intersects the common hinge axis of all three arms. The intersection of the hinge axis with the horizontal drafting surface represents the point source of the X-rays. A graduated rule is fixed to the free end of A, perpendicular to A, parallel to the drafting surface. The perpendicular distance of its graduated edge from the hinge axis corresponds to that between the C-arm X-ray source and detector. The transverse scale of A rests on the upper horizontal faces of S1 and S2, each of which is provided with a clamping mechanism so that settings of the edges of S1 and S2 on the scale may be fixed

a) Have image

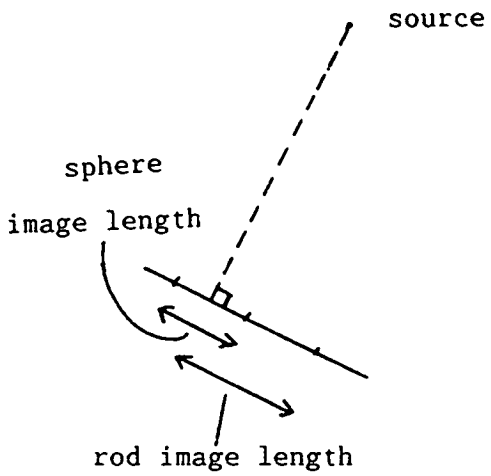

b) Draw rays and position marker spheres

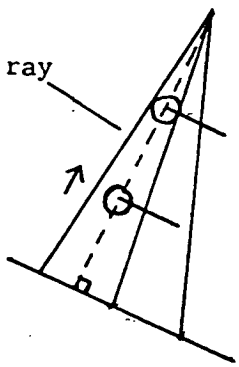

c) Rotate sphere to position the rod

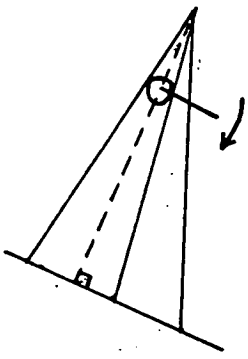

d) Marker correctly positioned with respect to the source and detector

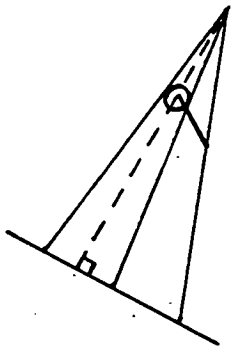

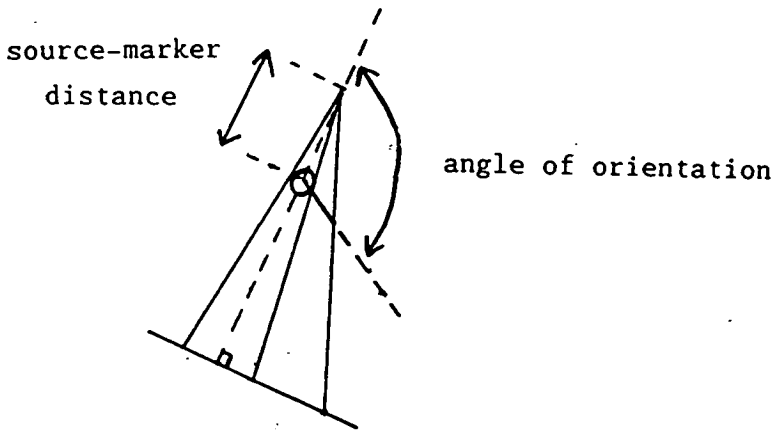

Figure 3.6 - Basic steps in optical determination of viewing angle.

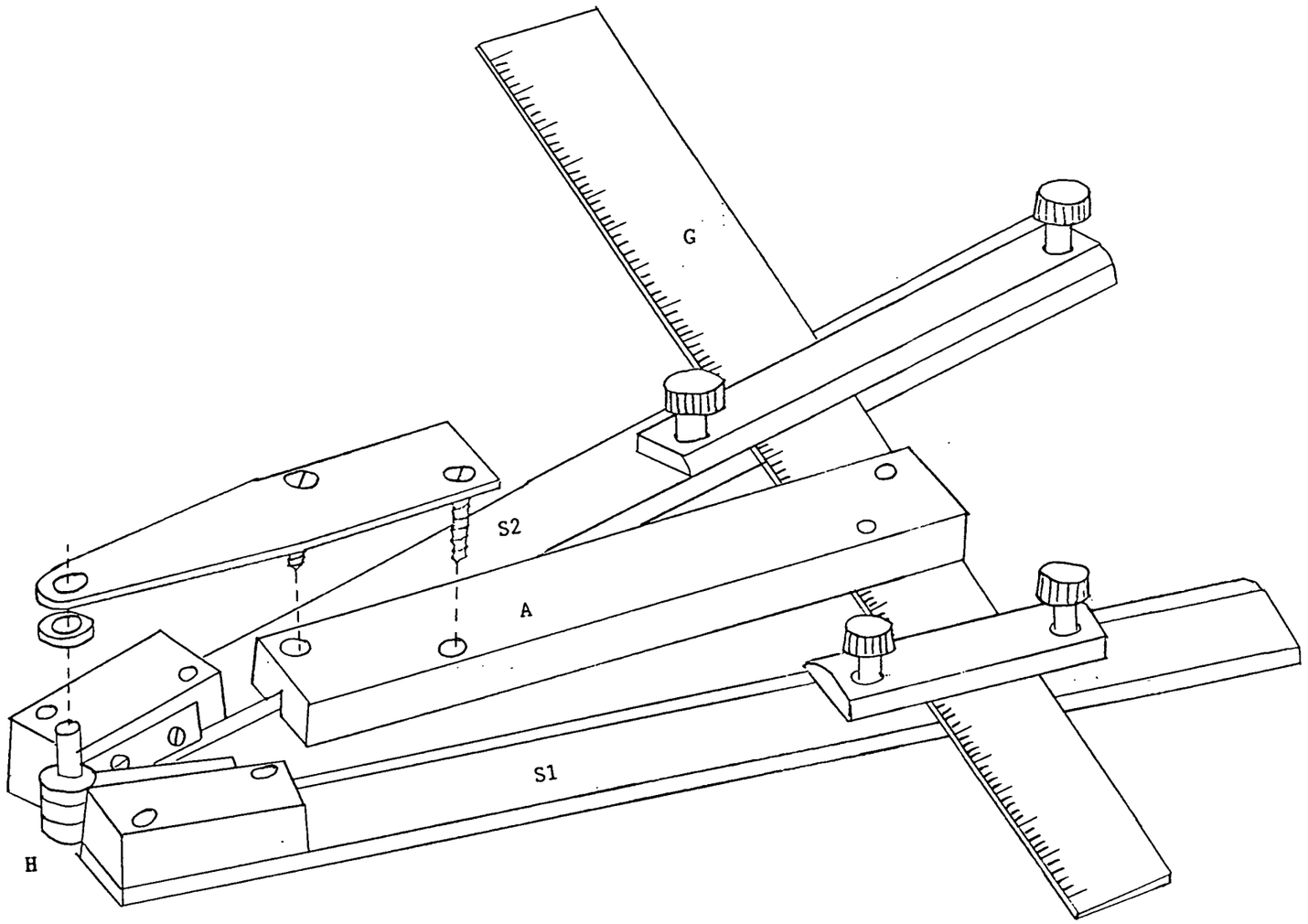

Figure 3.7 - The lesion plotter apparatus.

during subsequent manipulations. The sphere of the marker system is represented in 2-D by a disc, fixed to the drafting surface, having a small steel ball bearing mounted at the centre of its upper surface, which locates in the vee-groove of the arm A. The disc centre defines the centre of the sphere of the marker system; a removable pin in the drafting table represents the other end of the marker rod, point Q.

3.4.3. System Variables

The proposal under evaluation is that the position of a lesion (coordinates x,y) is to be determined relative to the marker from measurements of apparent or image distances between lesion and marker sphere and of apparent marker dimensions obtained in two views. The operating variables are the distance of the source from the marker and the angles of orientation of the two C-arm views relative to the marker rod. Parameters are the sphere diameter and the rod length.

3.4.4. Operation of the Mechanical Analogue

The arm S1 is set and locked at a graduation on the transverse scale such that its inner edge is at a distance from the vee groove axis corresponding to the radius of the image of the sphere. The instrument is then placed on the drafting surface so that the vee groove engages in the steel ball. The whole apparatus is then made to slide in the direction of the vee-groove, maintaining contact between the latter and the fixed ball and reducing the distance between the hinge the disc until S1 comes into contact with the disc periphery. The distance between the hinge axis and the disc centre now registers the correct source-marker distance corresponding to the observed radius of the image of the sphere. The ball is locked to the vee groove at this setting and the equipment is now rotated about the

ball until the arm, s2, which has previously been clamped to the scale at the division representing the observed rod image length, contacts the pin representing the end Q of the marker rod. The pin is then removed. Keeping the apparatus at this orientation, the arm S2 is moved to read on the scale the image length of the distance of the lesion from the centre of the marker sphere. A line is then drawn on the drafting surface along the straight edge S2 to represent possible lesion positions. The whole procedure is repeated using data derived from a different view, and the lesion taken to lie at the intersection of the two lines.

3.4.5. Reproducibility of the Mechanical Analogue

Before making more exhaustive trials with this system it is desirable to know how reproducible the apparatus itself is without the involvement of measurement errors. This was determined by setting and locking the scale readings, removing and then replacing the instrument on the draughting surface in engagement with the ball. At angles in the range 10° - 50° results are a pencil line width different at the end of the arm but at 60° - 90° these differences become much larger, up to 10 pencil widths, although in the region of the actual lesion they are much reduced (2 pencil widths). This suggests that it is the rotation of the apparatus to contact with the pin representing the marker end which is at fault. The apparatus itself is fairly reproducible.

3.4.6. Excluded Angles

It is noted that there are two cases for which results will not be achieved using this apparatus. At 0° and 180° pin Q will not be located as the cylinder at P obstructs the view. Also when the lesion lies between -R′ and R′, the sphere image radius, on the scale, i.e. on a region of the drafting surface obscured by arm

A, its position cannot be recorded on the scale.

3.4.7. Effects of Induced Errors

The half scale image lengths of the marker rod (P'Q'), the sphere radius (P'R') and the distance of the lesion from point P (P'L'), as shown in Figure 3.8, were determined over the angle range 10° - 170° and + or - 1mm errors induced onto all the scale settings (± 0.5mm in the case of the sphere radius). The 8 possible combinations of the induced errors on the 3 lengths have been investigated as shown in Figure 3.9. The lozenge formed by the outermost lines for each view is taken to be the largest error occurring.

Results are charted in Appendix 1.

At small angles in the range 10° - 30° the lines drawn are fairly reproducible but at larger angles the spread is much more diverse. Over the range 60° - 90° results are sometimes not obtainable. This is because as the centre line nears the perpendicular the marker image is close to its maximum viewed length which changes very slowly with increments in angle. Hence when induced errors are involved the combination of these errors becomes indefinitely large: As the apparatus is rotated about P the arm S2 acts as a tangent to a circle with centre P and radius greater than length PQ and contact with point Q is impossible, as shown in Figure 3.10.

The lesion is taken to lie within the quadrilateral or lozenge formed by the intersection of the extreme error bounds. The results noted for the uncertainties of lesion centre location are the radii of the smallest circle within which the error lozenge can be inscribed, as shown in Figure 3.11. The circle radius is thus an inverse measure of the accuracy of lesion location. The

Figure 3.8 - The variables used during use of the mechanical analogue.

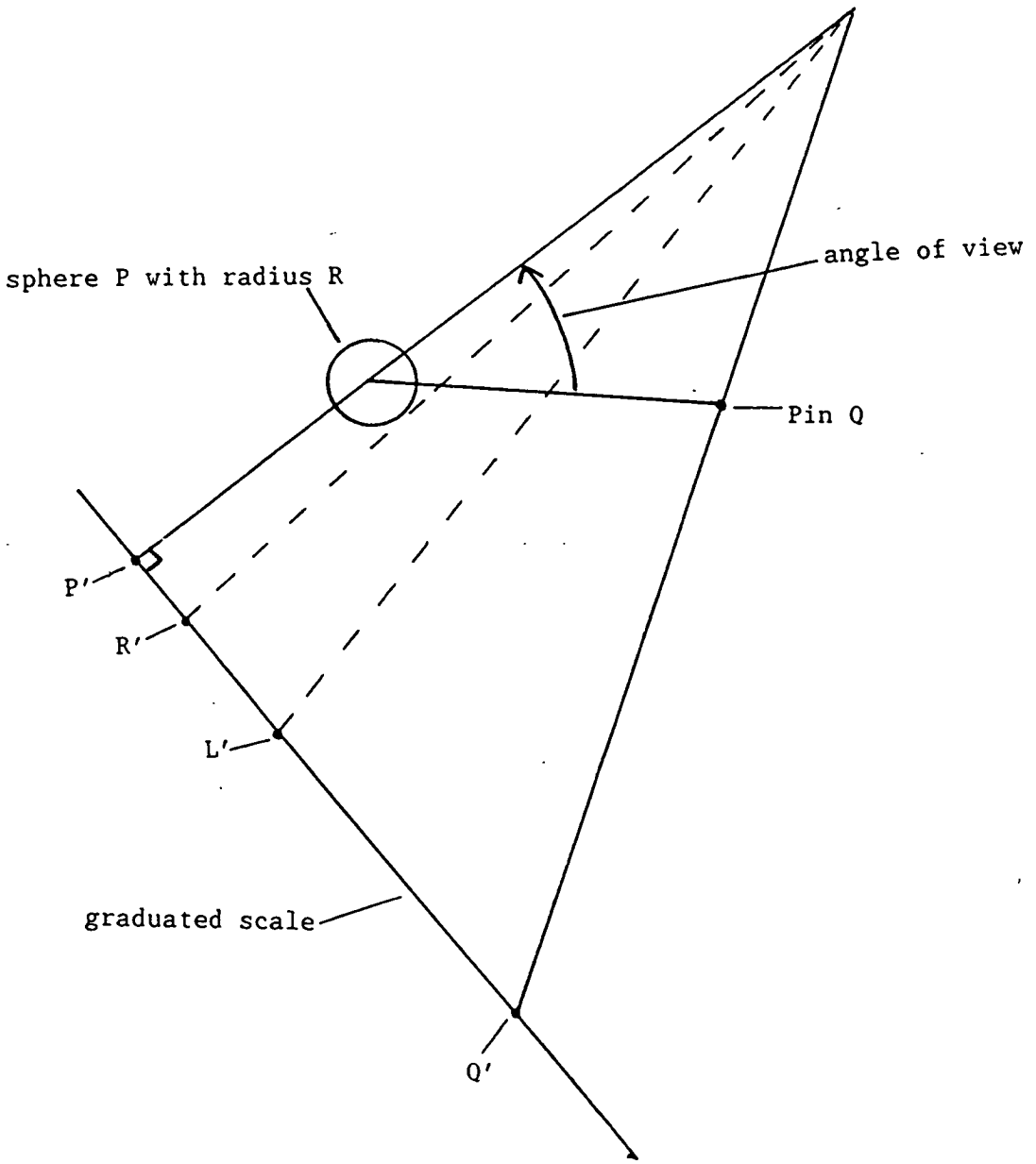

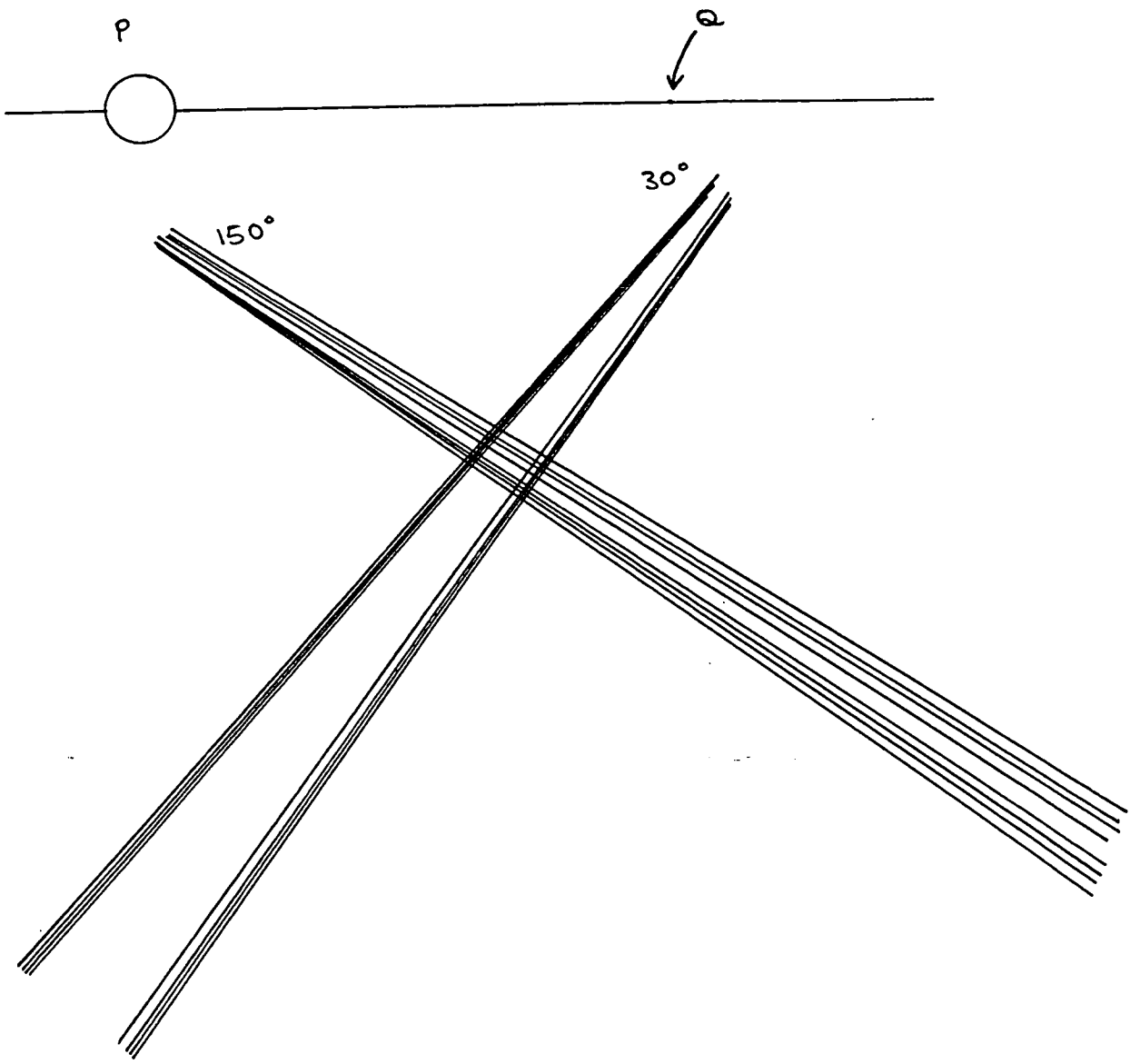

Figure 3.9 - Comparison of 8 possible combinations of the induced errors on the 3 lengths P'R', P'Q', P'L'. The lines drawn represent the line along which the lesion would be expected to lie.

Figure 3.10 - A diagram to illustrate how unobtainable readings can occur when induced errors are involved.

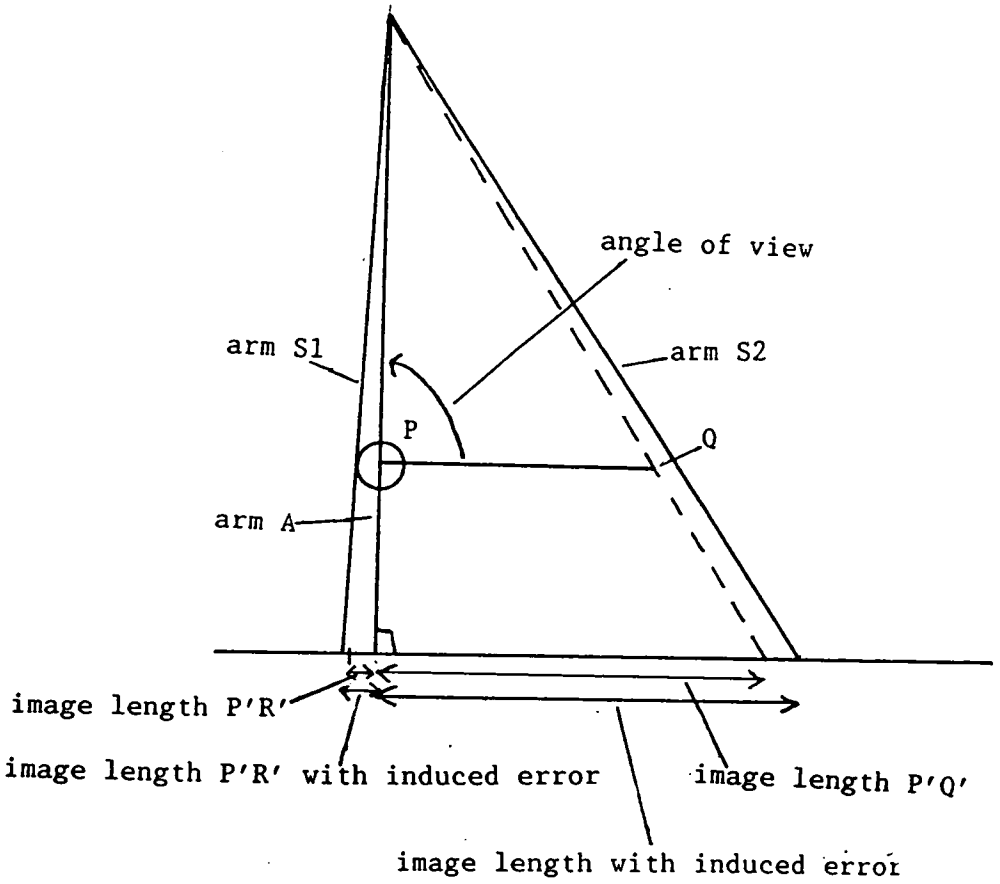

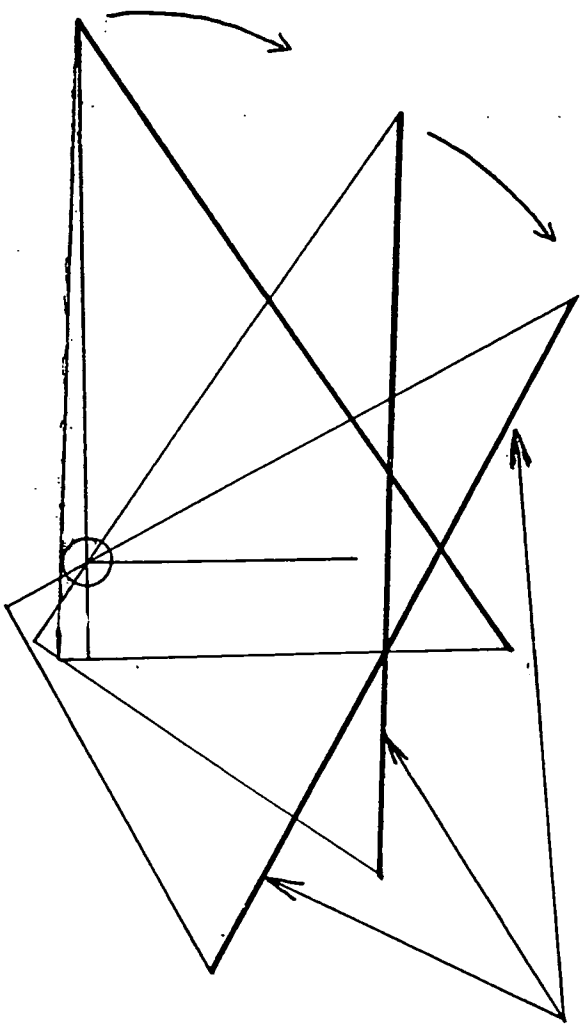

various positions of arm S2 on rotation

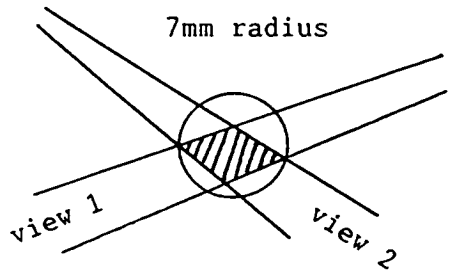

Figure 3.11 - The lesion area or 'lozenge' showing how the error is measured.

values found for this radius are associated with the half scale equipment with induced errors of + or - 1mm. The value for the error lozenge radius will correspond to induced errors of + or - 2mm in the full scale case, as shown in Figure 3.12. + or - 1mm induced error in the full scale case will produce an error lozenge radius half the size of that obtained for the half scale case.

It is generally observed that results are better at acute angles of 10°, 20°, 160°, 170° for one viewing direction relative to axis PQ paired with a small angle in the other quadrant for the other direction of view. A 90° separation between the two viewing directions would intuitively be expected to give the best results but this is not the case. A 110° - 130° separation proves best.

3.5. Effect of Marker Dimensions And Patient and Marker Positioning

3.5.1. Sphere Diameter

The effect of changing marker dimensions is also investigated and it has been found that increasing the sphere diameter from 2cm to 4 cm decreases the errors involved in the position estimation and increases the allowable range of angle pairs. Charts 7&11, 8&12 and 1&13 illustrate the effect of changing sphere diameter. It is assumed that + or - 0.5 cm (in the full scale case) will be satisfactory for the estimation of the lesion position. This corresponds to + or - 1cm lozenge radius in the charts. Such acceptable values have been stepped off in the charts in Appendix 1.

3.5.2. Marker Length

Increasing the marker length from 10cm to 15cm does not, surprisingly, appear to have a beneficial effect. There is a

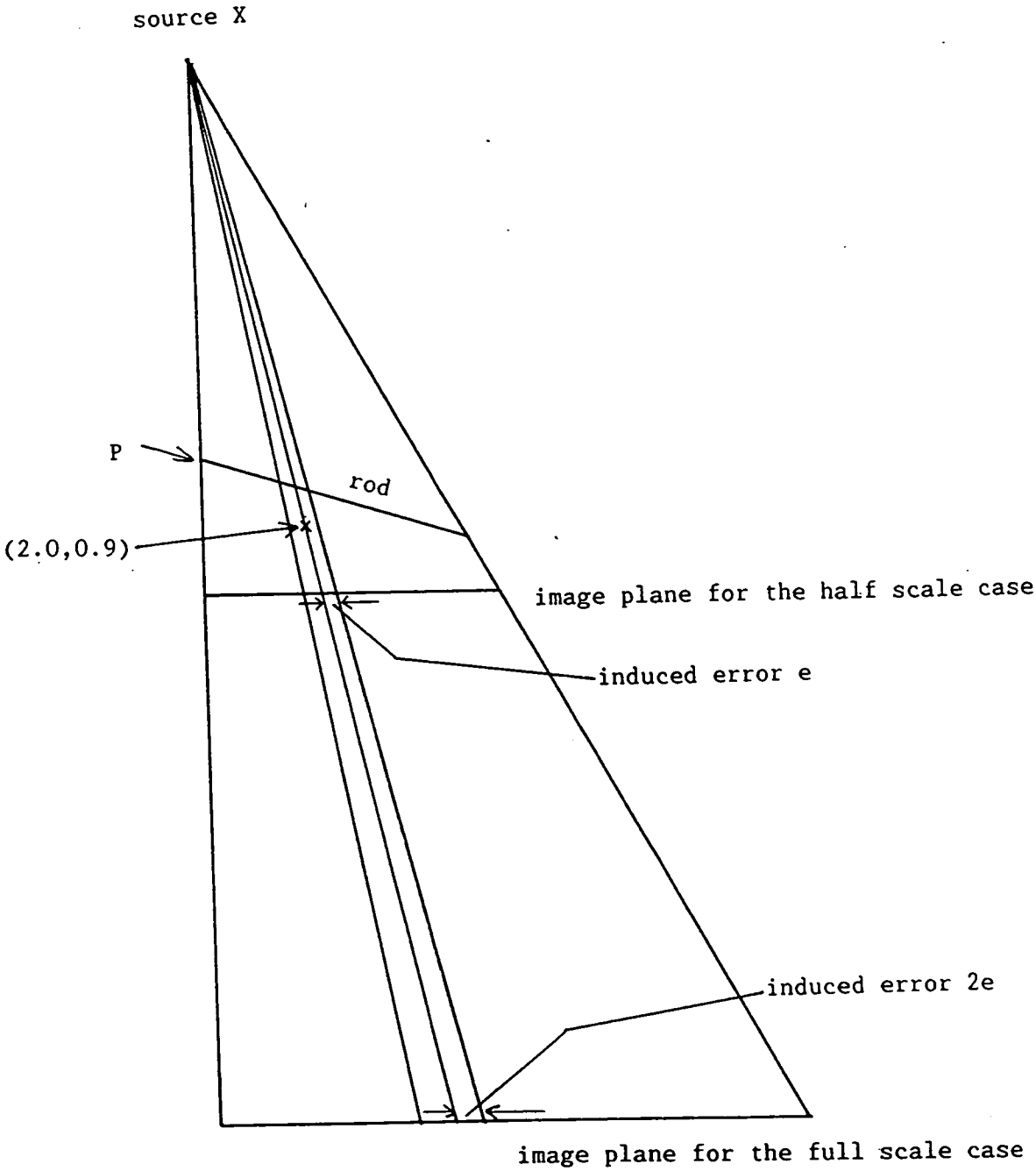

Figure 3.12 - Diagram illustrating the relevance of the error lozenge results obtained from the half scale apparatus to the full scale case.

small difference in errors over the better values and a slight increase in errors at other values. Results are illustrated in Charts 1 & 14 and 2 & 15.

3.5.3. Source-Patient Distance

A decrease in the distance between the source and the patient has the effect of improving the results slightly in all regions, but more noticeably in those which are worst. It acts by magnifying the images to a greater extent, thus reducing the percentage errors involved in the measurements, but the effects are not so large as to improve the range of angles over which best accuracy is obtained (Charts 1, 2, & 3; 7 & 8; 8 & 9; 10, 11 & 12).

3.5.4. Marker Position Relative to the Lesion

The position of the lesion relative to point P, the centre of the marker sphere, is also important. The closer the lesion is to P the more accurately its position may be determined. For example, at 14cm from P the best accuracy is $\pm$ 0.3cm but at 6.4 cm from P this reduces to $\pm$ 0.2 cm (only a very small angle range is observed for 6.4 cm as the lesion is obscured by the disc in the range 120° - 170°) and the range of angles over which acceptable values are obtained greatly increases from a 70° separation to a 40° separation (Charts 4, 5 & 6).

3.5.5. Effect of Additional Angle Information

In order to utilise viewing angles in the 60° - 90° region (i.e. the region which intuitively should reveal the best result) it would in principle suffice to use angular information from the C-arm machine itself. As the machine is neither rigid nor stable the best accuracy using position transducers would however, probably be $\pm$ 5°. To estimate the consequential errors in the

viewing angle region of 60° - 90° the apparatus is set to the correct source-patient distance using sphere images and locked into position as before and is then rotated until the arm lies at the designated angle, the lesion distance is set and the line representing possible lesion positions drawn along the edge of S2 in the usual manner. This method proves to be more reproducible than when angles in this range are estimated from measurements of PQ image length, but the error bounds and hence the error 'lozenges' are large. In several cases, however, paired with sharp angles, estimates fall within the satisfactory region.

If, instead of position transducers, an optical device were to be used over the whole angle range with $\pm$ 0.5° error the error lozenges produced would be much smaller. For example, in the case of Charts 4 & 13 the angle of separation required is reduced from 70° to 40°.

Therefore if an optical device could be provided to measure viewing angles with this accuracy over the whole angle range it would be more advantageous to concentrate on this avenue of approach than to persist with angle determinations using the marker system. If, on the other hand less accuracy of angle determination was available a combination of the two methods will prove necessary.

3.6. Conclusions

The existing biopsy technique has been examined and it appears that some of its faults might be avoided by use of a rotatable X-ray machine. A rod and sphere marker has been developed to overcome the difficulties of variable image magnification and viewing angle determination inherent in the use of such machines for lesion location and the effects of errors of image measurement upon accuracy of lesion location have been examined

using a two dimensional mechanical analogue of the proposed X-ray system. Results from this analysis suggest that lesions of 2cm diameter or even less may be accurately located using dimensional information obtained from a radio-opaque marker provided that image measurements can be reliably taken to within $\pm$1mm. Smaller lesions may be accurately located provided that the angles of view are carefully selected.

The optimum procedure leading to the best possible estimate of lesion position is to use information from at least two close views taken from sharp angles in opposite quadrants using a marker with as large a sphere as is reasonably convenient with the marker positioned above and close to the lesion. The sphere diameter appears to have a larger effect upon the accuracy than the source-patient distance.

CHAPTER 4

DEVELOPMENT AND TESTING OF MEASUREMENT TECHNIQUES FOR ACCURATE LESION LOCATION.

4.1. Introduction

A reference marker has been developed which has been shown to allow accurate determination of lesion position from the dimensions of X-ray images. It is now necessary to develop a means of obtaining dimensional information for images of the marker and lesion from the C-arm T.V. monitor to within an accuracy of $\pm$ 1mm. Here we consider what technique of image processing would best serve this purpose.

4.2. Image Analysis Applications

Much work has already been done on image analysis techniques applied to robotics but so far successful applications have been limited. One such application is automated inspection i.e. quality control of objects on a conveyor belt where all objects are required to be identical (within stated tolerances). A camera, in a fixed position above the conveyor belt and focussed on it, televises each object passing through its field of view. The televised image is processed and the object either accepted or rejected. A robot arm removes the offending object from the conveyor.

This application involves both image processing and pattern recognition. To enable this pattern recognition the computer must be 'taught' exactly what to look for.

This teaching phase involves 'showing' different orientations of the object to the camera. Significant characteristics are memorised by the computer to act as a reference description. This description is comprised of parameters which are not affected by

either object position or orientation on the focussed surface, such as area, perimeter, second moment of area, etc. (118). It is hence important that each object is clearly separated from other objects around it, as well as illuminated to prevent shadowing which will result in image distortion. Inherent in this recognition phase is the assumption that the camera-object distance is constant, thus allowing apparent area, perimeter, etc to be used as identifying characteristics. This, however, dramatically limits the possible applications of the program.

4.3. An Image Analysis Technique - Digitisation

Digitisation is probably the most common image analysis technique for processing picture data. In this the image is decomposed into small areas or points called pixels.

4.3.1. Binary Digitisation

The simplest image analysis involves binary pictures, i.e. in which the pixels are composed of only two colours - black and white. Binary pictures are obtained by 'thresholding' in which each pixel is examined in turn and compared with a preset level. Pixels lying on one side of this level are set black, the remainder white. Binary image analysis techniques employ mainly edge following algorithms. Initially a point on the image boundary is found and the next connecting boundary point is located. This process is repeated until the initial point is once again reached, by which time the perimeter of the object has been traced. By registering the direction of each edge point relative to the previous point a description of the object outline is obtained. This description may be compared with a reference to enable an object to be accepted or rejected. To allow a good quality object which has been moved or rotated round in the image plane to be accepted the algorithm locates the centroid of the

image and rotates the image about this point until the two descriptions match.

Binary imaging techniques are applicable only when all of an object's possible orientations are limited to rotations in a plane parallel to the image plane. Obtaining satisfactory binary images, however, is often difficult. The image boundary between the object and background can become indistinct and lighting is hence critical. Binary images are therefore generally restricted to use with two-dimensional or thin objects. If two or more objects touch or overlap the outline is destroyed and all the objects are rejected.

4.3.2. Grey Level Digitisation

Digitisation, with each point having a grey level resolution, is most often used. A higher level of detail is obtained with grey level systems compared with the silhouette image obtained with binary digitisation.

4.3.3. Analysis Techniques

The major problem with digitisation systems is the separation of the object from the background. Shadows cause edge blurring and the image is hence complicated. Techniques capable of analysing the data exist but are complex, time consuming and restricted to simple tasks.

Such techniques work satisfactorily provided that the objects neither touch nor overlap each other.

4.3.3.1. Overlapping Objects

A method for locating touching or overlapping two-dimensional objects which contain recognisable features such as holes or

corners is described (119). It relies upon matching several, but not all, of the features of an object with its description and proposes the remaining part of the object's position in the layout. Repeating the procedure the general arrangement of the objects is achieved. Parts which do not fit in with the object description are regarded as defective and may be rejected. However, defective objects, with the defective part obscured are accepted.

4.3.3.2. Boundary Recognition Problems

Problems arise with all these analysis systems. Picture cells on the image boundary will be composed of more than one grey level and the cell will thus have an intermediate value resulting in boundary recognition problems. This effect is enhanced if the picture cells are large.

4.3.3.3. Noise Filtration

Noise in the picture may result in some cells having erroneous grey levels. Horn (120) recommends a process of filtering and mentions two methods:

-Comparing cells with neighbouring points and adjusting 'outliers' to have the maximum or minimum grey level of any of its neighbours.

-Comparing with neighbouring cells and using the neighbourhood average.

These filtering processes cannot, however, be applied at an image boundary and their use is therefore limited to image recognition.

4.4. The C-arm Image

Generally, in the case of the C-arm monitor a high resolution, digitised grey level system exists. It is desired to pick out the marker and the lesion from the televised image but the associated image analysis is extremely complicated for several reasons:

-Although the sphere is of uniform diameter its image diameter varies, depending upon its distance from the detector. Thus although the general shape will remain the same at the image plane the important reference parameters will vary (i.e. diameter, perimeter, area, e.t.c.).

-It is possible that the sphere will appear as overlapping another object on the image. Although the overlapping sphere may not be lost the grey level across the circle varies and it is difficult to specify a set threshold value to determine the outlines in the overlapped area.

-No two lesions are of the same size or shape. Hence they cannot be recognised in any way by the computer.

-The ribs appear in any view of the chest and lungs and overlap with the sphere and lesion images. Although their outlines may be clear they drastically complicate the situation. Even if it were possible to accurately locate the marker images in isolation it would be extremely difficult to separate them from those of the ribs.

4.4.1. Low Resolution Analysis

The high resolution digitised image from the memoryboard is time consuming to analyse. Lower resolution digitisation would reduce image processing time but induces inaccuracies into the system. The error analysis carried out previously revealed how sensitive

estimates are of lesion position, calculated by means proposed in Chapter 3, are to small errors in image measurement, especially when viewing has to be done from certain directions.It is hence necessary to reject low resolution digitisation as a step in obtaining image dimensions in this case.

4.4.2. High Resolution Analysis

If it were possible to carry out this analysis at a high resolution, a complex image digitising system involving several threshold values would be required, i.e. a multiple grey level system. This, however, would require a lot of computer space to cover the complete analysis. The image appears on the T.V. monitor showing ribs, marker, lesion, internal organs, etc in varying grey levels. The particular grey levels are very dependent upon the particular patient (how fat or thin he or she is) and the lesion position within the lung, the characteristics and state of the X-ray machine, its mA and kV settings, the absorption of the trolley bedding, etc. Thus variable threshold values for the grey level changeover are necessary and it is impossible to stipulate exactly in which grey levels each object will appear. The marker will be semi-opaque and 'change colour' at the overlap region.

To provide a satisfactory automated image analysis procedure would thus in itself be a large project of dubious outcome. It was therefore decided that image recognition procedures should be rejected in the current programme and image analysis information input to the computer manually.

4.5. Manual Image Analysis System

A system has been devised to input the required image information. A BBC microcomputer, connected to a genlocking system, as shown in Figure 4.1, allows a computer generated

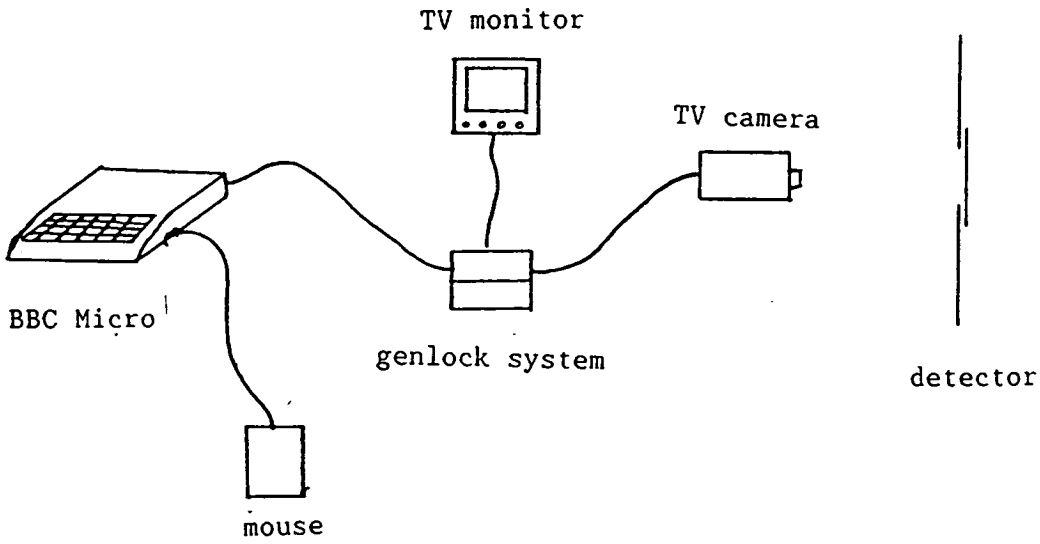

Figure 4.1 - Data collecting system

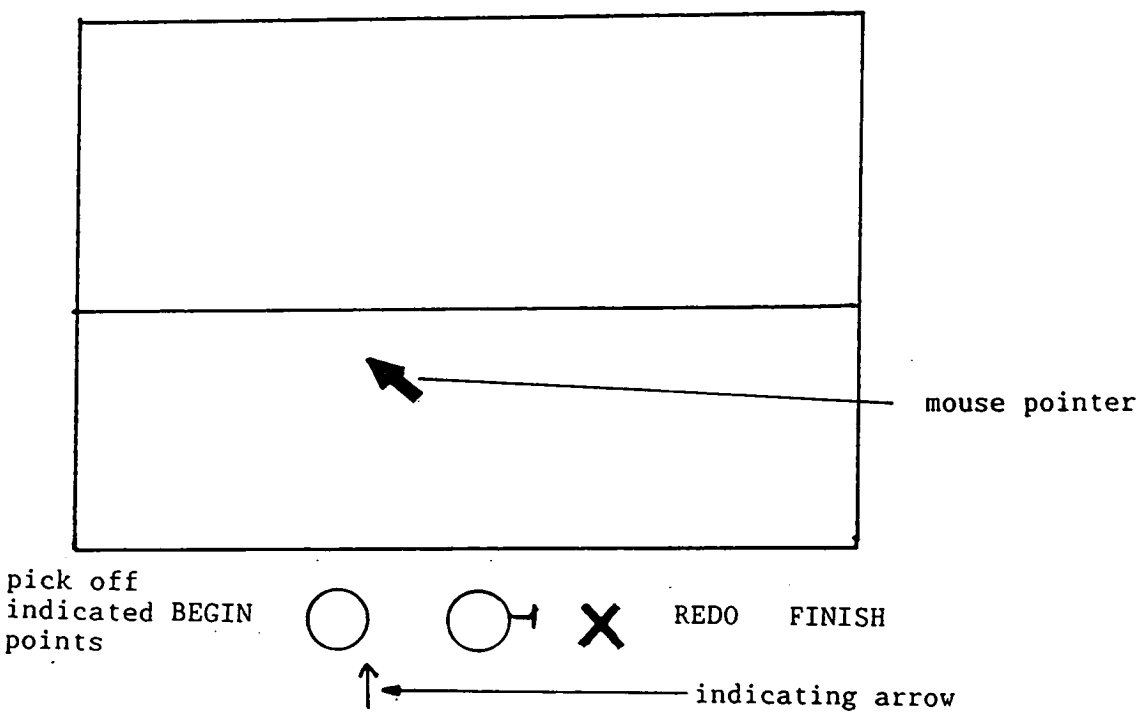

Figure 4.2 - The computer generated menu

picture to be superimposed on the video picture on the monitor. An AMX mouse is connected to the computer and a mouse-controlled pointer is displayed on the T.V. screen, superimposed over the X-ray image. The mouse is moved on a flat surface until the screen pointer is positioned over the relevant point. Pressing the mouse button causes the x and y coordinates of the designated point to be registered with the computer

Using this equipment a computer generated 'menu', as shown in Figure 4.2, is superimposed over the X-ray image and appears along the bottom of the screen. The menu contains symbols representing all the information required for lesion location . An arrow indicator, travelling along the bottom of the menu, indicates which feature of the image is to be measured and registered next and the operator moves the mouse until its screen pointer lies over the required point. Pressing a mouse button registers the position of the point into the computer and the menu indicator moves to point at the next piece of information required. If an inputting error is made simply positioning the pointer over the word 'REDO' and pressing a mouse button moves the indicator backwards. The correct information can hence be input.

Once all the information has been input to the computer the pointer is positioned over the word 'FINISH', the button pressed and the registered variables are used to calculate the distance of each sphere from the X-ray source and the angle of view and postulates a line along which the lesion must lie. Inputting a further image from a different view results in another line. Solving the two simultaneous equations reveals the lesion position relative to the marker.

4.6. An Optical Simulator

It was necessary to evaluate this technique extensively. However,

access to the C-arm machine, located in the City Hospital at Edinburgh, is limited: Medical staff, naturally, have priority over its use. Therefore a full scale model of the C-arm set-up was designed and built. Visible light is used in this model instead of X-rays, conveniently forming similar images without risk to personnel.

4.6.1. The Apparatus

The apparatus is illustrated in Figure 4.3. A light source with a 250W bulb and adjustable iris set to a small aperture is used to represent the X-ray point source. A 17cm diameter translucent plastic screen set 93cm away from this point source represents the X-ray detector. This section of the apparatus is surrounded by black screens to reduce interference from background light. A black and white T.V. camera with a 16mm lens is mounted on a three-axis adjustable support behind the plastic screen on which it is focussed. The image signal is sent to the black and white T.V. monitor so that the C-arm source and image detector are thus modelled.

4.6.2. The Patient Model

When using the C-arm X-ray machine itself the patient remains stationary and the different views are taken by rotating the C-arm. Literal modelling of this would require a large framework to support the various pieces of equipment and maintain them at the correct relative positions. In this simulation, therefore, the imaginary patient is rotated and the relatively large optical equipment remains fixed on the bench. A two dimensional system has again been used to prevent a cluttered system.

Throughout the diagnostic procedure the actual patient must remain in a fixed relation to the marker. Accordingly, in this simulation the patient is represented simply by a rigid structure

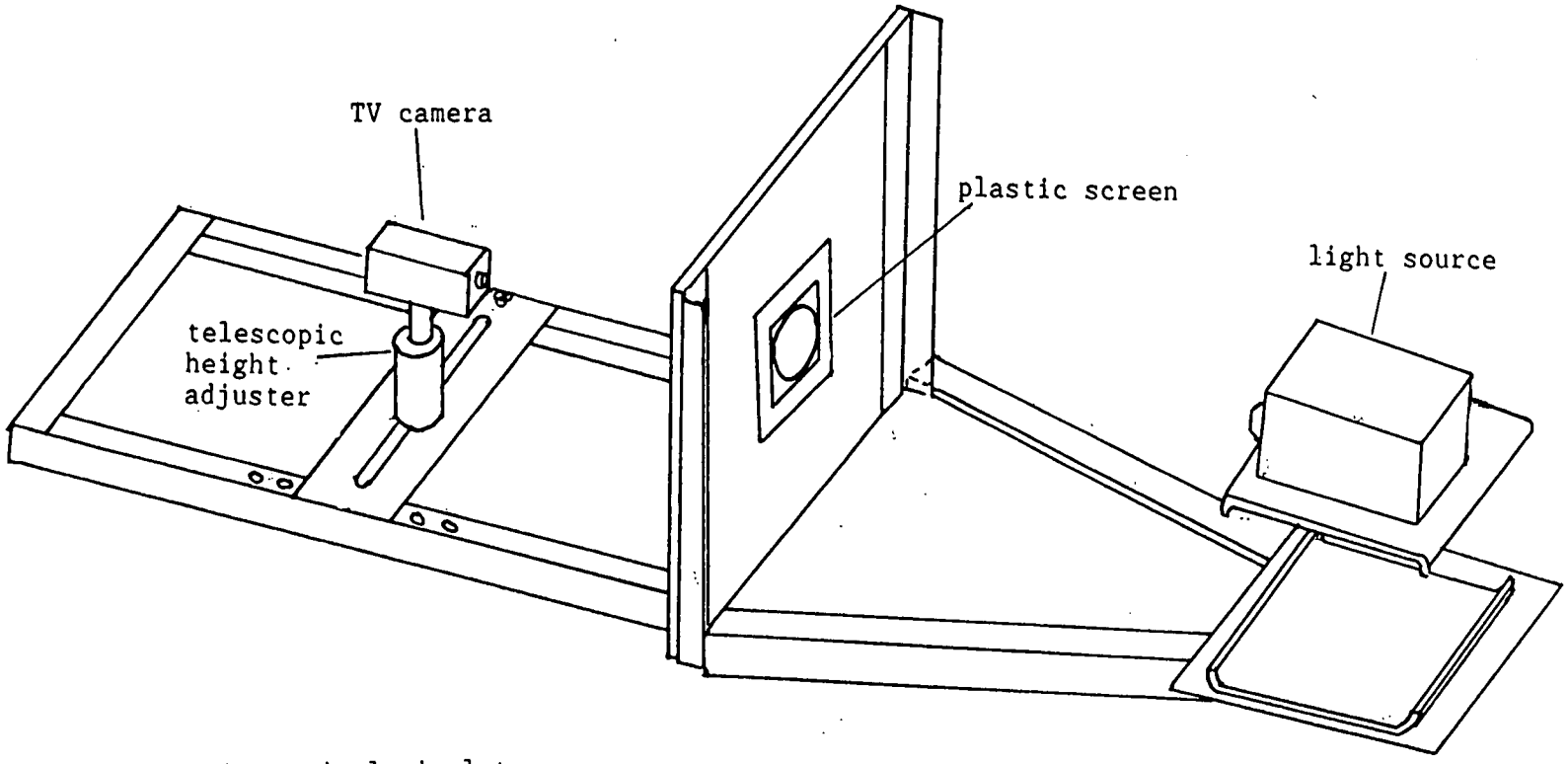

Figure 4.3 - The optical simulator

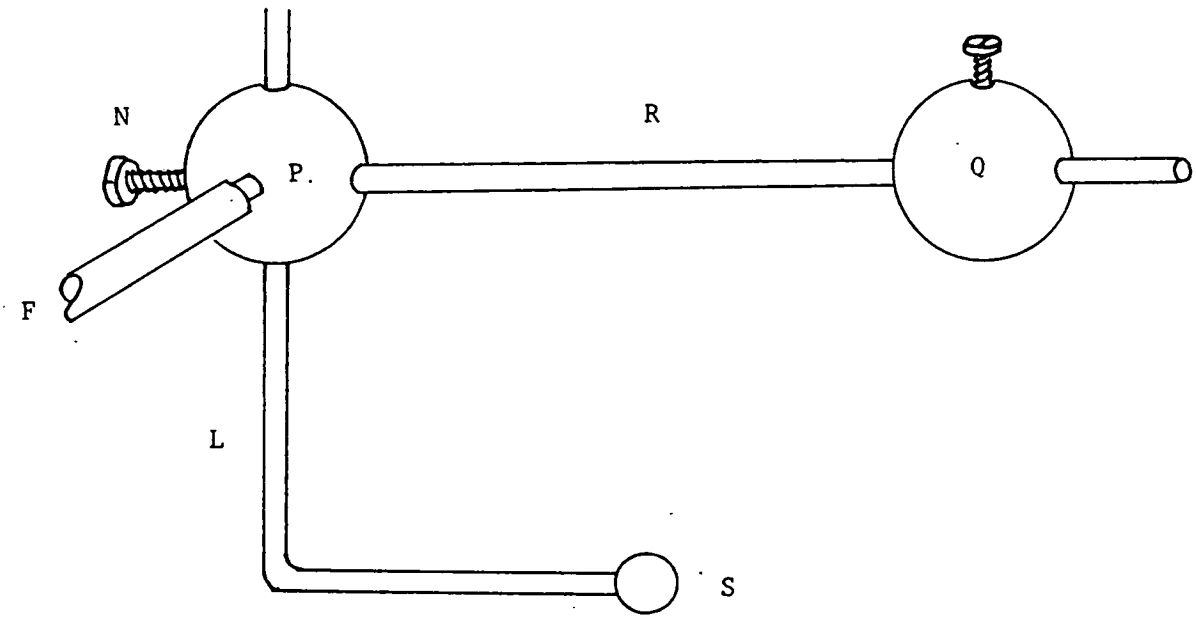

Figure 4.4 - Marker and lesion system

comprising the 2-dimensional marker and the lesion which are constructed from spheres and connecting rods , as shown in Figure 4.4. One sphere, P, is used to determine the scaling factor, F, mentioned previously, and the centres of this and of a second sphere, Q, define the ends of the marker rod, R. R is a sliding fit in a diametral hole in Q, which can be locked in place at any convenient distance from P by a screw. This enables the length of R to be varied. The 'lesion', a smaller (1cm diameter) sphere, S, is fixed to the end of one arm of an L-shaped rod, L. The longer arm of L is a sliding fit in a diametral hole in P, in which it can be locked in place with a nylon screw. This marker sphere, together with the associated system of rods and spheres, can turn about a fixed support, F, so that the 'patient' can be rotated relative to the optical system. As in the 2-dimensional mechanical system, this axis of rotation was made perpendicular to the plane PQS containing the two marker spheres and the 'lesion'.

4.7. Distortion Effects

Graduated rulers were televised and the image measurements from the T.V. monitor reveal that distortion effects with this apparatus are negligible.

A sphere of known diameter was positioned at various distances between the source and detector. Measurements of its image reveal that the optical system approaches pinhole optics with negligible error.

4.8. Calculation Method

The method of lesion position calculation is similar to that used in the mechanical analogue analysis: It differs in that sphere Q (the additional sphere used to indicate the position of the rod end) is now used to obtain an estimate of the marker viewed

length, MVL. The image and actual diameters of sphere Q are used to obtain the conversion factor, F, between the TV image and lengths referred to point Q, the end of the marker rod. This conversion factor is used to obtain an estimate of the marker viewed length, MVL, from the televised image.

$$MVL = \frac{\text{TV image length}}{F}$$

The true rod length is known and thus the angle of view, θc, is thus calculated, as shown in Figure 4.5.

The position of the lesion is measured relative to the centre of sphere P. A cartesian coordinate system is used, the centre of P representing the origin, the marker PQ (normally approximately horizontal in the intended clinical application) as the X-axis and the perpendicular to PQ at P (approximately vertical when the patient is horizontal) as the Y-axis, as shown in Figure 4.6. All viewed lengths are referred to the plane through point P, parallel to the image plane, as shown in Figure 4.7. Thus the dimensions of the images are found as their projections on the x-axis. The calculation method for lesion location is detailed in Appendix 2.

4.9. Reproducibility of Results

Reproducibility of results has been investigated. Six sets of readings were taken, in sequence, from identical views. The raw image data was not processed at this stage but stored on a disc. This has been repeated for views in the θc angle range 0° to 180° for the identical marker and lesion arrangement. All the collected data was then processed. Every set of readings was paired with every other set and the lesion position estimated. 36

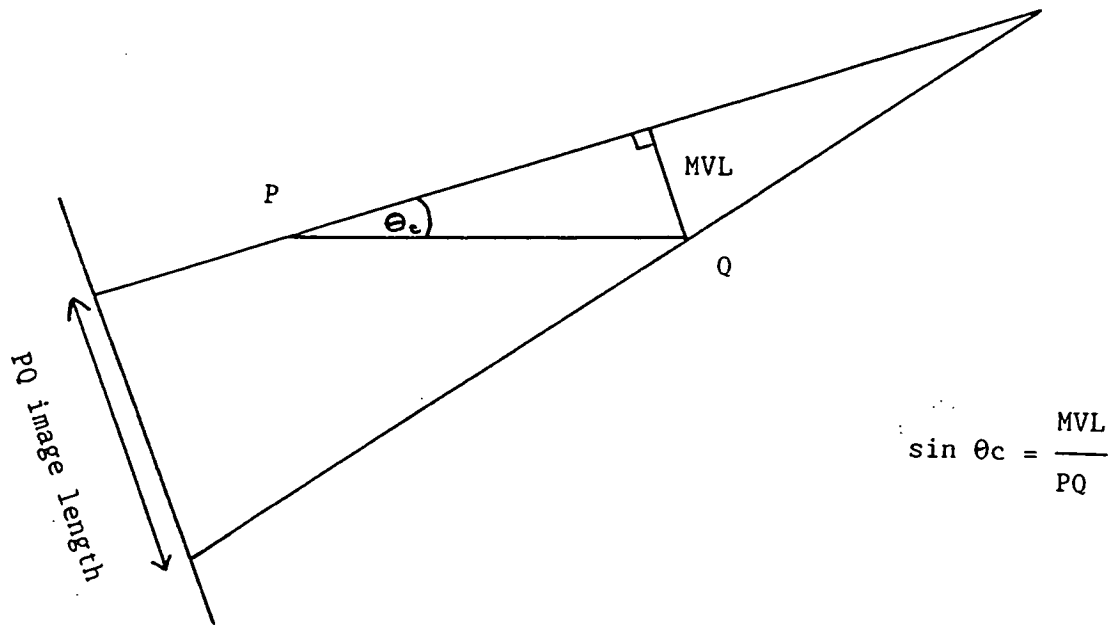

Figure 4.5 - Illustrating how the marker viewed length (MVL) is referred to point Q.

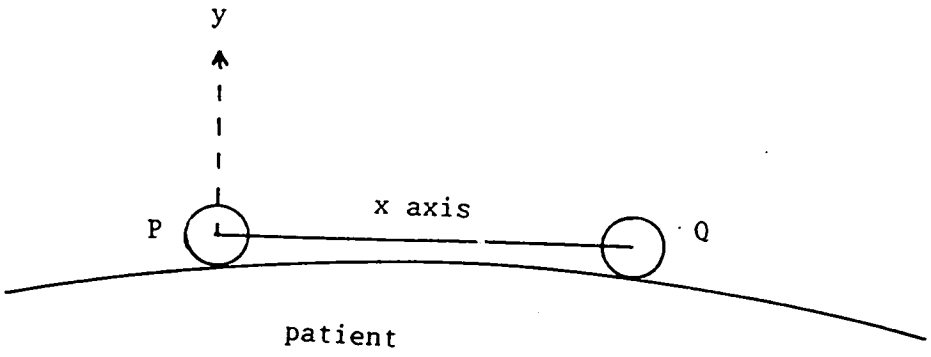

Figure 4.6 - Illustrating the cartesian coordinate axes.

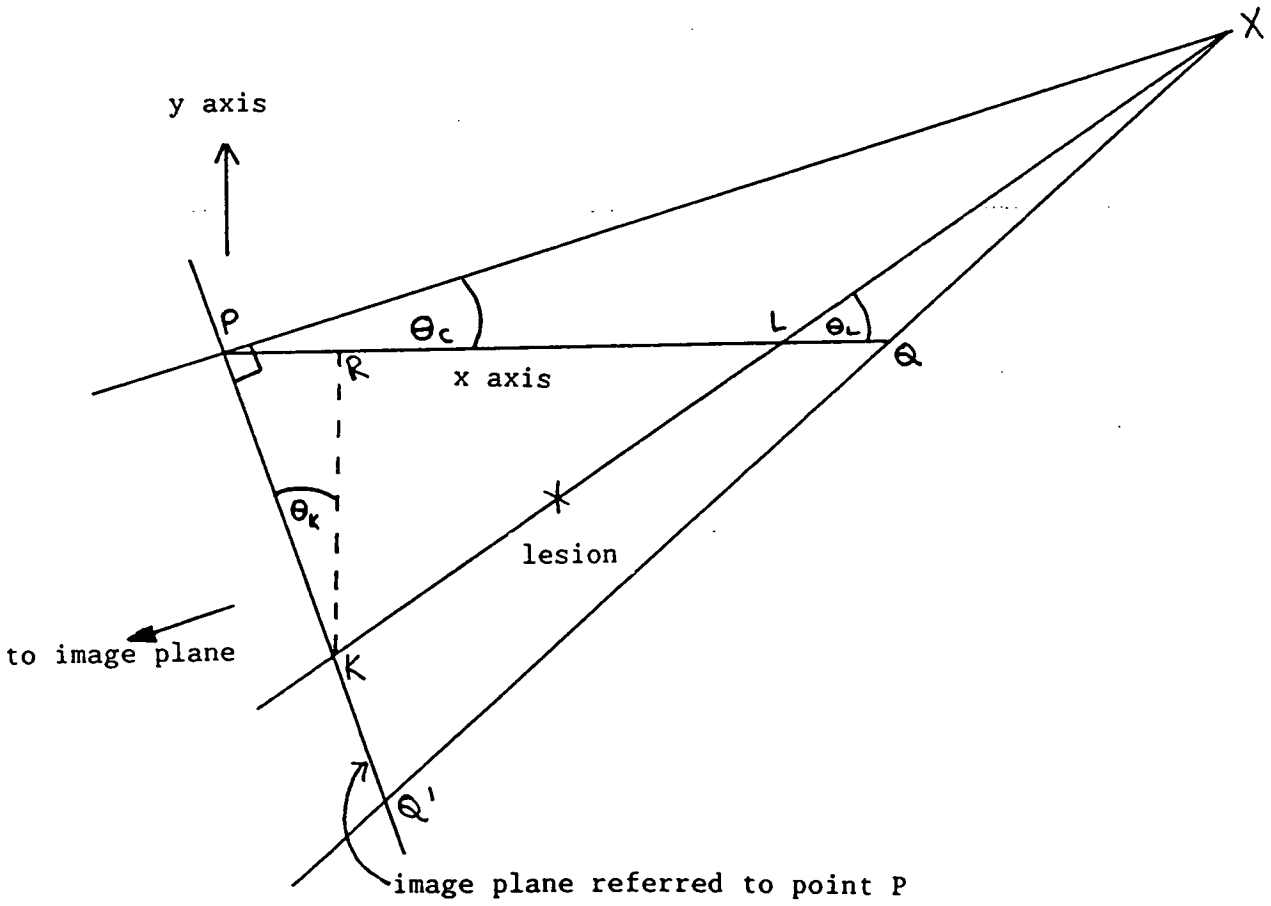

Figure 4.7 - Geometrical basis of lesion location.

estimates of lesion position are obtained from nominally identical pairs of views. The general reproducibility trend is shown in Figure 4.8, in which the spread of these estimates of lesion position is plotted on a vertical scale against the corresponding viewing angles. The general form of such plots reflects the original sensitivity analysis results obtained with the mechanical analogue, ie best reproducibility is obtained at Oc separations of between 90° and 110°, etc. However the results over the range 85°-95° in Figure 4.8 above are misleading, as on several occasions the calculated image length was larger than the actual rod length and therefore the angle of view θc could not be calculated. To avoid the program crashing it was modified in such a way that such data are intercepted and a message to this effect is printed on the screen, before the program continues as before.

It is instructive to determine how results from lesion targetting by the purely optical technique, shown in Figure 4.9 compare with those obtained using angles determined independently (eg read from the C-arm, using position transducers). Lesion estimates based on direct measurements of viewing angles are shown in Figure 4.10 over the range 0°-180° at the same lesion position as for the optical technique and using otherwise identical data as used to construct Figure 4.9. Results of the two methods are readily compared with the aid of Figure 4.9 and 4.10 to determine which is most appropriate over what angular range. Over the range 70°-110° the precision of the lesion location using the angle input method is much better, giving precise location within 1 cm, allowing this range to be used if the viewing angle can be accurately determined by some additional means.

4.10. Redundant Measurements

The error analysis carried out experimentally on the mechanical analogue revealed how susceptible lesion location is to small

Figure 4.8 - Spread of results of reproducibility tests of lesion plotting from the optical simulator. The vertical scale represents the range of estimated lesion positions.

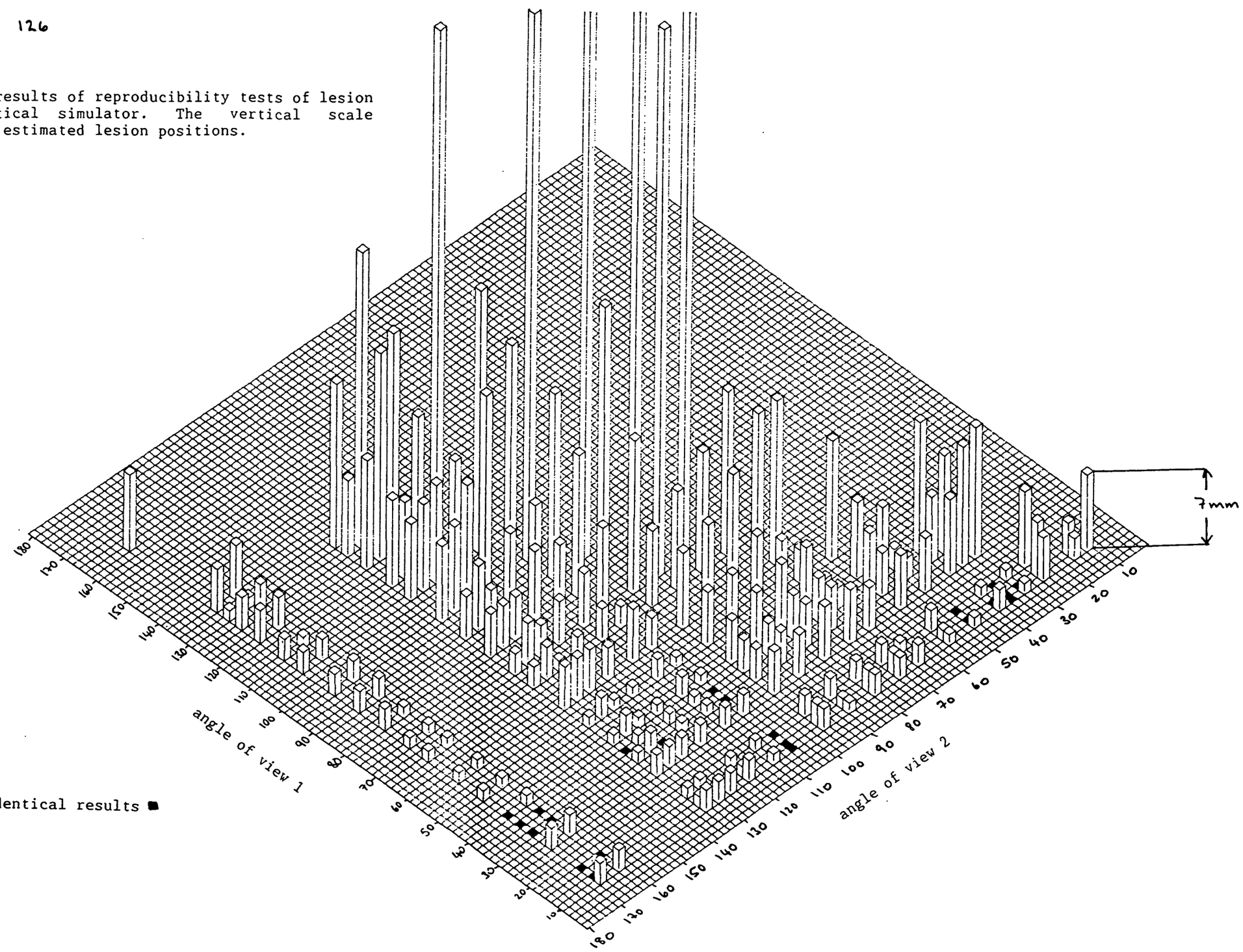

identical results ■

Marker dimensions
sphere diameter 2.5cm
rod length varies from 4.3cm to 19.1cm, depending upon the viewing angle.
lesion position (6.1,3.6)

Figure 4.9 - Results of lesion location error circle generated by data collection errors as a function of viewing angles, using optical data only.

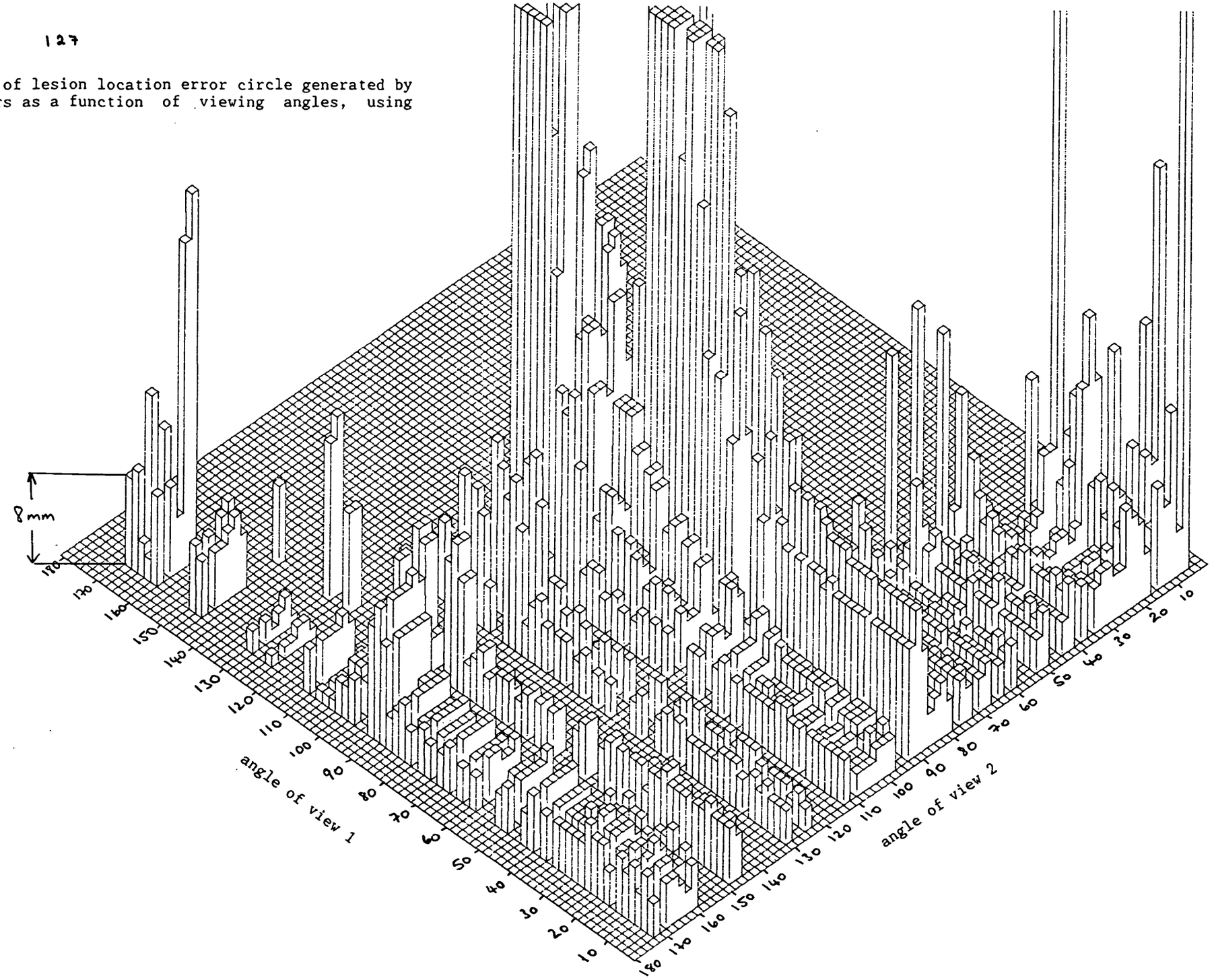

Marker dimensions
sphere diameter 2.5cm
rod length varies from 4.5cm to 19.1cm, depending upon the viewing angle.
lesion position (6.6,3.8)

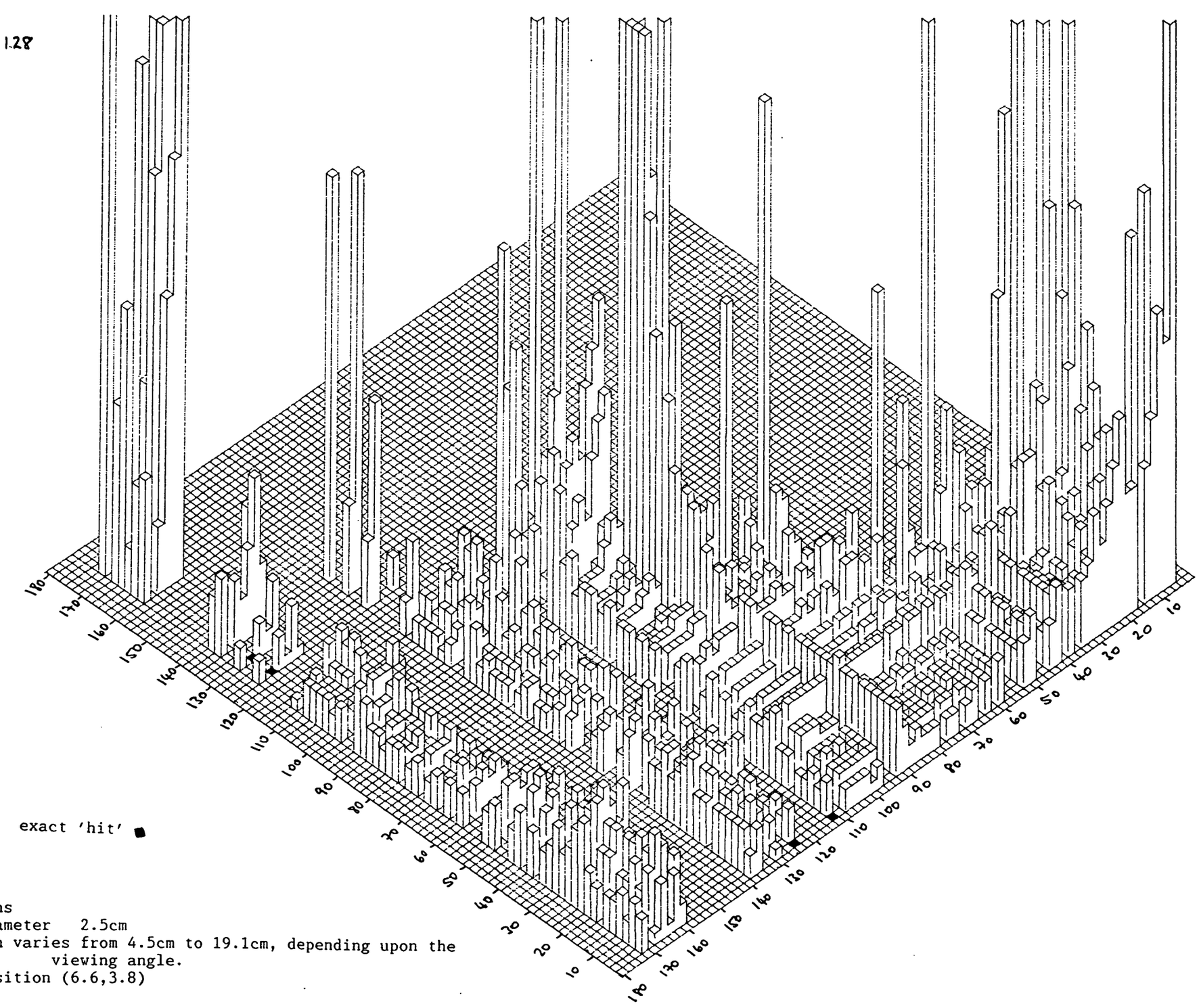

Marker dimensions
sphere diameter 2.5cm
rod length varies from 4.5cm to 19.1cm, depending upon the viewing angle.
lesion position (6.6,3.8)

Figure 4.10 - Radius of lesion location error circle generated by data collection errors as a function of viewing angles, using optical data supplemented by direct measurements of viewing angle.

errors, especially at angles of view within the 60°-120° range. It is desirable to know more generally, for the optical system, how accurate or precise any estimate of lesion position is likely to be and to what extent it is feasible, if necessary, to use redundant measurements to improve these estimates.

4.10.1. Mathematical Analysis

There are five measurements associated with each image: Two tangent locations for each of the two marker spheres and the lesion location. It is possible to express the lesion equation

$$y=(PL_i-x)\tan(\theta L_i)$$

in terms of the five directly measurable variables and hence in principle to analyse the effects of errors in these variables on the final lesion estimate. Since errors occur in both the independent and dependent variables and the problem is non-linear, the set of equations, detailed in Appendix 3, is complicated and appears insoluble. It has hence been put aside and experimental studies undertaken.

4.10.2. Results Improved by use of Additional (Redundant) Measurements

At least two views are required to estimate the two dimensional lesion position (x,y). In the case of redundant measurements n views are taken, where n>2. This provides $d=\sum_{i=1}^{n}(i-1)$ estimates of lesion position. By combining these d estimates a more accurate single estimate, (x,y)av is obtainable. There are several methods of combining these estimates, the most basic being simple averaging, ie

$$x_{av}=\frac{\sum_{i=1}^{d}(x_i)}{d} \qquad y_{av}=\frac{\sum_{i=1}^{d}(y_i)}{d}$$

Table 4.1 shows the percentage of simple average results which lie within 1cm and 0.5cm errors for different lesion positions when using sets of three views.

Since data has not been collected from similar viewpoints the results at the different lesion positions cannot be compared directly. Certain ranges of view have been omitted. These omissions arise for two different reasons:

a) The lesion is obscured by one of the marker spheres. In the optical analogue the spheres are opaque and thus if the lesion is situated behind one of them it will be completely obscured. In the X-ray system however the spheres will be semi-opaque, showing up on the monitor but still revealing dense structures behind them. Thus this range of views will not be forbidden in the X-ray system (provided that the lesion is sufficiently dense).

b) The lesion is offscreen. If the lesion lies deep within the body then at sharp angles either the marker or the lesion may lie offscreen. Reducing the marker rod length may, in some cases, decrease the overall image size but generally this problem is inherent with both the optical and X-ray systems.

Consequently an overall improvement in results is apparent if the obscured range lies close to 90° or a deterioration in results if the range lies away from 90°.

From studies of errors associated with the three viewing angles it is apparent that the results are most markedly improved where errors are largest,ie when one or more of the angles lie close to

Table 4.1 - Percentage of results which are within the indicated error bounds for different lesion positions when using redundant measurements.

Lesion Position	% within ±1cm error	% within ±0.5cm error
0,2.4	83.6	77.5
0,4.8	84.5	70.2
0,7.2	46.5	33.5
-0.2,10	52.2	21.9
-0.4,14.2	36.0	15.1
2.9,2.3	88.4	77.8
3.0,4.8	49.5	24.6
3.0,7.2	56.9	43.5
2.9,9.9	24.1	13.9
2.9,15	32.7	10.5
6.0,2.4	66.2	50.0
6.1,3.6	98.6	88.2
6.4,4.2	82.1	61.9
6.1,4.8	63.4	47.5
6.1,6.1	63.8	54.6
6.6,8.6	23.2	11.5
9.8,2.4	86.9	67.0
9.8,4.8	27.2	11.5
10.3,7.4	38.5	23.1
10.2,9.8	20.7	9.1

90°.

4.10.3. Quadrant Flips

Occasionally, however, results when utilising views around 90° are noticeably erroneous, often ridiculously so. Even the application of redundant measurements has little overall effect. For example, consider the following viewpairs:

28°, 87°, 63° give 4.5cm error
19°, 60°, 63° give 5.8cm error

Such results occur when one or more of the viewing angles are assigned to the wrong quadrant. This tends to occur in the 60°-120° range (In the above two examples a viewing angle of 117° has been wrongly assigned as 63°.) The further the viewing angle from 90° the worse is the final position estimate should such a quadrant 'flip' occur, ie an 85° view may assume a 95° view position, an error of 10°, whereas a 75° view may assume a 105° view position, a 30° error.

The quadrant is determined within the computer program by comparison of the image and actual diameters of the two identical marker spheres to calculate their distances from the X-ray source. Combining these distances with the rod length an estimate of the source x-coordinate is made and the quadrant thus determined. Close to 90° these spheres are roughly the same distance away from the source and thus their image diameters are similar: The slightest error in their measurement can result in a large error in these calculated distances and thus result in the adoption of the wrong quadrant.

4.10.3.1. Location of Quadrant Flip Occurrences

It is desirable to locate and correct such erroneous quadrant

allocations or 'flips'. This is done within the program by flipping every angle in the 60°-120° range as it occurs and calculating the different possibilities of lesion position when paired with another angle. If only one of the view pairs lies in this flip range then two lesion position estimates result, but for two pairs within the flip range then four estimates are obtained per angle pair.

A series of tests is applied within the program to each position estimate to eliminate the ridiculous or obviously erroneous positions. These elimination tests take several forms, depending upon how many views lie within the 60°-120° range. A flowchart describing the process is shown in Figure 4.11.

Initially any estimate which lies above the patient's body or further than 25cm from sphere P, as illustrated in Figure 4.12, is eliminated. If, during this removal of estimates all pairs involving one angle in one quadrant are eliminated then that quadrant is removed as a possible viewpoint for that angle and the remaining quadrant assumed correct, as described in Appendix 4.

Once the system can no longer be reduced by the above method then all remaining possible viewing angles are organised into sets of three possible views, as in Appendix 5, and the corresponding lesion estimates tested to ensure that they all lie within the constraints described above. The first set that provides a complete group of estimates is assumed correct (the sets are ordered so that those requiring the least amount of alterations to calculated viewing angles appear first). If there is no complete set of estimates then either the original calculated viewing angles are assumed (if the number of possible angle flips is 3) or the set with the smallest separation between its estimates is chosen. The system is thus reduced until all

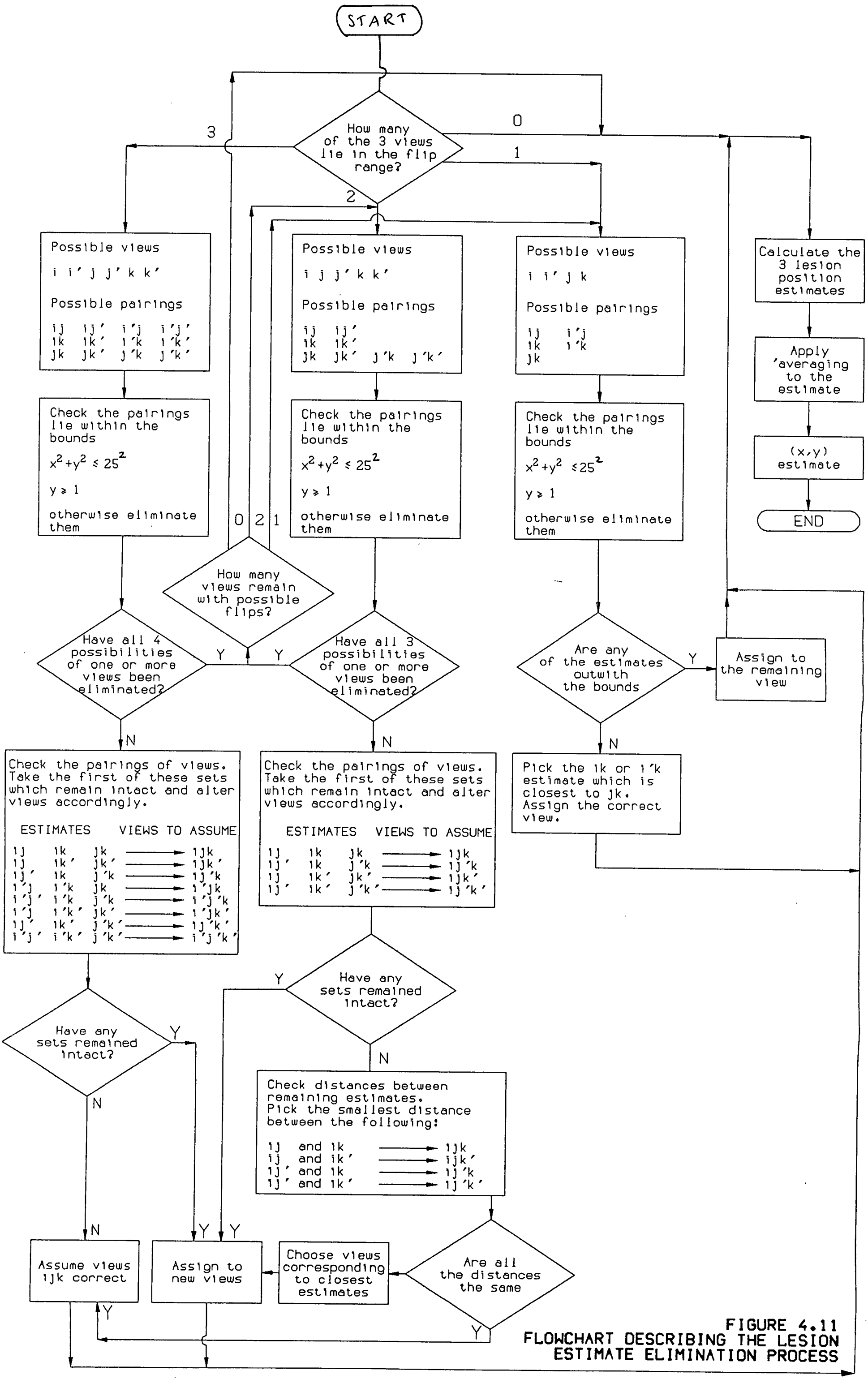

FIGURE 4.11
FLOWCHART DESCRIBING THE LESION ESTIMATE ELIMINATION PROCESS

Figure 4.12 - Constraints on acceptable lesion estimates.

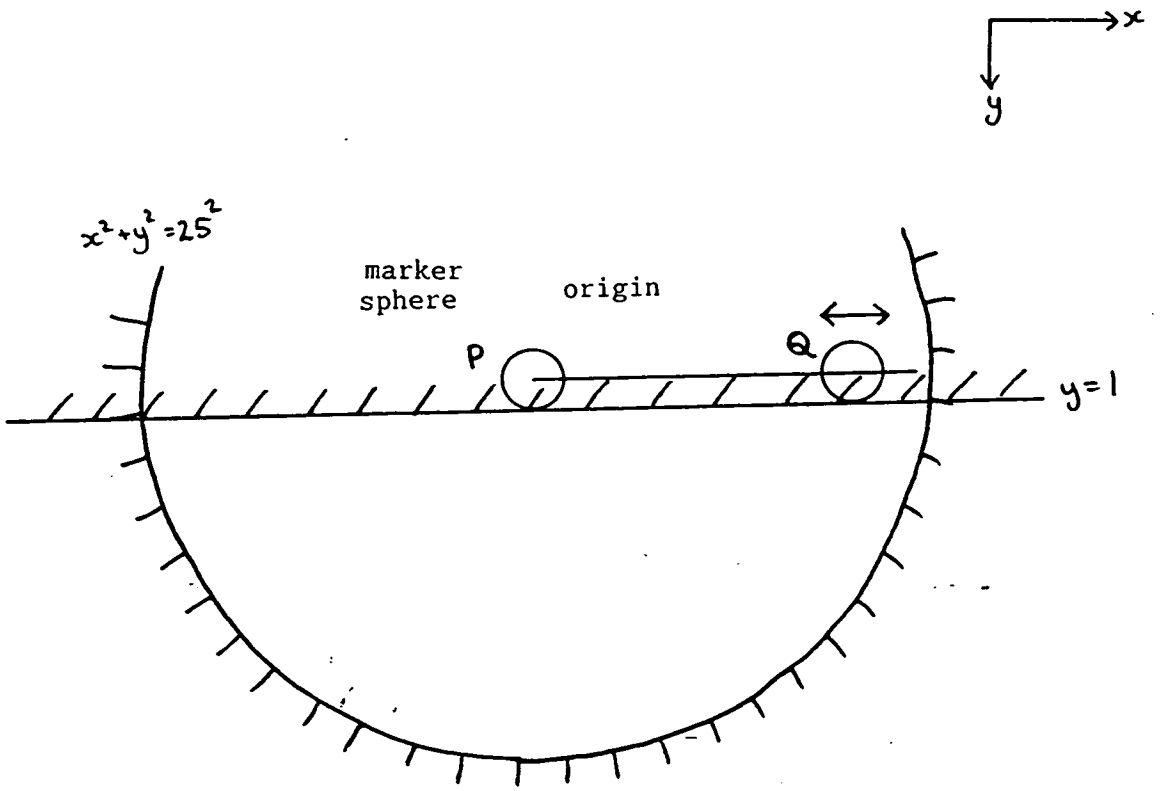

Figure 4.13 - Effects of simple averaging and quadrant flips on lesion position estimates during redundant measurements.

Lesion position (0,7.2)

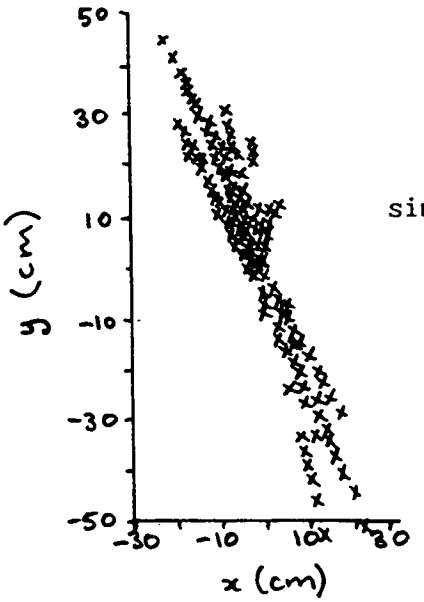

simple averaging

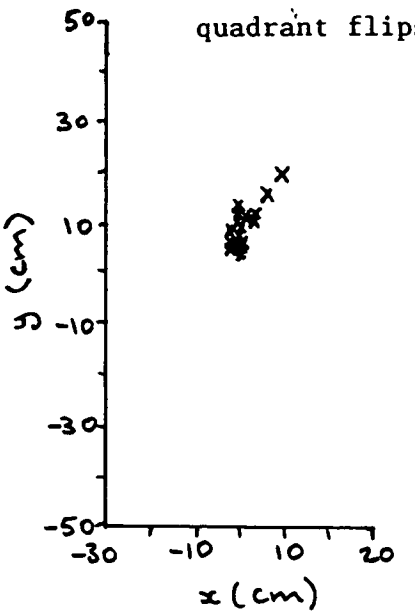

quadrant flips with simple averaging

possible flip angles are assigned to a quadrant and the lesion position estimates calculated. An example, shown in Figure 4.13 and based on lesion position (0,7.2), illustrates the overall effects of all these changes.

4.10.4. Application of Quadrant Flips to Redundant Measurements

Table 4.2 shows the percentage of average results within 1cm and 0.5cm errors for different lesion positions with induced quadrant flipping. The raw data used was identical to that used to generate the results in Table 4.1. In most cases the quadrant flipped results are a great improvement. For example, comparing Table 4.1 and Table 4.2 , at lesion position (10.3,7.4), averaged results have improved from 38.5% to 70.2% within 1cm error and from 23.1% to 40.5% within 0.5cm error. This difference is large because the viewing range is small and the number of wrongly assigned angles is large. However, in a few cases results are slightly worse. At lesion position (6.1,3.6) all angles are initially correctly assigned. Over one third of the angles lie within the 60°-120° flip range. On applying quadrant flips a few angles are reassigned and hence results deteriorate slightly, for example from 98.6% to 96.9% within 1 cm error and 88.2% to 87.0% within 0.5cm error on simple averaging. These tend to occur when either 3 similar angles or 2 similar and a third close to 90° are used, ie all 3 pairings give bad estimates.

Hence, generally, applying quadrant flips improves results greatly and should be used with redundant measurements. Some results are shown in Figure 4.14 as plots of percentage within error range against error, superimposed on the original results obtained without applying quadrant flips. Once again graphs at

Table 4.2 - Percentage of results which are within the indicated error bounds when quadrant flips are induced.

Lesion Position	% within +1cm error	% within +0.5cm error
0,2.4	96.9	91.2
0,4.8	97.7	84.8
0,7.2	85.4	68.9
-0.2,10	52.2	21.9
-0.4,14.2	36.0	15.1
2.9,2.3	96.8	85.8
3.0,4.8	78.9	42.9
3.0,7.2	91.0	72.7
2.9,9.9	51.8	23.2
2.9,15	32.7	10.5
6.0,2.4	89.7	75.1
6.1,3.6	96.9	87.0
6.4,4.2	83.3	60.7
6.1,4.8	88.1	72.3
6.1,6.1	90.3	77.6
6.6,8.6	28.4	11.3
9.8,2.4	87.0	69.4
9.8,4.8	54.1	27.6
10.3,7.4	70.2	40.5
10.2,9.8	29.6	10.2

Figure 4.14 - Graphs of percentage of results within the error range against error (cm) for different lesion positions.

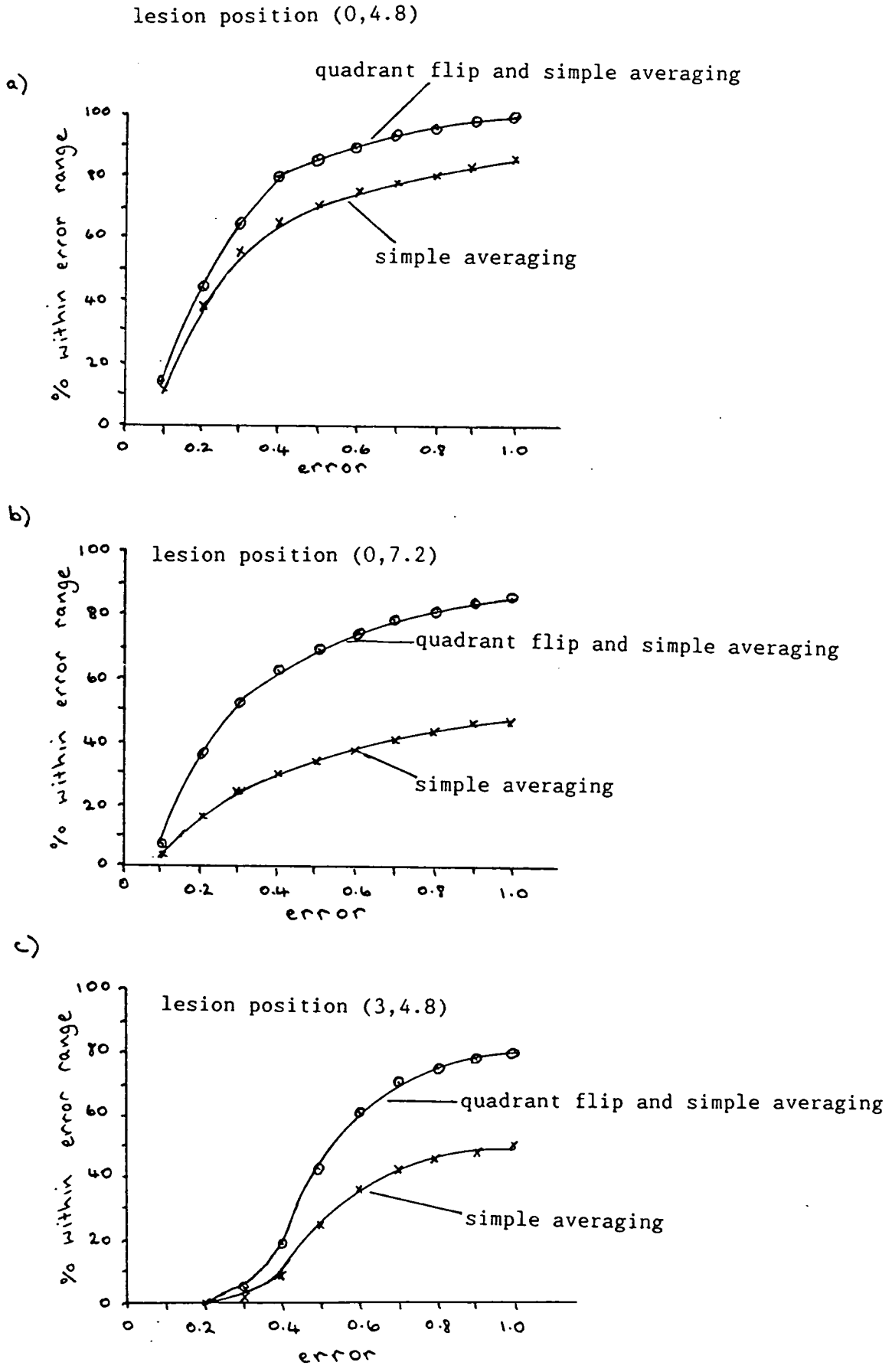

d)

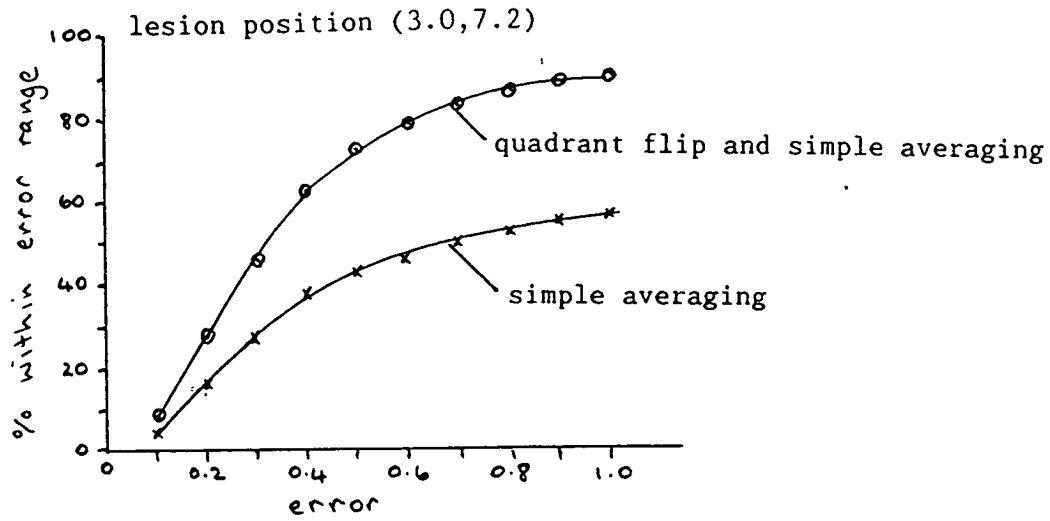
lesion position (3.0,7.2)
% within error range
100
80
60
40
20
0
0
0.2
0.4
0.6
0.8
1.0
error
quadrant flip and simple averaging
simple averaging

e)

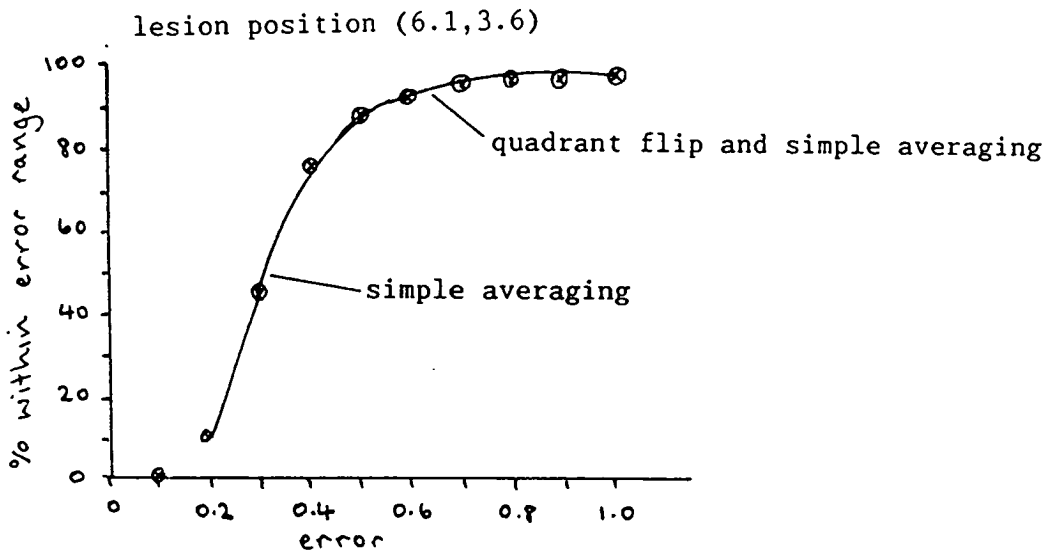
lesion position (6.1,3.6)
% within error range
100
80
60
40
20
0
0
0.2
0.4
0.6
0.8
1.0
error
quadrant flip and simple averaging
simple averaging

f)

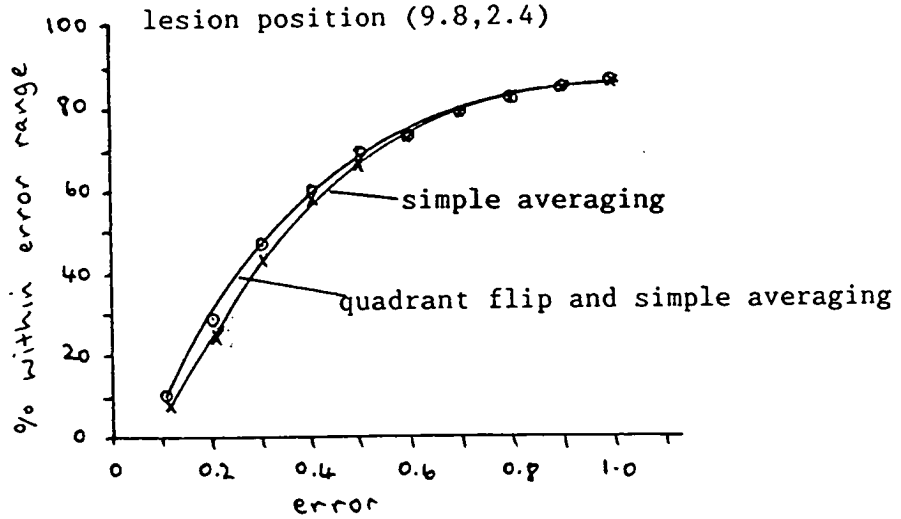
lesion position (9.8,2.4)
% within error range
100
80
60
40
20
0
0
0.2
0.4
0.6
0.8
1.0
error
simple averaging
quadrant flip and simple averaging

different lesion positions cannot be directly compared.

4.11. Attempts at Estimate Improvement

4.11.1. Application of Lesion Constraints on the Possible Estimates

In an attempt to further improve the lesion location estimation procedure the bounds within which acceptable estimates lie were reduced by application of a further constraint on lesion depth. The maximum depth below the patient's skin at which a lesion must lie, assuming that the patient lies either prone or supine, is 6 inches, ie 15cm, as shown in Figure 4.15. (6 inches is also the maximum length of biopsy needle available). The marker sphere radius is 1.25 cm and hence the vertical lesion distance from P when that touches the skin surface may reach a maximum of 16.5cm. Allowing for errors and some working clearance between the patient and marker, the constraint on depth has been set at 20cm maximum.

Results for shallow lesions are identical to those previously observed. However for deep lesions, for example (-0.4,14.2) results are noticeably worse. This occurs because often when a 90° view is involved the inaccurate true estimate may lie deeper than 20cm and is hence eliminated from the averaging process. The depth constraint has therefore been relaxed back to 25cm.

4.11.2. Alteration of the Applicable Range for Quadrant Flips

Narrowing the flip range from 60°-120° again causes results to deteriorate as many results which have been wrongly assigned are then ignored. Increasing the range to 55°-125° improves results for lesion position (3.0,4.8) as shown in Figure 4.16, which has one angle flipped from 125 to 55°. However, more generally,

Figure 4.15 - Typical human body dimensions

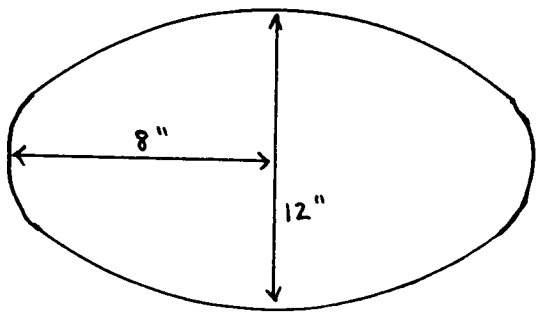

Figure 4.16 - Graphs of percentage within error range against error for lesion position (3.0,4.8)

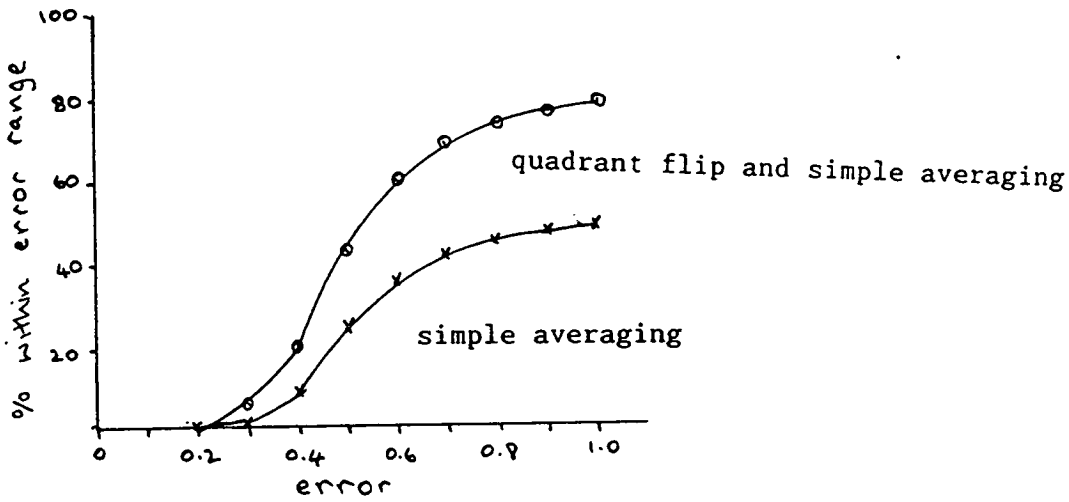

a) Quadrant flip range 60°-120°

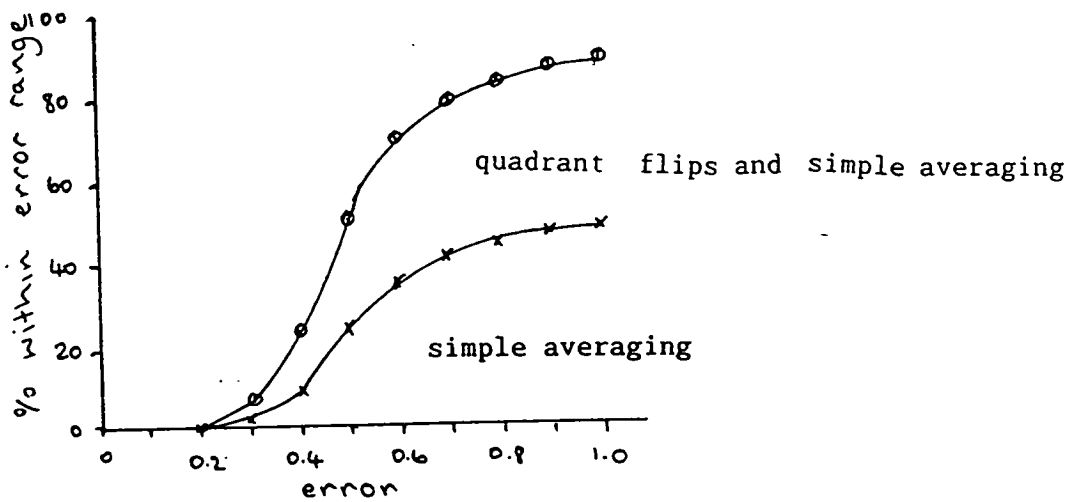

b) Quadrant flip range 55°-125°

results deteriorate. The quadrant flip range is hence taken as 60°-120° and the constraints on lesion position estimates as:

$$x^2 + y^2 < 25^2$$

$$y > 1.0$$

4.12. Number of Views (Extent of Redundancy) Necessary to Ensure Accurate Lesion Position Estimate

It is necessary to decide upon a strategy for the number of views which must be taken.

If the surgeon is provided with information regarding good/bad views and uses only good views, then only two such views are required.

However, in some cases, two good views are not always available, for example when the lesion is obscured except for a very small range of angles. This can occur when the lesion lies in the apex of the lung and can be viewed only from close to 90°. In this case redundant measurements must be used.

To obtain any more than three views becomes excessively time consuming and increases unacceptably the total dose of radiation. Therefore a maximum of three views should be used.

As the surgeon may not be privileged to information regarding good/bad views, three views should be used as standard.

An alternative possibility is for the computer to 'ask' for another viewpoint should one of the initial two views lie in a bad range.

Quadrant flips should be used when redundant measurements are necessary.

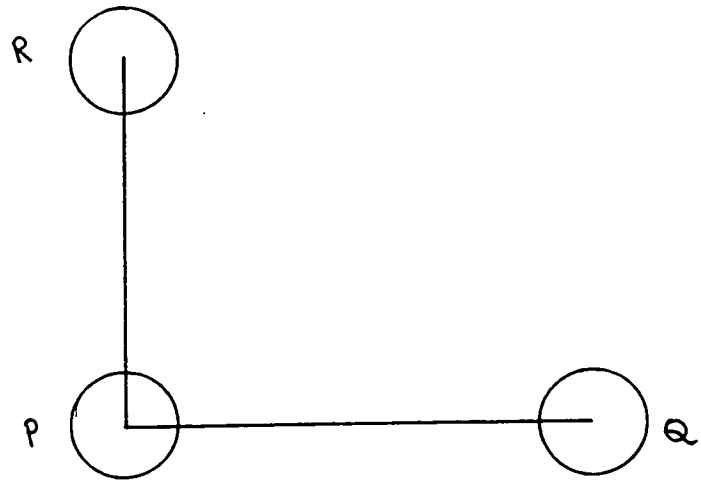

Figure 4.17 - Perpendicular marker arrangement for the two dimensional situation.

Figure 4.18 - Quadrant determination from the image appearance.

1st quadrant view

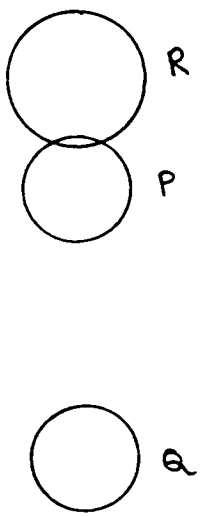

In the 1st quadrant R will lie on the opposite side of P to Q.

2nd quadrant view

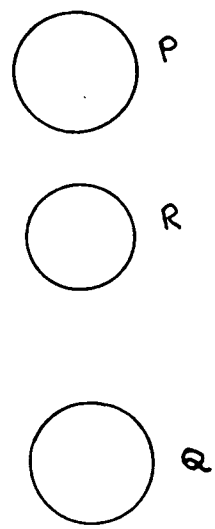

In the 2nd quadrant R will lie on the same side of P as Q.

4.13. Improvement of Angle Estimation

Accuracy for viewing angles close to 90° may be improved by substituting a nearly vertical rod perpendicular to the original marker rod presently used, as shown in Figure 4.17. Changes in viewed rod length with angle are hence large when close to 90°. To use this method, however, is not as simple as it first appears. Although the calculated angle may be more accurate the quadrant cannot be determined merely by combining the calculated distance from the X-ray source to the sphere with rod length as before. Hence additional information is required. The system may be completely defined by inclusion of the original horizontal marker, ie by using two marker rods perpendicular to each other. The spheres P and Q on the horizontal rod enable the quadrant to be determined as previously. However this involves quadrant flips. Alternatively, and probably more accurately, examining the relative image positions of spheres P, Q and R will determine the quadrant, as shown in Figure 4.18. However the image becomes cluttered for the two dimensional situation with the lesion and the three spheres, all of which must be uniquely distinguishable, lying on the image line. This is undesirable since it leads to operator confusion when picking off the image points with the mouse. Hence for the two dimensional machine a single marker rod is used as standard although for a later three dimensional machine a perpendicular marker arrangement for each rotation plane may be less clumsy since the image will appear as a plane, not as a single line and the images hence appear more spread out.

4.14. Conclusions

Due to the complexity of the X-ray image field containing anatomical structures, suspected lesion and reference marker, it

is not practicable to identify the relevant image points automatically by using conventional image analysis techniques. A manual system, which depends on the skill of the operator to recognise relevant features, and using a mouse pointer to measure their dimensions, has been devised and tested and found to give sufficiently accurate and reproducible estimates of lesion position when using a full-scale optical analogue of the C-arm machine and patient arrangement. Redundant measurements have been demonstrated to improve results when viewing angles are in the range 60°-120° from the horizontal reference marker. Quadrant flips further improve the estimates. Use of a perpendicular marker would eliminate the need for redundant measurements and additional X-ray takes. However imaging requires location of three spheres instead of two. The image becomes cluttered and confusing and the perpendicular marker is hence not recommended.

CHAPTER 5.

DEVELOPMENT OF THE BIOPSY MACHINE.

5.1. Introduction

Methods have been established for image analysis and position location of 'hidden' objects by using an optical reference marker. It remains to combine all these techniques and develop a biopsy machine which will enable accurate positioning of a biopsy needle to sample the lesion. The various design stages of the machine are detailed in the sections that follow.

5.2. Basic Operations.

It is necessary to examine the proposed sequence of operations (based on the existing biopsy method) which will be carried out during the computerised biopsy procedure. Figure 5.1 outlines the basic procedures.

5.3. Design Criteria

At this stage several points are apparent:

1) The positions of the marker (on or near the patient's chest), the lesion, the chosen needle insertion point on the skin must be known relative to some common reference.

2) The surgeon must choose the point, on the patient's skin, at which the needle will be inserted. At this stage he will know the calculated lesion position. The insertion point must be chosen to allow a direct approach towards the lesion avoiding ribs, arteries, and other internal organs such as the heart. Some means of registering this chosen location for the insertion point with the controlling computer is therefore necessary.

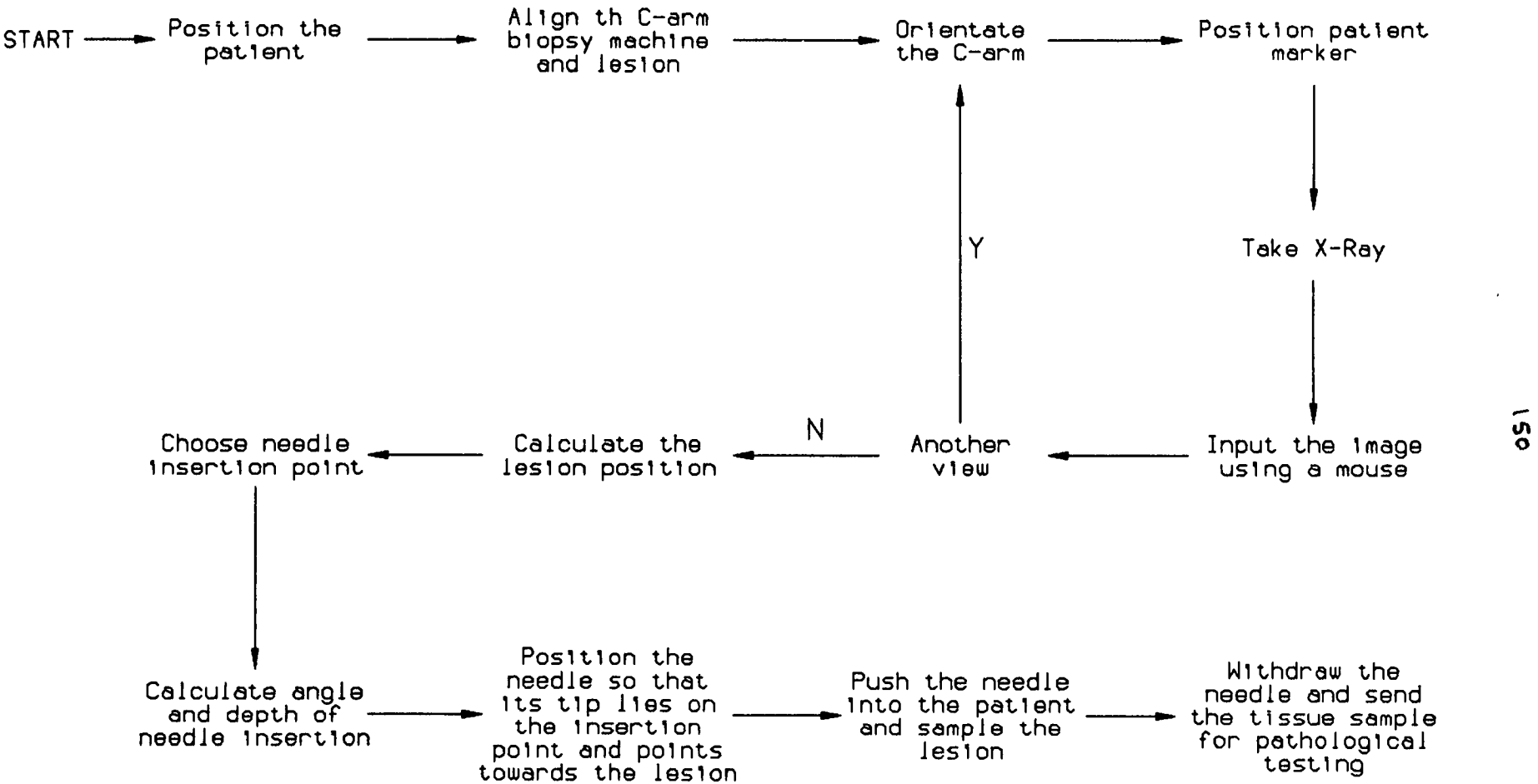

FIG 5.1 - Proposed sequence of operations for the computerised biopsy procedure

Several conclusions have been drawn from previous analyses:

1) The marker rod length must be adjustable to allow a wider range of viewing angles.

2) The marker should be positioned as close as possible to the patient (and thus to the lesion) for most accurate results.

3) A bar, positioned above and close to the patient's chest, will assist in reproducibility of breath holding.

4) The marker rod length may be adjusted between views, provided that the sphere representing the origin (for lesion location), remains fixed.

5) The patient (and supporting trolley) must remain in the same position between views - only the X-ray machine may be moved.

6) The needle must remain sterile.

7) The machine must be capable of accommodating needles of various lengths and thicknesses.

It is apparent that the machine must comprise three distinct functional parts: A patient marker, an insertion point indicator and a needle holder/angling device. All three must be able to be freely positioned wherever required relative to the patient but their positions, and that of the lesion, must be known relative to some fixed datum. Some connection must therefore exist between the frame of the machine and all three devices.

5.4. The Biopsy Machine.

A horizontal arm, cantilevered from the floor, spanning the patient and trolley and having the necessary devices suspended from it was chosen as the most suitable method of support and is shown in Figure 5.2.

It was decided to fix the three devices onto a single rail, along which each can travel. Transducers determine the relative positions of each device on the rail.

The devices are of two types: The marker and needle insertion point indicator require manual positioning relative to the patient but the needle positioning thereafter is fully specified and positioning may be done automatically. It seems prudent to mount the two manually positioned devices on the same carriage so that the rail may be less cluttered.

The machine therefore consists of a main rail from which two carriages are suspended: One is manually driven, the other is motorised.

5.4.1. The Manual Carriage.

The manual carriage contains both the patient marker and the needle insertion point indicator, both of which require to be positioned by the operator.

The manual carriage has a telescopic extension, the far end of which is connected to a linear transducer running the full length of the support rail: The position of the free end of the telescopic section on the rail at any instant can thus be determined.

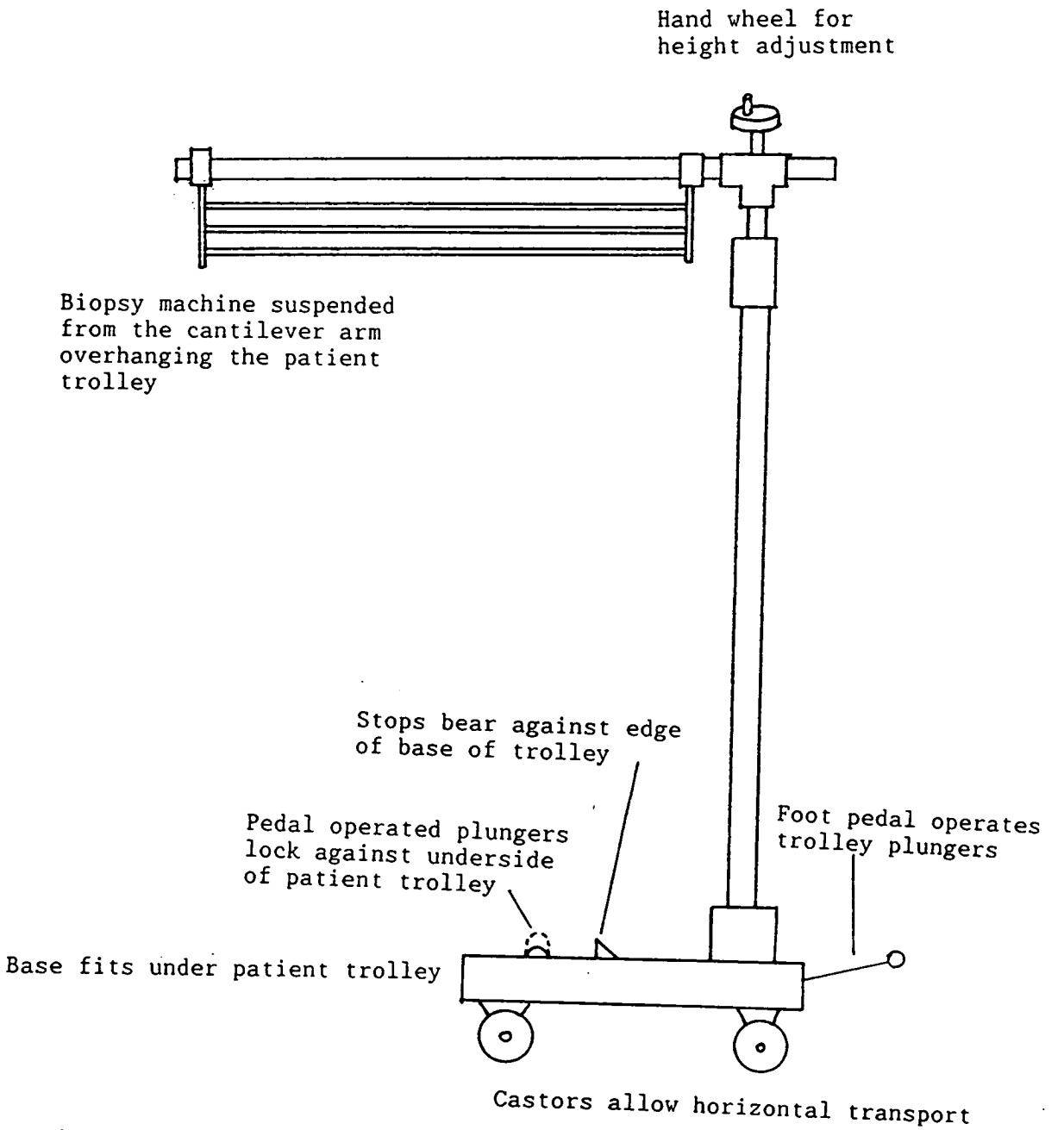

Figure 5.2 - The general arrangement of the machine support.

Normally the telescopic section is retracted into the main carriage and the two sections move as one along the rail. A manual lever on the main carriage faceplate enables the main carriage to be locked to the rail. This action at the same time releases the telescopic section and allows it around 15 cm of unrestricted movement away from the main carriage as shown in Figure 5.3. A further locking device on the telescopic section fixes it to the rail. Both locking levers act against continuous strip switches, adapted from those provided for bus passengers to sound the 'stop' bell. These also run the full length of the rail, and indicate to the computer when each locking action is completed.

5.4.1.1. The Patient Reference Marker.

The patient marker consists of two red lead coated (and thus semi X-ray opaque) 1-inch spheres fixed to rods or stems which project out from the manual carriage front and are arranged to lie with their centres on a nominally horizontal line, as shown in Figure 5.4. The line of centres is parallel to the direction of carriage movement along the rail, but displaced 10 cm out from the carriage front. The actual marker rod has been eliminated: The marker length is indicated by the distance between sphere centres. This has the benefit that the X-ray image appears less cluttered.

One sphere, whose stem is attached to the main carriage, is used to represent the origin in lesion position calculations. When not in use it can be folded away.

A second sphere is mounted on the telescopic section of the manual carriage. The line of centres of the two spheres, parallel to the rail, is used as the x-axis in calculation of the lesion position. Since the second sphere is fixed to the telescopic

Figure 5.3 - The telescopic section of the manual carriage

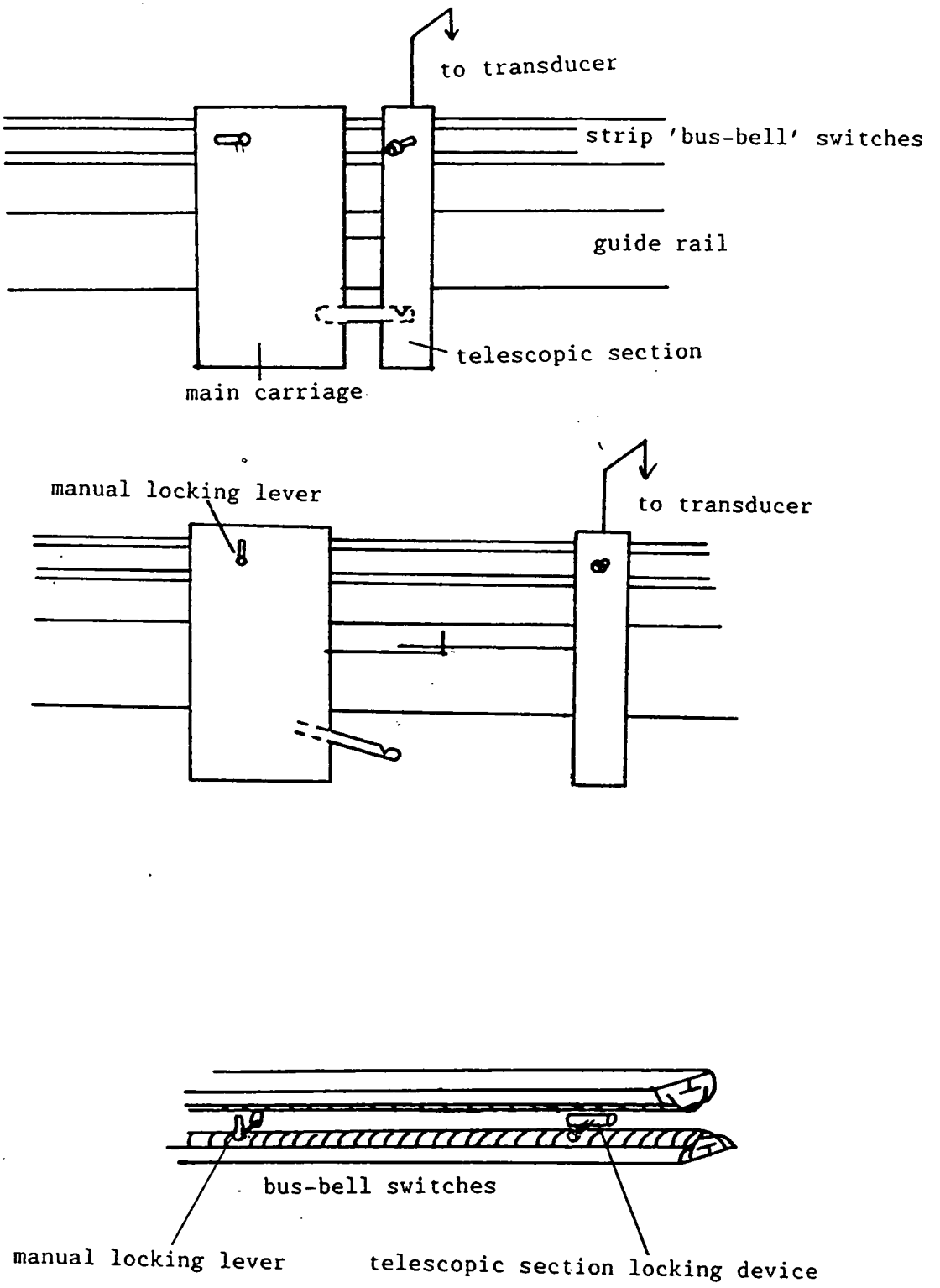

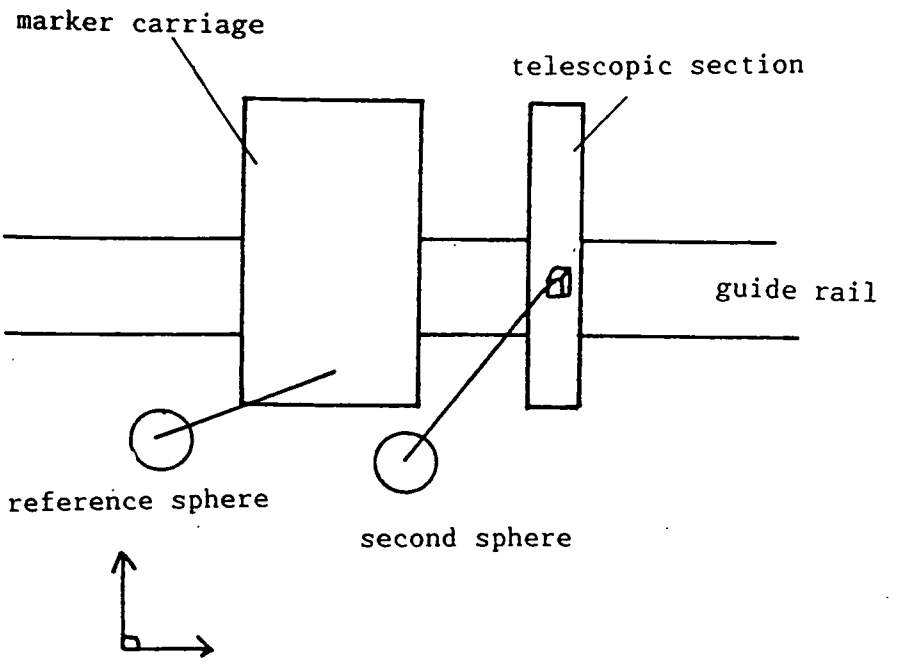

Figure 5.4 Marker arrangement

section the separation distance between the two spheres can be easily altered. The linear transducer, although connected only to the telescopic section and the second sphere, can register both sphere positions. The position of the second sphere is first registered while the telescopic section carrying it is retracted and secured to the main section of the manual carriage on which the reference sphere is mounted. The main carriage is then locked in position on the rail by clockwise movement of a lever which at the same time releases the telescopic section. That section, and the second sphere, can then be moved the desired distance away from the first. Its new position is measured by the linear transducer and is then registered by the action of locking the telescopic extension to the rail. The difference between the two transducer readings, plus the offset between the two spheres when the telescopic section is closed, gives the true marker length, ie the distance between the sphere centres. The spheres are arranged so that their lowest points are well below the carriage structure. The patient marker spheres can thus be placed in contact with, or very close to the skin surface and thus as close as possible to the lesion allowing more accurate calculation of the lesion position. They may also assist in breath holding reproducibility instead of the chest bar previously recommended.

5.4.1.2. Needle Insertion Point Indicator.

The needle insertion point indicator is a small metal ring which is fixed to an arm forming part of the support of the reference sphere. The entire assembly is mounted on a vertical slide on the front of the manual carriage. To register an insertion point the sphere is folded out of the way and the indicator ring is swung into position about a vertical axis through a quarter turn, as shown in Figure 5.5. The indicator moves with the manual carriage along the rail but lies 5 cm closer to the rail than the marker spheres.

Figure 5.5 - The insertion point indicator

a) original position

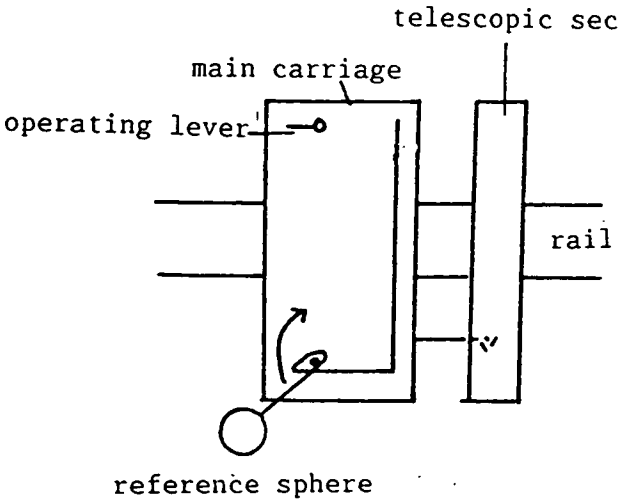

b) sphere folded away

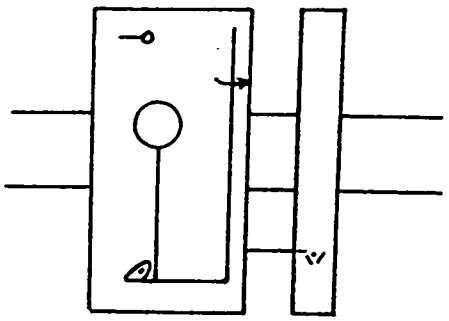

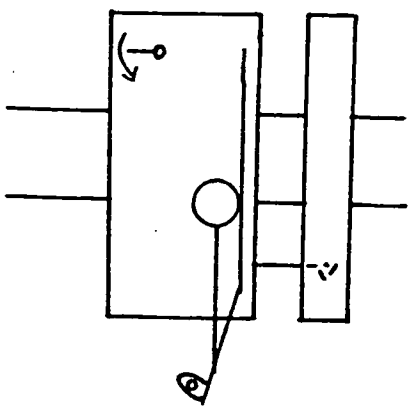

c) needle insertion point indicator pulled out

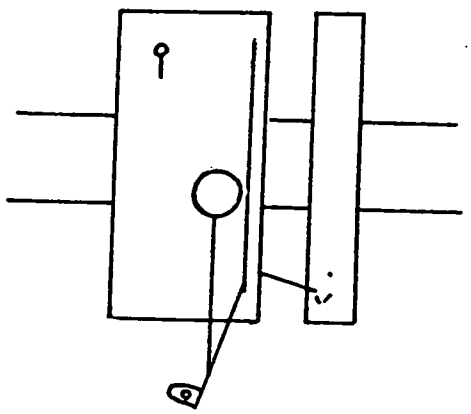

d) needle insertion point locked in x position. Telescopic section and slide now free for movement in the y direction

The manual carriage is slid along the rail until the indicator is positioned vertically above the chosen insertion point. the carriage is locked in place using the same locking lever as was used for the marker positioning but now rotated anti-clockwise, closing the lower 'bus-bell' switch. This action registers the position of the manual carriage on the linear transducer, thus giving the x-coordinate of the indicator. At the same time the anti-clockwise movement of the lever locks the main carriage to the rail and frees the telescopic section. It also couples the latter to the insertion point indicator pulley system. Turning a small knob on the main carriage front works the pulley and moves the indicator down its slide and at the same time moves the telescopic section away from the main carriage, as illustrated in Figure 5.6. When the indicator touches the patient's chest the surgeon indicates by keystroke to the computer to register the transducer reading. The difference between the x-coordinate reading and the latter reading indicates the depth through which the indicator has moved. Adding on the known depth or y displacement offset from reference sphere P gives the y-coordinate of the chosen insertion point . The insertion point is thus specified relative to sphere P, as illustrated in Figure 5.7.

5.4.2. The Motorised Carriage.

Once all the manual inputs have been entered and the lesion position calculated by the computer it remains to position the needle for accurate lesion sampling. This is done automatically.

The motorised carriage is served by three 1.8° four-phase stepper motors located in the fixed framework of the machine. A nut, fixed in the carriage, engages a multi-start leadscrew extending the full length of the rail One motor turns the screw and so traverses the carriage along the rail. A 10-turn potentiometer

a) horizontal coordinate

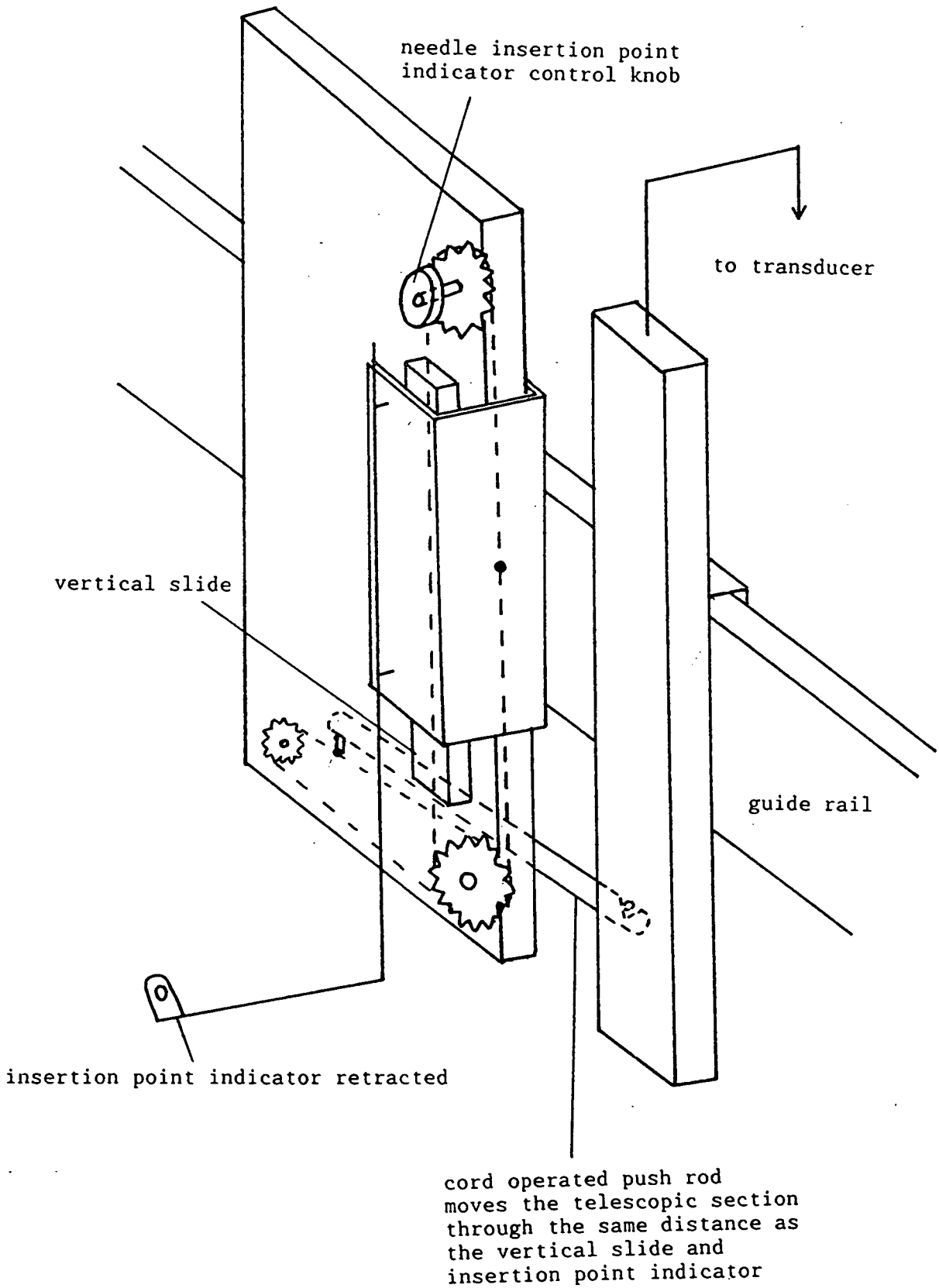

Figure 5.6 - The manual carriage as used for needle insertion point indication

b) vertical coordinate

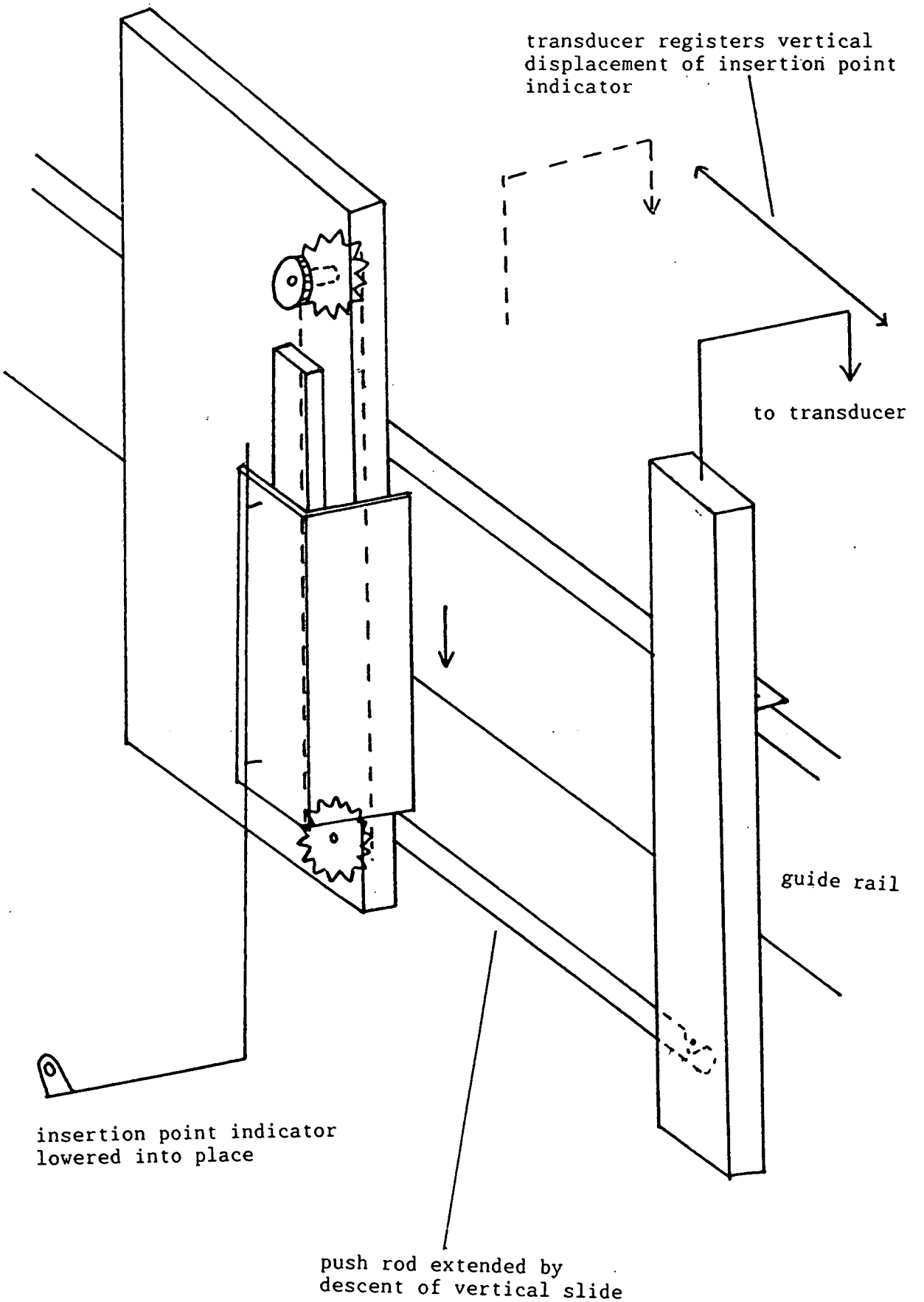

Figure 5.7 - Insertion point coordinate calculation

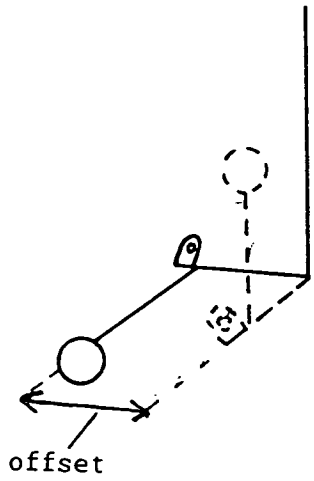

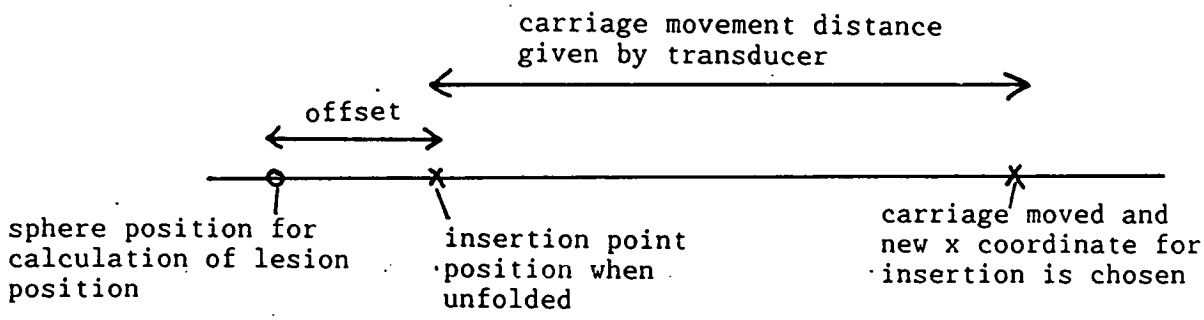

x-coordinate = registered transducer reading at chosen
insertion point
- registered reading at original marker position
+ offset

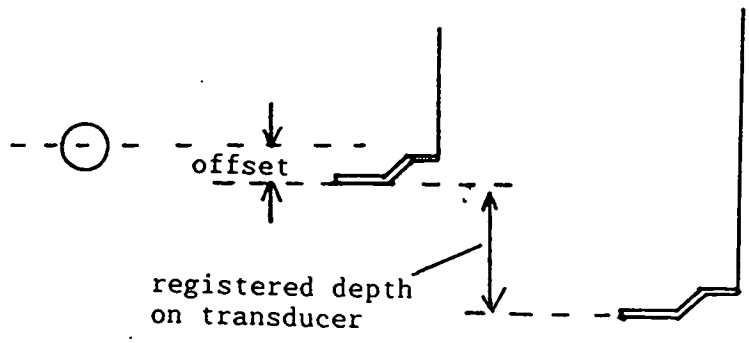

y-coordinate = transducer reading after indicator lowered
- transducer reading for x-coordinate
+ offset

registers the position of the carriage. 20 turns of the screw are required for the carriage to traverse the full rail length and so the 10-turn potentiometer is located on the low speed side of a 2:1 step-up gearbox as shown in Figure 5.8.

The two further motors each turn splined shafts, placed one above the other, parallel to the rail and extending its full length. 10-turn potentiometers, at the free ends of the shafts, indicate the number of shaft rotations. The shafts pass through nuts, shown in Figure 5.9, and are free to slide upon them but constrained by the splines to turn with them. Each nut is journalled in a ball race fixed in the motorised carriage and is coupled to a toothed wheel connected, via a toothed belt, to a pulley wheel on each of two gearboxes which are contained within the carriage (illustrated in Figure 5.10).

The two gearboxes installed inside the carriage lie one behind the other and the output shaft from the back gearbox runs through the bore of a hollow tube which forms the front gearbox output shaft. The needle guide is secured directly to the outer tubular shaft; the chain-wheel which drives the needle depthing mechanism is secured to the inner shaft. Turning the upper shaft operates the front gearbox and angles the needle guide shown in Figure 5.11. The angling is restricted to approximately + or - 90° from the vertical by two stops on the front carriage face. These prevent unwinding of an anti-backlash spring located between the needle guide and the front face of the carriage.

Needle insertion is not motorised but a motorised depthing mechanism is included. The lower splined shaft drives the back gearbox and turns the shaft which passes through the front gearbox and needle guide. A sprocket wheel on the end of this shaft engages an endless chain behind the needle slideway. This chain passes over tensioning wheels mounted on the slideway. One

Figure 5.8 - Motorised carriage drive unit

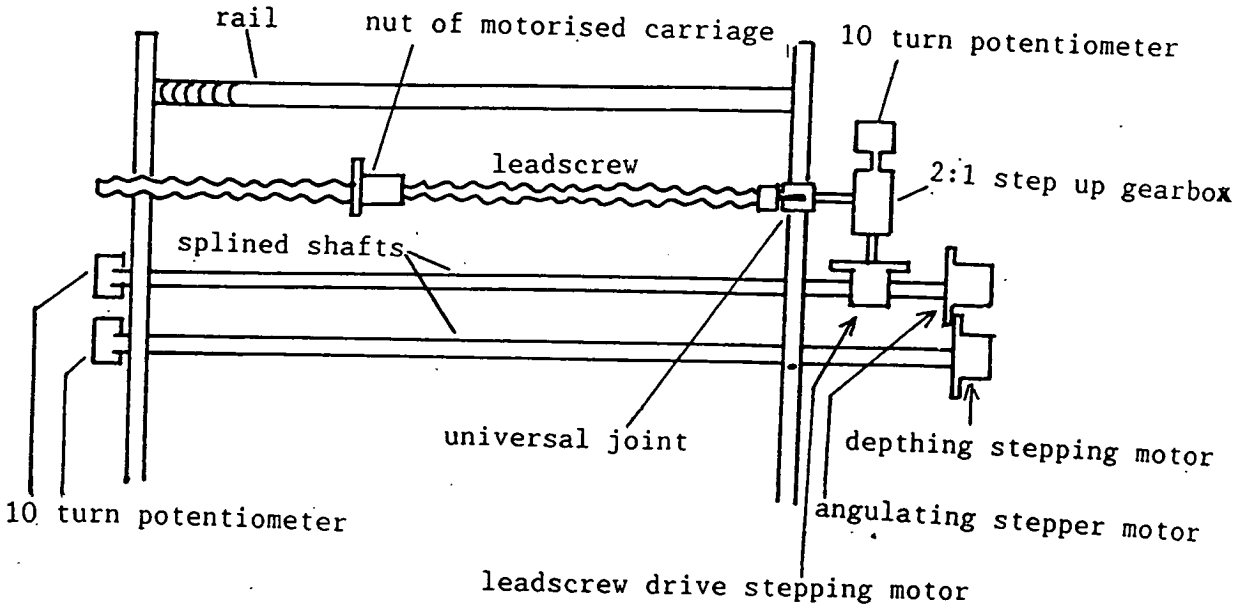

Figure 5.9 - Splined shaft, nut and drive adaptor

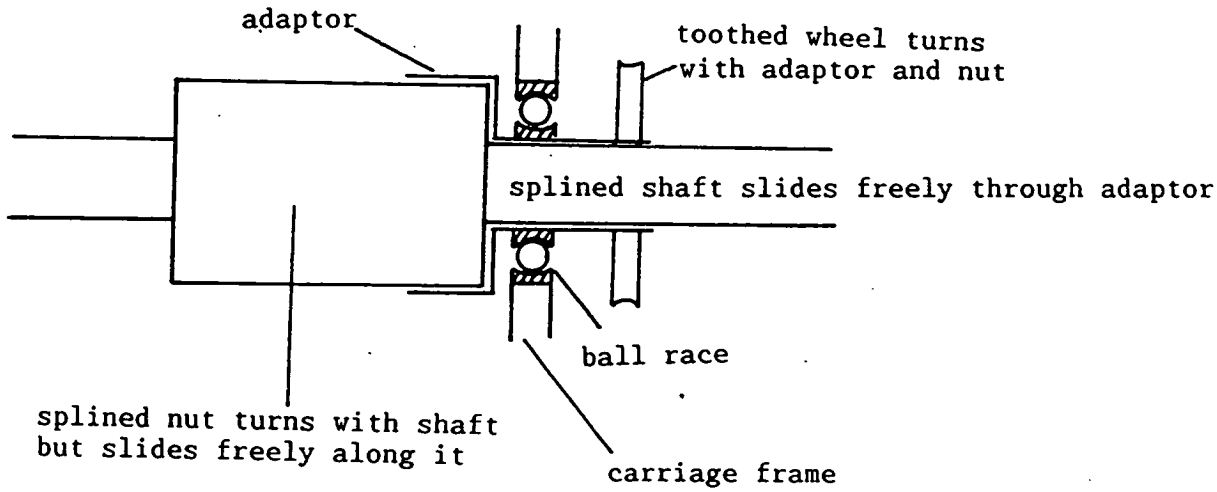

Figure 5.10 - Connections between the drive shafts and the motorised carriage. Main carriage with faceplate removed.

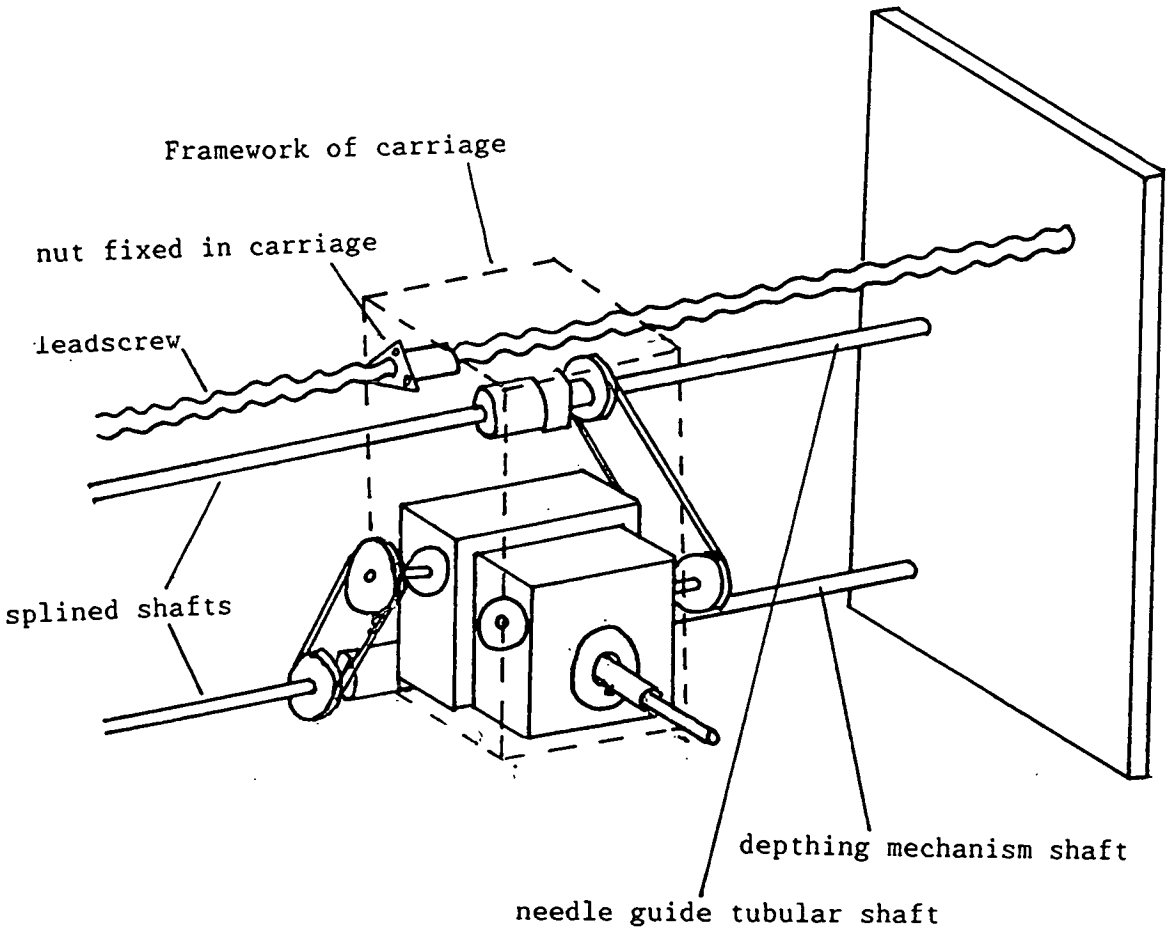

Figure 5.11 - Needle guidance mechanism

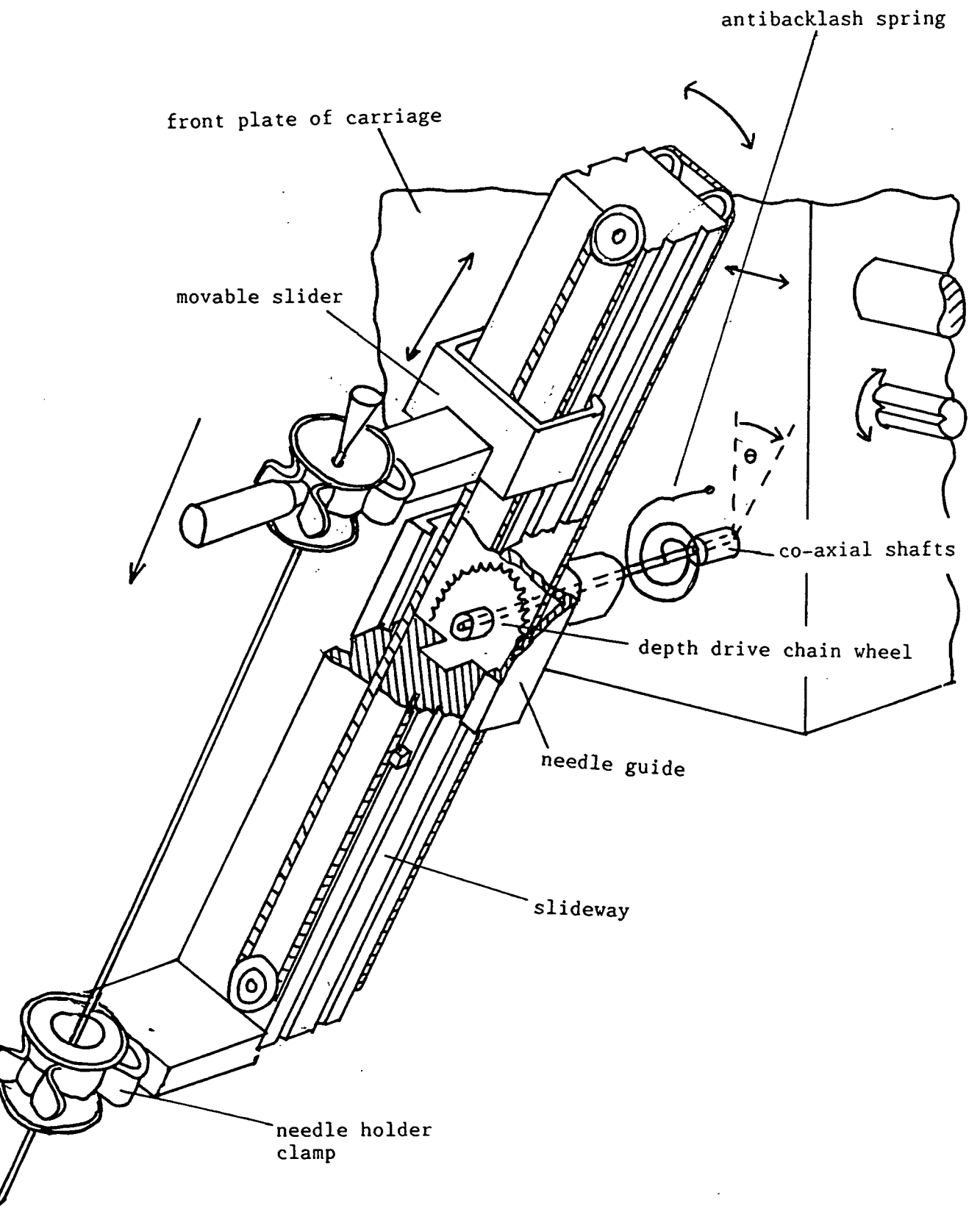

of these drives a shaft extending through the slideway to the front, where it carries a second sprocket wheel which drives a further chain, positioned on the front of the slideway. A metal stop is carried by this second endless chain. A slider free to move up and down the needle slideway is locked to the upper end of the needle and cannot pass the stop on the chain, unless manually over-ridden by deflection of a spring latch.

The biopsy needle, which must remain sterile, fits central holes drilled in each of two sterile brass holders, as shown in Figure 5.12. These holders fit into two clamps- one fixed on the lower end of the needle slideway and the other to the slide end. The upper holder can be locked to the needle. Moving the slider causes the needle to slide through the lower holder and out (and into the patient's chest). Several sizes of these close fitting needle holders will be required - one for each different gauge of biopsy needle.

The needle stop is carried by an endless chain whose setting is uniquely determined by the angular position of the depthing sprocket wheel. Thus when the latter has turned through the computed angle corresponding to the required depth of needle insertion , the needle slideway may be slid downwards through the guide as necessary without altering this depth. Thus the lower needle holder may be brought into contact with the patient's skin to give maximum support and guidance to the needle during subsequent insertion, without affecting the depth of penetration allowed by the stop setting.

5.4.2.1. Additional Equipment Necessary.

Basic electronic circuits are necessary in addition to the main biopsy machine equipment. The motors are driven by drive boards (one board per motor) which control the motor turning direction and speed. Speed is controlled by varying the rate of motor

Figure 5.12 - Needle holders

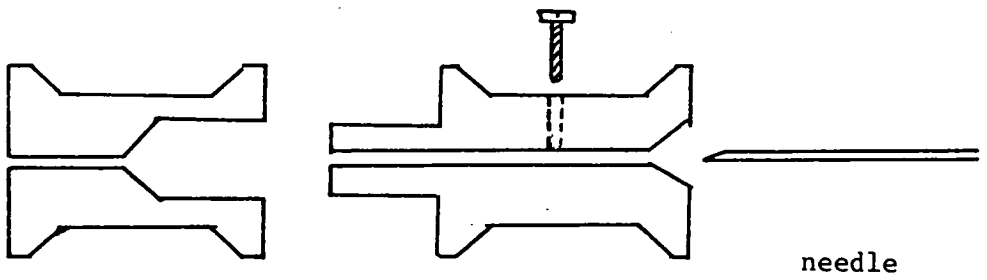

stepping. Each time the board receives a negative pulse the motor shaft turns through 1.8°. By varying the square wave period the stepping rate, and hence the motor speed, is changed.

Transistor switches are used in all digital inputs and outputs from both the analogue and printer ports. LED's are also included on the motor clock inputs to indicate which line is operating and to assist in fault finding should any connections become faulty.

5.5. Control Of the Biopsy Machine.

A BBC Master personal computer is used to control and monitor the biopsy machine operation. The biopsy machine requires inputs/outputs for several different functions. The equipment and their requirements are detailed in Table 5.1.

The BBC has several, easily accessible input and output ports available for digital and analogue(inputs only) signals as well as a 5V power supply, a 1.8V power supply and an earth line. These are shown in Table 5.2.

However, the AMX mouse operates from the user port and these last channels are not available for use.

It is hence obvious that the four analogue input channels on the 'analogue in' port be used to register the readings from the three potentiometers and the linear transducer. The analogue input voltage range is 0-1.8V. The 0V and 1.8V output pins can be used to supply the power to the transducers.

The two digital inputs on 'analogue in' can be used to register when the two strip or bus-bell switches are operated i.e. when the different sections of the carriage are locked in place and hence which action is underway.

Table 5.1. - Equipment Input/Output Requirements

EQUIPMENT	FUNCTION	COMPUTER CONNECTIONS	NO OFF
Linear Transducer	Indicates the position of the telescopic section of the manual carriage (and hence positions of the main section and entry point indicator).	+5V 0V 1 Analogue Input	1
10-Turn Potentiometers (3)	Control and indicate position of motorised carriage, needle angling and depthing devices.	+5V 1 Analogue Input	3
Drive Board	Drives the motors and controls the motor step rate and direction of rotation. Each board requires an independent power supply of 15-30V.	+5V 0V 2 Digital Outputs	3
Bus-bell Switches (2)	Indicate when the manual carriage is locked in place and identify significance transducer signals.	+5V 0V 1 Digital Input	2

Table 5.2 - BBC Hardware Ports

PORT	INTERNAL POWER SUPPLIES AVAILABLE	CONNECTIONS AVAILABLE
Analogue In	+5V +1.8V 0V	4 Analogue Inputs 2 Digital Inputs
6522 A side 8-bit parallel printer port	+5V 0V	8 Digital Inputs and/or Outputs
6522 B side 8-bit user port	+5V 0V	8 Digital Inputs and/or Outputs

The motor drive boards require two digital computer inputs each - one to control the motor turning direction, the other to control the 'clock', i.e. the rate at which each motor step is made. A ground connection is also required.

All digital inputs and outputs are via transistor switches. These switches prevent accidental overloading of the computer, which would result in component failure. The 'clock' outputs have, in addition, LEDs, which flicker as the clock signal changes. This assists in fault finding if faulty connections arise.

A general overview of the arrangement of computer, biopsy machine equipment and associated electronic connections is shown in Figure 5.13. Figures 5.14 and 5.15 show more detailed diagrams of the connections.

5.6. Machine Alignment.

Machine alignment is a process of trial and error which involves minute adjustments to the positions of various equipment items.

5.6.1. Efficient Mechanical Running.

It is essential that the splined shafts and leadscrew are aligned with the main rail. The drive motors used have a low maximum torque, above which they slip. They have been selected on the principle that if anything should go wrong the motors will slip rather than continuing to drive the shafts and carriage, which could cause irreparable buckling to the machine. If the shafts are slightly mis-aligned the torque required to drive the carriage is sometimes excessive and the motor thus slips. The helical screw has one unattached free end and thus alignment is automatic. The splined shafts, however, are attached to potentiometers which are fixed to the endplate. Although they are

Figure 5.13 - Biopsy machine and associated drive equipment

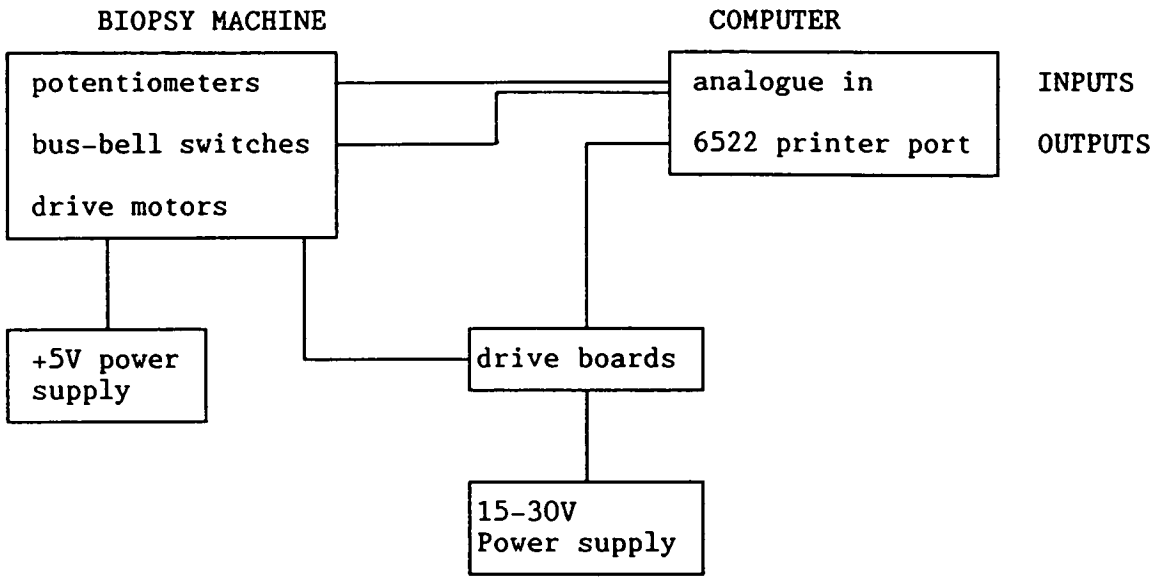

Figure 5.14 - Connections to the analogue input port

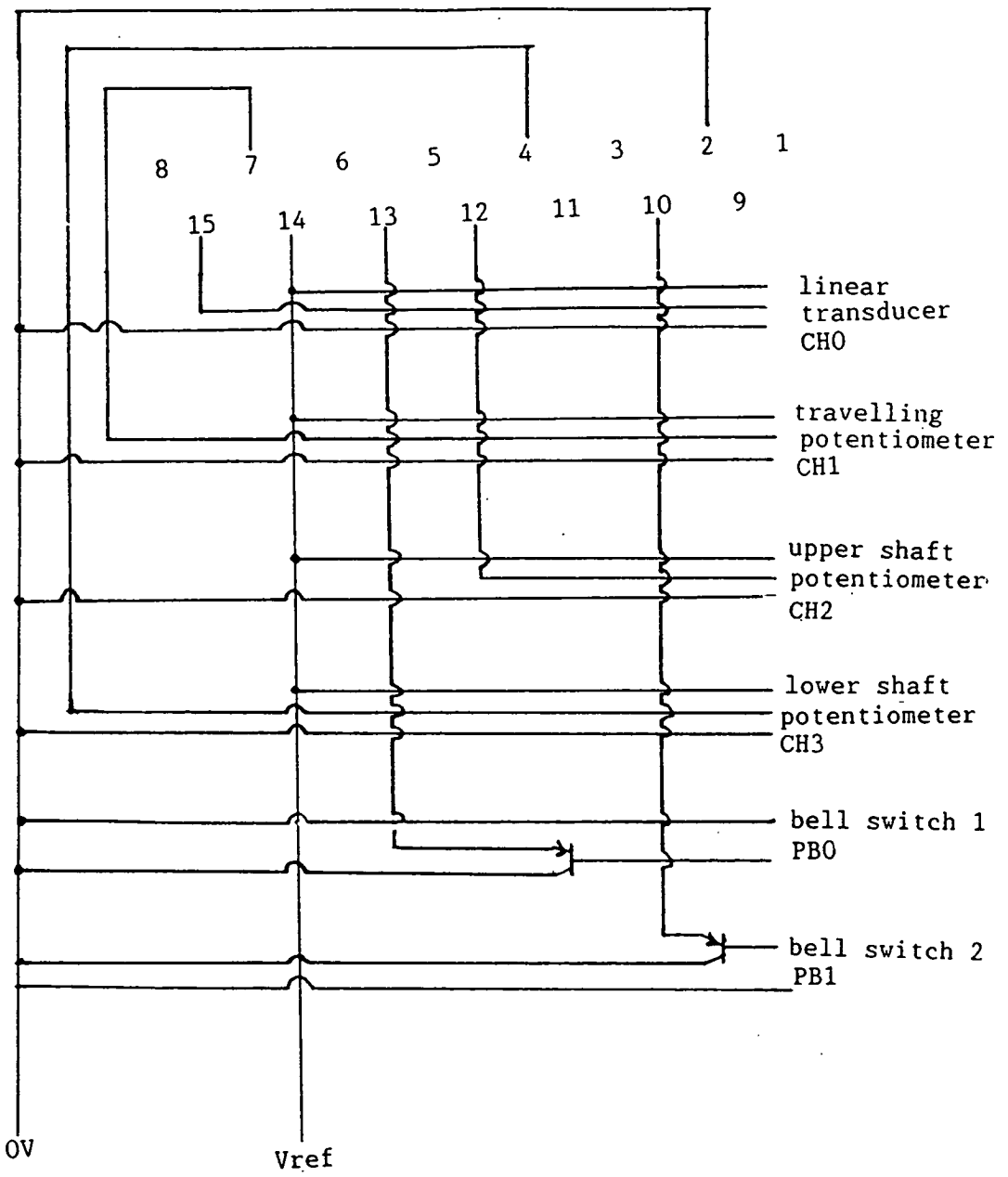

Figure 5.15 - Connections to the 6522 printer port, motors and motor drive boards.

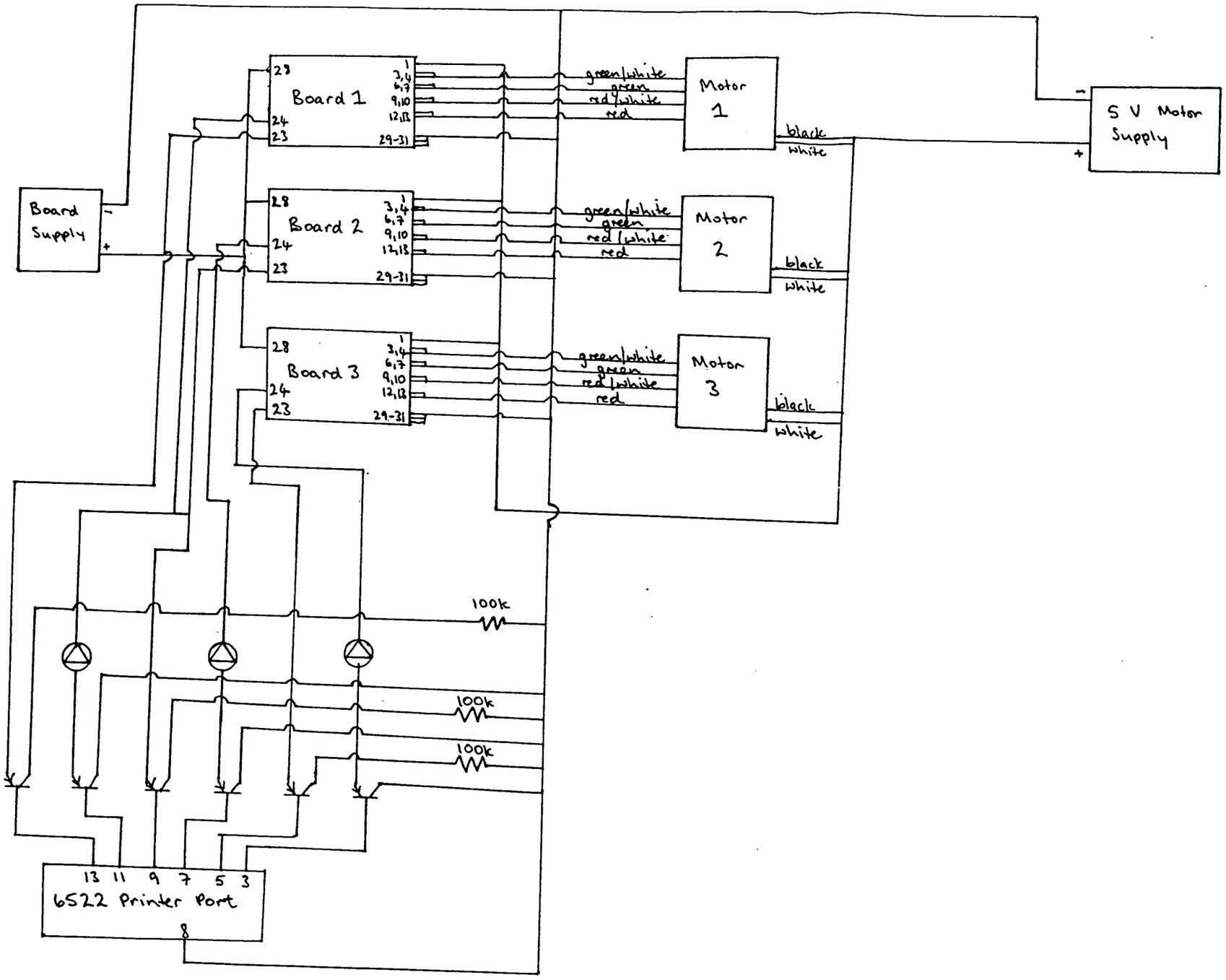

connected at either end by universal joints this does not ensure automatic self alignment. It is critical, therefore, that careful shaft alignment is done each time that the link between the shaft and the drive motor is broken or any piece of equipment at the shaft drive end is moved, however slightly.

5.6.2. Device Alignment.

Any misalignment of the marker and needle devices can have drastic effects on the final needle positioning. The centres of the horizontal spheres define the x-axis for all calculations and needle positioning. It is essential, therefore, that these spheres lie on this axis when the carriage is at any position on the rail. Some independent external means of registering the sphere centres at various carriage positions is therefore necessary.

A transparent Perspex mapping board has been constructed to assist in relating positions of different objects within the field of machine operation and is shown in Figure 5.16. The flexible board is stiffened by four metal strips which are fixed along each edge. A hole has been drilled in each corner of the board. Two 'claw' hooks latch over the main support bar from which the biopsy machine is suspended. Two wooden strips are fixed to the hooks. Metal spacers, fixed to the wooden strips contact the rail supports and have been designed to allow the wooden strips to hang approximately vertical. Four long bolts pass through holes drilled in the wooden strips and are locked to the wood. The bolts fit through the holes drilled in the corners of the Perspex board. Nuts fitted to the bolt on either side of the board enable it to be fixed in place on the bolts but at a large distance from the wooden strips. By adjustment of the nuts on each bolt the board can be positioned parallel to the needle movement plane and close up to the marker spheres.

Figure 5.16 - The mapping board.

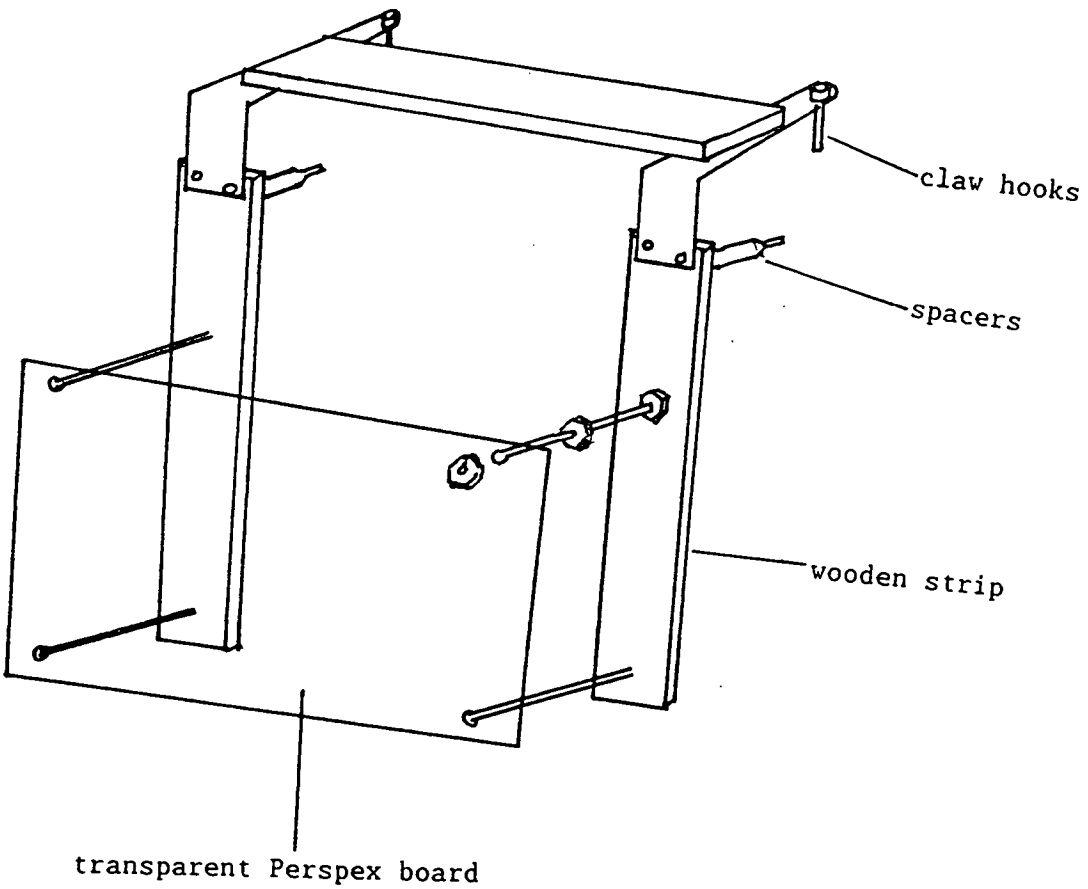

It is essential that the marker sphere centres lie in a line parallel to the plane of needle movement. The two spheres have different adjustments available. The reference sphere on the main carriage (and connected to the needle insertion point indicator) has a vertical adjustment facility: The axial position of the vertical shaft assembly (to which the sphere and indicator are fixed) can be altered relative to the slide, as shown in Figure 5.17.

The sphere which is fixed to the telescopic section has a single adjustment which moves the sphere obliquely to the needle plane. The rod, to which the sphere is attached, lies at an angle to the carriage face, projecting downwards. A screw adjustment, at the back of the folding section, allows minor alteration of this angle and thus moves the sphere both vertically in the forwards/backwards direction, as shown in Figure 5.18.

The mapping board is placed over the supports and hung in front of the machine. The needle carriage is moved along the rail and the needle projected out from the holder. A toolmaker's set square is used to find the perpendicular between the Perspex board and the needle tip and the relative perpendicular distance measured. Several measurements are made and compared. The board position is adjusted, using the locking nuts, until the board lies parallel to the needle movement plane (i.e. until the measured needle-board distance remains constant for different needle positions).

The sphere, fixed to the telescopic section, is adjusted until the line of centres of the two spheres is parallel to the board (and thus the needle plane) as shown in Figure 5.19. The sphere, attached to the main carriage, is then raised/lowered until the line of the two spheres is parallel to the rail on which the carriages run, as shown in Figure 5.20. The manual carriage is

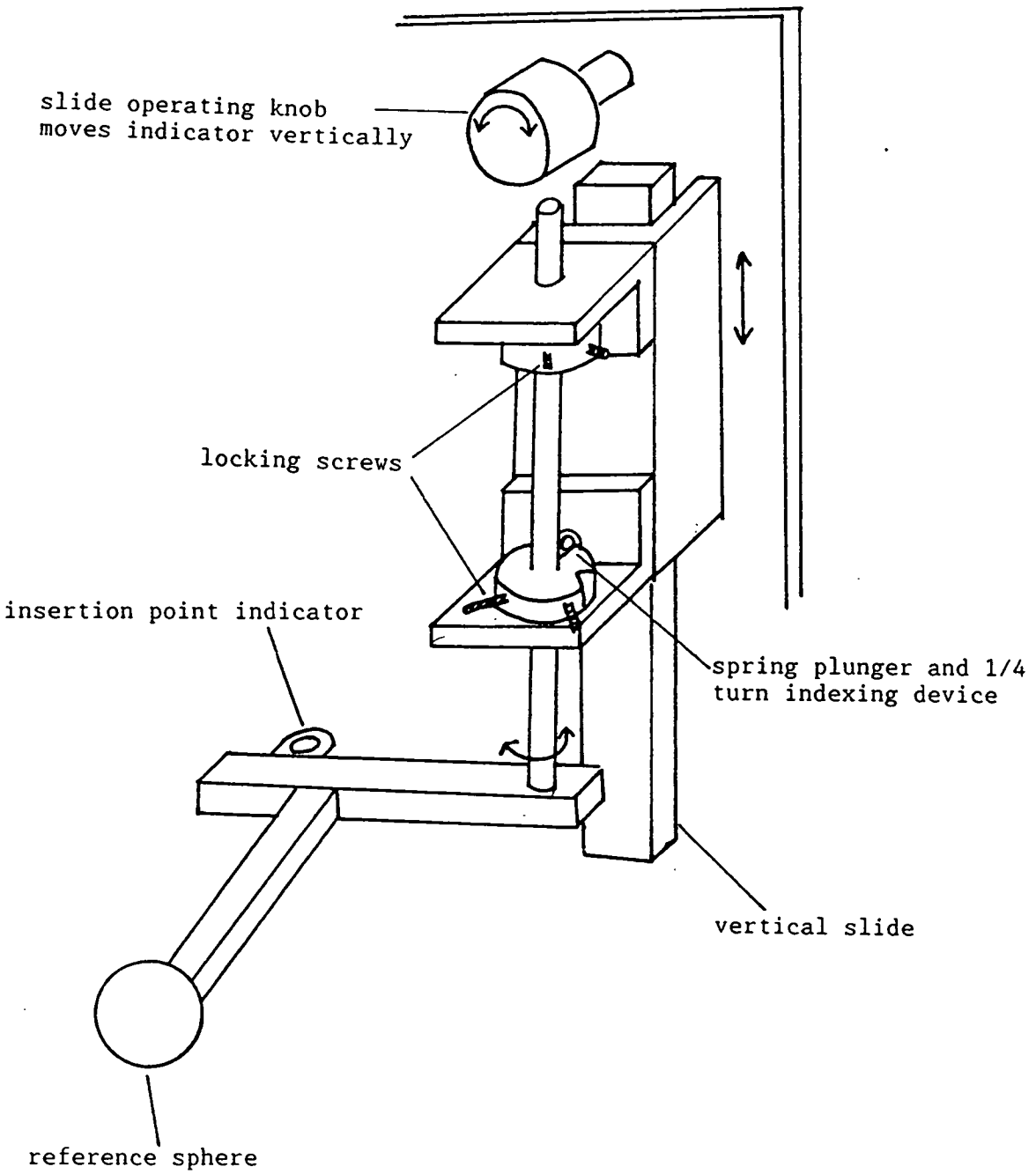

Figure 5.17 - The manual carriage

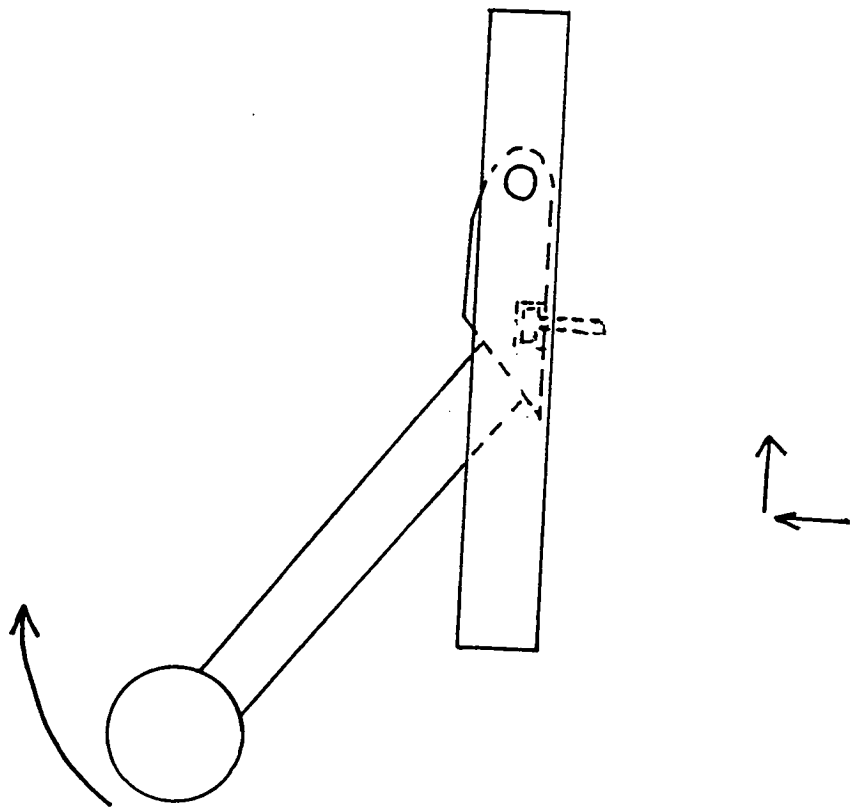

Figure 5.18 - Sphere on the telescopic section

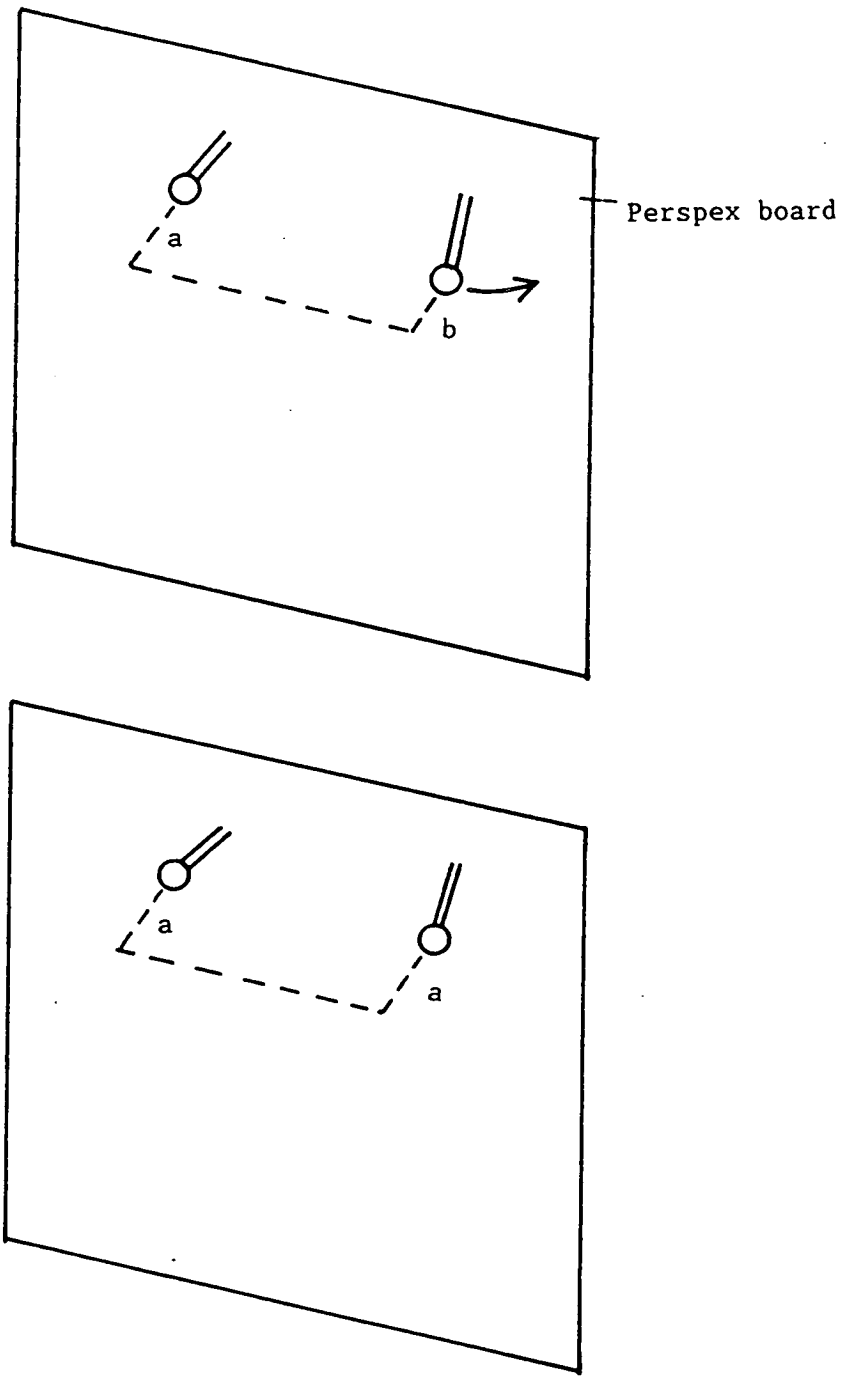

Figure 5.19 - Alignment of the spheres with the plane of the needle movement.

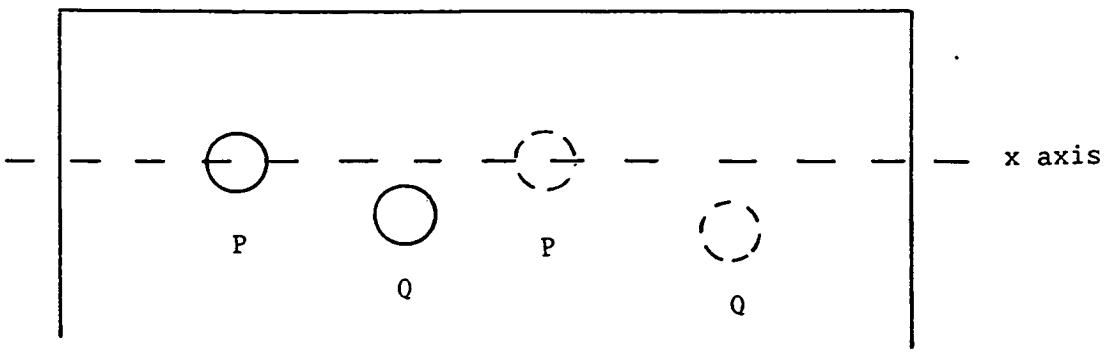

incorrect alignment

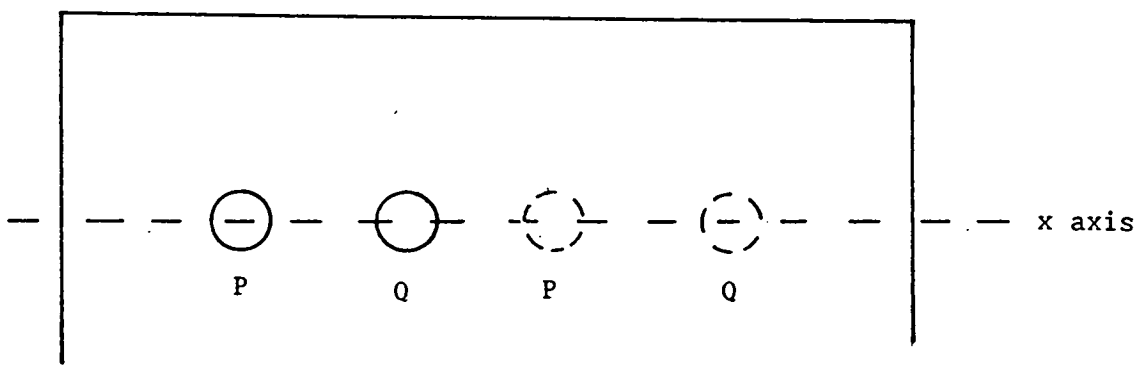

correctly aligned

Figure 5.20 Alignment of the spheres with the carriage rail.

thus aligned with the needle carriage.

5.7. Machine Calibration

Several parts of the biopsy machine require calibration. The quantities to be determined in such calibrations are of two kinds:

a)Those measured once only for each machine, which thereafter remain fixed. Some are in the form of responses or gradients, representing the relationship between changes of transducer inputs and outputs. Examples include the responses of the linear transducer serving the manual carriage and of the three potentiometers on the motorised carriage. Others are constant offset lengths between equipment items which must be included in calibrations as illustrated in Figure 5.21. These calibrated values can be used within the software as constants.

b)Those which require frequent re-calibration. These are the actual transducer readings at known positions, which enable the precise position of the various movable parts to be determined, sometimes relative to each other. Generally, if the machine has not been dismantled, some of these positions will not change and a one-off reading could be used, as in a) above. However, this particular machine is a prototype development model which is frequently dismantled and altered. It is also a piece of precision machinery which is easily upset by any slight manhandling. Since it is frequently transported between establishments it is liable to get out of alignment and so such readings often need to be made afresh.

The transducer readings fluctuate slightly and so an averaging procedure has been used. When a transducer reading is required

Figure 5.21 - Offset distances between various items of equipment.

a) marker rod

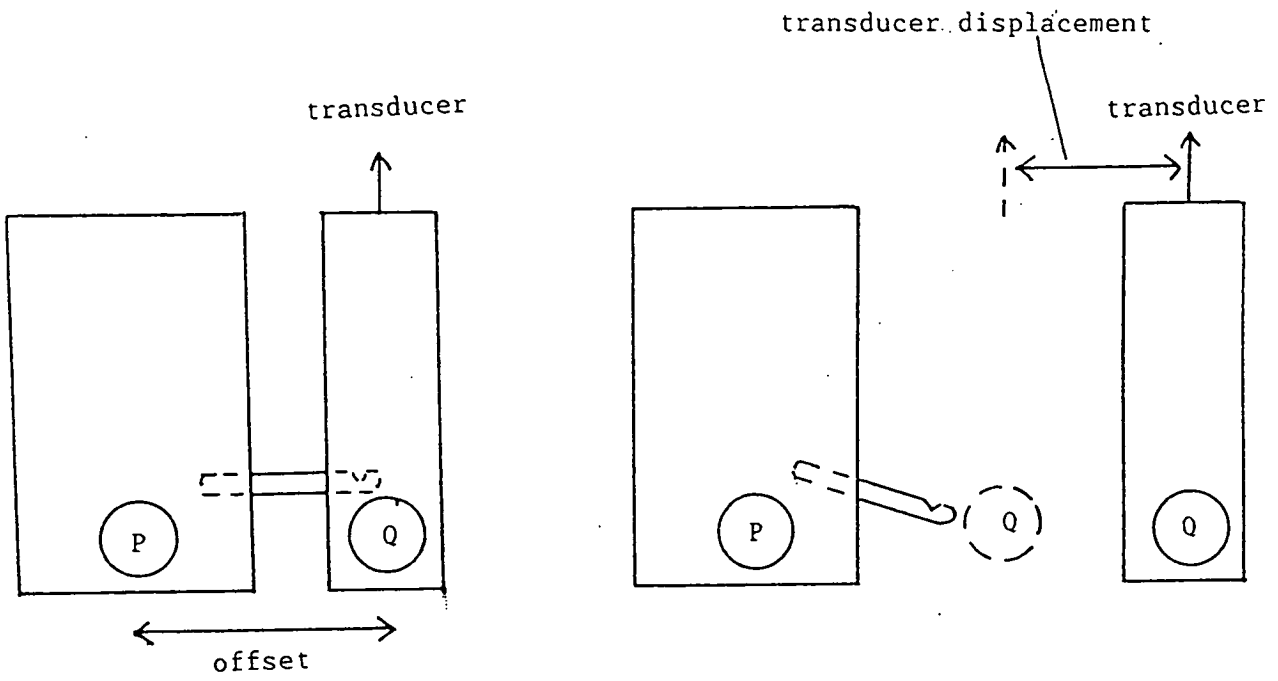

PQ = transducer displacement + offset

b) needle insertion point coordinates :

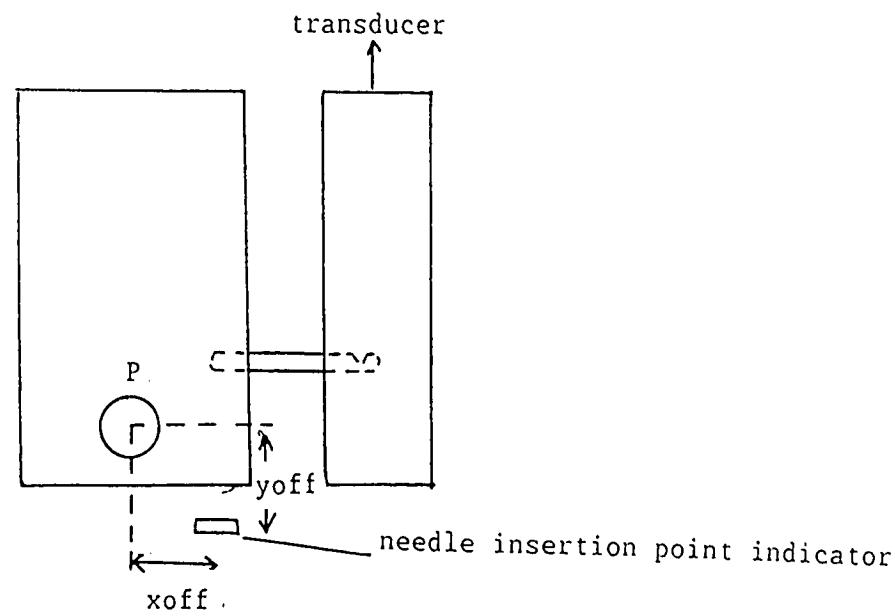

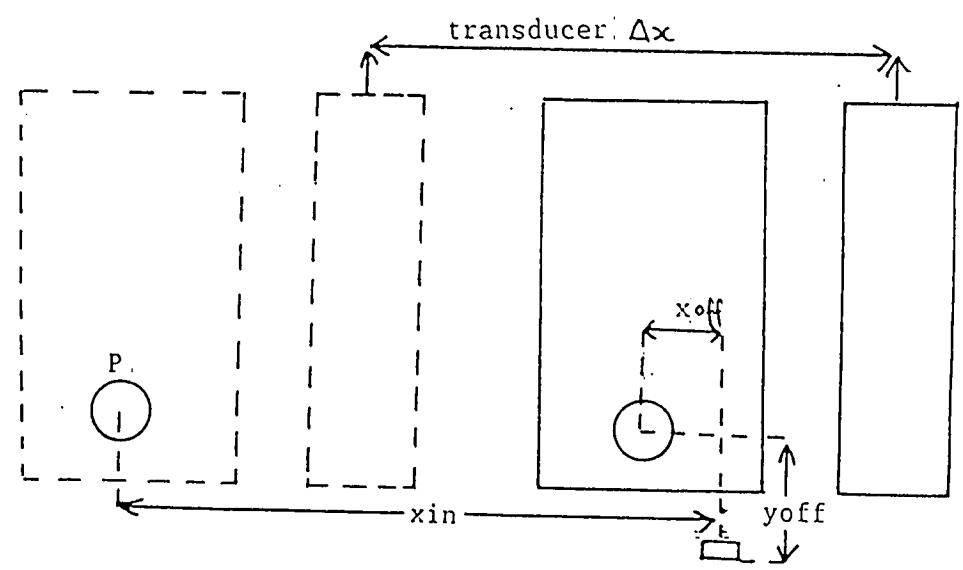

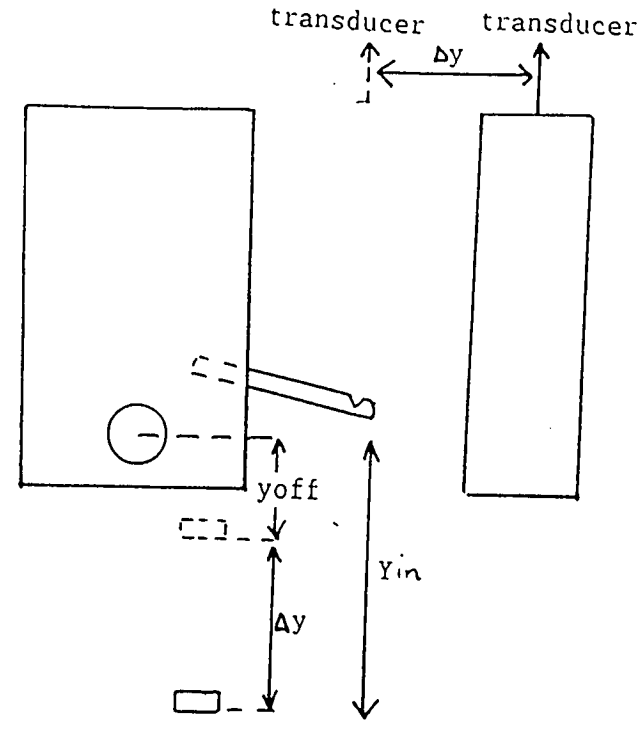

yin = yoff + Δ y

c) needle

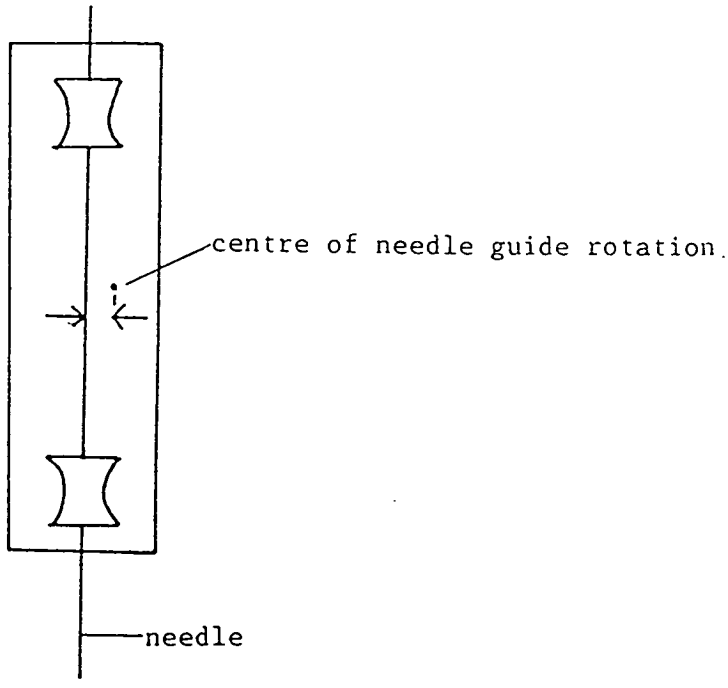

the computer takes 100 consecutive readings and then calculates the average value. This has been shown to provide sufficiently accurate values.

5.7.1. One-off calibrations

Five response or gradient calibrations are necessary - one for the linear transducer, one for each of the three potentiometers, and one for the secondary effect of angling on the depthing mechanism.

5.7.1.1. Linear Transducer:

The manual carriage is moved along the rail and transducer readings paired with the measured distance of the main sphere from the faceplate on the left hand (unsupported) end of the rail. A linear regression analysis has been applied to the results and details are provided in Table 5.3.

5.7.1.2. Leadscrew Potentiometer:

The motorised carriage is positioned at several points on the rail and readings paired with the measured distance of the axis of needle rotation from the unsupported end faceplate. A linear relationship has been obtained, and is shown in Table 5.3.

5.7.1.3. Depthing Potentiometer:

The depth stop on the chain is moved along the needle slideway. Distance moved is recorded against output reading. A linear relationship has again been obtained. However, angulation of the needle guide about the wheel driving the depthing chain, when that is stationary, inevitably has the same effect as rotating this driving wheel through the same angle (in the other

Table 5.3 Results of transducer and potentiometer calibrations.

Source	Measured Variable	Rate of Change of Transducer Output with Measured Variable	Correlation Coefficient	y intercept
Linear Transducer	Distance of reference sphere from left hand faceplate	-66.989 transducer units per cm	-0.99997	3476.9260 transducer units
Pot'meter on helical screw (i.e. travelling pot'meter)	Distance of reference sphere from left hand faceplate	66.9501 potentiometer units per cm	0.99999	-271.0200 pot'meter units
Pot'meter on angling device	Angle of Rotation	9.189 potentiometer units per degree	0.99999	2007.835 pot'meter units
Pot'meter on depthing device	Depth of needle insertion	94.8199 potentiometer units per cm	1.0000	580.8339 pot'meter units
Depth stop alterations with angling	Depth of needle insertion	-462.583 potentiometer units per cm	0.9994	10562.6 pot'meter units

direction) with the needle guide fixed; it alters the position of the needle depth stop. The alteration of set needle depth with guide inclination has to be measured so that it can be allowed for in the computations determining the positioning of the depth stop for a desired depth of needle penetration at known inclination, as below.

5.7.1.4. Angling Potentiometer:

To rotate the needle guide from one extreme angular position to the other requires 3.5 complete rotations of the splined driving shaft and its potentiometer. Potentiometer readings have been taken for every 10° of needle guide rotation. The position of the depth stop on the needle slideway has also been noted for each angle change and a substantial depth stop movement of around 7 cm noted over the entire 3.5 rotations. This must therefore be accounted for within the software.

5.7.2. Repeated Calibrations

These involve setting the various parts of the equipment in preselected and known positions thus indicating to the computer that the action is complete. The transducer reading is then taken to correspond to a known position coordinate.

5.7.2.1. Linear Transducer:

The manual carriage is positioned hard up against the left hand unsupported end. The distance of the sphere from the end faceplate is known and may thus be correlated with the transducer indication.

5.7.2.2. Angling Potentiometer:

The motorised carriage is driven into the middle portion of the

rail, thus providing adequate clearance for needle slideway rotation. The angling motor is driven until the transducer reaches the setpoint at which the needle slideway should be positioned perpendicular to the horizontal marker. Provided that the carriage has not been mishandled adjustments should not be necessary. If, however, adjustment is required, the guide and slideway assembly may be slid round on its supporting shaft against the friction of a clamping device by applying a slight overpressure.

5.7.2.3. Depthing Potentiometer:

Two possible methods have been evaluated:

a) Set the depth stop in a pre-indicated position and note the transducer reading. The needle does not need to be in place at this stage but this does require that the needle length is input into the computer at some stage prior to setting the depth stop for needling.

b)The needle (of any length) is inserted into the holders. The motor driven depth stop, as it is carried by the chain along the needle slideway, encounters a spring latch on the needle slider. The hinge is restricted from operating in one direction. If moving downwards, the stop deflects the latch hinge and passes freely down the slideway without moving the slider and needle. On moving upwards, however, it cannot open it. The slider and the needle, whose upper end is clamped to it, is therefore retracted through the lower holder by the motion of the driven chain. If the motion of the chain and stop is arrested when the tip of the needle lies flush with the base of the lower brass support then the depth indicator transducer reading corresponds to the tip of the needle lying at this known point. When the insertion depth is calculated

and input to the computer the depthing motor stop moves down appropriately and the slider can also be moved down by the same depth. The tip of the needle will therefore protrude from the end of the needle holder by the correct amount, i.e. it should lie in the lesion. The actual needle length is, therefore, irrelevant in this mode of calibration.

The latter method was chosen for this work.

5.7.2.4. Leadscrew Potentiometer:

The motor driven carriage is moved along to the right hand end of the rail. The distance between the needle guide and the left hand end faceplate is known. Since the same reference point is used, the motor driven carriage position is known relative to the manual carriage main sphere position. The two carriages, although working with different transducers, therefore use the same coordinate axes.

The above outlined calibration procedure is therefore performed at the start of every run.

5.8. Carriage Positioning.

Operating the entire unit from a real-time feedback control system from the transducers would be slow and would require elaborate corrections to avoid positional offsets and carriage overshoots. The stepper motors have been used, in addition to the transducers, to do the necessary equipment positioning. The motors have been calibrated, in much the same way as the transducers, and the number of steps necessary for each dimensional unit of change is known. The required number of motor steps is calculated, the motor stepped for this quantity and the transducers used to check the positions (since motor slip can

occur if a high frictional resistance exists or if the motor is run too fast). If any slight alterations are necessary, again the required number of steps is calculated and the process repeated until the transducer readings are correct.

5.8.1. Backlash

The biopsy machine is required to locate the needle tip to within a millimetre or so of a designated point by means of angular and linear movements applied at relatively large distances from that point. Thus any backlash effects in these controlling movements must be minimised. Backlash arises in several places:

Gearbox backlash affects carriage positioning, needle angling and needle depthing. The gearboxes purchased have low associated backlash. They are fitted, by the manufacturer, with anti-backlash spring-loaded split gears on the output shaft.

The effects of backlash would be most harmful in the angling of the needle guide. Accordingly a large preloaded torque is applied about the hollow shaft carrying the guide by a spring located between the guide and the carriage front plate. This spring is strong enough to maintain a resultant torque of constant direction, despite variations in the direction and magnitude of the gravitational torque acting on the needle guiding and depthing assembly at different inclinations.

Sprocket wheel and chain backlash will affect angling and depthing. This is minimised by correct adjustment of the chain tensioning wheels.

The leadscrew drive for the motorised carriage will have backlash positioning errors; but these are negligible for the proprietary ball-screw arrangement used.

Backlash effects are reduced by always using the same backlash extremes when positioning: Depthing is always done in the downwards direction; angling is done to the anti-clockwise extreme; and the motorised carriage (whose leadscrew backlash effects are limited by using an anti-backlash nut) is always positioned from the right hand end.

Rocking and twisting 'lost motion' errors in the positioning of the motorised carriage are essentially eliminated for the loads encountered here by the semi-kinematic design of the proprietary ball-slide and track arrangement used.

5.8.2. Biopsy Machine Positioning Accuracy

Direct measurements have been made of mechanical errors in the final needle positioning.

5.8.2.1. Procedure:

The machine calibration procedure is run through and the main marker sphere positioned and locked to the rail. The sphere position is thus registered and the origin for the coordinate system fixed (and known). The sphere position is marked on the mapping board using the square. The manual carriage is unlocked and moved to the end of the rail to allow the needle carriage unrestricted movement. The computer is given a lesion position and an insertion point and the needle tip is positioned accordingly by the stepper motors. The final tip position is then read on the mapping board.

Several different sets of trials have been done in an attempt to determine the effects of different variables on final positioning accuracy, as follows:

Table 5.4 and Table 5.5 - Final Needle Position at Different Lesion Depths but Maintaining Insertion Angle Constant.

Table 5.4 - Insertion Angle 135°

Lesion Position	Insertion Point	Final Needle Tip	Insertion Depth
(10,15)	(25,0)	(10,15)	21.1
(10,13)	(23,0)	(10,13.1)	18.4
(10,10)	(20,0)	(10,10.1)	14.1
(15,15)	(30,0)	(15,15.05)	21.2
(20,7)	(24,3)	(20,7.0)	5.7
(30,7)	(34,3)	(30,7.0)	5.7

Table 5.5 - Insertion Angle 90°

Lesion Position	Insertion Point	Final Needle Tip	Insertion Depth
(0,4)	(0,3)	(0.1,4.0)	1
(0,6)	(0,3)	(0.1,6.0)	3
(0,8)	(0,3)	(0,8.0)	5
(0,10)	(0,3)	(0,10.0)	7
(0,12)	(0,3)	(0,12.0)	9
(0,14)	(0,3)	(0.1,14.0)	11
(0,16)	(0,3)	(-0.1,16.0)	13
(0,18)	(0,3)	(0.18.0)	15
(0,20)	(0,3)	(-0.1,20.0)	17

Table 5.6 - Effect of variation in insertion point

Lesion Position	Insertion Point	Final Needle Tip	Angle of Insertion
(0,8)	(10,0)	(-0.2,8.1)	39
(0,8)	(9,0)	(-0.2,8.0)	41
(0,8)	(8,0)	(-0.1,8.1)	45
(0,8)	(7,0)	(0.0,8.0)	49
(0,8)	(6,0)	(-0.1,8.0)	53
(0,8)	(5,0)	(-0.1,8.0)	58
(0,8)	(4,0)	(0,8.1)	63
(0,8)	(3,0)	(0.8.0)	69
(0,8)	(2,0)	(0,8.1)	75
(0,8)	(1,0)	(0,8.0)	83
(0,8)	(0,0)	(0,8.0)	90
(0,8)	(-1,0)	(0.05,7.99)	97
(0,8)	(-2,0)	(0,7.9)	105
(0,8)	(-3,0)	(-0.05,7.9)	111
(0,8)	(-4,0)	(-0.2,7.9)	117
(0,8)	(-5,0)	(-0.15,7.95)	122
(0,8)	(-6,0)	(-0.2,7.95	127
(0,8)	(-7,0)	(-0.4,8.0)	131
(0,8)	(-8,0)	(-0.3, 7.95)	135
(0,8)	(-9,0)	(0.3,7.95)	139
(0,8)	(-10,0)	(-0.1,7.9)	141

5.8.2.2. Effects of depth of needle insertion (lesion depth)

The insertion angle is maintained constant and the lesion depth varied. Tables 5.4 and 5.5 illustrate the resultant needle tip position when two different insertion angles, 135° and 90°, are used. They indicate that needle positioning error does not appear to alter greatly with depth of insertion provided that the machine is correctly calibrated initially.

5.8.2.3. Effects of insertion point (angle of needle insertion)

The lesion position is maintained constant as the insertion point is moved along a line parallel to the marker. The coordinates of the needle tip after it has been pushed home are shown for each insertion point in Table 5.6, from which it is apparent that largest errors occur at sharper insertion angles. The best results are obtained when the needle is inserted perpendicular to the marker.

5.9. Conclusions

A biopsy machine has been developed, compatible with the current biopsy procedure and techniques. Throughout the design the aim has been to retain some of the subtle features of the existing practice by allowing manual interaction, as in the manual needle insertion which retains tactile sensitivity, enabling the operator to feel when the lesion has been penetrated.

Extensive machine testing has revealed that the mechanical needle positioning errors are small when compared with those arising from the image inputting and lesion position determination techniques. Errors of < 2mm in final placement of the needle tip relative to the lesion are normally achieved if the machine has been carefully calibrated beforehand. This is well within the

accuracy required to locate a lesion of < 2cm diameter.

CHAPTER 6

RESULTS AND CONCLUSIONS FROM TESTING OF THE BIOPSY MACHINE

6.1 Introduction

The biopsy machine and image analysis technique were both tested independently, as previously described, with the computer. It remained to connect all three sections together to test out the needle positioning accuracy of the networked equipment.

6.2. Preliminary Testing

Figure 6.1 indicates the network arrangement. Prior to testing with X-rays it seemed prudent to again verify and demonstrate to our medical colleagues the complete machine performance using an optical analogue , which more closely resembles the X-ray system. The optical simulator, described in section 4.6 was adapted so that it moves in a vertical plane and can be angled and positioned around the biopsy machine. The revised optical simulator is shown in Figure 6.2. Needle positionings have been done using a wide range of views. Reproducibility and error results in the final position are similar to those obtained previously, shown in Figures 4.8 and 4.9. It is obvious, from previous tests, that these errors are mainly the result of errors incurred during the image analysis procedure.

6.3. The C-arm X-ray Machine

The C-arm geometry has been described previously in Chapter 3.

The C-arm X-ray machine (Kalliscope D, supplied by CGR Medical Ltd) can be used to obtain either radiographic or fluoroscopic images. For this purpose the fluoroscope will be used for image analysis.

The X-rays hit an electron emitting screen below the detector

Figure 6.1 - The Machine Network

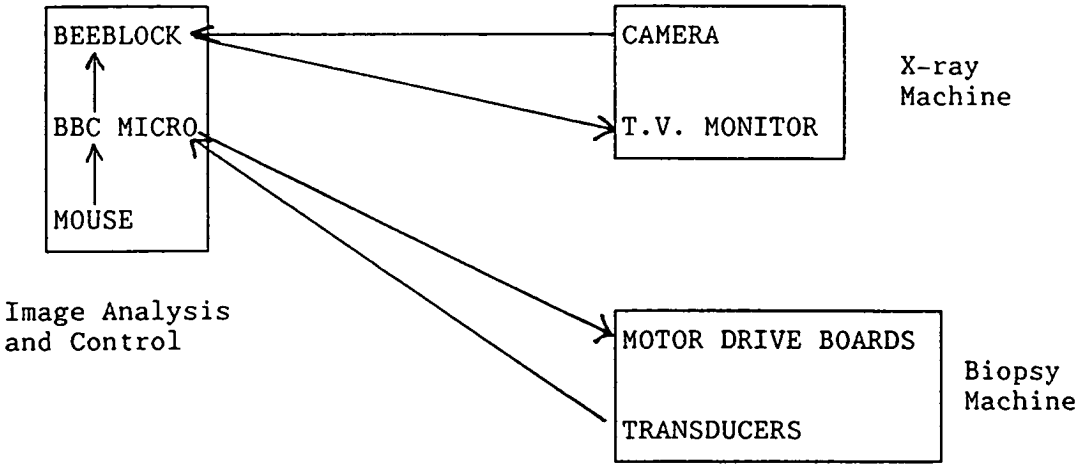

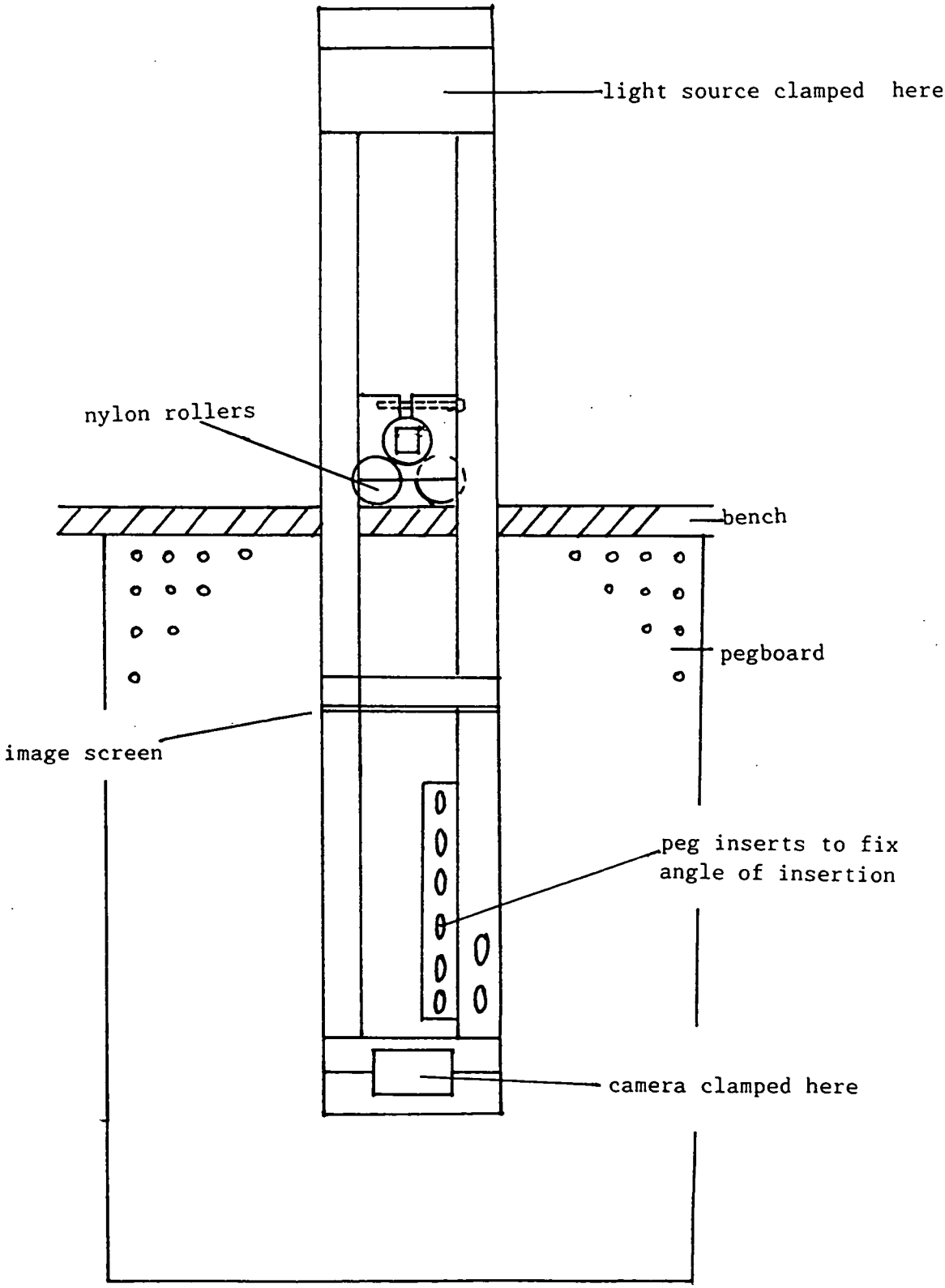

Figure 6.2 - The revised optical simulator for use with the biopsy machine prototype.

Figure 6.3 - The X-ray detector

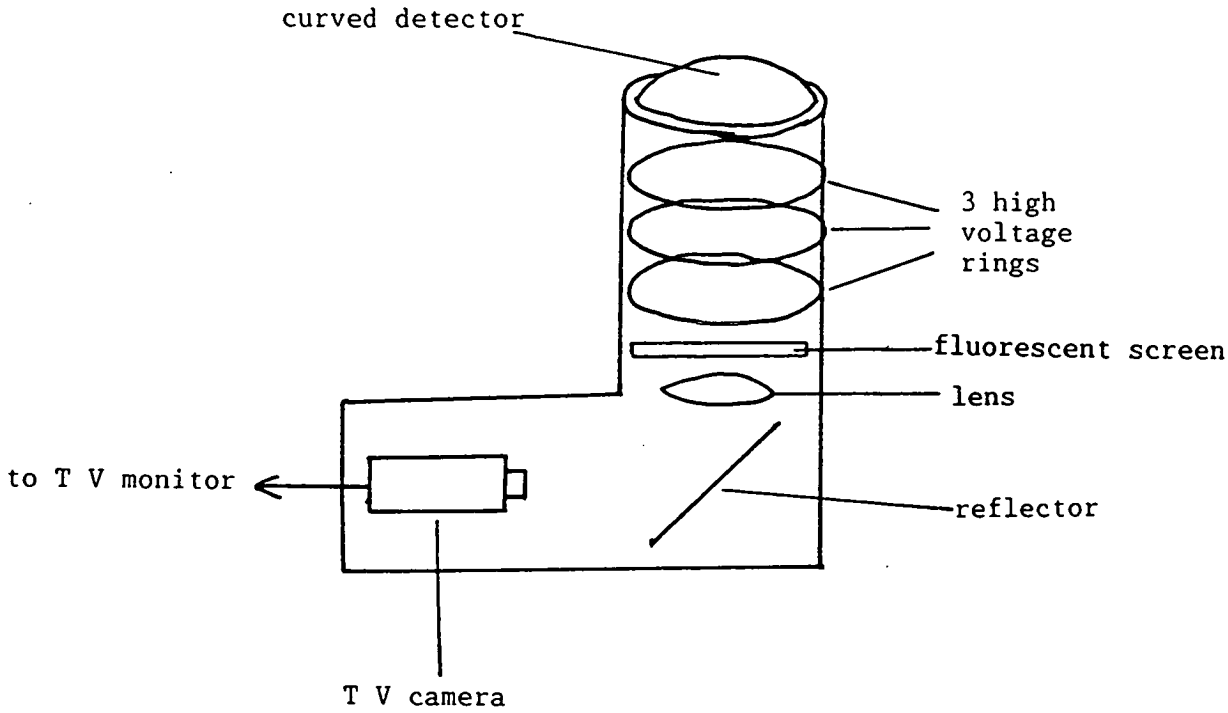

surface, as shown in Figure 6.3. The emitted electrons are then accelerated by a large voltage. Electrode rings, lying below the electron emitting screen focus the electrons before they hit a fluorescent screen and visible light is emitted. The light is focussed by lenses, reflected through 90° and the image is televised by a vidicon TV camera and digitised.

The C-arm displays its image information on two T.V. monitors. One is used while the C-arm is 'screening' and displays the moving, real-time image. The other displays a memorised image. A memory board is updated from the screened image many times a second. When the screening process is ceased the last memorised image is stored and is displayed on the second T.V. monitor.

6.4. Connection of the X-ray machine to the Biopsy Machine and Computer

The digitised signals from the memory board have been intercepted prior to the T.V. monitor and have been redirected to the genlock system. The superimposed video and computer output signals from the genlock have been input to the X-ray machine T.V. monitor. The C-arm memory board image and the output monitor thus replace the TV camera and TV monitor respectively in Figure 4.1, as shown in Figure 6.1. Image analysis on the X-ray image can hence be done.

6.5. X-ray assisted Biopsy Trial

A series of preliminary trials has been done using a metal wire ring of approximately 2cm diameter, fixed inside a polystyrene box with removable side, to represent the lesion and patient respectively. The dummy patient rests on the patient trolley and the equipment is arranged around it, as shown in Figure 6.4.

The biopsy machine, C-arm and trolley bases are clamped together

Figure 6.4 -General arrangement of the patient, biopsy machine, C-arm and patient trolley.

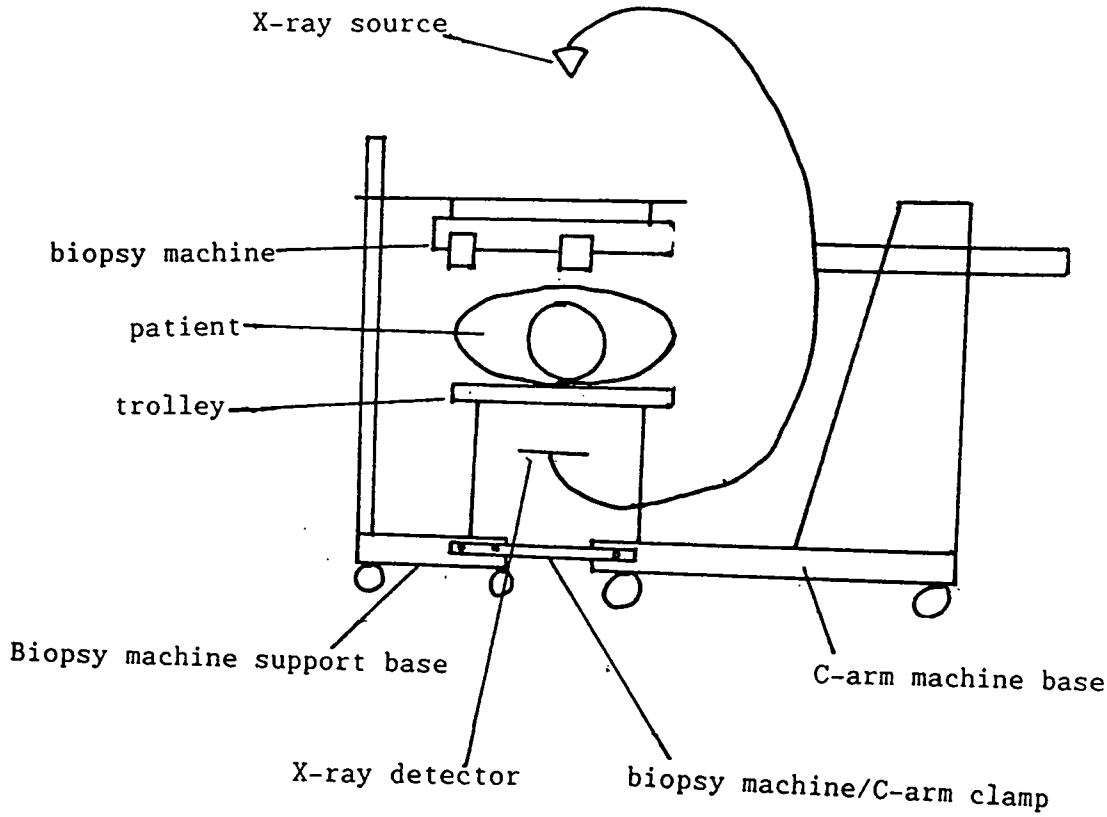

Figure 6.5 - The reference grid

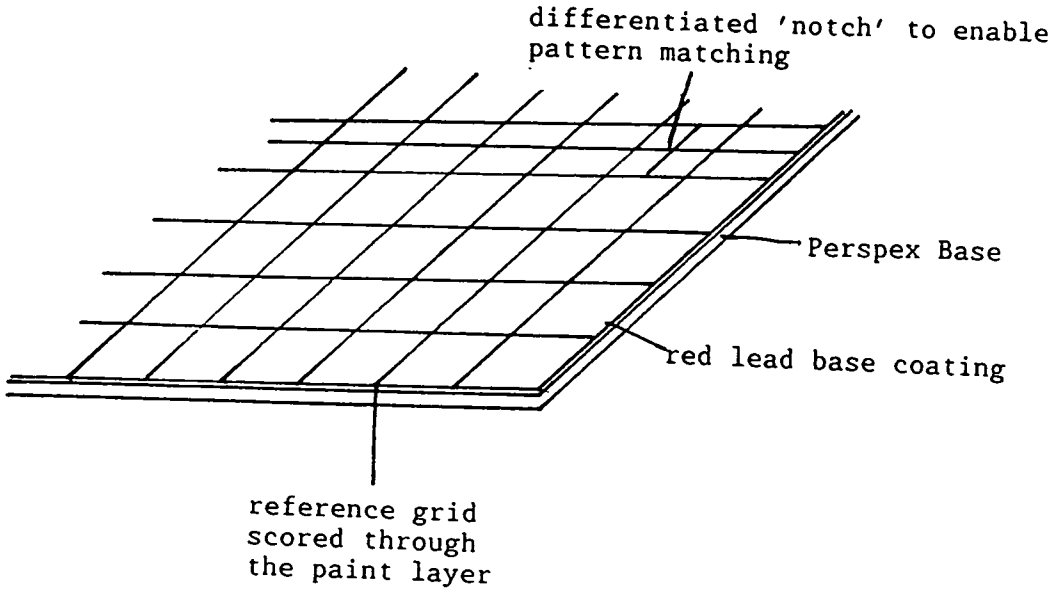

to prevent any uncontrolled relative movement during the biopsy procedure.

6.5.1. The procedure

The 'cantilever bridge', or overhanging arm, of the biopsy machine containing the marker and needle carriages, is swung round so as to lie parallel with the patient trolley. The bridge is raised until the lowest points of the marker spheres (the lowest points on the cantilever assembly) are at a greater height than the highest point of the 'patient' positioned on the trolley. The biopsy machine calibration procedure is run through and the cantilever arm is then swung across the patient and lowered so that the marker spheres are close to, or just touching the patient. The C-arm is positioned with the detector below the trolley and the source above the marker spheres, which project sufficiently from the main carriage support to allow the X-ray machine an unobstructed view of them. Preliminary screening is done to locate the lesion. The floating table top of the trolley bearing the patient is now moved longitudinally until the lesion lies in the same plane as the marker spheres. The main marker sphere is positioned with the aid of the TV monitor to ensure that the sphere and lesion are both visible on the screen. If necessary the marker is adjusted and screening recommenced. When in the correct position the first marker sphere is locked in place to the rail and the second sphere positioned, again by trial and error with the aid of the TV monitor. When it is finally in position and clamped in place screening is again done and the resulting image used for image analysis. The information is input to the computer using the mouse. The first view is then complete.

The C-arm is swung through a suitably large angle (see Chapter 4) and the second view begun. The lesion and the first marker sphere must not be moved - only the second marker sphere position may be

adjusted between views. The second view must therefore contain the lesion and first marker sphere. If these cannot be observed together on the screen then the viewing angle must be altered. The second marker sphere is then positioned to appear in view. If the second sphere cannot be brought into view then the viewing angle must be altered accordingly. The second image is thus obtained and image analysis done. The lesion position is then computed automatically.

Finally the telescopic section of the manual carriage is retracted, the marker spheres are folded away and the point of needle entry indicator is swung into position. The chosen point of needle insertion on the surface of the patient is then registered by the horizontal movement of the manual carriage and vertical movement of the indicator ring to coincide with that point.

The needle angling and depthing mechanism is then positioned automatically so that the needle will pass through the chosen entry point and reach the lesion.

6.5.2. Results of Preliminary Trials.

Repeated tests using the C-arm machine revealed large variable errors in needle placement which are inconsistent with previous results using the optical analogue. The problem lies in the calculated lesion position, not in the biopsy machine needle positioning. It therefore appears that the X-ray machine either introduces a further error or increases an error which has previously been small and insignificant.

6.6. Investigation to Find the Error Source

The likely error source appeared to be image distortion in the imaging system of the C-arm machine. To check this a reference

grid, shown in Figure 6.5 was constructed from Perspex sheet, coated in red lead paint. The paint layer was scored down to the original Perspex sheet to form a grid of squares of 1cm side. This grid was placed over the X-ray detector. The X-ray machine was run with the grid in place but minus the genlock and computer connections. It was immediately obvious from the image that massive image distortion occurred. The service engineer subsequently improved the image quality but a large amount of distortion still remained. The straight lines appeared as curves, especially around the outer edge of the circular image, as illustrated in Figure 6.6.

Possible sources of this error have been investigated, as follows:

a) Since the X-ray machine was tested using the grid without any connections to the video mixer or computer it is clear that the distortions arise from errors within the X-ray machine set-up.

b) The C-arm monitor was linked directly to the computer 'video out' and a computer generated grid drawn onto the screen. The grid appears undistorted in the centre and barrel-shaped at the extreme outer edge, as shown in Figure 6.7. This arises as a result of the monitor screen being slightly bevelled at the edges which causes a square grid to appear barrel shaped. This is normal and not significant for most of the field. The monitor is thus eliminated as the major source of distortion.

c) The memory board was tested by connecting the monitor to the X-ray detector as normal and placing the grid on the detector surface. One line of the grid was differentiated by a notch, as shown in Figure 6.5. A transparency was placed

Figure 6.6 - X-ray machine image distortion

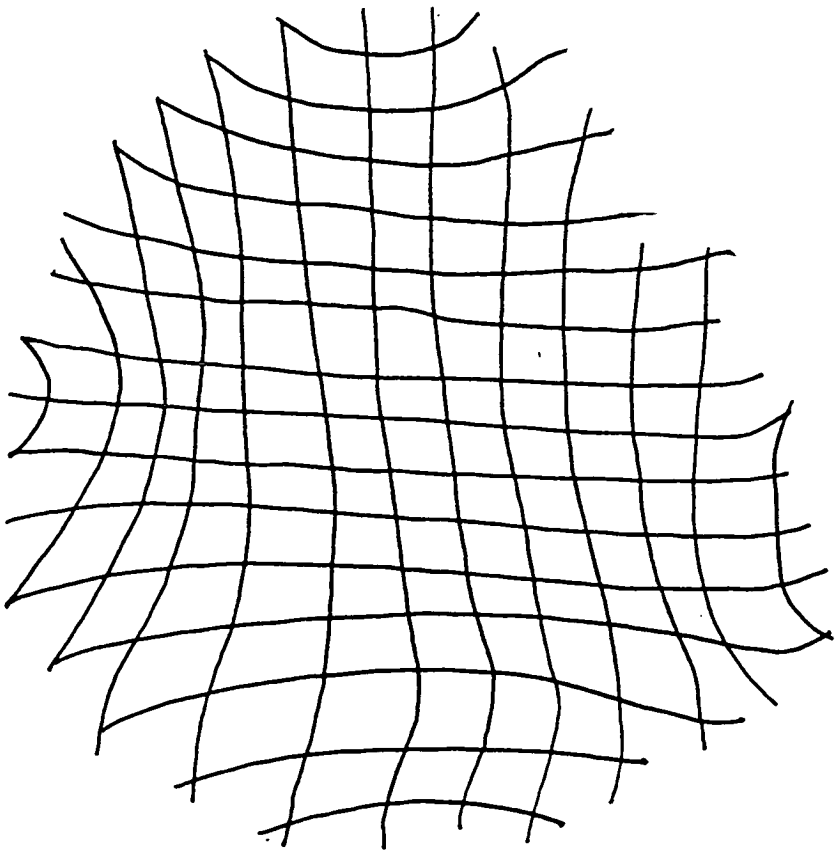

Figure 6.7 - The normal barrel-shaped image obtained from a T.V. monitor.

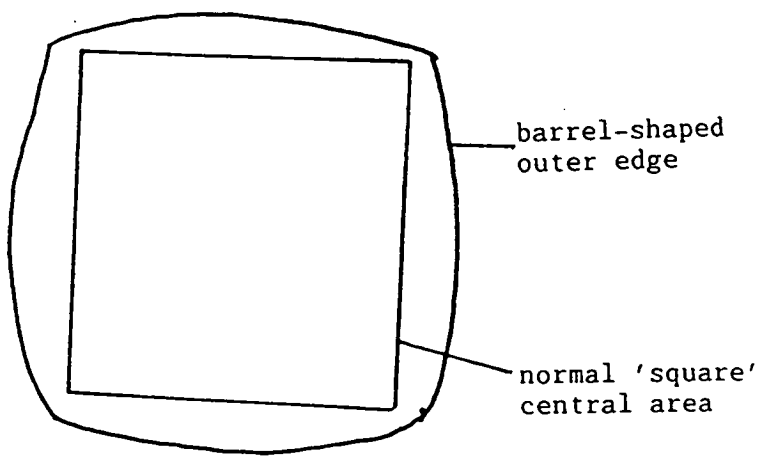

over the screening monitor surface and screening begun. While maintaining pressure on the foot switch (and thus keep the image on the first TV monitor) the differentiated line was traced onto the transparency. When the pressure is removed from the foot switch the memorised image was displayed on the 2nd monitor. The transparency was then removed from the screening monitor and replaced over the memorised image, ensuring that the notches matched. The memorised image was slightly magnified by about 11mm vertically and 4mm horizontally at the diagonals. However the transparency appeared similar to the memorised image, suggesting that the memory board does not cause the distortion effects.

d) Terrestrial magnetic or electrostatic field effects were investigated by angling the X-ray arm. The grid was fixed to the detector and the C-arm machine angled at 0, 45, and 90 degrees in the plane of the C-shaped arm as well as being tilted out of the plane by 90 degrees, as illustrated in Figure 6.8. Grid points on the resulting images were picked off using the mouse pointer and the nodal information stored on disc. Results revealed no apparent angling effects, although when a steel ruler was placed directly over the detector the image distorted badly. However the ruler has to lie right up against the detector before any effect is apparent. The patient trolley, partly fabricated in steel, might have had a larger effect than the steel ruler, so this was examined while the magnetic table locks were in operation. Little or no effect was apparent.

It is hence apparent that the distortion arises between the curved detector and the camera, perhaps in the detector itself or in the image intensifier. We were advised that in neither case could we hope to remedy the defect directly with the resources

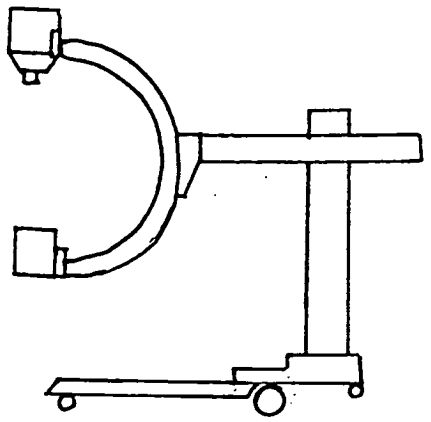

90° view

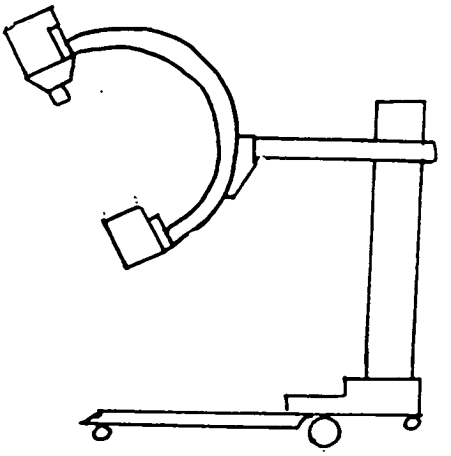

45° view

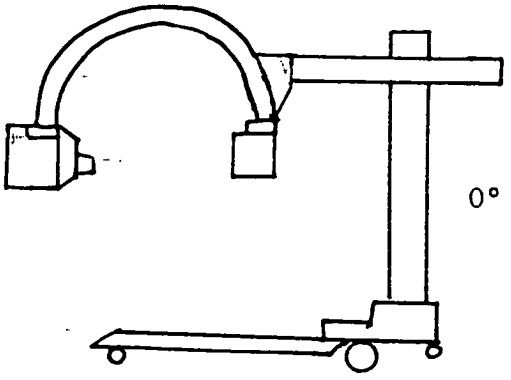

0° view

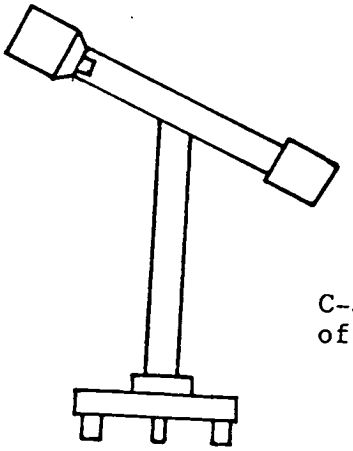

C-arm tilted out
of the plane

Figure 6.8 - Different C-arm angling positions used to determine terrestrial effects on the image

available to us.

6.7. Distortion Calibration

The Perspex grid was used to examine the precise nature and extent of the pincushioning distortion in an attempt to calibrate the output T.V. image.

The positions of the grid nodes on the T.V. monitor were input using the mouse and stored on disc. The procedure was repeated on successive X-rays taken over three hour periods at constant machine settings and the following noted:

a) The image stretches with time. The dimensions of the image circle on the T.V. monitor remain constant but the viewed area becomes gradually smaller as the gap between the grid lines increases. After around 1.5-2 hours the image size stabilises. It is interesting to note that throughout the warm-up period the horizontal part of the image does not alter significantly. However consecutive images are still not reproducible since the shapes of the distorted lines between views varies.

b) After the X-ray machine has been operated (or even just left on) for around two hours the digitised image has a tendency to spontaneously disappear after a short time, usually before all the information has been input to the computer.

c) The horizontal and vertical lines both vary in shape depending upon the position on the screen. Midway vertically down the image to the far left and far right the x coordinates have been stretched, turning the grid squares into rectangles. Midway across the image to the top and

bottom the y coordinates have been stretched , again giving rectangles but in a different elongation direction. On the outer edge of the image between the four areas mentioned above the squares become distorted in both directions, turning into parallelograms.

d) The y-coordinate stretches at a much faster rate than the x-coordinate. Over the entire three hour period the central x-line did not vary much although the x-lines at the top and bottom of the circular image stretch greatly.

e) The memorised image often displays horizontal interference smear lines. These lines obscure and further distort the image. They arise within the memory board when the screening process stops. The board updates its image from the screening monitor and saves the last image viewed. If, however, the new image is in the process of being saved when the screening is stopped then a combined image results and interference lines occur at the point at which the old and new image join. These interference lines may be small, severe or occasionally non-existent. The memory board in the C-arm machine at the time of our experiment was not that recommended by the manufacturers (the original broke down), but is an inferior board. This interference should not occur with the correct board in place.

f) The images are, unfortunately, not reproducible with time, especially in their y (vertical) dimensions and this immediately invalidates any attempt at complete image distortion calibration. However the image dimensions in the horizontal direction and close to the horizontal mid-line of the field do not appear to vary greatly and it appeared possible to calibrate and use this central horizontal section.

6.7.1. Attempts at Calibration using the Horizontal section.

Calibrations were done using the information obtained from the Perspex grid to relate the differences between TV image coordinates (x,y) to set distances on the image detector. However trials done using the polystyrene box 'patient' revealed that errors in needle placement are still unacceptably large.

6.8. Results of Patient Trials

Although it was apparent from the dummy patient trials that the C-arm X-ray machine has almost insoluble inherent problems, it was desired to assess the performance of the remaining equipment when used in a clinical situation. With the cooperation of medical staff of the Respiratory Diseases Unit of Edinburgh City Hospital, and with the full agreement of the patient, a lung cancer sufferer was positioned on the trolley with the biopsy equipment set up around him.

A short series of patient trials (not including the final needling stage) was then done using the C-arm equipment. The results are detailed below.

6.8.1. Ease of Positioning

The trolley top, patient and relevant parts of the biopsy machine must lie between the source and detector on either end of the C-shaped arm.

The source-detector separation distance is 93cm and hence the actual space available is very confined. The C-arm machine is far from rigid, even when locked to the trolley base, the structural members being fabricated of sheet metal and required to bear at their extremities the large overhung weights of the X-ray source

and detector. In positioning the unwieldy C-shaped arm it is difficult to avoid fouling either the underside of the trolley top with the detector or the biopsy machine with the X-ray source. The levers for C-arm adjustment are behind the main support framework and it is difficult to manoeuvre the arm and observe its progress at the same time. Collisions are thus inevitable. Setting or changing the angle of view invariably involves complicated sequences of angling, height adjustment and lateral movement of the arm because of the restricted clearance between this and the patient and trolley top.

The patient trolley construction (also supplied by CGR Medical Ltd) has a couch top 2m long by 600mm wide which presents inherent problems. Although the trolley table top is x-ray translucent it has heavy deep steel beams running its full length along each side. These supports, which double as electromagnetic locks for the floating table-top, unfortunately obstruct the C-arm angling. The biopsy machine supports, although designed to lie out of the X-ray plane, interfere with the bulky housing of the X-ray source. Thus the equipment is difficult to position and manipulation of the C-arm machine is a real struggle.

6.8.2. Available Angles of View

The bulky X-ray source and detector housings and particularly the excessive width of the patient trolley top and the depth and X-ray opacity of its longitudinal supporting beams restrict the C-arm movement and reduce the achievable viewing angle range. Thus only a small range of views is available, the exact values being dependent upon lesion depth relative to the marker spheres.

6.8.3. Ergonomics

The biopsy machine calibration is done before the machine is positioned over the patient, as shown in Figure 6.9 and is

Figure 6.9 - Position of the biopsy machine while the machine calibration is done.

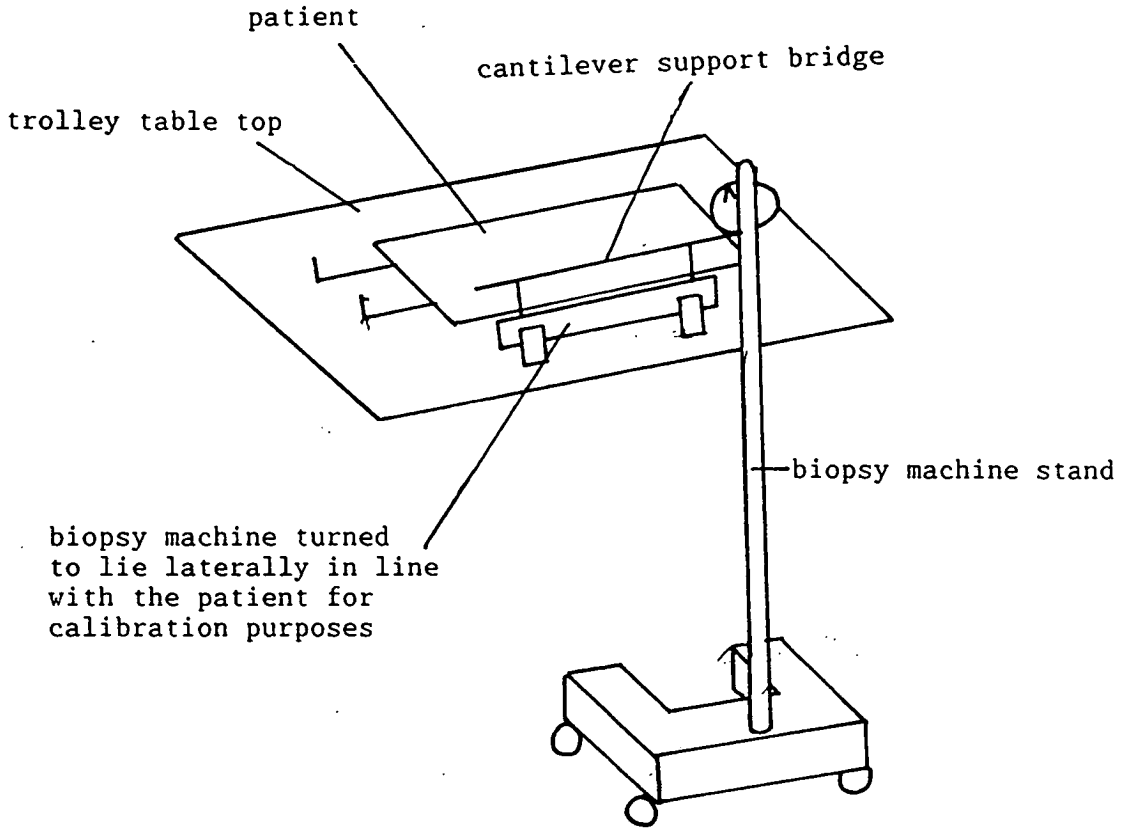

relatively simple. The cantilever is positioned over the patient. The actual alignment of the lesion and the marker spheres is done by screening and moving the floating table top until the lesion and spheres lie in line on the image. Arranging the views is more difficult. In principle the angle of view is chosen, the first sphere positioned and locked in place and then the second sphere. This however is difficult to do, since the sphere position must be altered manually and screening cannot be done while the surgeon's hands are within the X-ray field. Therefore a process of trial and error is necessary. On several occasions it became apparent, after the first sphere had been positioned and locked in place, that the second sphere would not fit into the image. Once locked in place the first sphere must not be moved until the entire screening process is complete (otherwise the entire process from machine calibration onwards must be repeated). The viewing angle must therefore be adjusted until the two spheres and the lesion can be observed in the view.

Having obtained one view it remains to locate a second view (at a suitably large separation angle away from the first view) in which the locked first sphere, the lesion and the second sphere can fit. Again a process of trial and error results.

C-arm manoeuvring constitutes the major problem.

The actual inputting of image data is relatively straightforward and does not impose problems.

Generally, the new biopsy procedure is not ergonomically sound. Even allowing for the fact that the procedure is new and strange to the medical team participating in these trials, many of the difficulties that appeared correspond to identifiable intrinsic faults.

6.8.4. Time Required for the Procedure

It follows from the above mentioned problems that the process is extremely time consuming and tedious to carry out. Most time is spent manoeuvring the C-arm to obtain a suitable viewing angle which shows all the necessary information. The existing biopsy procedure takes approximately 10 minutes from X-raying to final lesion sampling. The new procedure takes close to 30 minutes to perform. This is highly unsatisfactory: The patient, distressed anyway by his condition, will be further distressed by all the activities happening around him.

6.8.5. Image Clarity

When using the polystyrene dummy patient the spherical markers are very clear, obvious and also semi-translucent, allowing objects overlapped by them to be clearly observed. In the patient trials, however, the lesion proved difficult to see, even when large. The marker spheres are visible but sometimes difficult to pick out since they are obscured by the more dense patient.

6.8.6. Equipment Reliability

During the needle guide positioning the splined shaft drives of the angling and depthing mechanism frequently jammed. In test procedures in the lab the previous day the machine operated smoothly. The long shafts are precision made and carefully aligned. Transportation between establishments evidently misaligned the equipment.

6.9. Conclusions

Using the optical analogue the needle can be positioned to within 2 - 5mm of the centre of the lesion when selected viewing angles are used. The C-arm equipment is, however, clumsy to manoeuvre in

the obstructed environment of trolley, patient and biopsy machine. The viewing angle range is also drastically restricted by this environment and thus final needle positioning accuracy will be affected. In addition, because of poor imaging contrast and quality, it is often difficult to pick out the lesion even when it is large.

Quantitative readings cannot be taken from the equipment. Like most medical imaging systems, the C-arm X-ray machine is designed for qualitative not quantitative analysis and distortion of the image is hence large, irregular and not reproducible. It therefore appears that the lung biopsy machine developed here cannot be used in locating and sampling lung lesions with real time X-ray machines having the imaging characteristics of the C-arm machine used by us due purely to distortion.

The patient marker sphere system is large, clumsy, and difficult to position within a view, especially when the lesion lies deep within the patient's chest. Due to the patient density it is sometimes difficult to see the spheres on the image.

The actual positioning of the needle itself is accurate. Needle positioning on an actual patient has not been done but trials on polystyrene blocks have proved promising. However, this is in one respect, perhaps, an unrealistic test; the density and consistency of the tissue within the patient varies along the path of needle penetration and the needle, if large gauge, may consequently bend. No tests of needle guidance have been made in media of the consistency or variability of human tissue.

Tactility has been retained. The surgeon inserts the needle by hand by moving it along a slideway. The needle action still retains much of the sensitivity by which, in existing procedures, the surgeon may sometimes recognise a notable change in lung

consistency, often indicating that the lesion has been punctured.

If the biopsy machine is to be used in a commercial application then an alternative source of image information must be found, superior in that respect to the C-arm machine used by us. At the time of purchase (mid 1980's), we were advised that the machine was in every way representative of available machines of that general type and price range.

CHAPTER 7

FURTHER WORK

7.1. Introduction

Several factors currently limit the use of the developed biopsy machine:

The machine has been developed to operate in two dimensions only. This restricts the areas within the body which can be sampled by the biopsy needle.

Clinical trials have shown that the C-arm rotating X-ray machine, and probably any similar fluoroscopy machine is totally unsuitable for the required application due to large inherent image distortion.

Alternative imaging techniques are available but some cannot be used for imaging the lung. However the biopsy machine, although developed for sampling lung lesions, is not restricted to either respiratory medicine or to lesion sampling for diagnostic purposes.

7.2. A 3-dimensional machine

A lesion in the apex of the lung, for example, cannot be approached directly from either the anterior or posterior. The ribs are close together high in the chest and there is insufficient intercostal space for the needle to pass through. The scapula blocks any approach from the posterior. The apex can be approached by inserting the biopsy needle through the skin at a point low down in the chest wall and sharply inclining the needle in the cranial direction. This area of the lung cannot be approached using the 2-dimensional equipment.

7.2.1. Alterations Required

To be able to sample lesions lying outwith the existing needle sampling plane would require the following:

a) a further axis for image measurement. The existing image is already very cluttered when using the 2-dimensional marker: A less bulky 3-dimensional marker should be developed.

b) Needle movement in the lateral direction

c) Needle angling in the lateral plane. It is important that, during development of a 3-dimensional machine, a major aim should be to minimise the bulkiness of both the supporting equipment and the biopsy machine.

7.3. Alternative Sources of Image Information

Several alternative imaging systems are currently used in hospitals. These include X-ray plates or films, computerised axial tomography (CAT) and ultrasound.

7.3.1. X-ray plates or films

X-ray film displays essentially full scale, undistorted images. If the images are taken from different angles with the lesion and markers in view then all the necessary information will be contained on the films. At present the surgeon measures lengths directly, using a ruler, from two films obtained from perpendicular angles and then interprets the information to determine where the lesion lies relative to the marker positioned on the patient's chest . He then inserts a biopsy needle through the chest wall and into the lesion, estimating, rather than

calculating and measuring, the appropriate angles.

If the X-ray films are televised and the manual image analysis technique used to read off the relevant dimensional information then the biopsy machine can be used to position the needle more accurately. However the X-ray equipment is large and immobile which requires that the patient moves, rather than the equipment. As such the patient marker must be fixed to the patient rather than the biopsy machine. Some means of relating the marker position relative to the biopsy machine will be required.

7.3.2. Computerised Axial Tomography (CAT scanning)

CAT scanning involves the recording of 'slices' of the patient with an x-ray scanner. The records are then integrated by the CAT computer to give a cross sectional image. The CAT scanner equipment is immensely expensive in comparison with the C-arm and it is unlikely that such equipment will be available in every general hospital. This technique is more accurate and revealing than the C-arm machine and is marketed for its image measurement.

Internal software enables the coordinates of any indicated point to be calculated relative to the frame of reference within the equipment.

The developed patient marker will thus not be required: Only the coordinates of the needle insertion point require to be input to the computer relative to the same frame of reference as the lesion. In addition the insertion point must be known relative the biopsy machine. Thereafter the angle and depth of the needle insertion are determined and needling is done as normal through the indicated insertion point.

7.3.3. Ultrasound

Ultrasound, unlike X-rays does not produce harmful radiation and for that reason it is the generally preferred imaging technique. Ultrasound does not pass through air and cannot be used for viewing the lung. At other organs within the body, however, ultrasound can generate images with better detail than X-rays. It is a cheap and widely available technique. Like the CAT scanner, internal software enables accurate dimensional information to be obtained between two points indicated on the image. This eliminates the requirement of a patient marker to determine viewing angles, etc: Instead a frame of reference is required.

The needle insertion point requires to be input and hence requires an indicator to be positioned on the patient's chest which can also be viewed on the image. The needle can then be angled automatically and pushed home by the surgeon.

7.4. Alternative uses of the Biopsy Machine

Although the apparatus has been designed for lung lesion sampling for diagnostic purposes it may also be used for therapeutic purposes. Such possibilities include:

a) insertion of radioactive isotopes or powerful chemotherapeutic agents local to a lesion so that small localised doses of radiation or tumour-destroying drug may be given to a patient resulting in reduced side effects.

b) insertion of optic fibres into tumours which can then be destroyed by low power U.V. laser irradiation.

Both these require that the cancer is early and metastasis has not yet occurred. Many problems are common with those noted for the lung lesion case, such as respiratory motion.

7.5. Conclusions

Although it is evident that the developed 2-dimensional biopsy machine cannot be used with equipment of the C-arm type the equipment can be used with other imaging systems provided that the images are not randomly distorted. Alterations to the software and equipment are required for use with the alternative imaging equipment but these are mainly minor and not insurmountable. The developed biopsy machine can thus, with modifications, be used in a wider capacity than was originally intended for both diagnostic and therapeutic purposes in all parts of the body for which regular images can be obtained and which can be accessed by a biopsy needle.

NOMENCLATURE

A,B - known constants in the estimated differential equations for redundant measurements

C1,C2,C3 - known constants in equations for estimated precision, $_{ij}$

d - no of estimates of lesion position which may be calculated from n views

F - magnification factor to convert magnified TV image to corresponding true dimensions

g_i - constraint equation in redundant measurements

k - unknowns in redundant measurements, ie x and y

L_i - lesion position on TV image

$\hat{L}_i$ - estimate of Li in theoretical redundant measurement model

n- no of X-ray views taken

P - end of marker, indicated by sphere, to which all screen measurements are referred

p - no of dependent variables in the lesion equation gi=0

PL_i - point at which the X-rays from the source to the lesion cuts the marker PQ

PT_i, PB_i - diametrically opposite sides of sphere P on TV image

$\hat{PT}_i$, $\hat{PB}_i$ - estimates of PTi and PBi in theoretical redundant

measurement model

PQ - the marker length, which is measured between the centres of spheres P and Q

Q - end of marker PQ, indicated by sphere Q

QT_i, QB_i - diametrically opposite sides of sphere Q on TV image

$\hat{QT}_i$, $\hat{QB}_i$ - estimates of QTi and QBi in theoretical redundant measurement model

R - end of perpendicular marker PR, indicated by sphere R

x - distance from P, in the Q direction, along marker PQ (normally the lesion x-coordinate)

$X_{i,j}$ - independent variables in redundant measurements (ie PTi, PBi, ... etc)

$\hat{X}_{i,j}$ - estimates of independent variables in redundant measurements (ie $\hat{PTi}$, $\hat{PBi}$, ...etc)

$(x,y)_{av}$ - averaged estimate of lesion position obtained from redundant measurements

xoff - the horizontal offset distance between sphere P and the needle insertion point indicator when the latter is in its locked position

xin - horizontal distance of the needle insertion point from the original position of sphere P when positioned on the insertion point on the patients skin

y - depth below marker PQ (normally the lesion y coordinate)

Y_i - dependent variable in redundant measurements (taken to be L_i)

$\hat{Y}_i$ - estimate of the dependent variable in redundant measurements (taken to be L_i)

yin - vertical distance of the needle insertion point from the original position of sphere P when positioned on the insertion point on the patients skin

yoff - the vertical offset distance between sphere P and the needle insertion point indicator when the latter is in its locked position

Δx - horizontal distance through which the marker carriage is moved when positioning the needle insertion point indicator on the patients chest

Δy - vertical distance through which the telescopic section is moved when positioning the needle insertion point indicator on the patients chest

θ_{cL} - angle of orientation of the source to the marker (as shown in Figure 3.3) when the centre line of the X-ray passes through point P

θ_k, θ_c - angle of orientation of the source relative to marker PQ taken about point P

θ_L - angle at which the X-ray from the source to the lesion cuts PQ at point L

REFERENCES

1. Devesa S D, Silverman D T, Young J L, et al
'Cancer Incidence and Mortality Trends among Whites in the U.S. 1947-1984'
Journal of the National Cancer Institute V79, p701-770, 1987

2. Flenley D C, et al 'Concise Medical Textbook', 2nd Edition
Prepublished copy.

3. Flenley D C, Personal Communication

4. Carter S K, Glatstein E and Livington R B,
'Principles of Cancer Treatment', McGraw Hill, 1982

5. Weber M J, Journal of Biological Chemistry, V248, p2978-83, 1973

6. Chadwick C M, 'Receptors in Tumour Biology',
CUP, Cambridge, 1986

7. Roder J C, Kiesling R, Biberfield P, Andersson B,
Journal of Immunology, V121, p2509-17, 1978

8. Roder J C, Pross H F,
'The Biology of the Human Natural Killer Cell',
Journal of Clinical Immunology, V2, p249-263, 1982

9. Hande K R, Des Pres R M , 'Non Small Cell Carcinoma of the Lung', 'Recent Advances in Respiratory Medicine', Volume 3, edited by Flenley D C and Petty T L

10. Mason R J, 'Metabolism of Alveolar Macrophages'
'Respiratory Defence Mechanisms Part 2', edited by Brain

11. Byers V S , Baldwin R W, 'Immunology of Malignant Diseases',

MTP Press Ltd, Lancaster 1987, Chapter 1

12. Talmadge J E, Key M, Fidler I J,
'Macrophage Content of Metastatic and Non-metastatic Rodent Neoplasms'
Journal of Immunology, V126, p2245-2248, 1981

13. Treves A J, Cohen I R, Feldman M,
Journal of the National Cancer Institute, 1975 , p777-80

14. Ilfield, et al, International Journal of Cancer, 1973, p12,213

15. Matthews M J, Mackay B, Lukeman J,
'The Pathology of NSCC of the Lung',
'Seminars in Oncology', V10, p34-55, 1983

16. Rosenow E C, Carr D T,
'Bronchogenic Carcinoma',
Cancer Journal for Clinicians, V29, p233-245, 1979

17. Flenley D C, 'Respiratory Medicine', Chapter 14,
Bailliere Tindall, London, 1981

18. Crawford-Brown D J,
'Age Dependent Lung Doses from ingested 222Rn in Drinking Water',
Health Physics, V52, p149-156, 1987

19. Mattson M E, Kessler L G,
'The use of Tumour Related Epidemiologic Data on Smoking for Planning Cancer Control Programs',
Journal of Chronic Diseases, V40, Supplement 2, p25S-37S, 1987

20. Benhamou J, Benhamou E, Flamant R,

'Lung Cancer Risk associated with Cigar and Pipe Smoking',
International Journal of Cancer, V37, p825-829, 1986

21. 'Cancer - Principles and Practice of Oncology', edited by
DeVita V T, Hellman S, Rosenberg S A, 3rd edition,
Philadelhia: Lippencott, 1982

22. Pershagen G, Hrubec Z, Svensson C,
'Passive Smoking and Lung Cancer in Swedish Women',
American Journal of Epidemiology, V125, p7-24, 1987

23. Blot W J, Fraumeni J F,
'Passive Smoking and Lung Cancer'
Journal of the National Cancer Institute, V77, p993-1000, 1986

24. Akiba S, Kato H, Blot W J,
'Passive Smoking and Lung Cancer among Japanese Women',
Cancer Research, V48, p4804-4807, 1986

25. Wald N J, Nanchahal K, Thompson S G, Cuckle H J,
'Does Breathing Other Peoples Tobacco Smoke Cause Lung
Cancer?',
British Medical Journal, V293, p1217-1226, 1986

26. Dalager N A, Pickle L W, Mason TJ, et al,
'The Relation of Passive Smoking to Lung Cancer'
Cancer Research, V46, p4808-4811, 1986

27. Colditz G A, Stampfer M J, Willett W C,
'Diet and Lung Cancer: A Review of the Epidemiologic Evidence
in Humans',
Archives of Internal Medicine, V147, p157-160, 1987

28. Byers T E, Graham S, Haughey B P, et al,
'Diet and Lung Cancer Risk',

American Journal of Epidemiology, V125, p35-363, 1987

29. Pisani P, Berrino F, Macaluso M, et al,
'Carrots, Green Vegetables and Lung Cancer'
International Journal of Epidemiology, V15, p463-468, 1986

30. Hughes J M, Weill H, Hammad Y Y,
'Mortality of Workers Employed in Two Asbestos Cement Manufacturing Plants',
British Journal of Industrial Medicine, V44, p161-174, 1987

31. Coutts I I, Gilson J C, Kerr I H, et al,
'Mortality in Cases of Asbestosis Diagnosed by Pneumoconiosis Medical Panel',
Thorax, V42, p111-116, 1987

32. 'Cancer Control Objectives for the Nation: 1985-2000'
edited by Greenwald p, Sondik E J,
Published by NCI Monographs

33. Howe G R, Nair R C, et al,
'Lung Cancer Mortality (1950-1980) in Relation to Radon Daughter Exposure',
Journal of the National Cancer Institute, V77, p357-362, 1986

34. Halpern J, Whittenmore A S,
'Methods for Analysing Occupational Cohort Chart Data with Application to Lung Cancer in U. S. Uranium Miners',
Journal of Chronic Diseases, 40, 1987, Supplement 2, p79S-88S

35. Samet J M, Humble C G, Pathak D R,
'Personal and Family History of Respiratory Disease and Lung Cancer Risk',
American Review of Respiratory Diseases, V134, p466-470, 1986

36. Collins, Loeffler and Tivey,
'Observations on Growth Rates of Human Tumours'
American Journal of Roentgenology, V76, p988-1000, 1956

37. Spratt J S, Spjut H J, Ropier C I,
'The Frequency Distribution of the Rates of Growth and the Estimated Duration of Primary Pulmonary Carcinomas'
Cancer, V16, p687-693, 1963

38. Rigler L G,
'A Roentgen Study of Evolution of Carcinoma of the Lung',
Journal of Thoracic Surgery, V34, p283-297

39. Garland L H, Coulson W, Wollin E,
'The Rate of Growth and Apparent Duration of Untreated Primary Bronchial Carcinoma',
Cancer, 16, p694-707, 1963

40. Cameron I R, Bateman N T, 'Respiratory Disorders',
Edward Arnold, London, 1983

41. Godwin J D,
'The Solitary Pulmonary Nodule'
The Radiologic Clinics of North America, V21, p709-721, 1981

42. Selawry O S,
'Selective Treatment in Lung Cancer'
'Cancer Treatment: Endpoint Evaluation',
p343-357, edited by Stoll B A,
Published by John Wiley and sons, Chichester, 1983

43. Geddes D M,
'The Natural History of Lung Cancer: A Review Based on Rates of Tumour Growth',
British Journal of Diseases of the Chest, V73, p1-17, 1979

45. Melamed M R, Flehinger B J, Zaman M B,
'Impact of Early Detection on the Clinical Course of Lung Cancer'
The Surgical Clinics of North America, V67, p909-924, 1987

46. Boucot K R, Weiss W,
'Is Curable Lung Cancer Detected by Semi-annual Screening'
Journal of the American Medical Society, V224, p1361-1365, 1973

47. Rosen U W, Prolla J C, Gastal E S,
'Cytology in Diagnosis of Cancer Affecting the Lung',
Chest 63, p203-207, 1973

49. Brett G Z,
'Earlier Diagnosis in Lung Cancer'
British Medical Journal, V4, p260-264, 1969

50. Isherwood I, Best J K,
in 'Recent Advances in Respiratory Medicine: Volume 2'
edited by Flenley D C,
Published by Churchill Livingstone, Edinburgh 1980

51. Parbhoo S, Wahba A,
'Evaluating Response in Lesions of Lung Cancer and Central Nervous System',
in 'Cancer Treatment: Endpoint Evaluation'
edited by Stoll B A, John Wiley and Sons, Chichester, 1983

52. Niederman M S, Matthray R A,
'New Techniques for the Assessment of Interstitial Lung Disease',
Radiologic Clinics of North America, V21, p667-81, 1981

53. Sugarbaker P H, Dunnick N R, Sugarbaker E V, Chapter 11 in 'Principles and Practice of Oncology', edited by DeVita, Hellman, Rosenberg

54. Daar A S, Lennox E S, 'Tumour Markers and Antigens', in 'Tumour Markers in Clinical Practice' edited by Daar AS, Blackwell Scientific Publications, 1987

55. Bjorklund B, 'Tumour Products Reflecting Growth Activity', in 'Cancer Treatment: Endpoint Evaluation' edited by Stoll B A, John Wiley and Sons, Chichester, 1983

57. Springer G F, Parimal R D, Herta T, et al, 'Further Studies on the Detection of early Lung Cancer and Breast Carcinoma by T-antigen', in 'Tumour Markers in Cancer Control', p95-100 edited by Nieburgs H E, Holzner J H, Valli V E, Published by Alan R Liss Inc, New York, 1984

58. Carney DN, Ihde D C, Cohan M H, 'Serum Neuron-specific Enolase: A MArker for Disease Extent and Response', Lancet, p583-585, 1982

59. Rustin G J S, Bagshawe K D, 'Tumour Markers in Cancer chemothrapy', in 'Fundamentals of Cancer Chemotherapy', edited by Hellman K, McGraw Hill, New York, 1987

60. Rustin G J S, 'Circulating Tumour Markers in the Management of Human Cancer', in 'Tumour Markers in Clinical Practice',

edited by Daar A S, Blackwell Scientific Publications, 1987

61. Sloane J P S, Ormerod M G,
'Immunohistological Diagnosis of Tumours',
in 'Tumour Markers in Clinical Practice',
edited by Daar A S, Blackwell Scientific Publications, 1987

62. Kvale P A, Bode F R, Kini S,
'Diagnostic Accuracy in Lung Cancer. Comparison of Techniques used in Association with Flexible Fibreoptic Bronchoscopy',
Chest, V69, p752-757, 1976

63. Radke J R, Conway W A, Eyler W R, et al,
'Diagnostic Accuracy in Peripheral Lung Lesions: Factors Predicting Success with Flexible Fibreoptic Bronchoscopy',
Chest, V69, p176-179, 1976

64. Gibney R T N, Man G C W, King E G, et al
'Aspiration Biopsy in the Diagnosis of Pulmonary Disease'
Chest V80, p300-303, 1981

65. Rudd R M, Gellert A R, Boldy D, et al,
'Bronchoscopic and Percutaneous Aspiration Biopsy in the Diagnosis of Bronchial Carcinoma Cell-type',
Thorax, V37, p 462-465

66. Raynaud, Coman,
'Tumour Localisation using Radiomercury Labelled Compounds',
Tumour Localisation with Radioactive Agents,
IAEA, Vienna, 1976

67. Little A G, DeMeester T R, MacMahon H,
'The Staging of Lung Cancer',
Seminars in Oncology, 10, p56-70, 1983

68. Mountain C F,
'The New International Staging System for Lung Cancer',
The Surgical Clinics of North America, V67, p925-35, 1987

69. Sudlow M F,
'The Treatment of Lung Cancer',
Recent Advances of Respiratory Medicine,
edited by Flenley D C, Churchill Livingstone, Edinburgh

70. Burt M E, Pomerantz A H, Bains M S, et al,
'Results of Surgical Treatment of Stage III Lung Cancer
Invading the Mediastinum',
The Surgical Clinics of North America, V67, p987-1000, 1987

71. Jensik R J,
'Miniresection of small peripheral carcinomas of the lung',
The surgical Clinics of North America, 67, p951-958, 1987

72. Hansen H H, Rorth M,
'Small cell carcinoma of the lung' in
'Recent Advances in Respiratory Medicine',Volume 3,
edited by Flenley D C, Churchill Livingston, Edinburgh

73. Hellman S,
'Principles of Radiation Therapy', Chapter 7 in
'Cancer: Principles and Practice of Oncology', edited by
DeVita V T, Hellman s, Rosenberg S A, 3rd edition,
Philadelphia Lippencott, 1989

75. DeVita V T,
'Principles of Chemotherapy', Chapter 8 in
'Cancer: Principles and Practice of Oncology', edited by
DeVita V T, Hellman s, Rosenberg S A, 3rd edition,
Philadelphia Lippencott, 1989

76. Hellman K, Carter S K,
'Fundamentals of Cancer Chemotherapy',
McGraw Hill, New York, 1987

77. Boesden E, Davis W,
'Cytotoxic Drugs in the Treatment of Cancer',
Edward Arnold Ltd, London, 1989

78. Holmes E C,
'Treatment of Stage II Lung Cancer (T^1N^1 and T^2N^1)',
The Surgical Clinics of North America, V67, p945-949, 1987

79. Faber L P, '
Results of Surgical Treatment of Stage 3 Lung Cancer with Carinal Proximity',
The Surgical Clinics of North America, 67, p1001-1014, 1989

80. Chadwick C M,
'Antigens of normal and neoplastic cells' in
'Receptors in Tumour Biology',
edited by Chadwck C M, CUP, Cambridge, 1986

81. Markham N I, Sikora K,
'Monoclonal Antibodies and Solid Tumours' in
'Tumour Markers in Clinical Practice',
edited by Daar A S, Blackwell Scientific Publications, 1987

82. Harning S J,
'Interferon in Cancer Treatment', in
'Fundamentals of Cancer Chemotherapy',
edited by Hellman K, Carter S K, McGraw Hill, New York, 1987

83. Wanebo H J,
'Host Immunologic Impairment in Relation to Survival' in
'Cancer treatment: Endpoint Evaluation',

edited by Stoll B A, John Wiley and Sons, Chichester, 1983

84. Aisner J,
'Overview of Lung Cancer Research', Chapter 13 in
'Contemporary Issues in Clinical Oncology- Lung Cancer',
edited by Aisner J

85. Cox, Byhardt, Konaki, Seminars in Oncology, 10:81, 1983

86. Gray's Anatomy , Longman 1973, 35th Edition , p1183-1204.

87. Keith A,
'The Mechanics of Respiration in Man', in
'Further Advances in Physiology'
edited by Hill L,
Edward Arnold, London, 1909

88. Moran Campbell E J,
'The Respiratory Muscles and Mechanics of Breathing'
Lloyd Luke, London, 1958

90. Hoover C F,
'Diagnostic Signs from the Scaleni, Intercostal Muscles and the Diaphragm in Lung Ventilation'
Archives of International Medicine, V20, p701-715, 1917

91. Weiss P H, Baker J M, Potchen J,
'Assessment of Hepatic Respiratory Excursion',
Journal of Nuclear Medicine, V13, p758-9, 1972

92. Suramo I. Paivansalo M, Myllyla V,
'Cranio-caudal Movements of the Liver, Pancreas, and Kidneys in Respiration',
Acta Radiologica Diagnosis, V25, p129-31, 1984

93. Jones K R,
'A Respiration Monitor for use with CT body Scanning and other Imaging Techniques',
British Journal of Radiology, V55, p530, 1982

94. Wade O L,
'Movements of the Thoracic Cage and Diaphragm in Respiration'
Journal of Physiology, V124, p 193-212, 1954

97. Stringfield J T, Markowitz D J, Bentz R R, et al,
'The Effect of Tumour Size and Location on Diagnosis by Fibreoptic Bronchoscopy',
Chest, V72, p474-6, 1977

98. Ellis J H,
'Transbronchial Lung Biopsy via the Fibreoptic Bronchoscope: Experience with 107 Consecutive Cases and Comparison with Bronchial Brushing',
Chest V68, p524-532, 1975

99. Harrison B D W, Thorpe R S, Kitchemner P G, et al,
'Percutaneous Trucut Lung Biopsy in the Diagnosis of Localised Pulmonary Lesions',
Thorax, V39, p493-499, 1984

100. Berquist T H, Bailey P B, Cortese D A, Miller W E,
'Transthoracic Needle Biopsy: Accuracy and Complications in Relation to Location and Type of Lesion',
Mayo Clinic Proceedings, V55, p475-481, 1980

101. Lalli A F, McCormack L J, Zelch M, et al,
'Aspiration Biopsies of chest Lesions',
Radiology, V127, p35-40, 1978

102. Wightman A, Personal Communication

103. Westcott J L,
'Percutaneous Needle Aspiration of Hilar and Mediastinal Masses',
Radiology, V129, p323-329, 1981

104. Zavala D C, Schoell J E,
'Ultrathin Needle Aspiration of the Lung in Infectious and Malignant Disease',
American Review of Respiratory Diseases, V123, p125-131, 1981

105. Shields T W, Higgins G A, Matthews M J, Keehn R J,
'Surgical Resection in the Management of SCC of the Lung',
Journal of Thoracic and Cardiovascular Surgery, V84,
p481-488, 1982

106. Meyer J A,
'Indications for Surgical Treatment in Small Cell Carcinoma of the Lung',
The surgical Clinics of North America, V67, p1103-1155, 1987

107. Maurer L H, Tulloh M, Weiss R B, et al,
'A Randomised Modality Trial in SCC of the Lung',
Cancer, 45, p30-39, 1980

108. Inde D C, Makuch R W, Carney D N, et al,
'Prognostic Implications of Stage of Disease and Sites of Metastases in Patients with SCC of the Lung Treated with Intensive Combination Chemotherapy',
American Review of Respiratory Diseases, V123, p500-507, 1981

109. Martini N, Beattie E J,
'Results of surgical Treatment in Stage 1 Lung Cancer',
Journal of Thoracic and Cardiovascular Surgery, V74,
p499-504, 1977

110. Jensik R J, Faber L P, Kittle C F,
'Segmental Resection for Bronchogenic Carcinoma',
The Annals of Thoracic Surgery, V28, p475-483, 1979

111. Cooper J D, Pearson F G, Todd T R J,
Radiotherapy alone for Patients with Operable Carcinoma of the lung''
Chest, V87, p289-292

112. Williams D E, Pairolero P C, Davis C S, et al,
'Survival of Patients Surgically Treated for Stage 1 Lung Cancer',
Journal of Thoracic and Cardiovascular Surgery, V82, p70-76, 1981

113. Mountain C F, Carr D T, Anderson W A D,
'A System for the Clinical Staging of Lung Cancer',
American Journal of Roentgenology, V120, p130-138, 1974

114. Paulson D L,
'Carcinomas in the superior Pulmonary Sulcus',
Journal of Thoracic and Cardiovascular Surgery, V70,
p1095-104, 1975

115. Shields T W, Humphrey E W, Matthews M, et al,
'Pathological Stage Grouping of Patients with Resected Carcinoma of the Lung',
Journal of Thoracic and Cardiovascular Surgery, V80,
p400-405, 1980

116. Pairolero P C, Trastec V F, Payne W S,
'Treatment of Bronchogenic Carcinoma with Chest Wall Invasion',
The Surgical Clinics of North America, 67, p925-935, 1987

117. Martini N, Flehinger B J,
'The Role of Surgery in N² Lung Cancer',
The Surgical Clinics of North America, 67, p1037-1049, 1987

118. Robertson G I,
'Vision System Separates Gathering From Processing'
in 'Robot Vision',
edited by Alan Pugh, IFS Publications Ltd, U K, 1983

119. Bolles R C, Cain R A,
'Recognising and Locating Partially Visible Objects: The Local Feature-Focus Method' in
'Robot Vision',
edited by Alan Pugh, IFS Publications Ltd, U K, 1983

120. Horn B K P,
'Robot Vision',
MIT Press, London, 1986

Appendix 1

The following charts give the results of experiments with the mechanical plotter for the error radii, in cm, of the circles drawn around the lozenges representing the possible lesion positions (Figure 3.11), for lesions of different known coordinates (x,y) relative to the marker sphere centre and marker rod.

The figures down the side and along the top of the charts are the angles of view in degrees relative to the marker PQ, as illustrated in Figure 3.8.

In the case of the triangular charts the comparisons are drawn over two views taken at the same source-marker distance, XP, using the same marker dimensions, whereas when the complete table is filled the two views have been taken with at least one variable (other than orientation) different.

This is an attempt to identify lesions of at most 1cm radius on the half scale apparatus, ie radii of 0.5 cm at most, in the full scale case, and the object is to find acceptable ranges of angles over which this may be achieved. Such viewing angles correspond to the chart regions bounded by the stepped lines.

All charts, with the exception of Chart 13, use combinations of angle determination methods. Over the range 60°-90° angular information is assumed to come from the C-arm and is used directly. Outwith this range the marker is used to determine the angle optically (as shown in Figure 3.6).

Chart 1

Sphere diameter D=2cm
Source Marker distance Xp1=30cm
Xp2=30cm
Marker rod length PQ=10cm
lesion position (cm) = (10,10)

angle of view 2	Angle of View 1, degrees																	
	10	20	30	40	50	60	70	80	90	100	110	120	130	140	150	160	170	180
20	5.7																	
30	3.0	7.5																
40	1.7	2.4	6.6															
50	1.6	2.2	4.2	∞														
60	1.4	1.7	2.7	8.9	∞													
70	1.3	1.5	2.4	4.4	9.2	∞												
80	1.2	1.4	1.8	3.6	4.3	10.3	∞											
90	1.0	1.2	1.5	2.3	3.0	4.8	11.7	∞										
100	0.9	1.0	1.3	1.8	2.5	3.8	7.4	∞	∞									
110	0.7	0.8	1.5	1.5	1.9	2.6	3.9	7.3	∞	∞								
120	0.6	0.6	0.8	1.1	1.3	1.7	2.2	3.1	5.0	7.6	∞							
130																		
140																		
150	0.5	0.5	0.5	0.7	0.8	1.0	1.1	1.3	1.5	1.4	1.4	1.7						
160	0.5	0.5	0.6	0.6	0.8	0.9	1.0	1.2	1.3	1.2	1.2	1.3			5.4			
170																		
180																		

Chart 2

sphere diameter D=2cm
Source marker distance Xp1=40cm
Xp2=40
Marker rod length PQ=10cm
lesion position (cm)= (10,10)

Angle of View 1, degrees

angle of view 2

	10	20	30	40	50	60	70	80	90	100	110	120	130	140	150	160	170	180
20	4.2																	
30	2.3	6.2																
40	1.9	3.1	15.5															
50	1.7	2.3	4.1	∞														
60	1.4	1.9	2.9	7.8	∞													
70	1.2	1.6	2.1	3.9	25.0	∞												
80	1.2	1.4	1.8	2.8	5.9	8.1	∞											
90	1.0	1.2	1.5	2.2	3.6	4.2	9.5	∞										
100	1.0	1.1	1.4	2.0	3.1	3.4	6.3	∞	∞									
110	0.8	0.9	1.0	1.4	2.0	2.1	3.0	4.8	13.1	∞								
120	0.6	0.6	0.7	1.0	1.4	1.4	1.8	2.5	3.4	5.6	∞							
130																		
140																		
150	0.7	0.6	0.6	0.7	0.9	1.0	1.1	1.1	1.6	1.8	2.0	2.5						
160	0.8	0.6	0.6	0.7	0.9	0.9	1.0	1.2	1.4	1.4	1.6	1.7			8.2			
170	0.9	0.7	0.7	0.7	0.8	0.8	0.9	1.1	1.2	1.3	1.4	1.4			2.9	6.7		
180																		

Chart 3

sphere diameter D=2 cm
Source marker distance Xp1=50cm
Xp2=50cm
Marker rod length PQ=10cm
lesion position (cm)= (10,10)

Angle of View 1, degrees

angle of view 2

	10	20	30	40	50	60	70	80	90	100	110	120	130	140	150	160	170	180
20	5.0																	
30	2.4	6.8																
40	2.3	3.3	∞															
50	1.8	2.5	4.8	∞														
60	1.4	1.8	2.7	∞	∞													
70	1.3	1.6	2.3	3.7	∞	∞												
80	1.2	1.4	1.9	2.6	10.	11.	∞											
90	1.1	1.2	1.6	2.0	5.2	5.5	9.0	∞										
100	1.0	1.1	1.4	1.7	3.6	3.3	4.4	9.7	∞									
110	0.9	1.0	1.2	1.5	2.7	2.7	3.1	4.6	9.6	∞								
120	0.8	0.9	1.1	1.3	2.3	2.3	2.5	3.6	5.8	∞	∞							
130	0.8	0.8	0.8	1.0	1.6	1.7	2.2	2.3	3.0	4.6	12.1	∞						
140																		
150	0.9	0.9	0.9	0.8	1.3	1.3	1.3	1.6	1.9	2.3	3.0	3.5	5.4					
160	1.0	1.0	0.9	0.9	1.1	1.1	0.9	1.3	1.5	1.8	2.2	2.3	2.9		22.0			
170	1.1	1.0	0.9	0.9	1.1	1.0	1.0	1.1	1.4	1.4	1.6	1.7	1.9		4.0	7.0		
180																		

Chart 4

sphere diameter D=4cm
Source marker distance Xp1=30cm
Xp2=30
Marker rod length PQ=10cm
lesion position (cm)= (10,10)

Angle of View 1, degrees

angle of view 2	10	20	30	40	50	60	70	80	90	100	110	120	130	140	150	160	170	180
20	1.7																	
30	1.0	2.9																
40	1.0	2.0	5.9															
50	0.9	1.3	2.0	10.1														
60	0.9	1.3	1.7	3.8	∞													
70	0.9	1.2	1.5	2.5	5.5	∞												
80	0.9	1.1	1.3	2.0	3.0	9.7	∞											
90	0.8	1.0	1.2	1.7	2.2	4.2	11.0	∞										
100	0.5	0.6	0.7	1.0	1.3	2.2	3.3	8.6	∞									
110	0.3	0.4	0.5	0.7	0.9	1.4	2.1	3.1	6.4	∞								
120	0.3	0.4	0.4	0.6	0.8	1.2	1.7	2.1	3.1	3.3	7.3							
130																		
140																		
150	0.3	0.3	0.3	0.4	0.5	0.7	0.9	1.0	1.3	1.0	0.9	1.3						
160	0.3	0.3	0.3	0.4	0.4	0.7	0.8	1.0	1.0	0.8	0.8	0.9			3.1			
170																		
180																		

Chart 5

sphere diameter D=4 cm
source marker distance Xp1=30cm
Xp2=30
marker rod length PQ=10cm
lesion position (cm)= (5,4)

Angle of View 1, degrees

angle of view 2	10	20	30	40	50	60	70	80	90	100	110	120	130	140	150	160	170	180
20	1.0																	
30	0.5	1.1																
40	0.4	0.8	1.3															
50	0.3	0.7	0.7	2.2														
60	0.3	0.4	0.5	1.3	∞													
70	0.3	0.5	0.5	0.9	2.9	∞												
80	0.3	0.4	0.5	0.8	1.4	2.2	∞											
90	0.3	0.3	0.4	0.6	1.0	1.3	4.4	∞										
100	0.2	0.3	0.3	0.4	0.6	0.7	1.3	3.4	∞									
110	0.2	0.2	0.2	0.3	0.4	0.4	0.7	1.2	1.3	4.4								
120																		
130																		
140																		
150																		
160																		
170																		
180																		

Chart 6

sphere diameter D=4 cm
source marker distance Xp1=30cm
Xp2=30cm
marker rod length PQ=10cm
lesion position (cm) = (5,10)

Angle of View 1, degrees

angle of view 2	10	20	30	40	50	60	70	80	90	100	110	120	130	140	150	160	170	180
20	2.1																	
30	1.2	2.7																
40	1.1	1.7	4.8															
50	0.9	1.3	2.1	lge														
60	0.9	1.2	1.7	3.9	∞													
70	0.9	1.1	1.4	2.5	5.0	∞												
80	0.8	1.0	1.2	1.8	2.6	6.9	∞											
90	0.6	0.7	0.8	1.2	1.6	2.9	7.0	∞										
100	0.4	0.5	0.6	0.9	1.1	1.3	2.5	5.0	∞									
110																		
120																		
130																		
140	0.3	0.3	0.3	0.5	0.5	0.7	0.9	1.1	1.0	1.2								
150	0.3	0.3	0.3	0.4	0.5	0.6	0.8	0.9	1.1	0.9								
160																		
170																		
180																		

3.4

Chart 7

sphere diameter D1=2cm
D2=2cm
source marker distance Xp1=30cm
Xp2=40cm
Marker rod length PQ=10cm
lesion position (cm)= (10,10)

Angle of View 1, degrees

angle of view 2	10	20	30	40	50	60	70	80	90	100	110	120	130	140	150	160	170	180
10	4.8	2.6	2.0	1.4	1.4	1.2	1.2	1.1	1.0	0.8	0.7	0.6			0.6	0.7		
20	∞	10.2	3.8	2.1	1.9	1.6	1.4	1.3	1.2	0.9	0.7	0.6			0.6	0.6		
30	3.9	∞	∞	3.9	3.0	2.2	1.9	1.6	1.4	1.1	0.9	0.7			0.6	0.6		
40	2.4	4.4	∞	∞	13.1	4.5	3.1	2.4	2.1	1.7	1.4	1.1			0.7	0.7		
50	1.8	2.6	6.5	∞	∞	∞	8.8	4.5	3.3	2.7	2.0	1.5			0.9	0.8		
60	1.6	2.1	3.7	∞	∞	∞	∞	5.5	3.6	2.9	2.1	1.5			0.9	0.8		
70	1.4	1.7	2.4	6.1	∞	∞	∞	∞	6.8	4.9	3.0	2.0			1.0	0.9		
80	1.3	1.5	2.0	3.6	5.9	∞	∞	∞	∞	15.3	5.3	2.8			1.3	1.2		
90	1.1	1.3	1.7	2.6	3.5	6.1	lge	∞	∞	∞	lge	4.1			1.5	1.3		
100	1.0	1.2	1.4	2.2	2.9	4.6	10.5	∞	∞	∞	∞	9.3			1.6	1.4		
110	0.8	0.9	1.1	1.6	1.9	12.5	3.6	6.5	lge	∞	∞	∞			2.0	1.5		
120	0.6	0.6	0.8	1.0	1.3	1.6	2.0	2.8	3.9	4.5	9.0	∞			2.3	1.7		
130																		
140																		
150	0.6	0.6	0.6	0.7	0.9	1.0	1.2	1.4	1.6	1.5	1.5	1.9			∞	10.1		
160	0.6	0.6	0.6	0.6	0.8	0.9	1.0	1.2	1.4	1.2	1.2	1.4			5.4	∞		
170	0.7	0.6	0.7	0.6	0.7	0.8	0.9	1.1	1.1	1.1	1.0	1.2			2.3	4.3		
180																		

Chart 8

sphere diameter D1=2cm
D2=2cm
Source marker distance Xp1=30cm
Xp2=50cm
marker rod length PQ=10cm
lesion position (cm)= (10,10)

Angle of View 1, degrees

angle of view 2	10	20	30	40	50	60	70	80	90	100	110	120	130	140	150	160	170	180
10	2.8	1.8	1.6	1.2	1.2	1.1	1.0	1.0	0.9	0.8	0.6	0.6			0.7	0.7		
20	∞	4.4	2.9	1.8	1.7	1.5	1.3	1.2	1.1	0.9	0.8	0.6			0.6	0.7		
30	11.5	∞	12.6	3.2	2.7	2.2	1.8	1.6	1.4	1.2	1.0	0.8			0.6	0.7		
40	3.5	11.5	∞	13.1	6.0	3.5	2.5	2.1	1.8	1.5	1.3	1.0			0.7	0.7		
50	2.5	3.7	∞	∞	∞	∞	13.5	6.1	4.1	3.5	2.6	1.9			1.2	1.0		
60	1.8	2.2	3.7	∞	∞	∞	14.0	6.3	4.1	3.4	2.5	1.8			1.1	1.0		
70	1.5	1.9	2.7	9.3	∞	∞	∞	13.2	5.6	4.4	3.0	1.9			1.1	1.0		
80	1.3	1.6	2.2	4.0	7.4	∞	∞	∞	lge	10.2	4.8	2.7			1.3	1.2		
90	1.2	1.4	1.8	2.8	3.9	7.2	∞	∞	∞	∞	∞	3.9			1.5	1.3		
100	1.0	1.0	1.5	2.1	2.7	3.9	7.0	∞	∞	∞	∞	8.2			1.8	1.6		
110	1.0	1.0	1.3	1.7	2.1	2.8	3.8	6.5	∞	∞	∞	∞			2.5	1.9		
120	0.9	0.9	1.3	1.5	1.8	2.3	3.0	4.5	8.9	∞	∞	∞			2.8	2.1		
130	0.7	0.7	0.8	1.1	1.3	1.6	2.1	1.5	3.4	3.6	4.9	∞			4.0	2.5		
140																		
150	0.8	0.7	0.8	0.9	1.0	1.2	1.4	1.6	1.9	1.8	1.9	2.4			∞	∞		
160	0.7	0.7	0.7	0.7	0.9	1.0	1.2	1.3	1.5	1.4	1.4	1.6			6.3	∞		
170	0.8	0.7	0.7	0.7	0.8	0.9	1.0	1.1	1.2	1.1	1.1	0.7			2.4	4.2		
180																		

Chart 9

sphere diameter D1=2cm
D2=2cm
Source marker distance Xp1=40cm
Xp2=50cm
marker rod length PQ=10cm
lesion position (cm)= (10,10)

Angle of View 1, degrees

angle of view 2

	10	20	30	40	50	60	70	80	90	100	110	120	130	140	150	160	170	180
10	8.9	lge	3.4	2.3	2.0	1.6	1.4	1.3	1.1	1.0	0.9	0.8	0.7		0.9	0.9	1.0	
20	2.7	∞	∞	4.8	3.0	2.0	1.7	1.5	1.3	1.2	1.0	0.9	0.7		0.8	0.8	0.8	
30	1.8	3.7	∞	∞	6.5	3.0	2.5	1.9	1.6	1.2	1.2	1.0	0.8		0.8	0.8	0.8	
40	1.5	2.4	6.9	∞	∞	8.4	4.7	3.0	2.3	1.9	1.5	1.3	1.0		0.9	0.8	0.8	
50	1.4	2.0	3.4	12.2	∞	∞	∞	7.0	4.0	2.8	2.2	1.9	1.4		1.1	0.9	0.8	
60	1.3	1.7	2.7	5.1	∞	∞	∞	10.8	4.6	3.0	2.3	2.0	1.4		1.1	0.9	0.9	
70	1.1	1.4	2.1	3.2	∞	∞	∞	∞	lge	4.8	3.2	2.7	1.7		1.3	1.1	0.9	
80	1.1	1.4	1.8	2.4	8.0	8.8	∞	∞	∞	11.5	5.0	3.7	2.4		1.6	1.3	1.2	
90	1.0	1.2	1.5	2.0	4.8	4.8	7.6	∞	∞	∞	10.9	6.2	3.1		1.8	1.5	1.2	
100	0.9	1.1	1.4	1.8	4.0	4.0	5.4	lge	∞	∞	∞	∞	4.3		2.0	1.6	1.3	
110	0.7	0.9	1.1	1.3	2.7	2.5	2.9	4.5	10.2	∞	∞	∞	10.1		2.5	1.8	1.4	
120	0.6	0.6	0.8	1.0	1.8	1.7	1.8	2.4	3.4	5.9	∞	∞	∞		3.3	2.1	1.4	
130																		
140																		
150	0.7	0.7	0.7	0.7	1.2	1.1	1.1	1.4	1.6	1.9	2.5	2.9	2.9		∞	9.2	2.9	
160	0.8	0.8	0.7	0.7	1.1	1.0	1.0	1.2	1.4	1.6	2.4	2.1	2.6		lge	∞	5.0	
170	0.9	0.9	0.8	0.8	1.1	1.0	1.0	1.1	1.2	1.5	1.7	1.7	1.8		4.1	8.7	∞	
180																		

Chart 10

sphere diameter D1=4cm
D2=2cm
source marker distance Xp1=30cm
Xp2=30cm
marker rod length PQ=10cm
lesion position (cm)= (10,10)

Angle of View 1, degrees

angle of view 2	10	20	30	40	50	60	70	80	90	100	110	120	130	140	150	160	170	180
10	∞	3.3	1.7	1.2	1.2	1.2	1.1	1.0	0.9	0.6	0.5	0.4			0.4	0.5		
20	3.3	∞	3.1	2.2	1.5	1.4	1.3	1.2	1.1	0.7	0.5	0.5			0.4	0.4		
30	2.1	8.2	∞	7.2	2.6	2.2	1.9	1.5	1.4	1.0	0.7	0.6			0.5	0.5		
40	1.3	2.2	5.0	∞	∞	7.4	3.7	2.6	2.1	1.3	1.0	0.9			0.6	0.6		
50	1.3	2.0	3.3	∞	∞	∞	8.3	3.9	2.8	1.7	1.3	1.1			0.8	0.7		
60	1.1	1.6	2.1	4.6	∞	∞	∞	9.8	4.5	2.5	1.7	1.1			0.9	0.8		
70	1.1	1.4	1.7	2.8	6.3	∞	∞	∞	11.4	3.7	2.2	1.7			1.0	0.9		
80	1.0	1.2	1.4	2.2	3.4	10.0	∞	∞	∞	9.1	3.4	2.3			1.2	1.1		
90	0.9	1.0	1.2	1.7	2.3	4.3	11.1	∞	∞	∞	7.2	3.3			1.3	1.2		
100	0.7	0.9	1.0	1.5	2.0	3.5	7.0	∞	∞	∞	∞	3.7			1.2	1.1		
110	0.6	0.7	0.8	1.1	1.5	2.4	3.7	7.0	∞	∞	∞	6.5			1.2	1.1		
120	0.4	0.5	0.6	0.8	1.0	1.5	2.1	2.8	4.7	6.4	∞	∞			1.4	1.2		
130																		
140																		
150	0.4	0.3	0.3	0.5	0.5	0.8	1.0	1.2	1.4	1.1	1.1	1.6			∞	4.2		
160	0.4	0.4	0.4	0.4	0.5	0.7	0.9	1.0	1.2	1.0	1.0	1.1			3.1	∞		
170																		
180																		

Chart 11

sphere diameter D1=4cm
D2=2cm
source marker distance Xp1=30cm
Xp2=40cm
marker rod length PQ=10cm
lesion position (cm)= (10,10)

Angle of View 1, degrees

angle of view 2	10	20	30	40	50	60	70	80	90	100	110	120	130	140	150	160	170	180
10	4.7	1.9	1.3	1.2	1.0	1.1	1.1	1.0	0.9	0.6	0.5	0.5			0.5	0.6		
20	19.0	5.8	2.2	2.0	1.3	1.3	1.3	1.2	1.0	0.7	0.5	0.5			0.4	0.5		
30	2.6	∞	13.0	3.9	2.1	1.8	1.6	1.4	1.3	0.8	0.6	0.6			0.5	0.5		
40	2.0	4.4	∞	∞	7.0	3.9	3.0	2.1	1.8	1.2	0.8	0.8			0.7	0.6		
50	1.6	2.6	5.2	∞	∞	∞	7.6	4.2	2.9	1.9	1.4	1.2			0.8	0.8		
60	1.3	2.0	3.0	10.3	∞	∞	∞	5.3	3.4	2.1	1.5	1.3			0.8	0.8		
70	1.1	1.6	2.0	3.8	15.0	∞	∞	∞	6.3	3.0	2.0	1.5			1.0	0.9		
80	1.1	1.3	1.7	2.7	4.6	∞	∞	∞	∞	5.8	2.9	2.1			1.2	1.1		
90	1.0	1.2	1.4	2.0	2.9	5.8	∞	∞	∞	∞	5.0	3.0			1.4	1.2		
100	0.9	1.1	1.2	1.8	2.4	4.3	10.0	∞	∞	∞	∞	4.9			1.5	1.1		
110	0.7	0.8	0.9	1.2	1.5	2.3	3.4	6.0	∞	∞	∞	∞			1.7	1.4		
120	0.5	0.6	0.6	0.8	1.0	1.4	1.9	2.4	3.6	4.1	11.6	∞			2.0	1.5		
130																		
140																		
150	0.5	0.4	0.4	0.5	0.6	0.8	1.1	1.2	1.5	1.2	1.3	1.7			∞	8.3		
160	0.5	0.5	0.8	0.8	0.5	0.7	0.9	1.0	1.3	1.0	1.0	1.2			3.9	∞		
170																		
180																		

Chart 12

sphere diameter D1=4cm
D2=2cm
source marker distance Xp1=30cm
Xp2=50cm
marker rod length PQ=10cm
lesion position (cm)= (10,10)

Angle of View 1, degrees

angle of view 2	10	20	30	40	50	60	70	80	90	100	110	120	130	140	150	160	170	180
10	2.5	1.4	1.1	1.1	0.9	0.9	0.9	0.9	0.8	0.6	0.4	0.5			0.6	0.6		
20	∞	3.0	1.8	1.6	1.4	1.2	1.2	1.1	1.0	0.7	0.6	0.6			0.6	0.7		
30	4.9	∞	5.4	3.1	2.0	1.7	1.7	1.5	1.3	0.9	0.7	0.7			0.6	0.7		
40	2.6	∞	∞	∞	4.2	3.0	2.4	1.9	1.7	1.2	0.9	0.8			0.7	0.7		
50	2.0	3.6	12.3	∞	∞	∞	11.0	5.8	4.0	2.4	1.8	1.7			1.2	1.0		
60	1.6	2.2	3.0	11.0	∞	∞	11.0	6.0	4.0	2.5	1.8	1.5			1.0	1.0		
70	1.3	1.7	2.4	4.6	∞	∞	∞	12.8	5.6	3.0	1.9	1.6			1.0	1.0		
80	1.1	1.5	1.8	2.8	5.3	∞	∞	∞	∞	5.3	2.8	2.1			1.2	1.1		
90	1.1	1.2	1.5	2.2	2.3	6.5	∞	∞	∞	∞	4.8	3.0			1.5	1.3		
100	1.0	1.1	1.3	1.7	2.1	3.5	5.7	∞	∞	∞	∞	5.2			1.8	1.5		
110	0.9	1.0	1.1	1.5	1.7	2.8	3.6	5.8	∞	∞	∞	∞			2.2	1.8		
120	0.8	1.0	1.0	1.2	1.4	2.1	2.8	4.1	7.7	∞	∞	∞			2.4	2.0		
130	0.8	0.9	0.7	1.2	1.1	1.8	1.8	2.3	3.1	3.2	4.7	∞			3.7	2.2		
140																		
150	0.6	0.6	0.6	0.7	0.8	1.0	1.3	1.5	1.8	1.6	1.7	2.1			∞	∞		
160	0.5	0.5	0.5	0.6	0.7	0.9	1.0	1.2	1.3	1.2	1.2	1.5			4.7	∞		
170	0.5	0.5	0.5	0.6	0.6	0.7	0.9	1.0	1.1	0.9	1.4	1.1			2.0	3.4		
180																		

Chart 13

Using the optical technique. The construction is done using _0.5°, ie P'Q' location is not required.

sphere diameter D1=4cm
source marker lenth Xp=30cm
marker rod length PQ=10cm
lesion position (cm)= (10,10)

Angle of View 1, degrees

angle of view 2

	10	20	30	40	50	60	70	80	90	100	110	120	130	140	150	160	170	180
20	2.3																	
30	1.3	3.0																
40	0.8	1.4	2.8															
50	0.7	1.1	1.6	3.2														
60	0.6	0.8	1.1	1.5	3.6													
70	0.5	0.6	0.8	1.0	1.7	3.1												
80	0.4	0.5	0.6	0.7	1.1	1.5	3.4											
90	0.4	0.5	0.5	0.6	0.9	1.1	1.7	3.0										
100	0.3	0.4	0.5	0.5	0.6	0.8	1.1	1.5	3.1									
110	0.3	0.4	0.4	0.5	0.6	0.7	0.9	1.0	1.6	3.4								
120	0.3	0.3	0.4	0.4	0.5	0.5	0.6	0.7	1.0	1.4	3.1							
130																		
140																		
150	0.3	0.3	0.3	0.3	0.3	0.3	0.4	0.4	0.4	0.5	0.7	0.8						
160	0.3	0.3	0.3	0.3	0.3	0.3	0.3	0.4	0.4	0.4	0.5	0.6			2.1			
170																		
180																		

Chart 14

sphere diameter D=2cm
source marker distance Xp=30cm
marker rod length PQ=10cm
lesion position (cm)= (10,10)

Angle of View 1, degrees

angle of view 2

	10	20	30	40	50	60	70	80	90	100	110	120	130	140	150	160	170	180
20	4.1																	
30	2.1	6.9																
40	2.0	3.9	∞															
50	1.6	3.0	lge	∞														
60	1.6	2.5	5.5	∞	∞													
70	1.3	1.9	3.2	lge	9.5	∞												
80	1.2	1.7	2.6	6.3	4.6	∞	∞											
90	1.0	1.1	2.2	5.4	3.9	8.7	∞	∞										
100	0.9	1.2	1.7	3.3	2.7	4.3	8.1	∞	∞									
110	0.6	0.8	1.1	2.0	1.5	2.3	2.7	4.8	4.5	∞								
120	0.6	0.8	1.0	1.6	1.3	1.8	2.0	3.1	2.5	4.4	∞							
130																		
140																		
150	0.5	0.8	0.7	1.0	0.8	1.1	1.1	1.5	1.1	1.3	1.3	1.9						
160	0.5	0.6	0.6	0.9	0.9	1.0	1.0	1.3	0.9	1.1	1.0	1.4			5.0			
170																		
180																		

Chart 15

sphere diameter D=2cm
source marker distance Xp=40cm
marker rod length PQ=15cm
lesion position (cm)= (10,10)

Angle of View 1, degrees

angle of view 2

	10	20	30	40	50	60	70	80	90	100	110	120	130	140	150	160	170	180
20	4.5																	
30	2.5	7.9																
40	1.9	3.2	∞															
50	1.7	2.5	5.8	∞														
60	1.6	2.1	3.4	lge	∞													
70	1.4	1.7	2.5	5.7	8.2	∞												
80	1.2	1.4	1.9	3.3	3.8	8.2	∞											
90	1.1	1.3	1.6	2.5	2.8	4.4	9.2	∞										
100	1.0	1.2	1.7	2.7	3.0	4.8	11.6	∞	∞									
110	0.7	0.9	1.1	1.5	1.7	2.2	3.2	5.1	lge	∞								
120	0.7	0.7	0.9	1.2	1.3	1.7	2.2	2.9	4.8	5.9	∞							
130																		
140																		
150	0.8	0.7	0.6	0.8	0.8	1.0	1.2	1.3	1.7	1.5	1.7	2.0						
160	0.8	0.6	0.6	0.7	0.7	0.9	1.0	1.1	1.3	1.2	1.2	1.4			6.0			
170	0.9	0.7	0.7	0.7	0.7	0.9	0.9	1.0	1.2	1.1	1.1	1.1			2.6	4.9		
180																		

Appendix 2 - Lesion Position Estimation Method

For each view the viewing angle θ_c is determined. The lesion position is measured on each view relative to spheres P and Q. Figure 4.7 illustrates the situation.

The lesion position is determined as follows:

$\theta_k=\theta_c$

$KR=KP\cos\theta_k$

$PR=KP\sin\theta_k$

$\angle\hat{LXP}=\tan{-1}(KP/XP)$

$\angle\hat{XPL}=\theta_c$

$\angle\hat{XLP}=180-\hat{LXP}-\hat{XPL}$

$\theta_L=180-\hat{XLP}$

$$RL=\frac{KR}{\tan\theta_L}$$

$PL=PR+RL$

Thus for each view an estimate of θ_L and PL is obtained. Solving for both sets:

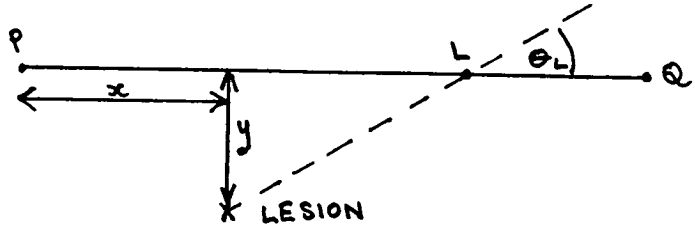

$$\tan\theta_L(1) = \frac{y}{PL(1)-x} \qquad \tan\theta_L(2) = \frac{y}{PL(2)-x} \qquad \theta_L \neq 90°$$

$$y = \tan\theta_L(1)[PL(1)-x] = \tan\theta_L(2)[PL(2)-x]$$

$$[\tan\theta_L(1) - \tan\theta_L(2)]x = PL(1)\tan\theta_L(1) - PL(2)\tan\theta_L(2)$$

$$x = \frac{PL(1)\tan\theta_L(1) - PL(2)\tan\theta_L(2)}{\tan\theta_L(1) - \tan\theta_L(2)}$$

$$x = \left[\frac{PL(1)\dfrac{\tan\theta_L(1)}{\tan\theta_L(2)} - PL(2)}{\dfrac{\tan\theta_L(1)}{\tan\theta_L(2)} - 1}\right]$$

$$y = [PL(1) - x]\tan\theta_L(1)$$

Hence the lesion position (x,y)

Appendix 3 - Least squares approximation of the lesion position using redundant measurements.

The following equations represent the minimised sum of squares for any non-linear model.

$$\sum_{j=1}^{n} (Y_j - \hat{Y}_j)\sigma_{Yj}^{-2} \frac{\partial g_j}{\partial B_k} = 0 \qquad k=1,\ldots,p \tag{1}$$

$$(X_{ik} - \hat{X}_{ik})\sigma_{Xik}^{-2} + (Y_i - \hat{Y}_i)\sigma_{Yi}^{-2} \frac{\partial g_i}{\partial \xi_{ik}} = 0 \tag{2}$$

where $i=1,\ldots,n$

p= no of dependent variables

n=no of sets of results

Along with the constraint equations:

$$g_i = 0 \quad i=1,\ldots,n \tag{3}$$

these may be solved for the unknowns $\hat{Y}_1$ ..,$\hat{X}_{11}$ ..and b_1, (the coefficients of X_{11}... and any constants)

In the model under consideration let L_i, the lesion point, be the independent variable, Y_i, and PT_i, PB_i, QT_i, QB_i the independent variables, X_{ik}.

$\hat{PT}_i$,$\hat{PB}_i$,$\hat{QT}_i$,$\hat{QB}_i$ and $\hat{L}_i$ are estimates of the dependent and independent variables and are regarded as unknowns.

The constants here are the lesion coordinates, x and y.

Since all the variables are read directly form the screen they have the same error, i.e. =constant.

Hence the above system becomes:

$$\sum_{j=1}^{n}(L_j-\hat{L}_j)\frac{\partial g_j}{\partial y} = \sum_{j=1}^{n}(L_j-\hat{L}_j) = 0 \qquad (4)$$

$$\sum_{j=1}^{n}(L_j-\hat{L}_j)\frac{\partial g_j}{\partial x} = \sum_{j=1}^{n}(L_j-\hat{L}_j)\tan(\hat{\theta}_{Lj}) = 0 \qquad (5)$$

$$(PT_i-\hat{PT}_i) + (L_i-\hat{L}_i)\frac{\partial g_i}{\partial \hat{PT}_i} = 0 \qquad i=1,\ldots n \qquad (6)$$

$$(PB_i-\hat{PB}_i) + (L_i-\hat{L}_i)\frac{\partial g_i}{\partial \hat{PB}_i} = 0 \qquad (7)$$

$$(QT_i-\hat{QT}_i) + (L_i-\hat{L}_i)\frac{\partial g_i}{\partial \hat{QT}_i} = 0 \qquad (8)$$

$$(QB_i-\hat{QB}_i) + (L_i-\hat{L}_i)\frac{\partial g_i}{\partial \hat{QB}_i} = 0 \qquad (9)$$

$$g_i = y-[\hat{PL}_i-x]\tan(\hat{\theta}_{Li}) = 0 \qquad (10)$$

where $\hat{PL}_i$ and $\tan(\hat{\theta}_{Li})$ are functions of $\hat{PT}_i$,$\hat{PB}_i$,$\hat{QT}_i$,$\hat{QB}_i$,$\hat{L}_i$.

Hence 5n+2 equations for 5n+2 variables

The general method of solution is to use equations (6)-(9) to solve for PT_i ,PB_i ,QT_i ,QB_i , in terms of L_i.

Substituting into (10) gives L_i in terms of x and y.

Inserting into (4) and (5) leaves two equations in x and y which are solved simultaneously. However the derivatives of gi are complicated, non-linear, trigonometric functions and analytical solution of (6)-(9) appears impossible.

By assuming that

$$\frac{\partial g_i}{\partial \hat{PT}_i} \approx \frac{\partial g_i}{\partial PT_i}$$

which seems reasonable since $\hat{PT}_i$ is an estimate of PT_i , the equations may be simplified by direct substitution of the known values of PT_i ,PB_i ,QT_i ,QB_i and L_i into these derivatives. The resulting derivatives are thus functions of x, of the form Ax+b, where A and B are known.

Substituting into (6)-(10) and rearranging the equations solves for $\hat{PT}_i$,... etc in terms of $\hat{L}_i$ and x. Putting these $\hat{PT}_i$,... values into (10) however leads to another non-linear equation in terms of $\hat{L}_i$, x and y which cannot be easily solved for $\hat{L}_i$.

Appendix 4 - Elimination of possible views to obtain the correct lesion estimate.

Assume that all 3 views lie in the quadrant flip range.

Possible views are:

i or i′
j or j′
k or k′

Possible estimates are formed from the following viewpairs:

ij ik i′j i′k jk j′k

ij′ ik′ i′j′ i′k′ jk′ j′k′

Tests on the bounds eliminate the following:

ij i′j′ j′k j′k′ ij′ ik ik′

All possible estimates involving view i have been eliminated, therefore view i′ must be correct.

The system has now reduced to 2 views with possible flips. The possible views are:

i′, j or j′, k or k′

Possible estimates are formed from the following viewpairs:

i′j i′j′ i′k i′k′ jk jk′ j′k j′k′

The tests on bounds have already eliminated

i'j' j'k j'k'

i.e. all estimates containing j', therefore view j is correct.

Possible views are now:

i', j, k or k'

Possible estimates remaining are:

Pick the jk or jk' estimate closest to i'j.

View k or k' hence assigned.

Appendix 5 - Reduction of Possible Viewing Angles by Testing Sets of Results.

Assume that the following views remain after applying constraints to the lesion estimates.

i or i′
j or j′
k

Sets of possible views	Corresponding lesion estimates
1) i j k	ij ik jk
2) i j′ k	ij′ ik j′k
3) i′ j k	i′j i′k jk
4) i′ j′ k	i′j′ i′k j′k

Assume that boundary conditions eliminate ij, ij′ and jk.

set 1) is eliminated by ij and jk

set 2) is eliminated by ij′

set 3) is eliminated by jk

set 4) remains complete therefore i′, j′, k are assumed to be the correct viewing angles, ie flip view i, flip view j, leave view k